Volume 6 - Number 1 - July 2020 - ISSN: 2426-3958

AsiaIntervention

Official Journal of the Asian Pacific Society of Interventional Cardiology (APSIC) and the Interventional Cardiology Foundation of India (ICFI)
www.asiaintervention.org

AsiaIntervention

Official Journal of the Asian Pacific Society of Interventional Cardiology

(APSIC) and the Interventional Cardiology Foundation of India (ICFI)

www.asiaintervention.org

Title: **Very rare giant coronary aneurysm.**

Authors: Rajeshwari Nayak, DNB; Yeramma Vijayachandra Reddy, M.D, DM, MRCP; Girinath Maligail Ramakrishnan, MS, Mch, FRCS; Rochita Ramanan, M.D; Sathyamurthy Immineni, M.D, DM; Jenifer Johnson, BS

Manuscript number: AIJ-D-18-00029

Manuscript submission date: 29 May 2018

Revisions received: 27 January 2019, 26 July 2019

Accepted date: 04 March 2020

Very rare giant coronary aneurysm

Rajeshwari Nayak[1 DNB], Yeramma Vijayachandra Reddy[2 M.D, DM, MRCP], Girinath Maligail Ramakrishnan[3 MS, Mch, FRCS], Rochita Ramanan[4 M.D], Sathyamurthy Immineni[5 M.D, DM], Jenifer Johnson[6 BS]

1. Fellowship in Heart Failure and Echo (Australia), Consultant cardiologist, Apollo hospitals, Chennai, India
2. Consultant cardiologist, Apollo hospitals, Chennai, India
3. Consultant cardiothoracic surgeon, Apollo hospitals, Chennai, India.
4. Consultant radiologist, Apollo hospitals, Chennai, India.
5. Consultant cardiologist, Apollo hospitals, Chennai, India.
6. Physician assistant. Apollo hospitals, Chennai, India.

Short running title:
Very rare giant coronary artery aneurysm

Corresponding author:

Dr Rajeshwari Nayak[1]mailing address: Apollo hospitals, No.21, greams lane, Off. Greams road, Chennai, Tamilnadu, India.
E-mail: drrajeshwari2006@yahoo.com

Conflict of interest statement:
None of the authors have conflicts of interest to declare

Funding :
Nil funding

Classifications:
Prior CABG; prior PCI; Aneurysm

Author image

Coronary artery aneurysm (CAA) are rare and giant CAA are even rarer. We describe an asymptomatic patient with a giant CAA of the RCA. A 65 year old, underwent echo (picture A&B) as part of his medical evaluation for life insurance policy which revealed a lesion in RA.

CAG revealed a giant aneurysm of the mid-segment of the RCA (picture F&G). CT coronary angiogram (CTA) revealed a large fusiform aneurysm, measured 32.1 mmx46mm (picture C, D, E).

Management options of percutaneous coronary intervention (PCI) with covered stent and surgical repair discussed. PCI was not a viable option as the artery proximal and distal to the aneurysm appeared highly ectatic.

He underwent surgical repair (picture H&I). CABG performed using saphenous vein grafts to the posterior descending artery and the acute marginal branches. The RCA proximal and distal to the aneurysm ligated. A third ligature placed around the origin of the acute marginal branch, achieving complete isolation of the aneurysm.

At 1 year follow-up, echo showed persisting RCA aneurysm. CTA showed aneurysm measuring 40mmx32mm, partially thrombosed with evidence of persistent filling from the native RCA. The large size of the aneurysm and the persistent filling by the RCA placed the patient at considerable risk of aneurysmal rupture and sudden cardiac death.

He underwent repeat surgery and RCA was ligated totally at its origin. At 1 year follow up after the second surgery, no echocardiographic evidence of persisting lesion. CTA revealed fully thrombosed RCA aneurysm.

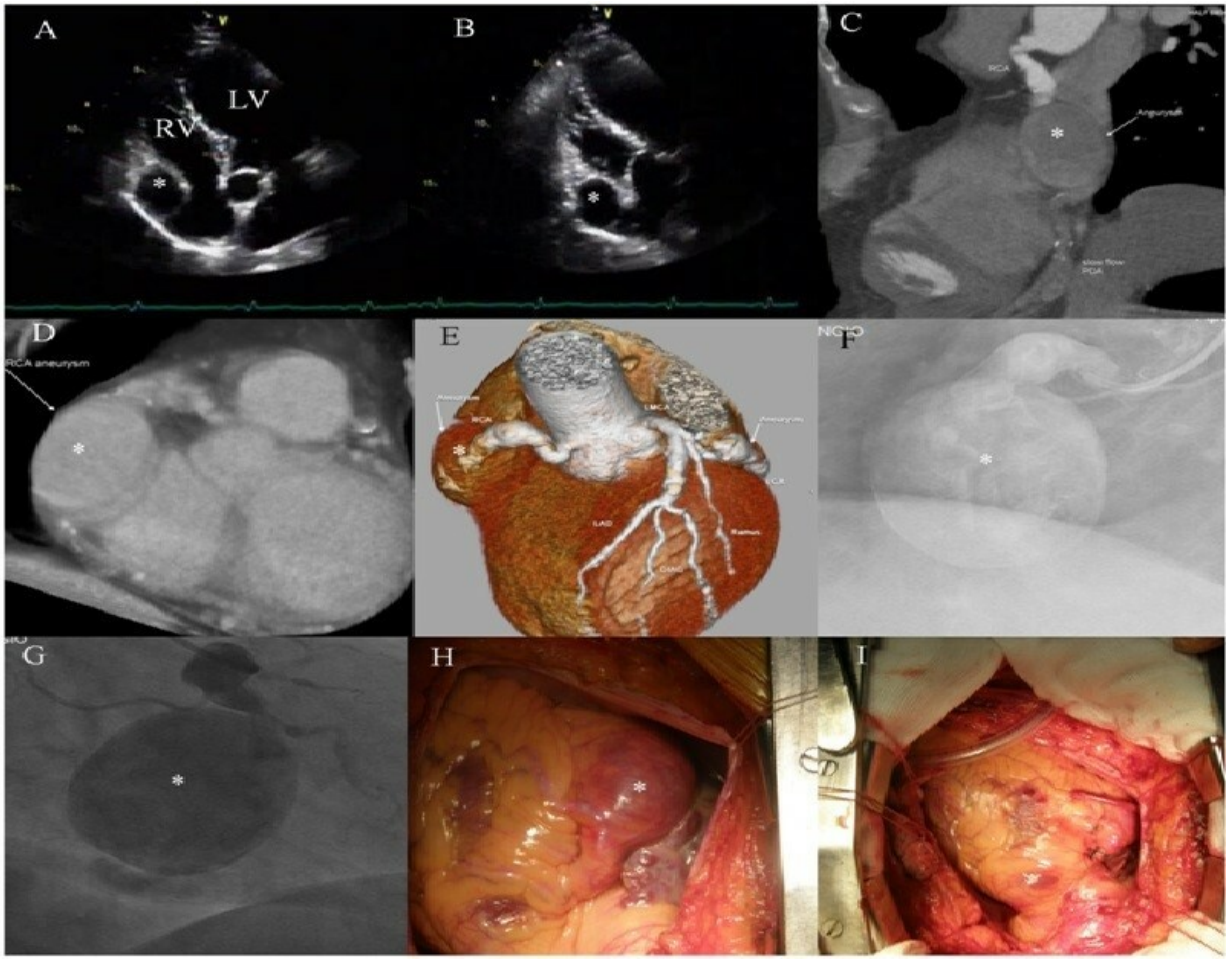

AsiaIntervention

Official Journal of the Asian Pacific Society of Interventional Cardiology

(APSIC) and the Interventional Cardiology Foundation of India (ICFI)

www.asiaintervention.org

Title: **Intracoronary Lithoplasty-Facilitated Expansion of an Undilatable Intra-Stent Lesion.**

Authors: Rattanachai Chanchai, M.D; Alfonso Ielasi, M.D; Antonio Silvestro, M.D; Maurizio Tespili, M.D

Manuscript number: AIJ-D-19-00021

Manuscript submission date: 02 May 2019

Revisions received: 19 July 2019

Accepted date: 04 March 2020

Intracoronary Lithoplasty-Facilitated Expansion of an Undilatable Intra-Stent Lesion

Rattanachai Chanchai, MD[1]; Alfonso Ielasi, MD[2]; Antonio Silvestro, MD[2]; Maurizio Tespili MD[2]

[1]Clinical and Interventional Cardiology Unit, Lanna Hospital, Chiang Mai, Thailand
[2]Clinical and Interventional Cardiology Unit, Sant'Ambrogio Cardio-Thoracic Center, Milan, Italy

Short title: Coronary lithoplasty and un-dilatable in-stent lesions

Classification: In-stent restenosis; Intravascular ultrasound; Other technique

The authors have no conflicts of interest to declare

Address for correspondence:

Alfonso Ielasi, MD, FESC

Clinical and Interventional Cardiology Unit, S. Ambrogio Cardio-Thoracic Center,

Via Faravelli 16, 20149, Milan, Italy.

Email: alelasi@hotmail.com

A 59-year-old male with a history of prior (12 years) PCI and drug-eluting stent (DES) implantation on proximal/mid right coronary artery (RCA) was admitted because of unstable angina. Coronary angiography revealed a focal in-stent restenosis (ISR) at the proximal RCA. **(Panel A)**

Pre-dilatation using a 3.5 mm non-compliant (NC) balloon inflated up to 30 atm was attempted with persistent under-expansion. **(Panel B)** Intravascular ultrasound (IVUS) revealed a heavily calcified neo-intimal plaque at the un-expanded site. **(Panel C)** The lesion was approached by a 3.5x12 mm (sized 1:1 to the reference artery ratio) coronary lithoplasty balloon (-LB- *Shock Wave Medical, USA*) inflated up to 4 atm before to release sequential lithotripsy runs at the lesion site resulting in a full LB and the NC (3.5 mm at 24 atm) expansion (**Panel D**). A new generation DES (3.5x15 mm) was finally implanted and post-dilated (4.0 NC balloon) at the target site obtaining a good final angiographic and IVUS result **(Panel E-F)**.

The use of a coronary LB was recently described as a novel option to facilitate the delivery of interventional equipment and improve stent expansion after modification of calcified plaques in native coronary arteries.[1] To date very little is known on the performance of the LB for the treatment of un-dilatable in-stent lesions. Our images highlight the importance of a new technology to overcome the potential limitations of currently available devices (i.e. rotational atherectomy, excimer laser, very high pressures NC balloons) for the treatment of resistant in-stent lesions.

Reference

1. Brinton TJ, Ali ZA, Hill JM, Meredith IT, Maehara A, Illindala U, Lansky A, Gotberg M, Van Miegehem NM, Whitbourn R, Fajadet J, Di Mario C. Feasibility of shockwave coronary intravascular lithotripsy for the treatment of calcified coronary stenoses. Circulation. 2019 Feb 5;139(6):834-836.

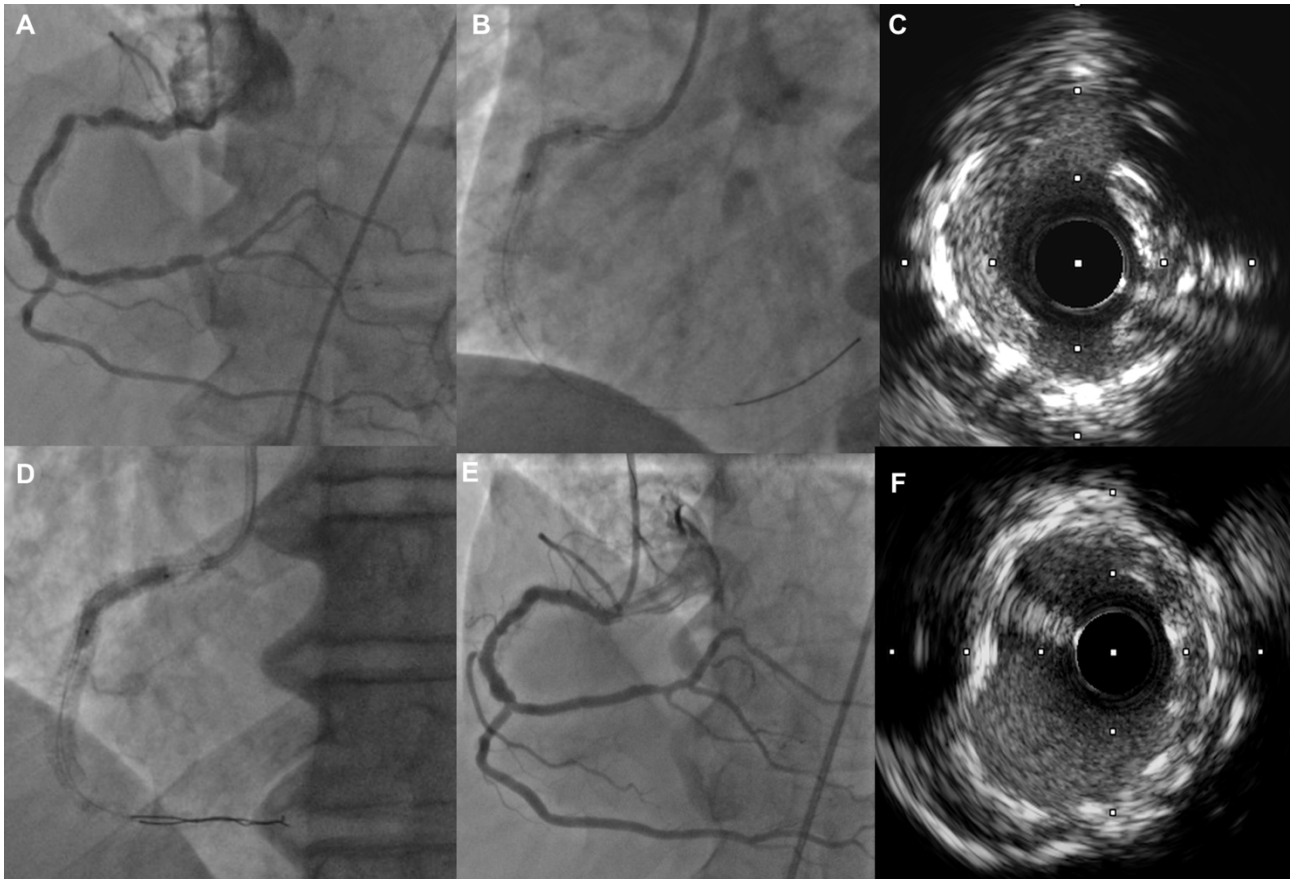

AsiaIntervention

Official Journal of the Asian Pacific Society of Interventional Cardiology

(APSIC) and the Interventional Cardiology Foundation of India (ICFI)

www.asiaintervention.org

Title: **Radiation doses during cardiac catheterization procedures in India – A multicentre study.**

Authors: Vijayakumar Subban, M.D, DM, FNB; Sophie Amelot, MS; Suma M Victor, DNB, DNB, FNB; Anil Potdar, M.D, DNB, MNAMS, FACC, FSCAI; Vishawanath Yadav, MBBS, DNB, DNB; Tejas Patel, M.D, DM, FACC, FSCAI; Sanjay Shah, M.D, DM; Thomas Alexander, M.D, DM, FACC, FICC, FCSI; Balakumaran Jeyakumaran, M.D, DM; Juno Angel, MSc, PGDCR; Mullasari S Ajit, M.D, DM, FRCP.

Manuscript number: AIJ-D-18-00044

Manuscript submission date: 20 July 2018

Revisions received: 30 November 2018, 01 May 2019, 11 July 2019

Accepted date: 04 March 2020

Radiation doses during cardiac catheterization procedures in India – A multicentre study

Short Title: Radiation Dose Study

VijayakumarSubban,[1] MD, DM, FNB; Sophie Amelot,[2]MS, Suma M Victor,[1] DNB, DNB, FNB, Anil Potdar[3], MD, DNB, MNAMS, FACC, FSCAI; Vishawanath Yadav[3],MBBS, DNB, DNB; Tejas Patel[4], MD, DM, FACC, FSCAI; Sanjay Shah[4], MD, DM; Thomas Alexander[5], MD, DM, FACC, FICC, FCSI; Balakumaran Jeyakumaran[5], MD, DM; Juno Angel[1], MSc, PGDCR; Mullasari S Ajit[1] MD,DM,FRCP.

[1] Institute of Cardiovascular Diseases, The Madras Medical Mission

[2] GE Healthcare, Buc, France

[3]Parisoha heart foundation Pvt.Ltd, Mumbai

[4]Apex Heart Institute , Ahmedabad

[5]Kovai Medical Centre and Hospital, Coimbatore

Corresponding author and contact details:

Dr. VijayakumarSubban

Institute of Cardio vascular Diseases

The Madras Medical Mission

4-A, Dr. J Jayalalitha Nagar

Moggappair, Chennai – 600037

Email: drkumarvijay@gmail.com

Conflict of interest statement: V Subban has received an institutional research grant from GE Healthcare. S Amelot is a GE Healthcare employee. Other authors have no conflicts of interest to declare.

Abstract

Aim:

Established, evidence-based measures of radiation are required to minimize its hazards, while maintaining adequate image quality. The aim of this study is to evaluate the data of radiation and to generate reference radiation levels for commonly performed coronary catheterization procedures in India.

Methods and results:

In this prospective, observational study, all procedures were performed in accordance with the established standards using Innova IGS 520/2100-IQ catheterization laboratories (GE Healthcare). Demographic, procedural and radiation data were collected. Dose reference limits (DRL) were established as the 75th percentile of the total distribution.

There were 2906 coronary angiograms (CAG), 750 percutaneous coronary interventions (PCI) and 715 coronary angiography + percutaneous coronary interventions (CAG + PCI). DRLs for Dose Area Product were: 19.6 Gy.cm2 for CAG, 49.8Gy.cm2 for PCI and 72.0 Gy.cm2 for CAG+PCI respectively. Median cumulative air kerma levels were: 185 mGy for CAG, 533mGy for PCI, and 891 mGy for CAG+PCI. Male gender, higher BMI, combining CAG+PCI, fluoroscopy time, number of cine frames, and image acquisition settings were significant contributors to increased radiation dose.

Conclusions:

This study established reference radiation dose levels for diagnostic and interventional coronary procedures in India, which were comparable and were in the lower range to international standards.

Classifications:

Radiation Protection, Other imaging modalities, Training and education

Abbreviations:

BMI: Body Mass Index

CAG: Coronary angiography

CAK: Cumulative Air Kerma

DAP: Dose Area Product

FT: Fluoroscopy Time

PCI: Percutaneous coronary Intervention

Condensed abstract:

To characterize the radiation doses received by patients during diagnostic and interventional **coronary** procedures and to establish provisional national reference levels for India, we studied radiation exposure data delivered during 4371 Coronary Angiography (CAG), or percutaneous coronary interventions (PCI) performed at tertiary cardiac institutions across India. 75th percentile of the distribution of Dose Area Product was: 19.6 Gy.cm2 (CAG), 49.8 Gy.cm2 (PCI), and 72.0 Gy.cm2 (CAG+PCI) respectively. This study allowed for the calculation of a DRL for diagnostic and interventional coronary procedures in India, these DRLs can be used as a benchmark for new or similar catheterization laboratories.

1. Introduction

Radiation based imaging has revolutionized the practice of modern medicine. Though it is used extensively in various fields of medicine, it remains the predominant modality for imaging in the cardiac catheterization laboratory. However, these procedures place both the patient and the laboratory personnel at risk from ionizing radiation. Excessive exposure to ionizing radiation may either have deterministic effect from direct injury to skin or stochastic effect in the form of neoplasms **(1).** Professional societies have emphasized the need to develop radiation safety programs for catheterization laboratories, which include essential parties responsible for protection and safety, training/education of the staff, radiation monitoring and, protective shielding **(2, 3).** Guidelines have proposed a dose threshold of 5 Gy or 500 $Gy.cm^2$, beyond which patients have to be on surveillance for skin injuries **(2).**

In India, approximately 1000 hospitals offer cardiovascular catheterization facilities across the country. The number of coronary interventional procedures increased from 1, 77,240 in 2012 to 3,73,579 in 2016 **(4).** An estimated 30% of these are multivessel or complex interventional procedures. In addition, approximately 30,000 non-coronary interventions are performed yearly and the number of diagnostic procedures is close to thrice the number of all other procedures performed **(4).** Though there has been a steady growth in the number of catheterization laboratories and the procedures over the years, systematic reporting of the patient radiation doses is not in practice in India. The aim of this study is to establish a baseline radiation reference dose for commonly performed coronary catheterization procedures in India and to compare them with established international standards.

2. Methods

2.1 **Study design and population**

This prospective observational study was conducted at 4 prominent tertiary cardiac centers across India. From June 2015 to January 2017, 4603 consecutive patients undergoing diagnostic and interventional **coronary** procedures were prospectively included in the study. All the procedures were performed in accordance with the participating center's established internal standards. Procedures were categorized into following 3 groups: Group I: coronary angiography (CAG), Group II: percutaneous coronary intervention (PCI), Group III: coronary angiography followed by adhoc percutaneous coronary intervention (CAG+PCI). Other procedures such as peripheral, endovascular, structural, electrophysiological, or pediatric catheterization were excluded. This study was approved by ethical review board, and all patients signed an informed consent prior to the procedure. Study was registered **with Clinical Trial Registry-India (CTRI), reference number: CTRI/2015/11/006359.**

2.2 Imaging Equipment

All procedures were performed using 3 Innova IGS 520 and 2 Innova 2100-IQ catheterization laboratories (GE Healthcare), installed between 2011 and 2015. All systems offered similar capability to customize dose and image quality among 5 "Dose Personalization" settings according to the preference of individual institution. The choice of configurable settings, as well as the selection of acquisition frame rates and normal versus low dose level preference was left to the physician's discretion. Together, configurable settings and selectable operational settings provided a typical 6:1 range in fluoroscopy and cine dose rate adjustments capability. The configurations of the systems and selectable settings of acquisition protocols with radiation dose limit (RDL) used at

the different hospitals are summarized in **Supplementary Table 1**. All systems provided built-in dosimetry capability, to monitor patient radiation data throughout the procedure.

2.3 Data collection

The following data were prospectively collected for each procedure: baseline demographics, clinical characteristics of the patient, radiation dose indicators from the system at the end of the procedure (Dose Area Product (DAP, $Gy.cm^2$) and cumulative Air KERMA (CAK, mGy), fluoroscopy time (FT, minutes));as well as other procedural data such as: procedure type, access route, number of vessels treated, number of stents implanted, duration of the procedure, procedural complications, quantity of contrast, use of adjunctive technology such as intravascular imaging, fractional flow reserve assessment and rotational atherectomy. In addition to the patient radiation data, other parameters such as acquisition mode, frame rate, radiation exposure data split between fluoroscopy and cine x-ray acquisition duration, and number of cine exposures were automatically recorded for each x-ray acquisition and were analyzed. For comparison between institutions, DAP rates were used to normalize differences in procedural time, which might be attributed to differences in operator's experience or complexity of the procedure (5). For each type of procedure, radiation data Reference Levels (RLs) were established as the third quartile of the total distribution (6). For this study, the 75th percentile of the distribution of DAP values was defined as Dose Reference Level (DRL).

2.4 Statistical Analysis

Statistical analysis was done using Microsoft® Excel® 2010 (Version 14.0.7165.5000) and Minitab®17 statistical software (2010) (Version 17.3.1, Minitab Inc.). Categorical variables are presented as numbers and percentages. Continuous variables are described

with mean ± standard deviation or median (with interquartile range) depending on their distribution. Kruskal-Wallis test was used for one-way analysis of variance for comparison of radiation data between sites. Comparison of radiation data was performed using the one -sided non-parametric 1 sample sign test when referenced data were provided as median to test the null hypothesis that no difference would be found between study and reference median and with alternative hypothesis that study median would be lower than reference median. Similarly, when referenced data was provided as mean, 1 sample t test was used. Multivariate analysis was performed for the patient subset of coronary interventions (PCI and CAG+PCI) to identify individual risk factors with logarithm-transformed DAP as the dependent variable using back-ward step wise analysis. All patients' related and image acquisition related characteristics listed above were used as covariates. Beta-coefficients are given after re-transformation [exp(beta coefficient)] to describe the relative influence of each variable on DAP. A 95% confidence level was used for all statistical calculations and a 'p' value of 0.05 or less was considered significant.

3. Results

Overall 4603 patients were included in the study, of these 4371 had analyzable data (195 incomplete radiation datasets, and 37 excluded from analysis as other type of procedures). Procedure distribution, demographic profile, cardiovascular risk factors and indications for procedure are summarized in **Table 1**. Majority of patients were males (71%). Diabetes and hypertension were prevalent at 39% and 42%, respectively. Most of the procedures were done electively (69%). The impact of BMI on the radiation is depicted in **Figure 1**, and there is a step-wise increase in DAPs in both PCI and CAG+PCI groups across increasing BMIs. This trend, however, is not seen in the CAG group. Procedural data are shown in **Table 2**. Transradial technique was used in 76% of the

patients. There were 2906 CAGs, 750 PCIs and 715 CAG + PCIs. Adjunctive technologies were used in 99 (2.9%) patients. On an average, there were 1.2 ± 0.4 vessels treated and 1.3 ± 0.6 stents implanted per each therapeutic procedure.

Procedure specific radiation data are summarized in **Table 3**. Reference levels for DAP, CAK, FT from the study for the above procedures were 19.6Gy.cm^2, 325 mGy, 4.5 min (CAG), 49.8Gy cm^2, 1016 mGy, 18.2 min (PCI), and 72.0Gy cm^2, 1461 mGy, 15.1 min (CAG+PCI) respectively. As expected, both DAP level, CAK level, and number of cine frame rates were higher when adhoc PCI were performed. Male gender, higher BMI, combining CAG+PCI, fluoroscopy time, number of cine frames, and image acquisition settings were significant contributors to increased radiation dose **(Table 4)**. Among the fluoro settings, using '7.5 fps RDL+Low' significantly decreased DAPs while '15 fps Smart IQ Low' did not show any statistical significance. On the other hand, 15 fps with either 'normal or Smart IQ Normal' adversely impacted the DAPs. Similarly, cine settings at 15fps when used with 'RDL+Low' notably reduced the radiation levels while other cine settings did not. There was significant dispersion of 75th percentile of DAP between the 4 centers for all procedures ('p'<0.05) (**figure 2**). The maximal range of median DAP between centers was 7-21 Gy.cm^2,13-52, and 20-57 Gy.cm^2 for CAG, PCI and CAG+PCI respectively. Institution 4 had the lowest DAP median for each of the 3 groups and this was the only institution which used '7.5frame/s RDL+ Low' settings for fluoroscopy.

Distribution of CAK is depicted in **Figure 3**. **Overall, 87.4% of the procedures were below 1 Gy, including 98% of CAG, 74% of PCI and 57% of CAG + PCI. 98.8% of the procedures were below the first notification threshold of 3Gy. 1% of the examinations attained a radiation dose between 3 and 5 Gy. Only 0.3% of (all PCIs (6 elective and 6 adhoc) exceeded the substantial radiation dose level of 5 Gy, above which patient follow up is recommended (2).** This category was inclusive of 3

patients with complex primary PCI , 4 PCIs for calcified lesions, 1 complex bifurcation PCI , 3 PCIs for chronic total occlusion , and 1 patient who had PCI related complications. However, lesion complexity data was not included in the study analysis as it was available for all patients. Comparison of radiation data from the current study with international references and recent literature is shown in **Figure 4** (6-16) as well as in **Supplementary Tables 2, and 3.** For each procedure category, the study median DAP and 75th percentile DAP were compared with data from previously published studies: 4 study datasets out of 31 had comparable or lower DAP for CAG and 9 out 40 had similar outcomes for PCI. This trend also continued with comparisons of CAK and FT.

4. Discussion:

The major observations of our study are: [1] DAP and CAK during diagnostic and interventional coronary procedures from a selection of Indian centers are comparable and in the low range in reference to the international standards. [2] Only 1% of the all procedures received a dose between 3Gy and 5 Gy and 0.3% of the examinations attained a dose above the cut off value 5 Gy. [3] There is considerable variation across the sites with regard to the radiation parameters. [4] Male gender, higher BMI, combining CAG+PCI, fluoroscopy time, number of cine frames, and image acquisition settings were significant predictors of higher DAP.

Historically, radiation dose during catheterization procedure varies widely based on age, BMI, radial route, previous bypass grafting, lesion complexity, equipment generation, technical settings and operator experience (17, 18). Gender-based patterns for radiation exposure across catheterization laboratories are unknown. In this study, male gender is an important predictor but women were under represented (29%) and significance of

this finding after adjustment for lesion complexity is not analyzed. However, in a study exploring mean effective radiation dose for nuclear cardiology procedures, it was shown women required slightly lesser radiation dose (9.6±4.5 mSv) than men (10.3±4.5mSv, p<0.001) (19). On the other hand the adverse relation between BMI and radiation dose is well established (18). Adhoc PCI increased DRLs significantly; with mean DAP 56.2± 42.7 Gy.cm^2 where as PCI group had a mean of 40.4 ±47.1 Gy.cm^2. In a study published by Truffa et al (20), the ad hoc group had lower total DAP 119.7 ± 70.7 Gycm^2, compared to staged group, 139.2 ± 75.3 Gycm^2 (p < 0.001), but the staged group's total DAP included the radiation during both CAG and PCI, thus cannot be compared to the present study. Fluoroscopy time, number of cine frames, and image acquisition settings are conventional risk factors of radiation (18).

All the hospitals participating in the study have used the same equipment for X-ray imaging but the choice of configurable settings was left to the physician's preference. The institution which recorded the lowest DAP means for all procedures, had the physicians opting for low frame rate as well as low radiation protocols for all the procedures. Preference of image technical settings between sites to accomplish a clinical task, operator's practice and awareness to radiation reduction techniques such as usage of collimation while limiting magnification, limitation of steep angulations, optimal placement of image receptor as close as possible to the patient, selection of lower frame rates and lower dose level preference, use of fluoro-store function instead of cine, impact the levels of radiation. Georges et al (17), in their analysis of 34,436 CAGs and 28,932 PCIs across 44 centers in France observed significant differences in the radiation doses between participating centers. The maximal range of median KAP between centers was 9-54 Gy.cm^2 and 16-126 Gy.cm^2 for CAG and PCI respectively. When comparison was made between centers delivering lower and higher radiation doses, old equipment,

routine left ventriculography, use of frame rates >7.5 fps were more frequent in centers delivering higher doses.

Incidence of high dose exposure varies between 0.1% and 1.0% among different studies (17). Historically, high radiation doses commonly occur in patients with high BMI and in those undergoing complex interventional procedures such as chronic total occlusions or calcified lesions or anomalous coronary arteries, or when procedure complications occur (21). Similar findings were observed in this study and are consistent with other published studies (17). None of the patients with radiation dose above 5 Gy reported skin injuries. However, the current study did not mandate follow up of patients who received high radiation doses.

The main objective of any radiation dose assessment is to minimize the detrimental effects of radiation by reducing its exposure in the catheterization laboratory. DRLs serve as a benchmark that gives an opportunity for the individual laboratories to compare their performance and to adapt policies to curtail unnecessary exposure to radiation. The DRLs from the current study were 19.6 Gy.cm^2 for CAG and 49.8 Gy.cm^2 for PCI and 72 Gy.cm^2 for CAG+PCI, considerably lower than the reference limits of other international studies (Supplementary tables 3 & 4). Various factors could have contributed to this. Indians with cardiovascular disease are known to have lower BMI when compared to other ethnicities (22). Most of the reference studies were published much earlier; hence, this study might have had the benefit of improved radiation awareness, better experience of the operators, and recent advances in technical equipment.

4.5 Limitations:

The current study has some important limitations. Radiation dose measurements were restricted to the selected 3 procedures (CAG, PCI, CAG+PCI) and hence no reference values can be deduced from this study for other catheterization procedures. Detailed

technical factors such as field of view, collimation, source-to-image distance, angulations have not been monitored. Lesion complexity and operator experience were not considered. There is no follow up of patients who have received high radiation doses and the adverse effects of these high doses have not been reported.

5. Conclusions:

DRLs for diagnostic and interventional coronary angiography procedures in India were calculated in this study. Despite variations across centers, radiation doses from a selection of tertiary cardiac care centers using similar equipment are comparable and are in the low range with reference to the international standards. The establishment of these DRLs can be used as a benchmark for new or similar catheterization laboratories.

Impact on daily practice:

The current study provides preliminary radiation exposure reference levels for commonly performed coronary procedures in India. This may serve as a reference for evaluation of radiation dose in individual catheterization laboratories to adapt policies and practices to improve their radiation doses.

Acknowledgment: The authors thank the support of Varun Gopinathand Bhavani who helped in this study.

Funding source: This work was supported in part by a GE Healthcare grant.

References: -

1. Kato M, Chida K, Sato T, Oosaka H, Tosa T, Munehisa M, Kadowaki K. The necessity of follow-up for radiation skin injuries in patients after percutaneous coronary interventions: radiation skin injuries will often be overlooked clinically. Acta radiologica.2012; 53:1040-4.
2. Chambers CE, Fetterly KA, Holzer R, Lin PJ, Blankenship JC, Balter S, Laskey WK. Radiation safety program for the cardiac catheterization laboratory. Catheter Cardiovasc Interv. 2011;77:546-56.
3. The 2007 Recommendations of the International Commission on Radiological Protection. ICRP publication 103. Annals of the ICRP. 2007; 37:1-332.
4. Khanna NN, Rao S. Growth of Interventional Cardiology in India: The Relevance of National Interventional Council (CSI–NIC). In: Sarat Chandra K, Bansal M, editors. Cardiology update 2017. Gurgaon, India: Elsevier; 2017. p. 211-9.
5. Hirshfeld JW, Jr., Balter S, Brinker JA, Brinker JA, Kern MJ, Klein LW, Lindsay BD, Tommaso CL, Tracy CM, Wagner LK, Creager MA, Elnicki M, Lorell BH, Rodgers GP, Weitz HH . ACCF/AHA/HRS/SCAI clinical competence statement on physician knowledge to optimize patient safety and image quality in fluoroscopically guided invasive cardiovascular procedures. A report of the American College of Cardiology Foundation/American Heart Association/American College of Physicians Task Force on Clinical Competence and Training. J Am Coll Cardiol.2004; 44:2259-82.
6. Establishing guidance levels in x-ray guided medical interventional procedures: a Pilot study — Vienna: International Atomic Energy Agency, 2008 — Safety reports series, ISSN 1020–6450, no. 59. 2009.

7. Padovani R, Vano E, Trianni A, Bokou C, Bosmans H, Bor D, Jankowski J, Torbica P, Kepler K, Dowling A, Milu C, Tsapaki V, Salat D, Vassileva J, Faulkner K . Reference levels at European level for cardiac interventional procedures. Radiat Prot Dosimetry. 2008;129:104-7.
8. D'Helft CJ, Brennan PC, McGee AM, McFadden SL, Hughes CM, Winder JR, Rainford LA. Potential Irish dose reference levels for cardiac interventional examinations. Br J Radiol. 2009;82:296-302.
9. Bogaert E, Bacher K, Lemmens K, Carlier M, Desmet W, De Wagter X, Djian D, Hanet C, Heyndrickx G, Legrand V, Taeymans Y, Thierens H. . A large-scale multicentre study of patient skin doses in interventional cardiology: dose-area product action levels and dose reference levels. Br J Radiol. 2009;82:303-12.
10. Hart D, Hillier MC, Wall BF. National reference doses for common radiographic, fluoroscopic and dental X-ray examinations in the UK. Br J Radiol. 2009;82:1-12.
11. Brnic Z, Krpan T, Faj D, Kubelka D, Ramac JP, Posedel D, Steiner R, Vidjak V, Brnić V, Visković K, Baraban V.. Patient radiation doses in the most common interventional cardiology procedures in Croatia: first results. Radiat Prot Dosimetry. 2010; 138:180-6.
12. Sanchez R, Vano E, Fernandez JM, Sotil J, Carrera F, Armas J, Rosales F, Pifarre X, Escaned J, Angel J, Diaz JF, Bosa F, Saez JR, Goicolea J. . A national programme for patient and staff dose monitoring in interventional cardiology. Radiat Prot Dosimetry. 2011;147:57-61.
13. Samara ET, Aroua A, De Palma R, Stauffer JC, Schmidt S, Trueb PR, Stuessi A, Treier R, Bochud F, Verdun FR.An audit of diagnostic reference levels in interventional cardiology and radiology: are there differences between academic and non-academic centres? Radiat Prot Dosimetry. 2012;148:74-82.

14. Miller DL, Hilohi CM, Spelic DC. Patient radiation doses in interventional cardiology in the U.S.: advisory data sets and possible initial values for U.S. reference levels. Medical physics. 2012; 39:6276-86.
15. Simantirakis G, Koukorava C, Kalathaki M, Pafilis C, Kaisas I, Economides S, Hourdakis CJ, Kamenopoulou V, Georgiou E.Reference levels and patient doses in interventional cardiology procedures in Greece. Eur radiol. 2013; 23:2324-32.
16. Georges JL, Belle L, Etard C, Azowa JB, Albert F, Pansieri M, Monsegu J, Barbou F, Trouillet C, Leddet P, Livarek B, Marcaggi X, Hanssen M, Cattan S, The Ray'act-Investigators. Radiation Doses to Patients in Interventional Coronary Procedures-Estimation of Updated National Reference Levels by Dose Audit. Radiat Prot Dosimetry. 2017;175:17-25.
17. Georges JL, Belle L, Ricard C, Cattan S, Albert F, Hirsch JL, Monsegu J, Dibie A, Khalife K, Caussin C, Maccia C, Livarek B, Hanssen M; RAY'ACT investigators. Patient exposure to X-rays during coronary angiography and percutaneous transluminal coronary intervention: results of a multicenter national survey. Catheter Cardiovasc Interv. 2014;83:729-38.
18. Journy N, Sinno-Tellier S, Maccia C, Le Tertre A, Pirard P, Pagès P, Eilstein D, Donadieu J, Bar O. Main clinical, therapeutic and technical factors related to patient's maximum skin dose in interventional cardiology procedures. Br J Radiol. 2012;85:433-42.
19. Shi L, Dorbala S, Paez D, Shaw LJ, Zukotynski KA, Pascual TN, Karthikeyan G, Vitola JV, Better N, Bokhari N, Rehani MM, Kashyap R, Dondi M, Mercuri M, Einstein AJ; INCAPS Investigators Group. Gender Differences in Radiation Dose From Nuclear Cardiology Studies Across the World: Findings From the INCAPS Registry. JACC Cardiovasc Imaging. 2016 Apr;9(4):376-84.

20. Truffa MA, Alves GM, Bernardi F, Esteves Filho A, Ribeiro E, Galon MZ, Spadaro A, Kajita LJ, Arrieta R, Lemos PA. Does Ad Hoc Coronary Intervention Reduce Radiation Exposure? - Analysis of 568 Patients. Arq Bras Cardiol. 2015 Nov;105(5):487-92.
21. Delewi R, Hoebers LP, Ramunddal T, Henriques JP, Angerås O, Stewart J, Robertsson L, Wahlin M, Petursson P, Piek JJ, Albertsson P, Matejka G, Omerovic E. Clinical and procedural characteristics associated with higher radiation exposure during percutaneous coronary interventions and coronary angiography. Circ Cardiovasc Interv. 2013;6:501-6.
22. Nag T, Ghosh A. Cardiovascular disease risk factors in Asian Indian population: A systematic review. J Cardiovasc Dis Res. 2013 Dec;4(4):222-8.
23. Abdelaal E, Plourde G, MacHaalany J, Arsenault J, Rimac G, Déry JP, Barbeau G, Larose E, De Larochellière R, Nguyen CM, Allende R, Ribeiro H, Costerousse O, Mongrain R, Bertrand OF; Interventional Cardiologists at Quebec Heart-Lung Institute. Effectiveness of low rate fluoroscopy at reducing operator and patient radiation dose during transradial coronary angiography and interventions. *JACC Cardiovascular interventions.* 2014;7(5):567-74.
24. Eloot L, Thierens H, Taeymans Y, Drieghe B, De Pooter J, Van Peteghem S, Buytaert D, Gijs T, Lapere R, Bacher K. Novel X-ray imaging technology enables significant patient dose reduction in interventional cardiology while maintaining diagnostic image quality. *Catheter Cardiovasc Interv*. 2015;86:E205-12.
25. Bracken JA, Mauti M, Kim MS, Messenger JC, Carroll JD. A Radiation Dose Reduction Technology to Improve Patient Safety During Cardiac Catheterization Interventions. *J IntervCardiol*.2015; 28:493-7.

26. Livingstone RS, Chase D, Varghese A, George PV, George OK. Transition from image intensifier to flat panel detector in interventional cardiology: Impact of radiation dose. *J Med Phys*.2015; 40:24-8.

27. Nakamura S, Kobayashi T, Funatsu A, Okada T, Mauti M, Waizumi Y, Yamada S. Patient radiation dose reduction using an X-ray imaging noise reduction technology for cardiac angiography and intervention. *Heart Vessels.* 2015; 31:655-63.

28. Varghese A, Livingstone RS, Varghese L, Kumar P, Srinath SC, George OK, George PV. Radiation doses and estimated risk from angiographic projections during coronary angiography performed using novel flat detector. *J ApplClin Med Phys*.2016; 17:433-441.

29. Ryckx N, Goy JJ, Stauffer JC, Verdun FR. Patient Dose Assessment after Interventional Cardiology Procedures: A Multi-Centric Approach to Trigger Optimisation. *RadiatProt Dosimetry*. 2016; 169:249-52.

30. Didier R, Magalhaes MA, Koifman E, Leven F, Castellant P, Boschat J, Jobic Y, Kiramijyan S, Nicol PP, Gilard M. The utilisation of the cardiovascular automated radiation reduction X-ray system (CARS) in the cardiac catheterisation laboratory aids in the reduction of the patient radiation dose. *EuroIntervention*. 2016;12: e948-e956.

31. Hansen JW, Foy A, Schmidt T, Ghahramani M, Chambers CE. Fluoroscopy pulse rate reduction during diagnostic and therapeutic imaging in the cardiac catheterization laboratory: An evaluation of radiation dose, procedure complications and outcomes. *Catheter Cardiovasc Interv*.2016; 89:665-670.

32. Jurado-Roman A, Sanchez-Perez I, Lozano Ruiz-Poveda F, López-Lluva MT, Pinilla-Echeverri N, Moreno Arciniegas A, Agudo-Quilez P, Gil Agudo A.

Effectiveness of the implementation of a simple radiation reduction protocol in the catheterization laboratory. *CardiovascRevasc Med*.2016 ;17 :328-32.

33. Wilson SM, Prasan AM, Virdi A, Lassere M, Ison G, Ramsay DR, Weaver JC. Real-time colour pictorial radiation monitoring during coronary angiography: effect on patient peak skin and total dose during coronary angiography. *EuroIntervention.* 2016;12: e939-e947.
34. Kastrati M, Langenbrink L, Piatkowski M, Michaelsen J, Reimann D, Hoffmann R. Reducing Radiation Dose in Coronary Angiography and Angioplasty Using Image Noise Reduction Technology. *Am J Cardiol.*2016; 118:353-6.
35. Tarighatnia A, Mohammad Alian AH, Ghojazadeh M, Farajollahi AR. Comparison of the patient radiation exposure during coronary angiography and angioplasty procedures using trans-radial and trans-femoral access. *J CardiovascThorac Res*.2016; 8:77-82.
36. Sinha SK, Mishra V, Afdaali N, Jha MJ, Kumar A, Asif M, Thakur R, and Varma CM. Coronary Angiography Safety between Transradial and Transfemoral Access. *Cardiol Res Pract*.2016; 2016:4013843.
37. Uniyal SC, Chaturvedi V, Sharma SD, Rawat A. Patient Dosimetry during Interventional Cardiac Procedures in a Dedicated Catheterization Laboratory. *RadiatProt Dosimetry*. 2017; 175:201-208.
38. Balter S, Brinkman M, Kalra S, Nazif T, Parikh M, Kirtane AJ, Moses J, Leon M, Feri A, Green P, Ali ZA, Liao M, Karmpaliotis D. Novel Radiation Dose Reduction Fluoroscopic Technology Facilitates Chronic Total Occlusion Percutaneous Coronary Interventions. *EuroIntervention*.2017:13: e1468-e1474.
39. Ordiales JM, Vano E, Nogales JM, Ramos J, López-Mínguez JR, Martínez G, Cerrato P, Álvarez FJ. Optimisation of imaging protocols in interventional cardiology: impact on patient doses. *J Radiol Prot*.2017 ;37 :684-696.

40. Gunja A, Pandey Y, Xie H, Wolska BM, Shroff AR, Ardati AK, Vidovich MI. Image noise reduction technology reduces radiation in a radial-first cardiac catheterization laboratory. *CardiovascRevasc Med*.2017 ;18 :197-201.

41. Faroux L, Blanpain T, Nazeyrollas P, Tassan-Mangina S, Herce B, Tourneux C, Metz D. Minimizing exposure to radiation in invasive cardiology using modern dose-reduction technology: evaluation of the real-life effects. *Catheter Cardiovasc Interv*. 2018;91:1194-1199.

42. Sciahbasi A, Ferrante G, Fischetti D, Miklin DJ, Sarandrea A, Schirripa V, Guarracini F, Arya A, Loreni G, Bruni A, Rigattieri S, Marini M, Vagnarelli S, Scevola G, Reimers B, Hindricks G, Cohen M. Radiation dose among different cardiac and vascular invasive procedures: The RODEO study. *Int J Cardiol.*2017 ;240 :92-96.

43. Ichimoto E, Kadohira T, Nakayama T, De Gregorio J. Efficacy of radiation dose reduction due to real-time monitoring and visualization of peak skin dose during coronary angiography and percutaneous coronary intervention. *CatheterCardiovascInterv*. 2017; 91:717-722.

44. Boland JE, Wang LW, Love BJ, Christofi M, Muller DW. Impact of New-generation Hybrid Imaging Technology on Radiation Dose during Percutaneous Coronary Interventions and Trans-femoral Aortic Valve Implantations: A comparison with conventional flat-plate angiography. *Heart Lung Circ*.2016 ; 25:668-75.

45. Chon MK, Chun KJ, Lee DS, Lee SY, Hwang J, Lee SH, Hwang KW, Kim JS, Park YH, Kim JH. Radiation reduction during percutaneous coronary intervention : A new protocol with a low frame rate and selective fluoroscopic image storage. *Medicine (Baltimore).* 2017;96: e7517.

46. Faroux L, Blanpain T, Nazeyrollas P, Tassan-Mangina S, Herce B, Tourneux C, Metz D. Trends in Patient Exposure to Radiation in Percutaneous Coronary Interventions Over a 10-Year Period. *Am J Cardiol*.2017 ;120 :927-930.

47. Gislason-Lee AJ, Keeble C, Egleston D, Bexon J, Kengyelics SM, Davies AG. Comprehensive assessment of patient image quality and radiation dose in latest generation cardiac x-ray equipment for percutaneous coronary interventions. *J Med Imaging (Bellingham).*2017; 4:025501

Figure legends:

Figure 1: Impact of BMI on patient radiation dose. BMI: Body mass index, DAP: Dose area product.

Figure 2: 75th percentile DAP data by institutions. DAP: dose area product; CAG: coronary angiography; PCI: percutaneous coronary intervention; CAG+PCI: coronary angiography followed by percutaneous coronary intervention

Figure 3: Cumulative Air Kerma distribution for all procedures (CAG, PCI, CAG+PCI) – Log scale. CAG: coronary angiography; PCI: percutaneous coronary intervention; CAG+PCI: coronary angiography followed by percutaneous coronary intervention

Figure 4: Cumulative DAP (Gy.cm^2) in comparison with international references for CAG and PCI categories. Median and Interquartile range are given, unless otherwise indicated. CAG: coronary angiography; DAP: dose area product; PCI: percutaneous coronary intervention.

Table 1:

	All procedures	CAG	PCI	CAG+PCI
Number	**4371**	**2906**	**750**	**715**
Institution 1 (%)	835 (19)	546 (19)	76 (10)	213 (30)
Institution 2 (%)	982 (22)	513 (18)	95 (13)	374 (52)
Institution 3 (%)	1147 (26)	778 (27)	274 (37)	95 (13)
Institution 4 (%)	1407 (32)	1070 (37)	304 (41)	33 (5)
Age (Mean, SD) years	57.7 ± 10.7	57.4 ± 10.7	58.0 ± 10.6	58.5 ± 11.0
Male (%)	3247 (71)	2073 (71)	572 (76)	602 (84)
Diabetes (%)	1795 (39)	1186 (41)	298 (40)	311 (43)
Hypertension (%)	1951 (42)	1318 (45)	310 (41)	323(45)
BMI* (Mean, SD) kg/m^2	26.0 ± 4.2	26.3 ± 4.3	26.1 ± 4.1	25.1 ± 3.5
BMI* <25 (%)	1923 (44)	1207 (42)	316 (43)	400 (57)
BMI* ≥ 25 to <30 (%)	1699 (39)	1148 (40)	311 (42)	240 (34)
BMI* ≥ 30 (%)	705 (16)	536 (19)	108 (15)	63 (9)
Prior PCI (%)	238 (5)	129 (4)	51 (7)	58 (8)
Prior CABG (%)	89 (2)	60 (2)	15 (2)	14 (2)
STEMI (%)	353 (8)	140 (5)	18 (2)	195 (27)
NSTEMI/Unstable Angina(%)	840 (18)	513 (18)	71 (9)	256 (36)
Elective (%)	3177 (69)	2256 (78)	658 (88)	263 (37)

* BMI data is available for 4327 patients

BMI- Body Mass Index, CAG- Coronary Angiography, PCI- Percutaneous Coronary Intervention, CABG- Coronary Artery Bypass Graft surgery, STEMI- ST-segment Elevation Myocardial Infarction, NSTEMI- Non ST-segment Elevation Myocardial Infarction.

Table 2:

ACCESS ROUTES*	**N (%)**
Radial (%)	3312 (76.0)
Femoral (%)	991 (22.8)
Bi femoral (%)	15 (0.3)
Radial + Femoral (%)	38 (0.4)
PROCEDURE TYPE	
CAG (%)	2906 (63.2)
PCI (%)	750 (16.3)
CAG+PCI (%)	715 (15.5)
No of vessels treated (Mean, SD)	1.2 ± 0.4
No of stents implanted (Mean, SD)	1.3 ± 0.6
AMOUNT OF CONTRAST MEDIA USED	
CAG (Mean, SD) ml	51 ± 9
PCI (Mean, SD) ml	150 ± 18
CAG+PCI (Mean, SD) ml	146 ± 35

ADJUNCTIVE TECHNOLOGIES USED	
Rotablator (%)	17 (0.5)
OCT (%)	17 (0.5)
FFR (%)	25 (0.7)
IVUS (%)	34 (1.0)
IABP (%)	6 (0.2)
PROCEDURE COMPLICATION	
Dissection (%)	11 (0.3)
Unsuccessful Procedure (%)	4 (0.1)
Thrombosis (%)	5 (0.2)
Occlusion (%)	15 (0.4)

*Information missing regarding access route for 15 procedures.

CAG- Coronary Angiography, PCI- Percutaneous Coronary Intervention, OCT- Optical Coherence Tomography, FFR- Fractional Flow Reserve, IVUS- Intravascular Ultrasound, IABP- Intra Aortic Balloon Pump.

Table 3:

	N	Mean ± SD	Median	25th Percentile	75th Percentile
Goup I: CAG Group I	2906				
DAP (Gy.cm^2)		15.8 ± 16.4	11.0	6.4	19.6
Fluoroscopy DAP (Gy.cm^2)		4.4 ± 8.9	1.9	0.9	4.5
Cine DAP (Gy.cm^2)		11.5 ± 9.7	8.4	5.1	14.5
CAK (mGy)		261±255	185	112	325
Fluoroscopy CAK (mGy)		63 ± 129	28	12	64
Cine CAK (mGy)		198 ± 162	150	91	251
Acquisition duration (min)		4.3 ± 4.5	2.8	1.7	5.1
Fluoroscopy time (min)		3.8 ± 4.4	2.4	1.3	4.5
Cine time (min)		0.5 ± 0.2	0.5	0.4	0.6
Number of cine frames		460 ± 204	427	320	552
Group II: PCI	750				
DAP (Gy.cm^2)		40.4 ± 47.1	25.7	12.5	49.8
Fluoroscopy DAP (Gy.cm^2)		20.8 ± 29.9	11.4	5.3	23.3
Cine DAP (Gy.cm^2)		19.5 ± 21.0	13.1	6.5	25.6
CAK (mGy)		825 ± 941	533	243	1016
Fluoroscopy CAK (mGy)		418 ± 591	229	98	488

Cine CAK (mGy)		406 ± 423	280	138	533
Acquisition duration (min)		15.1 ± 11	12.4	7.9	19.3
Fluoroscopy time (min)		14.1 ± 10.6	11.4	7.1	18.2
Cine time (min)		1.0 ± 0.6	0.8	0.6	1.3
Number of cine frames		885 ± 551	738	520	1128
Group III: CAG+PCI	715				
DAP (Gy.cm^2)		56.2 ± 42.7	45.8	27.3	72.0
Fluoroscopy DAP (Gy.cm^2)		25.0 ± 26.7	17.3	9.6	31.7
Cine DAP (Gy.cm^2)		31.2 ± 21.7	26.9	15.7	41.5
CAK (mGy)		1135 ± 939	891	526	1461
Fluoroscopy CAK (mGy)		494 ± 595	325	174	609
Cine CAK (mGy)		641 ± 454	539	324	861
Acquisition duration (min)		13.6 ± 9.3	11.7	7.7	16.3
Fluoroscopy time (min)		12.4 ± 9	10.6	6.7	15.1
Cine time (min)		1.2 ± 0.5	1.1	0.8	1.4
Number of cine frames		1039 ± 474	962	729	1245

CAG- Coronary Angiography, DAP- Dose Area Product, CAK- Cumulative Air Kerma.

Table 4:

Variables	'β'	SE	95% CI	'p'-value
Gender: male vs female	1.3311	1.04	(1.22-1.43)	<0.001
BMI (kg/m^2)	1.0300	1.00	(1.02-1.04)	<0.001
Procedure Type: PCI vs CAG+PCI	0.9205	1.04	(0.95-0.99)	<0.001
Fluoroscopy Time (min)	1.0276	1.00	(1.02-1.03)	<0.001
Number of cine frames	1.0006	1.00	(1.00-1.00)	<0.001
Fluoroscopy Setting				0.023
7.5fps RDL+ Low	0.6107	1.05	(0.56-0.67)	<0.001
15fps RDL+ Normal	1.6620	1.11	(1.37-2.04)	<0.001
15fps Smart IQ Low	0.9418	1.15	(0.71-1.24)	0.667
15fps Smart IQ Normal	1.3825	1.08	(1.18-1.61)	<0.001
Cine Setting				<0.001
15fps IQ Standard Low	0.6157	1.34	0.35-1.34)	0.096
15fps RDL+ Low	0.6480	1.08	(0.56-1.08)	<0.001
15fps RDL+ Normal	1.0367	1.13	(0.91-1.13)	0.769

CAG- Coronary Angiography, PCI- Percutaneous Coronary Intervention, BMI- Body Mass Index.Beta coefficients (β) are given after re-transformation [exp(beta coefficient)] to describe the relative influence of each variable.

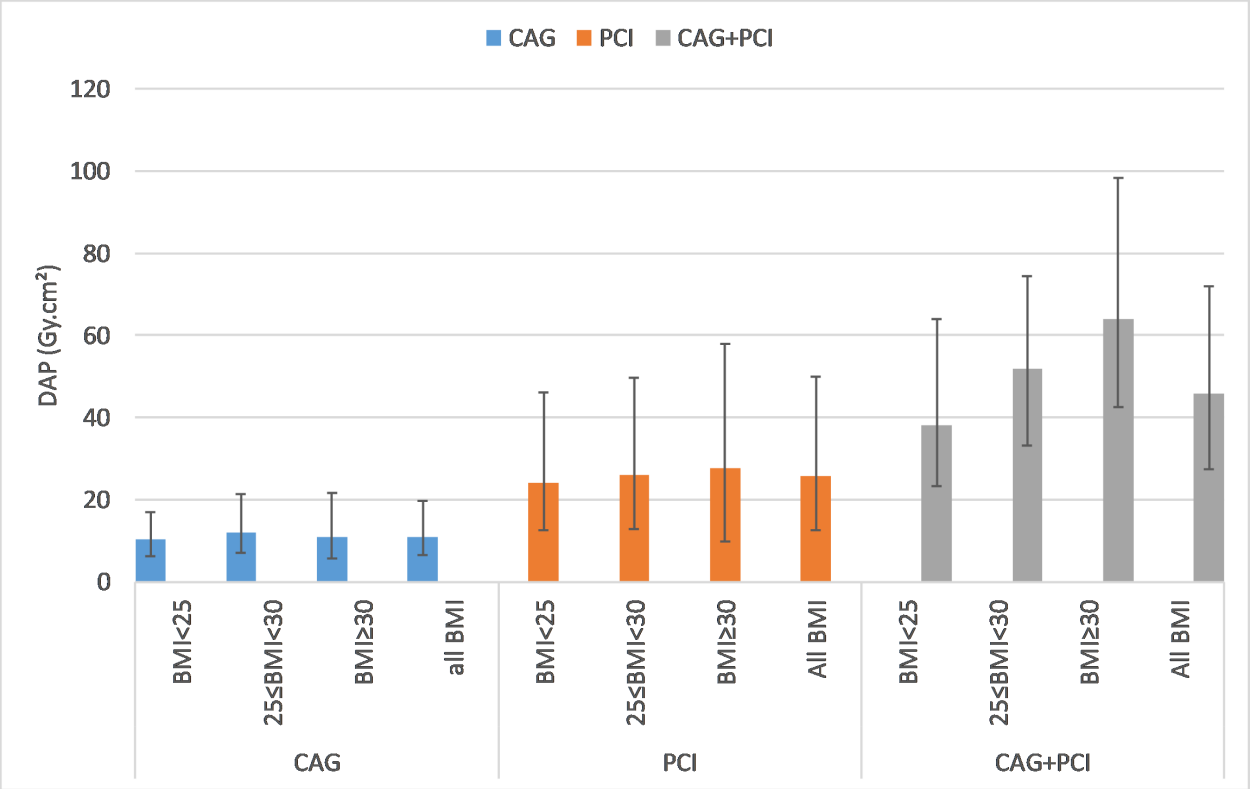

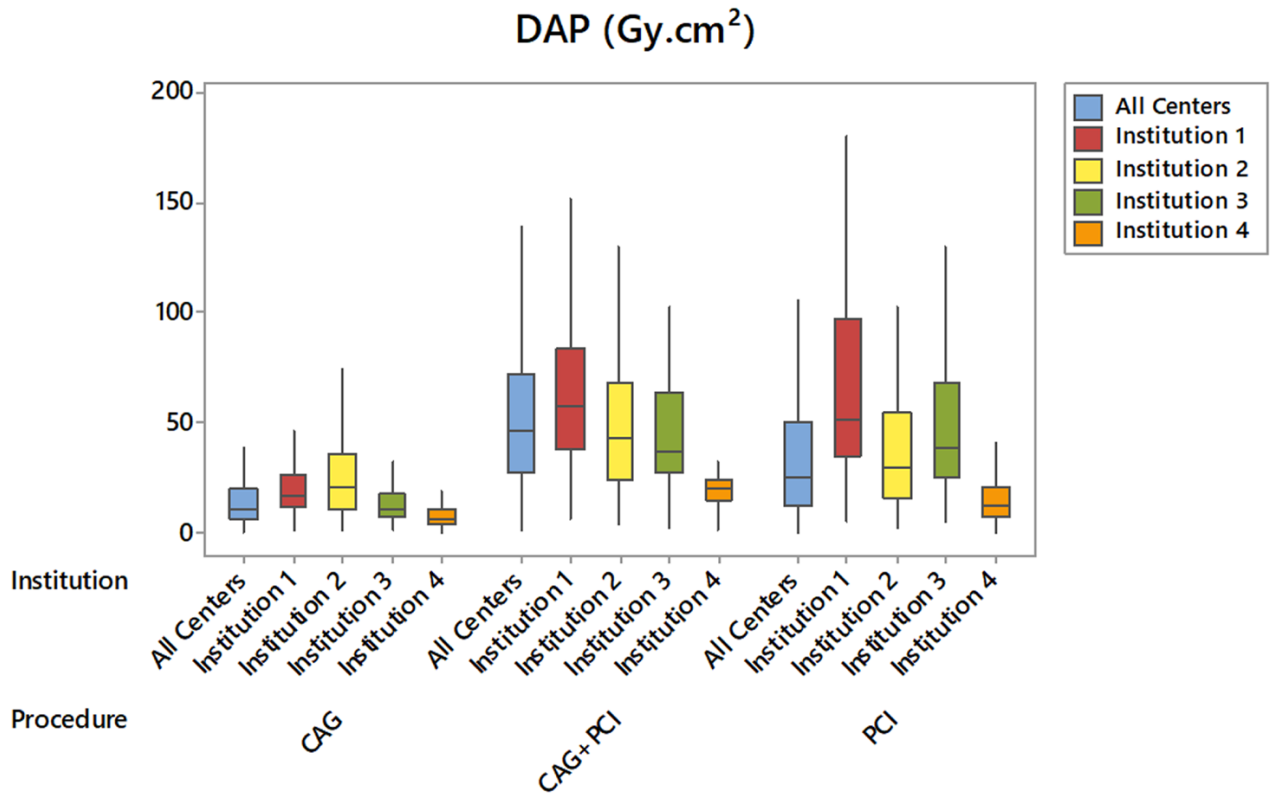

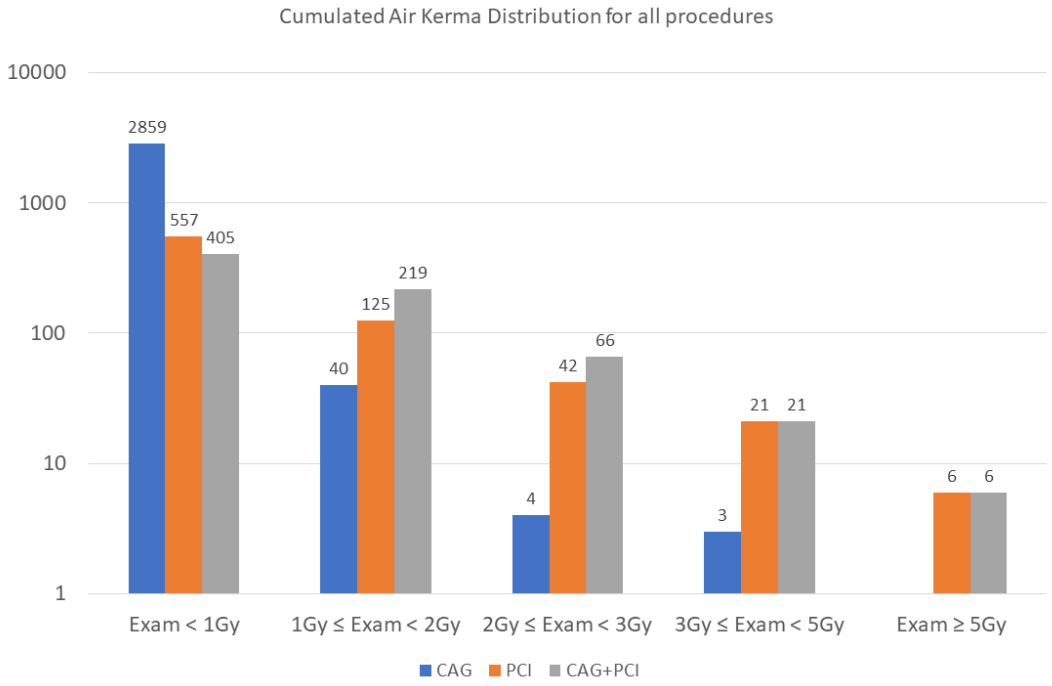

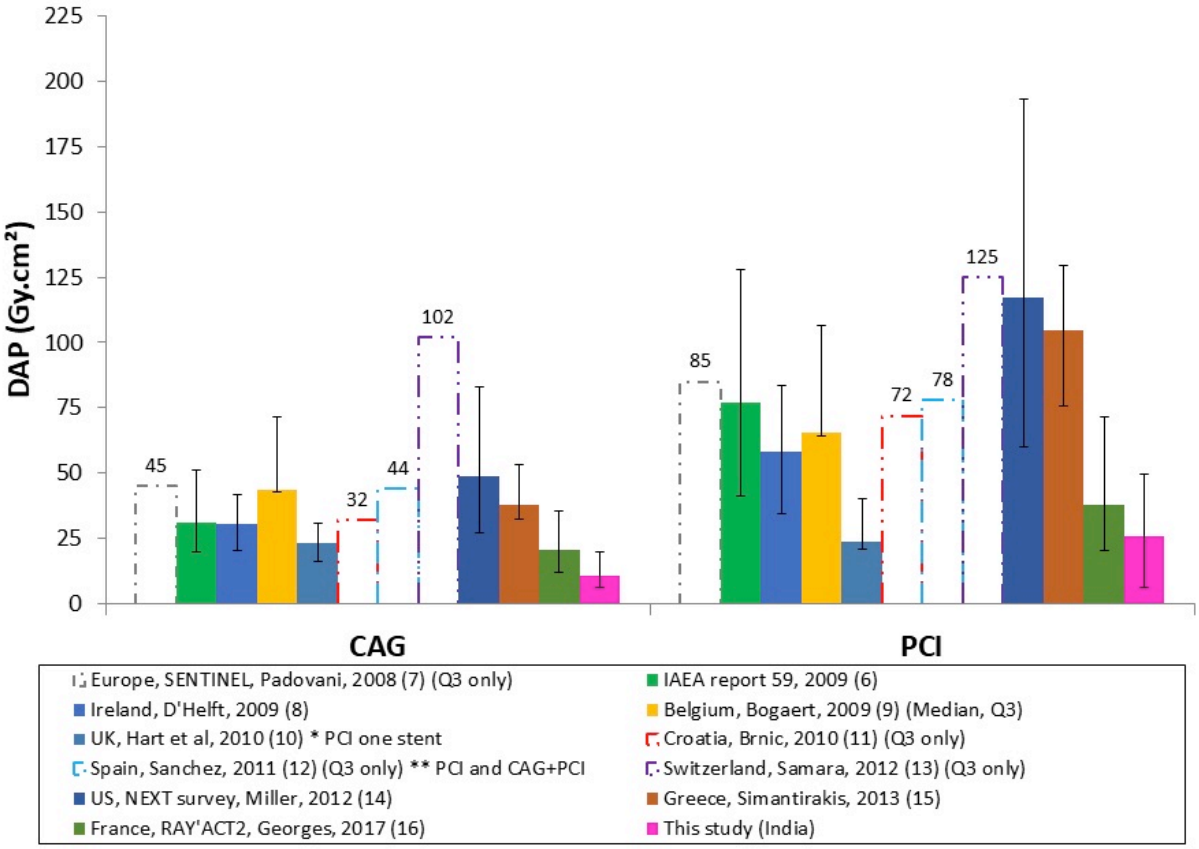

Supplementary data legends:

Supplementary Table 1: Sites Equipment and preferred acquisition protocol configurations.

Supplementary Table 2: Comparison with International References.

Supplementary Table 3: Comparison with recent literature data.

Supplementary Table 1: **Sites Equipment and preferred acquisition protocol configurations.**

Institutions	Equipments	Installed	Acquisition protocol configurations	
			Fluoroscopy	**Cine angiography**
1	Innova 2100-IQ	2011	15 frame/s RDL+ Normal	15 frame/s RDL+ Normal
	Innova 2100-IQ	2012	15 frame/s RDL+ Normal	15 frame/s RDL+ Normal
2	Innova IGS 520	2015	• Low dose protocol: 15 frame/s RDL+ Low • Improved Image Quality protocol: 15 frame/s Smart IQ Normal	• Low dose protocol: 15 frame/s RDL+ Low • Improved Image Quality protocol: 15 frame/s IQ standard Normal
3	Innova IGS 520	2012	15 frame/s RDL+ Low	15 frame/s RDL+ Low
4	Innova IGS 520	2013	7.5frame/s RDL+ Low	15 frame/s RDL+ Low

RDL- Radiation Dose Limit.

Supplementary Table 2: Comparison with International References.

Reference	Year	N	BMI (kg/m²)	Total DAP (Gy.cm²)	P-Value	CAK (mGy)	P-Value	FT (min)	P-Value	Number of exp. frames	P-Value	Site/country
CAG												
This Study – CAG	**2017**	**2906**	**26.3 ± 4.3**	**10.9 (6.4-19.6)**	**-**	**185 (112-325)**	-	**2.4 (1.3-4.5)**	**-**	**427 (320-552)**	**-**	**4 hospitals, India**
Europe (SENTINEL) (7)	2008	672	na	45[d]	-	na	-	6.5[d]	-	700[d]	-	9 centers, Europe
IAEA (6)	2009	2265	Height (m): 1.68[a]; Weight (kg): 78.5[a]	31.8 (20.8-49.4)	<0.001	700 (500-1000)	<0.001	5 (3-9)	<0.001	810 (655-1003)	<0.001	7 centers
Ireland (8)	2009	967	na	30.6 (20.2-41.7)	<0.001	na	-	na	-	na	-	14 hospitals, Ireland
Belgium (9)	2009	200	27[a] (19–49)[c]	43.8 (na-71.3)	<0.001	na	-	na	-	na	-	8 hospitals, Belgium
UK (10)	2009	na	Weight (kg): 75-85[c]	29[c]	-	na	-	4.5[c]	-	na	-	110 centers, UK
Croatia (11)	2010	138	28.2 (18.6-37.2)	25.3[a] (na-32)	<0.001	na	-	5.5[a] (na-6.6)	<0.001	554[a] (na-610)	<0.001	4 centers, Croatia
Spain (12)	2011	na	na	44[d]	-	na	-	8.0[d]	-	869[d]	-	6 hospitals, Spain
Switzerland (13)*	2012	311	na	87[a] (na-102)	<0.001	na	-	3.2[a] (na-10)	1.000	1039[a] (na-1549)	<0.001	23 centers, Switzerland
United States (NEXT Survey) (14)	2012	1326	na	46.2 (27.0-83.0)	<0.001	680 (440-1180)	<0.001	2.7 (1.8-5.4)	<0.001	na	-	United States
Greece (15)	2013	2572	na	37.9 (32.5-53.3)	<0.001	na	na	5.4 (4.1-5.7)	<0.001	na	-	26 centers, Greece
France, RAY'ACT-2 (16)	2016	51229	26.8 (24.2–30.1)	20.8 (11.8–35.7)	<0.001	294 (164–498)	<0.001	3.3 (2.1–5.7)	<0.001	404 (284–566)	1.000	61 centers, France
PCI												
This Study – PCI	**2017**	**750**	**26.0 ± 4.1**	**25.7 (12.5-49.8)**	**-**	**533 (243-1020)**	**-**	**11.4 (7.1-18.2)**	**-**	**738 (520-1128)**	**-**	**4 hospitals, India**
Europe (SENTINEL) (7)	2008	662	na	85[d]	-	na	-	15.5[d]	-	1000[d]	-	9 centers, Europe
IAEA (6)	2009	1027	Height (m): 1.68[a]; Weight (kg): 77.4[a]	53.3 (29.9-98.4)	<0.001	1900 (1100-3000)	<0.001	12 (7-20)	0.0772	881 (527-1465)	<0.001	

Ireland (8)	2009	463	na	58.1 (34.3-83.6)	<0.001	na	-	na	-	na	-	14 hospitals, Ireland
Belgium (9)	2009	118	28[a] (20–47)[c]	65.4 (na-106.6)	<0.001	na	-	na	-	na	-	8 hospitals, Belgium
UK (10)**	2009	na	Weight: 75-85[c] kg	50[e]	-	na	-	13.0[e]	-	na	-	28 centers, UK
Croatia (11)	2010	151	28.4 (18.6-38.9)	55.2[a] (na-72)	<0.001	na	-	15.5[a] (na-19)	<0.001	1067 (na-1270)	<0.001	4 centers, Croatia
Spain (12)***	2011	na	na	78[d]	-	na	-	22.0[d]	-	1762[d]	-	6 hospitals, Spain
Switzerland (13)	2012	119	na	91[a] (na-125)	<0.001	na	-	14[a] (na-19)	0.584	1277[a] (na-1837)	<0.001	23 centers, Switzerland
United States (NEXT Survey) (14)	2012	144	na	99.3 (60.0-193.0)	<0.001	1610 (1000-3120)	<0.001	10.1 (6.8-18.5)	1.000	na	-	United States
Greece (15)	2013	1899	na	104.7 (75.8-129.3)	<0.001	na	-	13.8 (11.0-17.8)	<0.001	na	-	25 centers, Greece
France, RAY'ACT-2 (16)	2016	6743	26.8 (24.2–30.1)	38.0 (20.3–71.4)	<0.001	668 (351–1285)	<0.001	9.8 (5.7–16.8)	1.000	537 (339–788)	1.000	61 centers, France
CAG +PCI												
This Study – CAG+PCI	**2017**	**715**	**25.1 ± 3.5**	**45.8 (27.3-72.0)**	**-**	**891 (526-1461)**	**-**	**10.6 (6.7-15.1)**	-	**962 (729-1245)**	**-**	**4 hospitals, India**
IAEA (6)	2009	817	Height (m): 1.69[a]; Weight (kg): 82.3[a]	92.9 (59.1-138.3)	<0.001	1900 (1300-2700)	<0.001	15 (10-24)	<0.001	1468 (1174-1976)	<0.001	7 centers
Ireland (8)	2009	134	na	77.1 (50.2-106.7)	<0.001	na	-	na	-	na	-	14 hospitals, Ireland
United States (NEXT Survey) (14)	2012	528	na	111.8 (73.0-199.0)	<0.001	1780 (1200-3000)	<0.001	10.8 (7.3-18.1)	0.1309	na	-	United States
France, RAY'ACT-2 (16)	2016	35479	26.8 (24.2–30.1)	46.4 (26.9–78.7)	0.3268	757 (433–1285)	1.000	9.8 (6.4–15.2)	0.9989	710 (501–991)	1.000	61 centers, France

Note. Radiation data values are given as median (IQR) and BMI as mean ± Standard Deviation; unless otherwise indicated.
FT fluoroscopy time; DAP dose area product; CAK cumulative air kerma.
[a] Mean; [b] third quartile; [c] Range; [d] Dose Reference Level (based on 75th Percentile); [e] 75th percentile of means of the rooms; na not available; * Data normalized to average size patient (height 1.70m and weight 70kg); **Single stent PCI; *** PCI and CAG+PCI combined
p-value from non-parametric 1 sample sign test when referenced data provided as median and 1 sample t test when referenced data provided as mean.

Supplementary Table 3: Comparison with recent literature data.

Author	Year	N	BMI (kg/m²)	Total DAP (Gy.cm²)	P-Value	CAK (mGy)	P-Value	FT (min)	P-Value	Number of exp. frames	P-Value	Site/country	Details
CAG													
This Study – CAG	**2017**	**2906**	**26.3 ± 4.3**	**10.9 (6.4-19.6)**	**-**	**185 (112-325)**	**-**	**2.4 (1.3-4.5)**	**-**	**427 (320-552)**	**-**	**India (4 sites)**	
Abdelaal (23)	2014	89	28.6 ± 5.6	23 (15–31)	<0.001	na	-	2.6 (1.8–4.5)	<0.001	na	-	Canada	1.Transradial access 2.Reduced Fluoro framerate group (7.5fps)
Eloot (24)	2015	35	26.1 (23.8–31.0)	8.8 (6.33-17.6)	1.000	na	-	2.9 (1.9-5.0)	<0.001	na	-	Belgium	Novel Imaging system
Bracken (25)	2015	88	26.8 (22.8-32.3)	20.1 (12.3-36.5)	<0.001	197 (124-360)	<0.001	5.5 (3.7-9.2)	<0.001	517 (337 - 657)	<0.001	USA	Dose reduction technology
Livingstone (26)	2015	222	na	24.4 ± 14.5	<0.001	na	-	3.9[a] (0.5-10.4)[c]	0.143	na	-	India	Flat panel detector
Nakamura (27)	2015	307	23.2 ± 3.7	52.0 (na-80.4)	<0.001	na	-	9.9 (na - 18.7)	<0.001	2510 (na-3378.5)	<0.001	Japan	Upgraded Imaging system
Varghese (28)	2016	140	25[a]	14.0[a] (4.0-37.6)[c]	1.000	231[a] (74-622)[c]	1.000	3.2[a] (0.5-10.5)[c]	1.000	525[a] (246-1063)[c]	<0.001	India	Novel imaging system
Ryckx (29)	2016	877	na	na (na-69)	na	na (na-41)	-	na (na-8.9)	-	na	-	Switzerland	
Didier (30)	2016	598	26.8 ± 5.0	27.1 (16.7-41.6)	<0.001	336 (207-507)	<0.001	na	-	na	-	France	Cardiovascular automated reduction x-ray system
Hansen (31)	2016	130	Height (m): 1.69[a] Weight (kg): 64.7[a]	44.0 (28.6-69.6)	<0.001	621 (405-909)	<0.001	8.5[a]	<0.001	na	-	USA	Reduced Fluoro framerate group (7.5fps)
Jurado-Roman (32)	2016	558	28.6 ± 5.7	43.3 ± 40.1	<0.001	na	-	8.0 ± 7.0	<0.001	na	-	Spain	Radiation Reduction Protocol
Wilson (33)	2016	617	27.6 ± 6.0	50.4 ± 37.0	<0.001	440 ± 376	<0.001	3.3 ± 3.0	1.000	na	-	Australia	

Author	Year	N	BMI (kg/m²)	Total DAP (Gy.cm²)	P-Value	CAK (mGy)	P-Value	FT (min)	P-Value	Number of exp. frames	P-Value	Site/country	Details
Kastrati (34)	2016	397	28.8 ± 5.0	9.8 ± 9.8	1.000	na	-	4.7 ± 4.4	<0.001	na	-	Germany	Cohort Noise Reduction technoogy
Tarighatnia (35)	2016	37	na	17.3[a] (6.3-36.6)[c]	<0.001	234[a] (75-526)[c]	1.000	3.3[a] (0.8-9.5)[c]	1.000	na	-	Iran	Transradial access
Tarighatnia (35)	2016	37	na	19.5[a] (6.8-107.8)[c]	<0.001	211[a] (87-433)[c]	1.000	1.8[a] (0.5-8.4)[c]	1.000	na	-	Iran	Transfemoral access
Sinha (36)	2016	921	23.8 ± 3.6	22.3 ± 3.46	<0.001	na	-	2.8 ± 1.3	1.000	na	-	India	Transfemoral access
Sinha (36)	2016	1076	24.9 ± 2.8	24.2 ± 4.21	<0.001	na	-	2.5 ± 1.2	1.000	na	-	India	Transradial access
Uniyal (37)	2017	40	Weight: 74 ± 9.5 kg	21.1 ± 19.8	<0.001	420 ± 373	<0.001	2.4 ± 2.9	1.000	360 ± 129	1.000	India	
Balter (38)	2017	307	na	34.0 (23.0-54.0)	<0.001	350 (230-540)	<0.001	6.4 (3.8-10.5)	<0.001	na	-	USA	Third Imaging configuration
Ordiales (39)	2017	195	29.9 ± 5.1	18.5 (na-na)	<0.001	220 (na-na)	<0.001	2.70 (na-na)	<0.001	449 (na-na)	<0.001	Spain	Period 5 Optimized Imaging protocol
Gunja (40)	2017	na	na	30.2 ± 23.5	<0.001	na	-	7.7 ± 5.9	<0.001	na	-	USA	Novel imaging system
Faroux(41)	2017	508	28.0 ± 5.4	12.4 ±13.0	1.000	176 ± 130	1.000	na	-	na	-	France	Novel imaging system
Sciahbasi (42)	2017	7631	28 ± 5	26 (16-46)	<0.001	na	-	3.0 (1.9-5.4)	<0.001	na	-	Italy, Germany, USA	Italy (4 sites), Germany (1), USA (1)
PCI													
This Study – PCI	**2017**	**750**	**26.0 ± 4.1**	**25.7 (12.5-49.8)**	**-**	**533 (243-1020)**	**-**	**11.4 (7.1-18.2)**	**-**	**738 (520-1128)**	**-**	**4 hospitals, India**	
Abdelaal (23)	2014	93	28.6 ± 5.6	55 (35–83)	<0.001	na	-	9.2 (5.7–15.0)	1.000	na	-	Canada	1. Transradial Access 2.Reduced Fluoro framerate group (7.5fps)
Nakamura (27)	2015	127	23.2 ± 3.7	85.8 (na-144.3)	<0.001	na	-	32 (na-52.9)	<0.001	3768 (na-6025)	<0.001	Japan	Upgraded Imaging system
Bracken (25)	2015	47	27.7 (25.1-32.8)	83.8 (47.5-118.5)	<0.001	980 (627.5-1370.5)	<0.001	17.7 (13.1-27.7)	<0.001	1045 (877-1387)	<0.001	USA	Dose reduction technology

Author	Year	N	BMI (kg/m²)	Total DAP (Gy.cm²)	P-Value	CAK (mGy)	P-Value	FT (min)	P-Value	Number of exp. frames	P-Value	Site/country	Details
Livingstone (26)	2015	75	na	63.6 ± 39.4	<0.001	na	-	12.49[a] (3.51-25.5)[c]	1.000	na	-	India	Flat panel detector
Sciahbasi (42)	2016	5465	27 ± 4	66 (40-109)	<0.001	na	-	10.4 (7.0-16.5)	0.9988	na	-	Italy, Germany, USA	Italy (4 sites), Germany (1), USA (1)
Kastrati (34)	2016	208	29.4 ± 6.7	24.8 ± 19.8	1.000	na	-	11.1 ± 7.1	1.000	na	-	Germany	Cohort Noise Reduction technology
Tarighatnia (35)	2016	74	na	43.4[a] (5.2-118.4)[c]	0.041	734[a] (86-2336)[c]	0.996	8.4[a] (1.0-21.1)[c]	1.000	na	-	Iran	Transradial access
Tarighatnia (35)	2016	74	na	52.8[a] (4.8-194.5)[c]	<0.001	855[a] (93-3464)[c]	0.188	8.8[a] (0.9-37.1)[c]	1.000	na	-	Iran	Transfemoral access
Jurado-Roman (32)	2016	160	28.6 ± 5.7	123.7 ± 91.6	<0.001	na	-	21.3 ± 14.6	<0.001	na	-	Spain	Radiation Reduction Protocol
Hansen (31)	2016	146	Height (m): 1.72[a]; Weight (kg): 64.8[a]	106.5 (67.5-143.1)	<0.001	1459 (947-6589)	<0.001	17.8[a]	<0.001	na	-	USA	Reduced Fluoro framerate group (7.5fps)
Didier (30)	2016	130	26.8 ± 4.3	26.6 (12.7-50.7)	0.4564	400 (188-840)	1.000	na		na	-	France	Cardiovascular automated reduction x-ray system
Ichimoto (43)	2017	57	29.3 ± 6.3	17.8 ± 13	1.000	205 ± 141	1.000	5.5 ± 3.0	1.000	na	-	USA	PCI with Dose Tracking System
Uniyal (37)	2017	50	Weight:77 ± 11 kg	97.0 ± 61.7	<0.001	2028 ± 1322	<0.001	15.7 ± 10.0	<0.001	888 ± 384	0.434	India	
Boland (44)	2016	30	Weight: 83 ± 16 kg	55.6 (27.0-91.5)	<0.001	551 (310-998)	0.2216	7.3 (5.4-11.0)	1.000	na	-	Australia	Novel imaging system
Chon (45)	2017	152	24.6 ± 3.3	123.4 ± 53.7	<0.001	1634 ± 718	<0.001	16.2 ± 8.8	<0.001	na	-	Korea	Radiation Reduction Protocol
Faroux (46)	2017	807	28.0 ± 5.4	19.94 ± 24.9	1.000	na	-	9.7 ± 11.2	1.000	na	-	France	Include only period 2 (2016)
Gislason-Lee (47)	2017	131	na	22.9 (na-na)	0.9844	na	-	12.5 (na-na)	<0.001	na	-	UK	Novel imaging system
Gunja (40)	2017	na	na	73.6 ± 59.3	<0.001	na	-	20.1 ± 12.6	<0.001	na	-	USA	Novel imaging system

Author	Year	N	BMI (kg/m²)	Total DAP (Gy.cm²)	P-Value	CAK (mGy)	P-Value	FT (min)	P-Value	Number of exp. frames	P-Value	Site/country	Details
Ordiales (39)	2017	90	29.9 ± 5.1	38.3 (na-na)	<0.001	473 (na-na)	0.9844	8.9 (na-na)	1.000	664 (na-na)	1.000	Spain	Period 5; Optimized imaging protocol
CAG+PCI													
This Study – CAG+PCI	**2017**	**715**	**25.1 ± 3.5**	**45.8 (27.3-72.0)**	**-**	**891 (526-1461)**	**-**	**10.6 (6.7-15.1)**	**-**	**962 (729-1245)**	**-**	**4 hospitals, India**	
Didier (30)	2016	228	26.7 ± 4	45.0 (26.6-75.1)	0.5888	672 (353-1082)	1.000	na	-	na	-	France	Cardiovascular automated reduction x-ray system
Ryckx (29)	2016	1527	na	na (na-150)	-	na (na-2014)	-	na (na-18.1)	-	na	-	Switzerland	
Jurado-Roman (32)	2016	442	28.6 ± 5.7	123.9 ± 48.8	<0.001	na	-	16.1 ± 9.4	<0.001	na	-	Spain	Radiation Reduction Protocol
Tarighatnia (35)	2016	52	na	56.5[a] (17.8-136.1)[c]	0.422	891[a] (251-2324)[c]	1.000	11.2[a] (3.5-25.7)[c]	1.000	na	-	Iran	Transradial access
Tarighatnia (35)	2016	52	na	67.4[a] (17.5-186.1)[c]	<0.001	1041[a] (301-2545)[c]	0.996	10.8[a] (2.4-42.3)[c]	1.000	na	-	Iran	Transfemoral access
Faroux (46)	2017	441	28.0 ± 5.4	26.7 ±20.0	1.000	471 ± 130	1.000	na	-	na	-	France	Novel imaging system

Note. Radiation data values are given as median (IQR) and BMI as mean ±Standard Deviation; unless otherwise indicated.
FT fluoroscopy time; DAP dose area product; CAK cumulative air kerma.
[a] Mean; [b] third quartile; [c] Range; [d] Dose Reference Level (based on 75th Percentile); na not available.

p-value from non-parametric 1 sample sign test when referenced data provided as median and 1 sample t test when referenced data provided as mean

AsiaIntervention

Official Journal of the Asian Pacific Society of Interventional Cardiology (APSIC) and the Interventional Cardiology Foundation of India (ICFI)

www.asiaintervention.org

Title: **A Novel Technique: Passing Through Bulky Calcified Nodules Projecting Into a Popliteal Artery Using a TruePath Crossing Device.**

Authors: Yuji Nishimoto, M.D; Rei Fukuhara, M.D; Masanao Toma, M.D; Yukihito Sato, M.D, PhD

Manuscript number: AIJ-D-19-00020

Manuscript submission date: 01 May 2019

Revisions received: 18 July 2019

Accepted date: 04 March 2020

A Novel Technique: Passing Through Bulky Calcified Nodules Projecting Into a Popliteal Artery Using a TruePath Crossing Device

Authors: Yuji Nishimoto[1], MD; Rei Fukuhara[1], MD; Masanao Toma[1], MD; Yukihito Sato[1], MD, PhD

[1]Department of Cardiology, Hyogo Prefectural Amagasaki General Medical Center, Amagasaki, Japan.

Short running title: A Novel CanPath Technique

Corresponding author: Yuji Nishimoto, MD

Department of Cardiology, Hyogo Prefectural Amagasaki General Medical Center

2-17-77 Higashinaniwa-cho, Amagasaki 660-8550, Japan

E-mail: yuji.nishimoto@gmail.com

Conflict of interest statement: The authors have no conflicts of interest to declare.

Key words: Femoro-popliteal disease; Calcified stenosis; Atherectomy; Imaging modalities

An 84-year-old man presented with eccentric severe stenosis of the left popliteal artery (**Panels A and A'**). After crossing the lesion with a tapered tip 1g 0.014-inch guidewire, and dilatation with a 1.5 mm balloon, intravascular ultrasound (IVUS) demonstrated eccentric bulky calcified nodules (**Panels B and B'**). A conventional bigger balloon dilatation in this lumen would have caused an under-expansion, and therefore, we tried a novel CanPath technique: passing through bulky **Ca**lcified **n**odules using a True**Path** (Boston Scientific, Natick, Massachusetts), which consisted of a 0.018-inch wire with a rotating distal diamond-coated tip[1]. The CanPath technique, which is indicated for the longitudinal penetration of calcified nodules using the TruePath under fluoroscopy guidance, could create an intraluminal pathway. After performing this technique (**Panels C and C'**), IVUS demonstrated that the wire was located in the middle of the calcification (**Panels D and D'**;). After dilatation with a 4.0 mm cutting balloon, the IVUS revealed some cracks in the calcification (**Panels E and F**). Subsequent to dilatation with a 5.0 mm balloon, the final angiogram and IVUS demonstrated that the lesion had become well-expanded without a stent implantation (**Panels G and H**;). Freedom from any target vessel revascularization has lasted for 12 months.

The main advantage of the CanPath technique was the increased deliverability of the 0.014-inch system because of the 0.018-inch debulking effect, which should be investigated further. This technique has the limitation of its cost, which requires the TruePath and IVUS.

Acknowledgement: We would like to express our gratitude to Mr. John Martin for his grammatical assistance.

References

1. Bosiers M, Diaz-Cartelle J, Scheinert D, Peeters P, Dawkins KD. Revascularization of lower extremity chronic total occlusions with a novel intraluminal recanalization device: results of the ReOpen study. *J Endovasc Ther.* 2014;21:61-70.

Figure Legends

Figure. Procedural Images of the Angiogram and IVUS

Pre-procedural angiography reveals an eccentric severe stenosis with bulky calcified nodules projecting into the popliteal artery (**A and A'**, **white** color indicates calcification). After crossing the lesion with a tapered guidewire, and dilatation with a 1.5 mm balloon, the IVUS demonstrates eccentric bulky calcified nodules (**B and B'**, **white** color indicates calcification). After crossing the calcified nodules using the TruePath (**C and C'**), the IVUS shows the wire in the middle of the calcification (**D and D'**, **white** color indicates calcification). After dilatation with a 4.0 mm cutting balloon (**E**), the IVUS shows some cracks in the calcification (**F**, **white arrowheads** indicate cracks). The final angiogram and IVUS demonstrate the lesion has become well-expanded (**G and H**). IVUS=intravascular ultrasound.

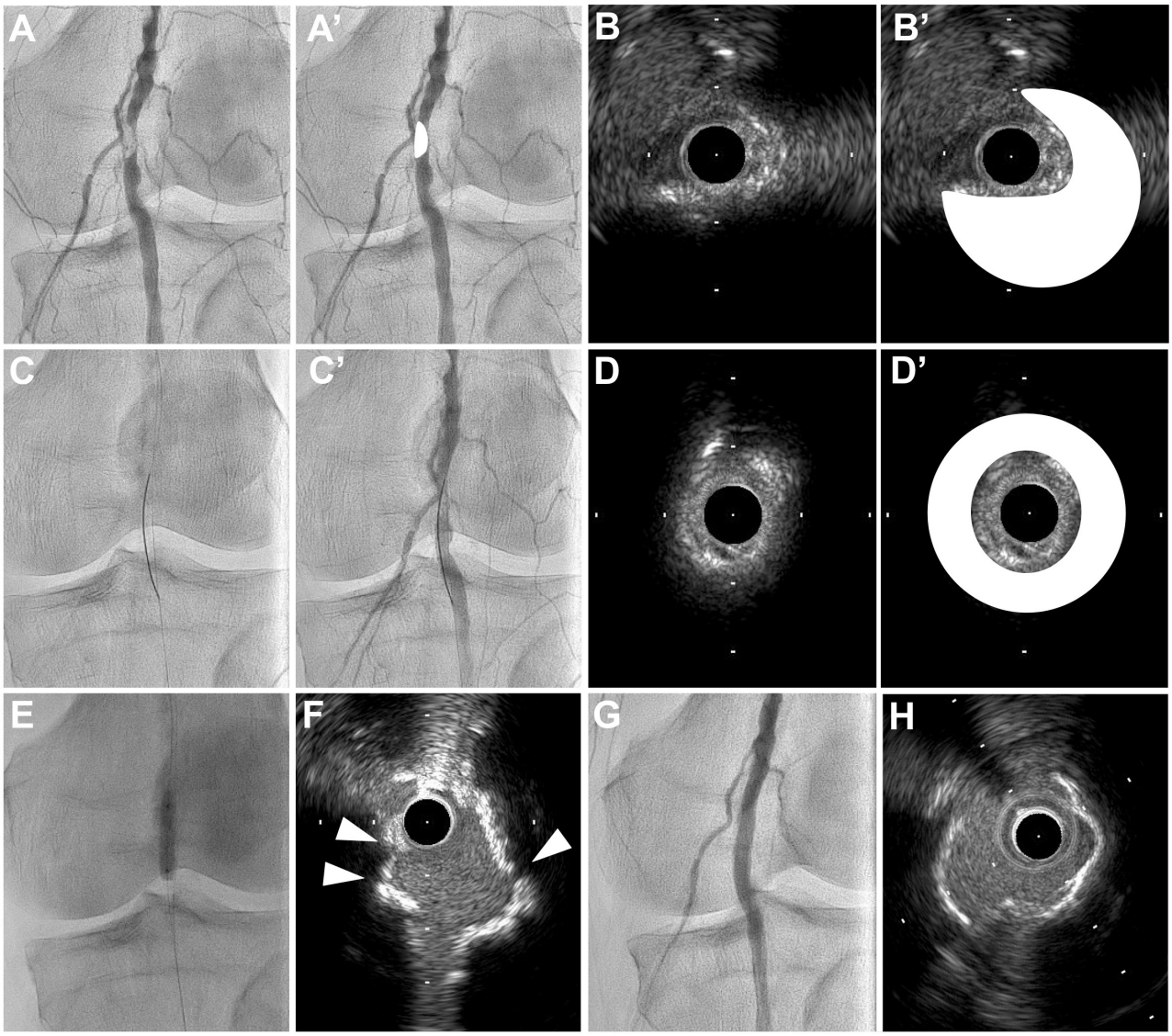

AsiaIntervention

Official Journal of the Asian Pacific Society of Interventional Cardiology

(APSIC) and the Interventional Cardiology Foundation of India (ICFI)

www.asiaintervention.org

Title: Successful management of shortening of overlapping segment and subsequent restenosis at the gap between two 2nd-generation stents in the left anterior descending artery.

Authors: Nozomi Kotoku, M.D, PhD; Yuki Ishibashi, M.D, PhD; Yasuhiro Tanabe, M.D, PhD; Akiyuki Kotoku, M.D, PhD; Hiroshi Yamazaki, M.D; Shingo Kuwata, M.D, PhD; Takanobu Mitarai, M.D; Kazuaki Okuyama, M.D, PhD; Kihei Yoneyama, M.D, PhD; Takumi Higuma, M.D, PhD; Tomoo Harada, M.D, PhD; Yoshihiro J Akashi, M.D, PhD

Manuscript number: AIJ-D-18-00060

Manuscript submission date: 09 December 2018

Revisions received: 14 May 2019, 08 June 2019, 06 July 2020

Accepted date: 04 March 2020

Successful management of shortening of overlapping segment and subsequent restenosis at the gap between two 2nd-generation stents in the left anterior descending artery

Nozomi Kotoku[1], MD, PhD; Yuki Ishibashi[1], MD, PhD; Yasuhiro Tanabe[1], MD, PhD;

Akiyuki Kotoku[2], MD, PhD; Hiroshi Yamazaki[1], MD; Shingo Kuwata[1], MD, PhD;

Takanobu Mitarai[1], MD; Kazuaki Okuyama[1], MD, PhD; Kihei Yoneyama[1], MD, PhD;

Takumi Higuma[1], MD, PhD; Tomoo Harada[1], MD, PhD; Yoshihiro J Akashi[1], MD, PhD

1. Division of Cardiology, Department of Internal Medicine. St. Marianna University School of Medicine, Kawasaki, Kanagawa, Japan

2. Division of Radiology, St. Marianna University School of Medicine, Kawasaki, Kanagawa, Japan

Corresponding Author: Yuki Ishibashi, M.D, PhD, FESC.

Division of Cardiology, Department of Internal Medicine,

St. Marianna University School of Medicine

2-16-1, Sugao, Miyamae-ku, Kawasaki-City, Kanagawa 216-8511, Japan

E-mail: ishibashi15@marianna-u.ac.jp

Short title: Shortening of overlapping segment

Classifications: MSCT; Optical coherence tomography; Drug-eluting stent

Conflict of interest statement: The authors have no conflicts of interest to declare.

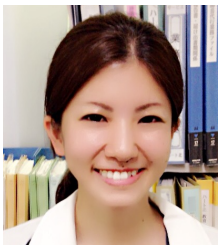

A 74-year-old man with silent myocardial ischemia was taken percutaneous coronary intervention to overlap with a 3.0 x 38 everolimus-eluting stent (EES; Xience Alpine®) and a 2.5 x 16 everolimus-eluting platinum chromium stent (PtCr-EES; Promus premier®) in the mid-portion of left anterior descending artery (LAD). Nine months after the stent implantation, the patient was readmitted to our hospital due to exertional chest pain. Coronary angiography (CAG) revealed significant restenosis at the mid-portion of the tortuous LAD segment.. Coronary computed tomography showed the distal stent fracture and shortening of overlapping segment. Optical coherence tomography (OCT) was also performed for the detailed examination. No significant luminal narrowing of the fractured segment was found (OCT, 3.97 mm^2); whereas the minimum lumen area of the gaps between the two stented segment was 1.07 mm^2 (OCT). A 3.0 x 12 PtCr-EES was successfully overlapped the gap segment, from the proximal to the previously overlapped segment. Follow-up CAG at 9 month after the 2nd procedure resulted in no clinical events.

In the present case, the quantitative CAG analysis suggested that shortening of overlapping segment and the gap between the two 2nd-generation DESs might

occur due to 1) straightening vessel curves after metallic stent implantation and 2) geometric changes caused by stent placement **(Figure 1)**.

After created the gap between the two 2nd-generation DESs in the LAD caused by continuous stress during cardiac cycle, mechanical stress imposed on the stent edge would cause vessel wall injury and inflammation characterised by deposition of platelets and fibrin, as well as adhesions of circulating neutrophils and macrophages, which might lead to restenosis.

Previous studies reported that the PtCr-EESs with higher bending flexibility has greater fracture resistance against severer angulation ranges compared with the other 2nd generation drug-eluting stents. In this case, the PtCr-EES was thus selected for significant restenosis at the gap between the two metal stents.

Figure legends

Figure 1. Quantitative coronary angiography (QCA) showed the changes of angulation and curvature.

A) QCA before 1st procedure.

B) QCA after 1st procedure; straightening the vessel curves after metal stent implantation.

C) QCA before 2nd procedure. The angulation and curvature in C) were increased compared with those in B).

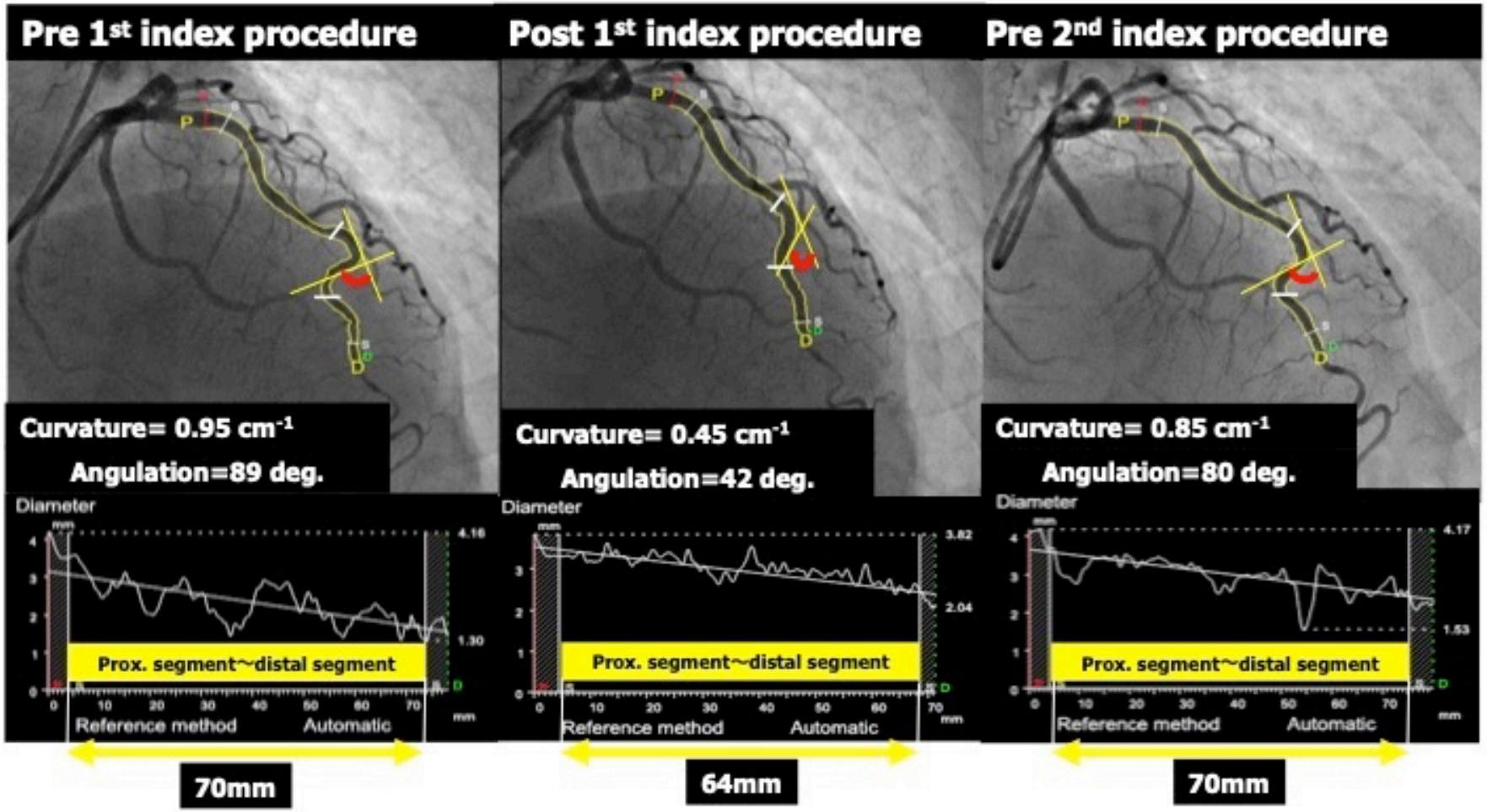

AsiaIntervention

Official Journal of the Asian Pacific Society of Interventional Cardiology

(APSIC) and the Interventional Cardiology Foundation of India (ICFI)

www.asiaintervention.org

Title: Impact of Transcatheter Aortic Valve Size on Leaflet Stresses: Implications for Durability and Optimal Grey Zone Sizing.

Authors: Yue Xuan, PhD; Danny Dvir, M.D; Andrew D. Wisneski, M.D; Zhongjie Wang, PhD; Jian Ye, M.D; Julius M. Guccione, PhD; Liang Ge, PhD; Elaine E. Tseng, M.D

Manuscript number: AIJ-D-19-00005

Manuscript submission date: 14 January 2019

Revisions received: 22 April 2019, 06 June 2019

Accepted date: 05 July 2019

Impact of Transcatheter Aortic Valve Size on Leaflet Stresses: Implications for Durability and Optimal Grey Zone Sizing

Yue Xuan[1], PhD, Danny Dvir[2], MD, Andrew D. Wisneski[1], MD, Zhongjie Wang[1], PhD, Jian Ye[3], MD, Julius M. Guccione[1], PhD, Liang Ge[1], PhD, Elaine E. Tseng[1], MD.

[1]Department of Surgery, University of California San Francisco and San Francisco VA Medical Centers, San Francisco, CA; [2]Division of Cardiology, University of Washington, Seattle, WA; [3]Division of Cardiovascular Surgery, St. Paul's Hospital and Vancouver General Hospital, Vancouver, BC, Canada.

Short running title: Transcatheter valve size impacts leaflet stresses

Corresponding Author:

Elaine E. Tseng, MD

Division of Cardiothoracic Surgery

UCSF Medical Center

500 Parnassus Ave., Suite 405W, Box 0118

San Francisco, CA, 94143-0118, USA.

Email: elaine.tseng@ucsf.edu

Presented at EuroPCR on May 17-20, 2016 in Paris, France.

Conflict of Interest Statement: Drs. Tseng and Ge are founders of ReValve Med, Inc. Drs. Dvir and Ye are consultants for Edwards Lifesciences. The remaining authors have no conflicts of interest to declare.

First author portrait:

Abstract

Aims: As indications for transcatheter aortic valve replacement (TAVR) continue to expand towards younger and lower-risk patients, durability becomes an increasingly important question. Durability decreases as leaflet stresses increase, but the impact of transcatheter heart valve (THV) size on stress is unknown. Patient annulus sizes can fall within "grey zones" between 2 TAVR sizes. Our aim was to examine the impact of balloon-expandable THV size on leaflet stresses.

Methods and Results: SapienXT 23mm, 26mm, and 29mm sizes (Edwards Lifesciences, Inc) underwent micro-computed tomography scanning to create THV computational models then loaded to systemic pressure using finite element software. THV leaflet maximum principal stresses were 1.69MPa (23mm), 1.70MPa (26mm), and 2.12MPa (29mm) at mean arterial pressure. For intermediate annulus sizes, undersizing the larger THV yielded lower leaflet stresses than oversizing the smaller THV.

Conclusions: Increasing THV size yielded greater leaflet maximum principal stresses, which could suggest a relationship between THV size and long-term durability.. For annulus "grey zones" sizes, undersizing the larger THV resulted in lower leaflet stresses than oversizing the smaller THV. These results may influence optimal device sizing, as THV durability remains an important, unanswered question.

Classifications: Aortic stenosis, Degenerative valve, Paravalvular leak, TAVI

Abbreviations:

TAVR = transcatheter aortic valve replacement

THV = transcatheter heart valve

SAVR = surgical aortic valve replacement

AS = aortic stenosis

FEA = finite element analyses

FE = finite element

mm = millimeter

kPa = kilopascal

MPa = megapascal

PVL = paravalvular leakage

LVOT = left ventricular outflow tract

Condensed abstract

Durability of bioprostheses is a complex interaction of patient factors and valve design, but is related to mechanical stresses on valve leaflets. Balloon-expandable transcatheter heart valves (THV) underwent micro-computed tomography to develop precise geometry of stent, Dacron, and leaflets for computational modeling. Dynamic finite element simulations to systemic pressure were performed to determine impact of THV size on leaflet stresses. Increasing THV size resulted in increased leaflet stresses, which may impact long-term durability. However, when annulus size fell within grey zones between two THV sizes, undersizing the larger THV resulted in lower leaflet stresses.

Introduction

Transcatheter aortic valve replacement (TAVR) has revolutionized treatment of severe aortic stenosis (AS) and expanded indications from inoperable and high-risk patients to intermediate- and potentially soon to low-risk patients[1-5]. Improving TAVR outcomes by reducing paravalvular leakage (PVL) has required optimal transcatheter heart valve (THV) sizing, which is primarily based on ECG-gated computed tomography angiography (CTA)[6-9]. Selection of the appropriate THV size to implant is based on aortic annulus sizing, which is dynamic dependent on timing of the cardiac cycle. Timing of CTA image acquisition during diastole vs systole impacts annulus size measurements, and systolic gating to measure maximum annulus area is primarily used for THV size selection[8]. Some patients' annulus sizing falls within areas of "grey zones" between two THV sizes, which can both be considered appropriate. Clinical decision-making is often guided by parameters such left ventricular outflow tract (LVOT) calcification and risk of annular rupture[10], anticipation of degree of PVL[6, 7, 9], sinus effacement, and sinotubular junction dimensions.

However, degree of THV under- or over-sizing, impacts the deployed THV shape and leaflet coaptation[11, 12]. Such changes in THV configuration can impact leaflet stresses. Prior THV biomechanical studies have suggested that greater leaflet stresses accelerate THV degeneration and limit long term durability[13-17]. There is no method to directly measure leaflet stresses, thus computational methods such as finite element analysis (FEA) are valuable for providing such data, which assess failure modes. Accurate finite element (FE) models require precise 3D geometry in zero-stress state, material properties, and physiologic loading conditions. Our previous FEA studies have determined THV leaflet stresses on specific sizes of first-[16], second-[17], and third-generation[15] SAPIEN,

Sapien XT, and Sapien 3 under quasi-static loading conditions based on micro-CT images. However, the impact of THV size on THV leaflet stresses is unknown. For each generation of Edwards balloon-expandable THV, there has existed "grey zones" where either of 2 sizes of THV are suitable. Thus, it is helpful to examine leaflet stresses of different sizes of THV and also to understand the impact of under- or oversizing THV within the annular "grey zones."

Edwards Sapien XT, a second-generation bovine pericardial balloon expandable valve, was designed with a cobalt-chromium stent with fewer rows and columns between the commissures compared to the first-generation SAPIEN allowing reduction in THV profile for smaller delivery systems[18]. In Sapien XT sizing chart, 23mm XT was optimal for annulus diameters of 19-22mm, and areas of 300-380mm^2, while 26mm XT was optimal for diameters of 23-25mm, and areas of 415-490mm^2. As such, a grey zone existed between diameters of 22-23mm, and areas of 380-415mm^2 in which either size 23mm or 26mm XT could be chosen for a given patient. Similarly, 29mm XT was optimal for annulus diameters of 26-28mm, and areas of 530-620 mm^2 [19]. Thus, between diameters of 25-26mm, and areas of 490-530mm^2, either 26mm or 29mm XT could be chosen for a patient. Choosing the smaller THV would result in THV oversizing (overexpansion of a smaller sized THV), while choosing the larger THV would result in THV undersizing (underexpansion of a larger sized THV). Based upon our availability of 3 sizes of commercial Sapien XT, our goal in this study was to determine THV leaflet stresses with increasing THV size to understand the impact of choosing a given THV size on future long-term durability using XT THVs as an example.

Materials and Methods

Commercial 23mm, 26mm, and 29mm Edwards Sapien XTs had been obtained. Fully expanded THV assembly consisted of 3 components: cobalt-chromium stent, dacron skirt, and bovine pericardial leaflets. Suture connections between different components were included to enable accurate simulation of the assembly with its connections. The process to determine THV stress distribution included: 1) microCT scanning of each individual THV, 2) 3D reconstruction of THV components, 3) FE simulation to mimic *in-vivo* blood pressure and deployment, and 4) post-processing and data analysis to determine stresses on leaflets and stent.

Transcatheter Aortic Valve Reconstruction

Sapien XTs were imaged with desktop cone-beam micro-computed tomography scanner (microCT-40; Scanco Medical AG, Baseldorf, Switzerland) in different orientations and intensities to distinguish stent and leaflet geometries as previously described[15-17]. High-resolution DICOM (Digital Imaging and Communications in Medicine) radiologic images were imported into image processing software MeVisLab (http://www.mevislab.de/). Images were manually segmented to separate THV stent vs. leaflets and obtain the most accurate representation of each of the three TAVR sizes. Reconstructed geometries were then imported into GeoMagic Design (3DSystems, Rock Hill, SC, USA) to create the geometric model, which was used to generate volumetric mesh in TrueGrid (XYZ Scientific Applications, Inc, Pleasant Hills, CA). Convergence studies were performed to determine optimal mesh density. The mesh was refined until the stress results varied <5% for two subsequent mesh refinements[20]. Ultimately, 20,988 elements were chosen for the leaflets on the 23mm, 26mm, and 29mm Sapien XT, 6,336 elements for the stent, and 1,848 elements for the dacron skirt. Leaflets, stent, and dacron were precisely reconstructed and aligned to create the entire THV model. Leaflets

were attached to dacron and stent along suture lines. Geometry and mesh of a representative THV are shown (Figure 1). Stent geometry was modeled using 3-dimensional brick elements, while leaflet geometry was modeled using nonlinear shell elements.

Finite Element Analyses

Deployment and dynamic systemic pressure loading were performed using ABAQUS (Dassault Systems, Waltham, MA). Contact definitions between the pairs of inner leaflets, leaflet and stent, leaflet and dacron, and stent and dacron were defined to most accurately represent the contact interaction behavior. THV leaflet geometries were sutured to the stent at the commissure area and sutured to the dacron mesh along the bottom edge as seen in Figure 1. Leaflets of Sapien XT are composed of bovine pericardium which is specially treated to resist calcification, a proprietary process that is also used for corresponding surgical Carpentier-Edwards Magna pericardial valves (Edwards Lifesciences, Inc, Irvine, CA). Biaxial stretch testing of these surgical valve leaflets(n=12 with 35 valve leaflets) was performed to determine material properties of THV leaflets[21] and the constitutive material model was previously described[16, 17]. A nonlinear regression Levenberg-Marquardt least squares algorithm in MATLAB (version 2014a) was used to fit experimentally obtained stresses to find the best-fitting material constants.

Pressure loading was applied to the fully expanded THV at nominal geometry or to the deployed geometry. Superior surfaces of leaflets and all the surfaces of stent were subjected to dynamic loading of systemic pressures. After the initial pressurization, cardiac cycles of 800ms duration were applied. Each cardiac cycle was composed of 300ms ramp upwards to maximum systolic pressure, followed by 500ms ramp downwards to minimum diastolic pressure.

A repeatability study to verify the stress results was performed and the repeatability was satisfactory. One of the study authors (Z.W.) independently re-created the models of all 3 sizes of Sapien XT from the micro-CT images, and ran pressure loading simulations. Stress distribution on the leaflet and stent of each size was nearly identical to the original model, and variation of the peak stress magnitudes was 6.28% ± 3.84% (mean±SD) which was within the range of the previous interobserver study[22].

.

Results

For Sapien XT leaflets, maximum principal stresses across the entire leaflet, including sutured regions were 1.69MPa, 1.70MPa, and 2.12MPa for 23mm, 26mm, and 29mm XT, respectively at mean arterial pressure of 93.3mmHg (Figures 2a-c). Minimum principal stresses across the entire leaflet, including sutured regions were –0.37MPa, -0.29MPa and -0.24MPa for 23mm, 26mm, and 29mm XT, respectively at mean arterial pressure (Figure 2d-e). Maximum and minimum principal stresses for each region in 23mm, 26mm, and 29mm XT are listed in Table 1. Positive stress values correspond to tensile stress where THV leaflets are stretched to provide coaptation, while negative stress values represent leaflet compression or bending where redundant tissue was compressed in order to coapt. Peak stresses occurred at tips of leaflet commissures along the attachment with the stent in 23mm and 29mm XT and occurred at the bottom suture of leaflet to the dacron in 26mm XT (Figure 2). In contrast, regions of free leaflet margin at the top and leaflet belly at the bottom, had lower peak stresses for all three sizes.

Stress distribution on leaflets of each THV size was analyzed and plotted on histograms (Figure 4). Surface areas of each leaflet were 304mm^2, 338mm^2, and 392mm^2 for 23mm, 26mm, and 29mm XT, respectively. Median values of maximum principal

stresses were 0.32MPa, 0.35MPa, and 0.41MPa with increasing THV size, 23mm, 26mm, and 29mm XT, respectively. Examining the most frequent leaflet stress values by histogram, they fell within the range of [300, 400], [400, 500] and [500, 600] kPa for the 23mm, 26mm, and 29mm XT, respectively (Figure 4).

To determine THV leaflet stresses for annulus sizes within the grey zones, we deployed 23 and 26mm XT within annulus of area 398mm^2 which clinically would require balloon oversizing 23mm XT and undersizing 26mm XT. When deployed within the same size annulus, leaflet stresses were compared. Stress distribution in the undersized 26mm XT was greatly shifted towards lower stress levels (Figure 5), while stress distribution in oversized 23mm XT did not change significantly from its fully expanded position and overall, had higher frequencies of high stress concentrations than 26mm XT. Similarly, we deployed the 26mm and 29mm XT within grey zone of annulus area 511mm^2 . Leaflet stresses on the undersized 29mm XT again were greatly shifted towards lower stress levels (Figure 6), while oversized 26mm XT showed minimal change in stresses from its nominal geometry but overall had higher frequencies of larger stress concentrations than the undersized 29mm XT.

For Sapien XT stent, maximum principal stresses at mean arterial pressure were 54.91MPa, 47.33MPa, and 53.11MPa, for 23mm, 26mm, and 29mm XT, respectively; minimum principal stresses at mean arterial pressure were -52.12MPa, -48.78MPa, and -50.17MPa, for 23mm, 26mm, and 29mm XT, respectively (Figure 3). Peak stresses occurred on the stent in proximity to the simulated patient annulus and at distal frame elements.

Discussion

Edwards balloon-expandable THVs, approved by US Food and Drug Administration in late 2011, have revealed no structural valve dysfunction with maintenance of low gradients and excellent valve area at 5 years[4]. While short-term durability appears adequate, long-term follow-up for durability of these valve designs is needed. Biomechanical studies using FEA can provide insight into mechanisms of valve degeneration by non-invasive approaches. Our current study investigated the impact of THV size from the same generation of balloon expandable THVs on leaflet and stent stresses, which may impact bioprosthetic valve durability. Stresses on leaflets and stents of three different sizes of Sapien XT were computationally determined and compared. Our study established the benchmark to access the size effect on the long-term durability of bioprosthetic THV, as indications for TAVR continue to expand to lower risk and younger patient populations.

Peak Stress and Size

Three different sizes of second-generation Sapien XT were available for different annulus dimensions. Commonly, patient annulus areas would fall into the grey zone between two THV sizes. In this study, peak stresses on THV leaflets irrespective of region increased with increasing THV size when examining THV expanded to nominal dimension. Overall, median stresses for the entire leaflet increased with increasing THV size at nominal, fully expanded deployment states (Figure 4). This is explained since the in-plane force is roughly equal to the product of pressure and cross-sectional area. Thus, a larger valve has greater total force on the leaflets because of its larger cross-sectional area for the same pressure loading. Our results suggest that THV size selection may potentially impact long-term durability.

Optimal TAVR Sizing

Clinically, optimal TAVR sizing balances ideal hemodynamics with risks, such as conduction disorders and annular rupture. From hemodynamics standpoint, larger TAVR size minimizes transvalvular gradient and PVL, and maximizes effective orifice area to decrease patient-prosthesis mismatch. PVL results from lack of congruence between annulus and THV, and is related to undersized THV prosthesis, device malpositioning, heavily calcified bulky native aortic valve cusps, and/or bicuspid valve[23]. Larger baseline annular coronal and oblique sagittal dimensions were found in patients with significant PVL[24]. Low cover index was also associated with PVL, suggesting THV oversizing was necessary to reduce PVL[25]. From patient-prosthesis standpoint, larger THV size leads to less patient-prosthesis mismatch[26], which impacts mortality[27]. On the other hand, oversizing THV can compress the conduction system, increase the rate of permanent pacemaker implantation, and increase risk of annular rupture when LVOT calcification is present[25].

In this study, we examined the impact of oversizing a smaller THV vs undersizing a larger THV for annulus sizes within the grey zone, and examined differences in leaflet stresses as a potential indicator for long-term durability. Undersizing the larger THV led to significantly lower leaflet stresses than oversizing the smaller THV, which may be another consideration clinically when choosing between two TAVR sizes. Overall, for annulus sizes that were clearly within the 23, 26, or 29mmXT sizing guidelines, the larger THV had higher peak stresses which may lead to earlier THV bioprosthetic degeneration. In comparison, other computational studies examined how THV underexpansion affects leaflet stress, concluding that peak leaflet stress increased with more underexpansion[12],[28]. For a given THV size, greater degrees of underexpansion were

unfavorable compared to nominal deployment[12],[28]. However, in these prior studies, only 1 THV size was tested with varying degrees of underexpansion, and did not account for an alternative THV size option for a given annulus size.

TAVR physicians must exercise their best judgment when choosing optimal THV size within the grey zones based upon current practices, the finite number of THV sizes available, patient anatomy, including LVOT calcification, sinus effacement, sinotubular junction dimensions, as well as optimal hemodynamics minimizing PVL, to achieve ideal clinical outcomes. With multi-factorial risk factors for bioprosthetic valve degeneration, choosing THV size based upon leaflet stresses to optimize long-term durability is yet one additional procedural consideration that could be factored into clinical decision-making to offer the benefit of longevity. Further clinical study will be needed to correlate calculated leaflet stress results with valve durability and loss of collagen integrity.

Limitations

The 23mm, 26mm, and 29mm Sapien XT were chosen for controlled comparisons within one generation of balloon-expandable THV to investigate the impact of size on THV leaflet stresses. Given limited access to THV for research purposes, complete sizes of Sapien 3 were not available to conduct this study. Given Sapien 3 also has grey zones that accept either an oversized smaller THV or an undersized larger THV, these computational simulations examining leaflet stresses in a similar leaflet design across sizes are still translatable clinically. This study did not take into account leaflet damage from crimping and ballooning process which occurs during TAVR. Studies have demonstrated that crimping physically damages THV leaflets and may weaken leaflets and increase leaflet stresses[1]. We did not destroy our THV to test its leaflets for exact material properties given the rarity of obtaining THVs and need for future TAVR experimental *in vitro* testing,

which were beyond the scope of this study. As such we utilized excised leaflets from surgical bioprostheses to determine material properties for THV leaflets. While treatment processes for both Edwards valves are expected to the same, thinner pericardial leaflets used in TAVR may have slightly different material properties[6] than were represented here. As stent and leaflet stresses cannot be directly measured, there was no suitable method to perform experimental validation of stresses. Complex fluid-structure interaction simulations were not incorporated and were beyond the present scope of this study. Lastly, patient-specific simulations of each of the THV sizes were not performed given a single patient would only be able to provide a post-TAVR CT of one THV size and not yield suitable information regarding the 2nd THV size when choosing between two sizes.

Conclusions

We studied the impact of balloon expandable THV size on leaflet and stent stress in this study by comparing the same generation of THV with three available sizes. Larger THV sizes had greater leaflet stresses and may be more prone to earlier degeneration. On the other hand, when choosing between two THV sizes within grey zones of annulus sizing, undersizing the larger TAVR resulted in lower leaflet stresses than oversizing the smaller THV. Sizing THV currently takes into account annular measurements from CTA, as well as potential for PVL, patient-prosthesis mismatch, and risk of permanent pacemaker implantation and annular rupture. The results from this study shed light on another factor, leaflet stresses and THV size. Correlation with further clinical studies will be essential to correlate stresses with valve durability.

Impact on Daily Practice: For some patients, measured annulus size falls within the grey zone of THV sizing and is suitable for two THV sizes, depending on the degree of

oversizing/undersizing. We performed finite element analyses of 23mm, 26mm, and 29mm second-generation balloon expandable THV to determine the impact of device size on leaflet stresses, as a surrogate for durability. Larger THV sizes had higher peak leaflet stresses. However, at annulus sizes within the grey zone between two THV sizes, stresses were reduced when using an undersized larger THV than oversized smaller THV deployed in the same annulus size. The choice to size upwards in the grey zone may lead to improved long-term valve durability.

Funding: The study was funded by the University of California Proof of Concept grant #246590, National Institutes of Health R01HL119857, and American Heart Association Postdoctoral Fellowship 16POST31420013.

Conflict of Interest Statement: Drs. Tseng and Ge are founders of ReValve Med, Inc. Drs. Dvir and Ye are consultants for Edwards Lifesciences. The remaining authors have no conflicts of interest to declare.

References

1. Deeb GM, Reardon MJ, Chetcuti S, Patel HJ, Grossman PM, Yakubov SJ, Kleiman NS, Coselli JS, Gleason TG, Lee JS, Hermiller JB, Jr., Heiser J, Merhi W, Zorn GL, 3rd, Tadros P, Robinson N, Petrossian G, Hughes GC, Harrison JK, Maini B, Mumtaz M, Conte J, Resar J, Aharonian V, Pfeffer T, Oh JK, Qiao H, Adams DH, Popma JJ. 3-year outcomes in high-risk patients who underwent surgical or transcatheter aortic valve replacement. *J Am Coll Cardiol*. 2016;67:2565-2574.
2. Grover FL, Vemulapalli S, Carroll JD, Edwards FH, Mack MJ, Thourani VH, Brindis RG, Shahian DM, Ruiz CE, Jacobs JP, Hanzel G, Bavaria JE, Tuzcu EM, Peterson ED, Fitzgerald S, Kourtis M, Michaels J, Christensen B, Seward WF, Hewitt K, Holmes DR, Jr., Registry SAT. 2016 annual report of the society of thoracic surgeons/american college of cardiology transcatheter valve therapy registry. *J Am Coll Cardiol*. 2017;69:1215-1230.
3. Kapadia SR, Leon MB, Makkar RR, Tuzcu EM, Svensson LG, Kodali S, Webb JG, Mack MJ, Douglas PS, Thourani VH, Babaliaros VC, Herrmann HC, Szeto WY, Pichard AD, Williams MR, Fontana GP, Miller DC, Anderson WN, Akin JJ, Davidson MJ, Smith CR. 5-year outcomes of transcatheter aortic valve replacement compared with standard treatment for patients with inoperable aortic stenosis (partner 1): A randomised controlled trial. *Lancet*. 2015;385:2485-2491.
4. Mack MJ, Leon MB, Smith CR, Miller DC, Moses JW, Tuzcu EM, Webb JG, Douglas PS, Anderson WN, Blackstone EH, Kodali SK, Makkar RR, Fontana GP, Kapadia S, Bavaria J, Hahn RT, Thourani VH, Babaliaros V, Pichard A, Herrmann HC, Brown DL, Williams M, Davidson MJ, Svensson LG, Akin J. 5-year outcomes of transcatheter aortic valve replacement or surgical aortic valve replacement for high surgical risk patients with aortic stenosis (partner 1): A randomised controlled trial. *Lancet*. 2015;385:2477-2484.
5. Nishimura RA, Otto CM, Bonow RO, Carabello BA, Erwin JP, 3rd, Fleisher LA, Jneid H, Mack MJ, McLeod CJ, O'Gara PT, Rigolin VH, Sundt TM, 3rd, Thompson A. 2017 aha/acc focused update of the 2014 aha/acc guideline for the management of patients with valvular heart disease: A report of the american college of cardiology/american heart association task force on clinical practice guidelines. *J Am Coll Cardiol*. 2017;70:252-289.
6. Leber AW, Eichinger W, Rieber J, Lieber M, Schleger S, Ebersberger U, Deichstetter M, Vogel J, Helmberger T, Antoni D, Riess G, Hoffmann E, Kasel AM. Msct guided sizing of the edwards sapien xt tavi device: Impact of different degrees of oversizing on clinical outcome. *International journal of cardiology*. 2013;168:2658-2664.
7. Stahli BE, Nguyen-Kim TD, Gebhard C, Erhart L, Frauenfelder T, Tanner FC, Falk V, Landmesser U, Nietlispach F, Luscher TF, Maier W, Binder RK. Prosthesis-specific predictors of paravalvular regurgitation after transcatheter aortic valve replacement: Impact of calcification and sizing on balloon-expandable versus self-expandable transcatheter heart valves. *J Heart Valve Dis*. 2015;24:10-21.
8. Murphy DT, Blanke P, Alaamri S, Naoum C, Rubinshtein R, Pache G, Precious B, Berger A, Raju R, Dvir D, Wood DA, Webb J, Leipsic JA. Dynamism of the aortic annulus: Effect of diastolic versus systolic ct annular measurements on device selection in transcatheter aortic valve replacement (tavr). *J Cardiovasc Comput Tomogr*. 2016;10:37-43.
9. Binder RK, Webb JG, Willson AB, Urena M, Hansson NC, Norgaard BL, Pibarot P, Barbanti M, Larose E, Freeman M, Dumont E, Thompson C, Wheeler M, Moss RR, Yang TH, Pasian S, Hague CJ, Nguyen G, Raju R, Toggweiler S, Min JK, Wood DA, Rodes-Cabau J, Leipsic J. The impact of integration of a multidetector computed tomography annulus area sizing

algorithm on outcomes of transcatheter aortic valve replacement: A prospective, multicenter, controlled trial. *Journal of the American College of Cardiology*. 2013;62:431-438.
10. Barbanti M, Yang TH, Rodes Cabau J, Tamburino C, Wood DA, Jilaihawi H, Blanke P, Makkar RR, Latib A, Colombo A, Tarantini G, Raju R, Binder RK, Nguyen G, Freeman M, Ribeiro HB, Kapadia S, Min J, Feuchtner G, Gurtvich R, Alqoofi F, Pelletier M, Ussia GP, Napodano M, de Brito FS, Jr., Kodali S, Norgaard BL, Hansson NC, Pache G, Canovas SJ, Zhang H, Leon MB, Webb JG, Leipsic J. Anatomical and procedural features associated with aortic root rupture during balloon-expandable transcatheter aortic valve replacement. *Circulation*. 2013;128:244-253.
11. Sun W, Li K, Sirois E. Simulated elliptical bioprosthetic valve deformation: Implications for asymmetric transcatheter valve deployment. *J Biomech*. 2010;43:3085-3090.
12. Abbasi M, Azadani AN. Leaflet stress and strain distributions following incomplete transcatheter aortic valve expansion. *J Biomech*. 2015;48:3663-3671.
13. Martin C, Sun W. Comparison of transcatheter aortic valve and surgical bioprosthetic valve durability: A fatigue simulation study. *J Biomech*. 2015;48:3026-3034.
14. Martin C, Sun W. Simulation of long-term fatigue damage in bioprosthetic heart valves: Effects of leaflet and stent elastic properties. *Biomechanics and modeling in mechanobiology*. 2014;13:759-770.
15. Xuan Y, Dvir D, Wang Z, Mizoguchi T, Ye J, Guccione JM, Ge L, Tseng EE. Stent and leaflet stresses in 26-mm, third-generation, balloon-expandable transcatheter aortic valve. *J Thorac Cardiovasc Surg*. 2018.
16. Xuan Y, Krishnan K, Ye J, Dvir D, Guccione JM, Ge L, Tseng EE. Stent and leaflet stresses in a 26-mm first-generation balloon-expandable transcatheter aortic valve. *J Thorac Cardiovasc Surg*. 2017;153:1065-1073.
17. Xuan Y, Krishnan K, Ye J, Dvir D, Guccione JM, Ge L, Tseng EE. Stent and leaflet stresses in 29-mm second-generation balloon-expandable transcatheter aortic valve. *Ann Thorac Surg*. 2017;104:773-781.
18. Rodes-Cabau J. Transcatheter aortic valve implantation: Current and future approaches. *Nat Rev Cardiol*. 9:15-29.
19. Www.Accessdata.Fda.Gov/cdrh_docs/pdf13/p130009s034d.Pdf. In: Lifesciences E, ed. Edwards sapienxt transcatheter heart valve with the ascendra + delivery system instructions for use. Irvine, CA.: Edwards Lifesciences L.L.C. ;2015: p. 1-32.
20. Sinclair G, Beisheim J, Sezer S. Practical convergence-divergence checks for stresses from fea. International ANSYS Users Conference and Exhibition, Pittsburgh, PA https://www ansys com/-/media/ansys/corporate/resourcelibrary/conference-paper/2006-int-ansys-conf-28 pdf;2006.
21. Azadani AN, Chitsaz S, Matthews PB, Jaussaud N, Leung J, Tsinman T, Ge L, Tseng EE. Comparison of mechanical properties of human ascending aorta and aortic sinuses. *Ann Thorac Surg*. 2012;93:87-94.
22. Teutelink A, Cancrinus E, van de Heuvel D, Moll F, de Vries J-P. Preliminary intraobserver and interobserver variability in wall stress and rupture risk assessment of abdominal aortic aneurysms using a semiautomatic finite element model. *Journal of vascular surgery*. 2012;55:326-330.
23. Zegdi R, Ciobotaru V, Noghin M, Sleilaty G, Lafont A, Latremouille C, Deloche A, Fabiani JN. Is it reasonable to treat all calcified stenotic aortic valves with a valved stent? Results from a human anatomic study in adults. *J Am Coll Cardiol*. 2008;51:579-584.

24. Delgado V, Ng AC, van de Veire NR, van der Kley F, Schuijf JD, Tops LF, de Weger A, Tavilla G, de Roos A, Kroft LJ, Schalij MJ, Bax JJ. Transcatheter aortic valve implantation: Role of multi-detector row computed tomography to evaluate prosthesis positioning and deployment in relation to valve function. *Eur Heart J*. 2010;31:1114-1123.
25. Detaint D, Lepage L, Himbert D, Brochet E, Messika-Zeitoun D, Iung B, Vahanian A. Determinants of significant paravalvular regurgitation after transcatheter aortic valve: Implantation impact of device and annulus discongruence. *JACC Cardiovasc Interv*. 2009;2:821-827.
26. Deeb GM, Chetcuti SJ, Yakubov SJ, Patel HJ, Grossman PM, Kleiman NS, Heiser J, Merhi W, Zorn GL, 3rd, Tadros PN, Petrossian G, Robinson N, Mumtaz M, Gleason TG, Huang J, Conte JV, Popma JJ, Reardon MJ. Impact of annular size on outcomes after surgical or transcatheter aortic valve replacement. *Ann Thorac Surg*. 2018;105:1129-1136.
27. Pibarot P, Weissman NJ, Stewart WJ, Hahn RT, Lindman BR, McAndrew T, Kodali SK, Mack MJ, Thourani VH, Miller DC, Svensson LG, Herrmann HC, Smith CR, Rodes-Cabau J, Webb J, Lim S, Xu K, Hueter I, Douglas PS, Leon MB. Incidence and sequelae of prosthesis-patient mismatch in transcatheter versus surgical valve replacement in high-risk patients with severe aortic stenosis: A partner trial cohort--a analysis. *J Am Coll Cardiol*. 2014;64:1323-1334.
28. Martin C, Sun W. Transcatheter valve underexpansion limits leaflet durability: Implications for valve-in-valve procedures. *Annals of biomedical engineering*. 2017;45:394-404.

Figure 1a: Transcatheter Heart Valve Leaflet Assembly

Regions of interest studied for stress distribution in leaflets: upper leaflet free edges; lower leaflet belly; and sutured leaflet edges.

Figure 1b: Transcatheter Heart Valve Mesh

Representative mesh of 23mm SapienXT with leaflet assembly and stent frame.

Figure 2: **Maximum and Minimum Principal Stresses on Transcatheter Heart Valve Leaflets**

Maximum (a-c) and minimum (d-f) principal stresses on entire leaflet of 23mm, 26mm, and 29mm SapienXT at mean arterial pressure.

Figure 3: **Maximum and Minimum Principal Stress on Transcatheter Heart Valve Stent**

Maximum (a-c) and minimum (d-f) principal stresses of stent of 23mm, 26mm, and 29mm SapienXT at mean arterial pressure.

Figure 4: Histogram of Leaflet Stress Values

Histogram of leaflet stress distribution for three Sapien XT sizes. Circled bar indicates range with highest frequency.

Figure 5: Leaflet Stress Histogram for 23mm and 26mm Deployed to 398mm^2

Histogram of stress distribution on leaflets of 23mm and 26mm Sapien XT deployed to 398mm^2. The y-axis value represents the number of elements in the model experiencing the specified range of stress defined by the x-axis bin-width.

Figure 6: Leaflet Stress Histogram for 26mm and 29mm Sapien XT Deployed to 511mm^2

Histogram of stress distribution on leaflets of 26mm and 29mm Sapien XT deployed to 511mm^2. The y-axis value represents the number of elements in the model experiencing the specified range of stress defined by the x-axis bin-width.

Table 1: Maximum and minimum principal stresses of transcatheter heart valve subregions by size.

	Max Principal Stress (MPa)			Min Principal Stress		
	23XT	26XT	29XT	23XT	26XT	29XT
Upper leaflet	1.69	1.43	2.12	-0.17	-0.13	-0.24
Lower leaflet	0.77	1.61	1.11	-0.15	-0.20	-0.11
Leaflet Sutured Region	1.14	1.70	1.66	-0.37	-0.29	-0.20
Stent	54.91	47.33	53.11	-52.12	-48.78	-50.71

MPa: Megapascal

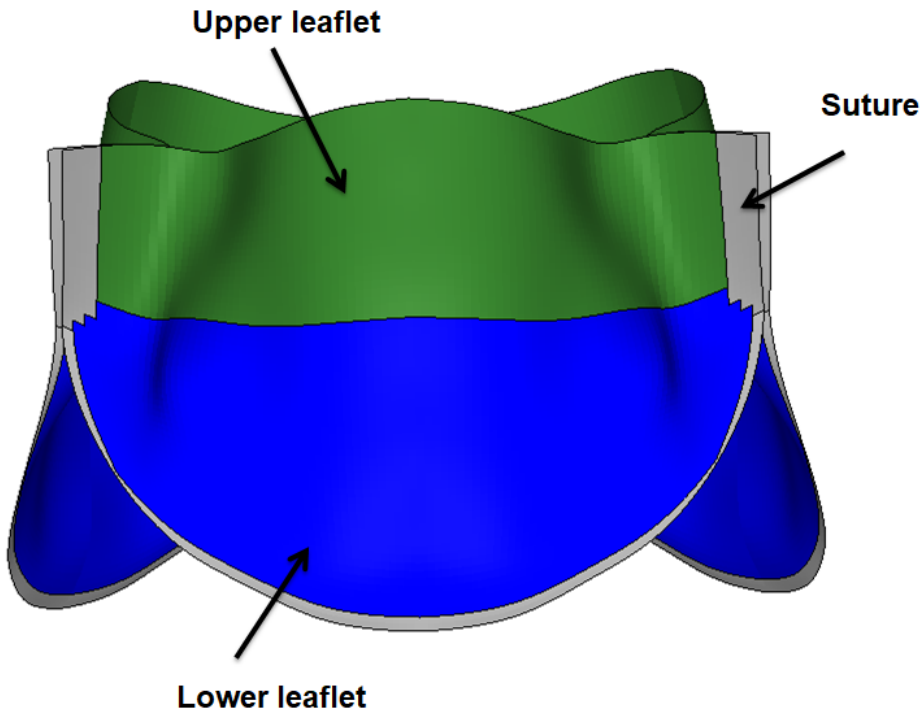

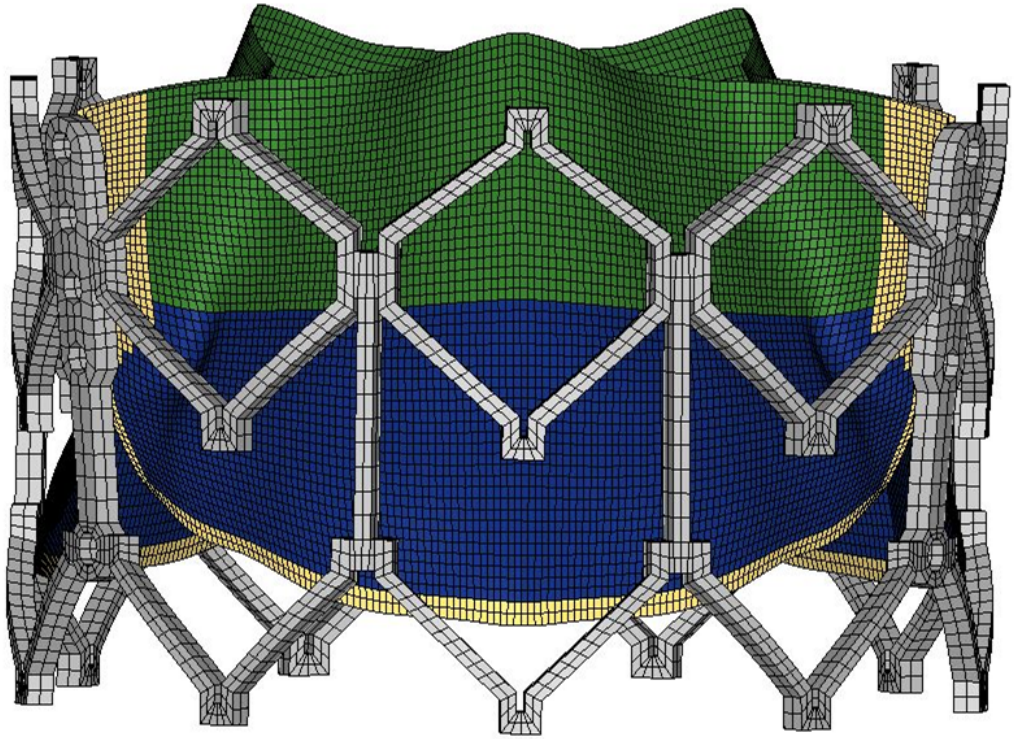

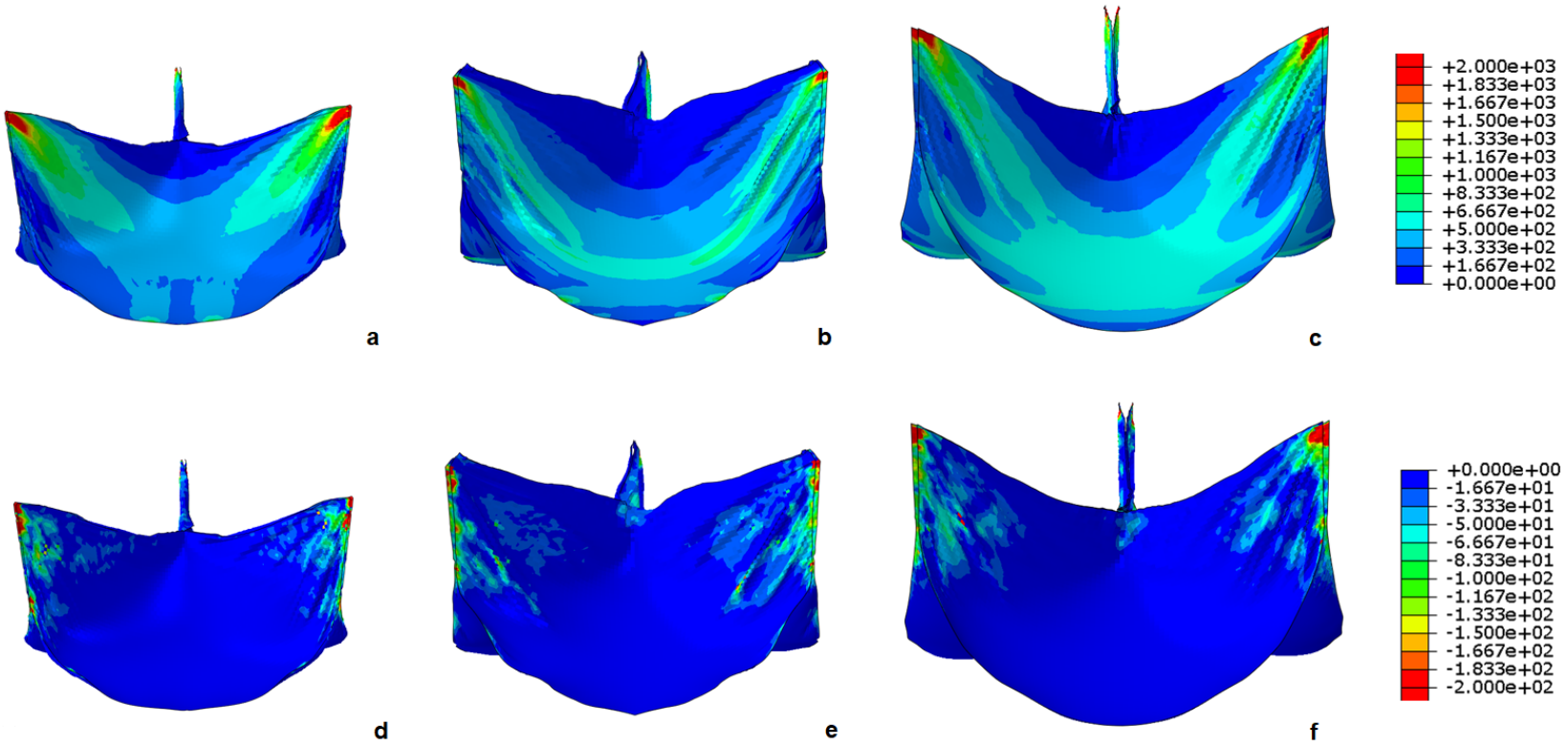

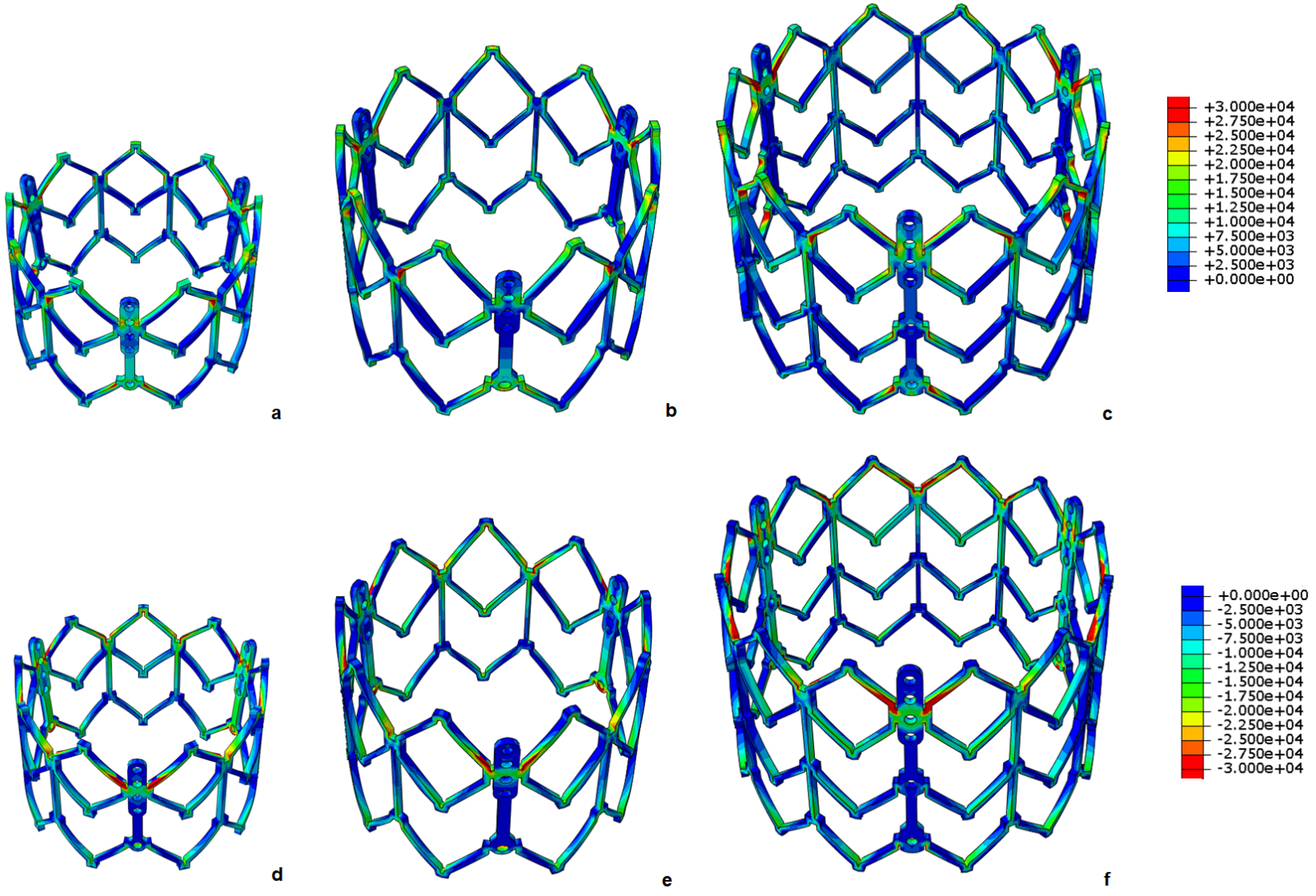

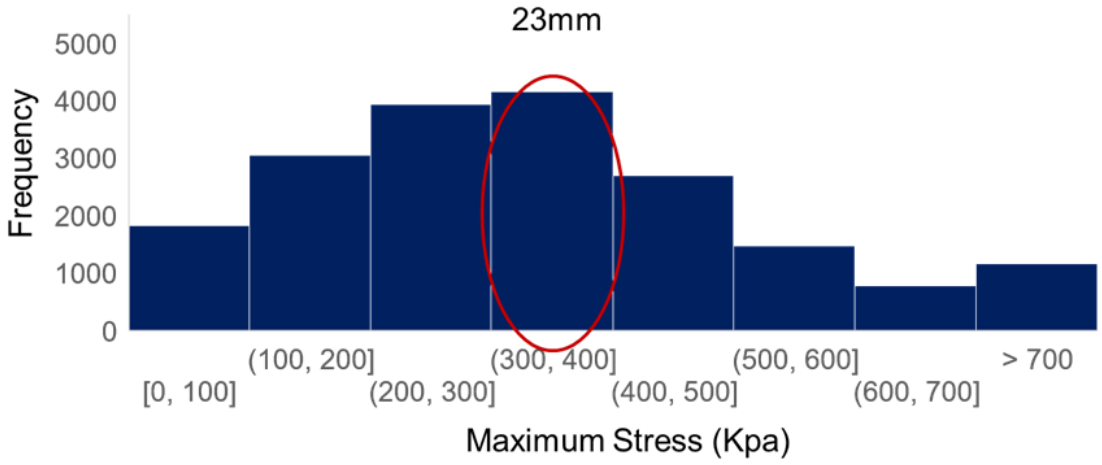

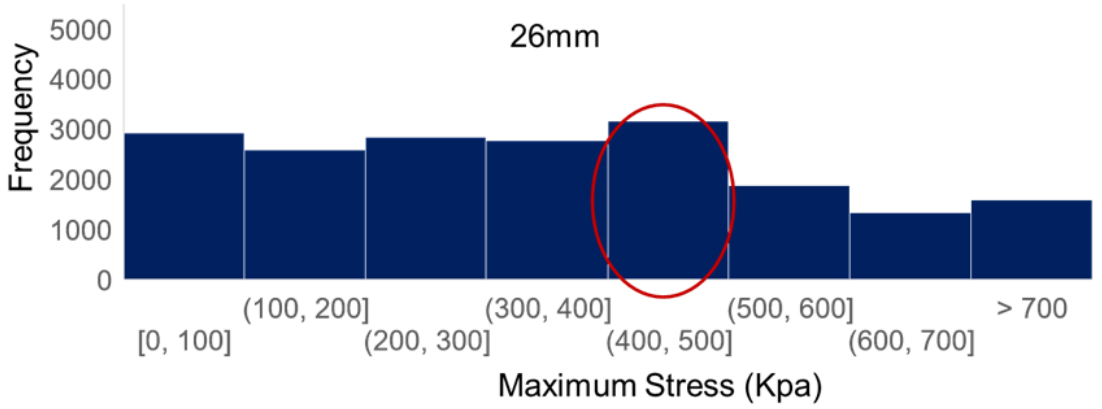

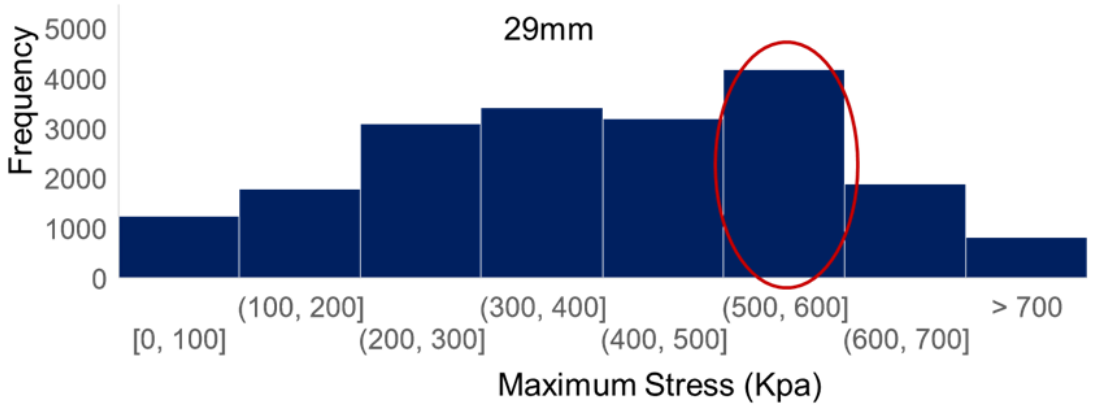

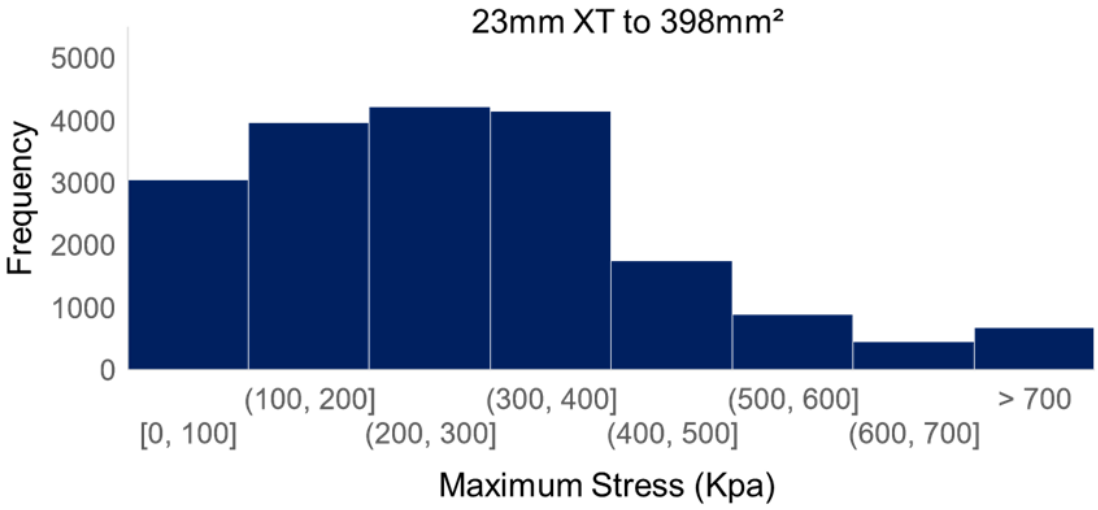

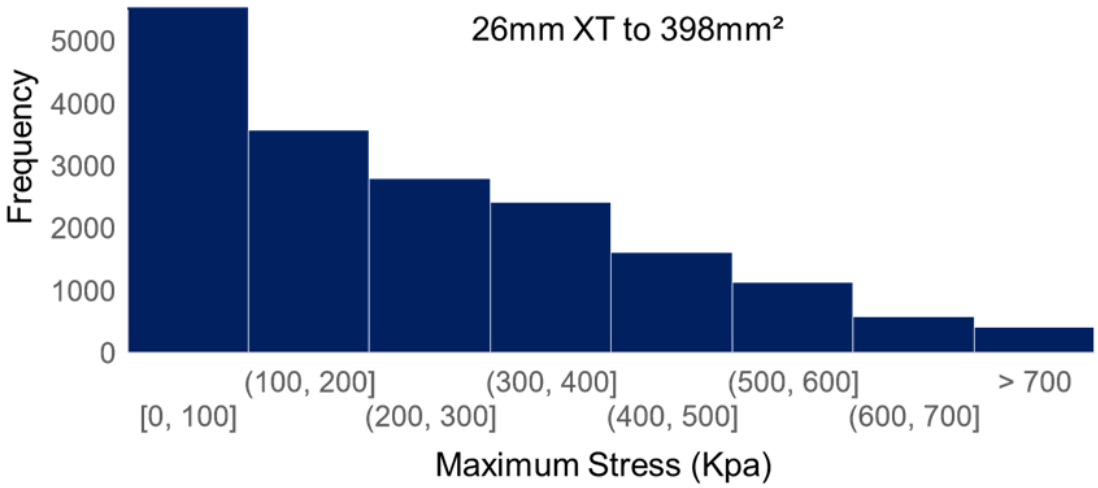

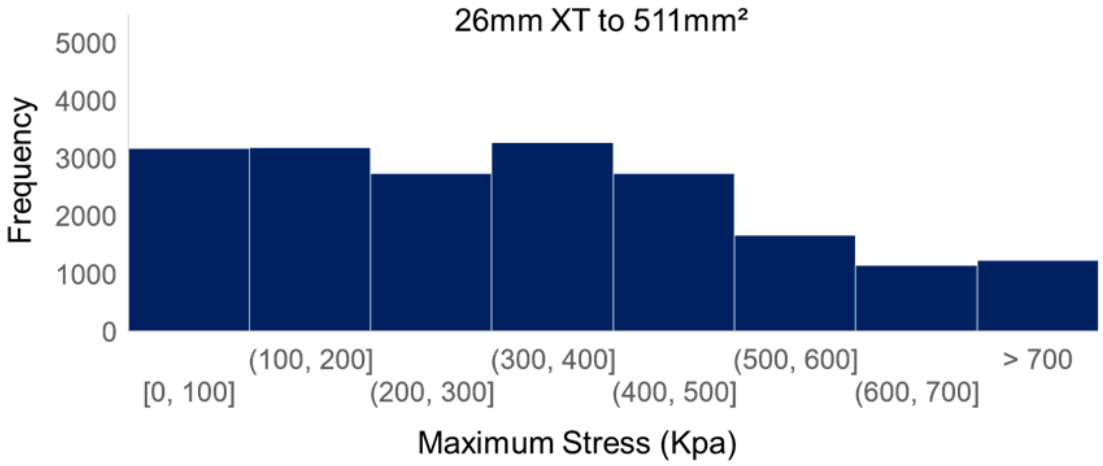

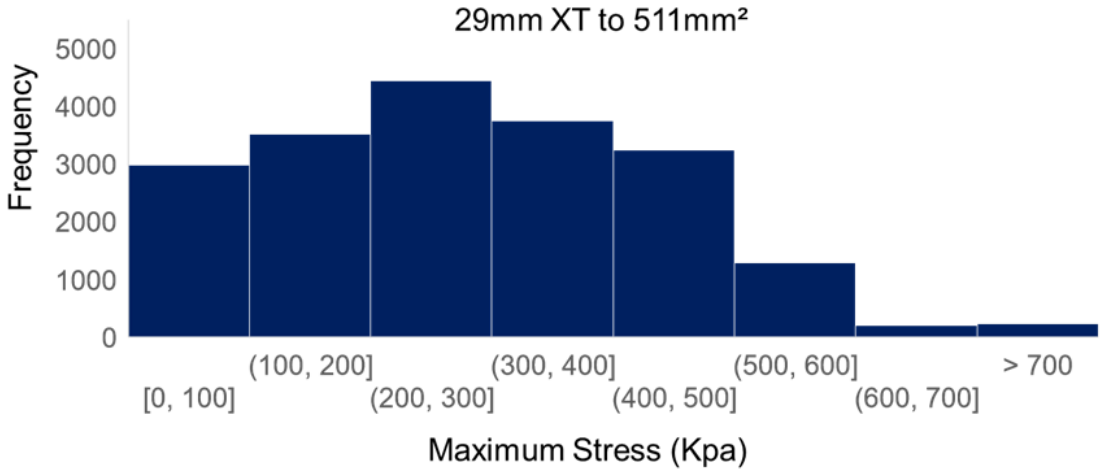

AsiaIntervention

Official Journal of the Asian Pacific Society of Interventional Cardiology

(APSIC) and the Interventional Cardiology Foundation of India (ICFI)

www.asiaintervention.org

Title: **Prediction of post-intervention fractional flow reserve (FFR) in diffuse or sequential coronary stenosis considering the residual trans-stent pressure gradient.**

Authors: Xiaoyang Song, M.D; Naritatsu Saito, M.D; Yoshiaki Kawase, M.D; Yusuke Yoshikawa, M.D; Erika Yamamoto, M.D; Munenori Okubo, M.D; Hiroki Shiomi, M.D; Shin Watanabe, M.D; Takeshi Kimura, M.D; Hitoshi Matsuo, M.D

Manuscript number: AIJ-D-19-00015

Manuscript submission date: 28 April 2019

Revisions received: 24 July 2019, 11 March 2019, 27 May 2019

Accepted date: 9 June 2020

Prediction of post-intervention fractional flow reserve (FFR) in diffuse or sequential coronary stenosis considering the residual trans-stent pressure gradient

Xiaoyang Song[1], MD; Naritatsu Saito[1], MD; Yoshiaki Kawase[2], MD; Yusuke Yoshikawa[1], MD; Erika Yamamoto, MD[1]; Munenori Okubo[2], MD; Hiroki Shiomi[1], MD; Shin Watanabe[1], MD; Takeshi Kimura[1], MD; Hitoshi Matsuo[2], MD

1. Department of Cardiovascular Medicine, Kyoto University Graduate School of Medicine, Kyoto, Japan
2. Department of Cardiovascular Medicine, Gifu Heart Center, Gifu, Japan

Short running title: Post-intervention FFR in diffuse/sequential lesion

Address for Correspondence

Naritatsu Saito, MD, PhD

Address: 54 Shogoin-Kawahara-cho, Sakyo-ku, Kyoto, 606-8507, Japan

Department of Cardiovascular Medicine, Kyoto University Graduate School of Medicine, Kyoto, Japan

Email address: naritatu@kuhp.kyoto-u.ac.jp

Conflict of interest statement:

The authors have no conflicts of interest to declare.

Abstract

Aims:

Prediction of post-intervention fractional flow reserve (FFR) in a diffuse or sequential coronary lesion is difficult due to complex hemodynamic interactions between individual stenosis. Furthermore, the existence of a residual intra-stent pressure gradient makes the prediction difficult. We developed an equation predicting the post-intervention FFR in a diffuse/sequential lesion in consideration with intra-stent FFR gradient. The present study aims to validate the equation in an in-vitro model and in clinical data.

Methods and Results:

In the in-vitro experiment, three sequential coronary stenosis were made with a collateral flow. The correlation coefficient of the predicted FFR and the actual post-intervention FFR was 0.99, and the absolute difference was 0.008 ± 0.006 (n = 50). In the clinical data analysis, the correlation coefficient was 0.41, and the absolute difference was 0.06 ± 0.05 (n = 67). We applied a fixed value of intra-stent FFR

gradient and a collateral flow index so that the equation can be used in clinical practice. The correlation coefficient became 0.28 and the absolute difference became 0.06 ± 0.06.

Conclusions:

In clinical practice, prediction of post-intervention FFR in a diffuse/sequential lesion is difficult even when residual intra-stent pressure gradient is considered.

Classifications

Stable angina, Diffused disease, Fractional flow reserve

Abbreviations

FFR: fractional flow reserve, PCI: percutaneous coronary intervention, iFR: instantaneous wave free ratio, CFI: collateral flow index, NSTEMI: non-ST segment elevation myocardial infarction, STEMI: ST segment elevation myocardial infarction, LAD: left anterior descending artery, LCX: left circumflex artery, RCA: right coronary artery, QCA: quantitative coronary angiography, RFR: resting full-cycle ratio, dPR: diastolic pressure ratio, IVUS: intravascular ultrasound, OCT: optical coherence

tomography

Condensed abstract

We developed an equation predicting the post-intervention fractional flow reserve (FFR) in a diffuse/sequential lesion in consideration with intra-stent FFR gradient and validated the equation in an in-vitro model and in clinical data. The equation perfectly predicted post-intervention FFR of diffuse/sequential coronary lesions in the in-vitro model of coronary circulation. However, in clinical data analysis, prediction of post-intervention FFR in a diffuse/sequential lesion was difficult even when residual intra-stent pressure gradient was considered.

Impact on daily practice

Prediction of post-intervention fractional flow reserve (FFR) in a diffuse/sequential lesion is only possible in an in-vitro model. In clinical practice, prediction is difficult due to considerable errors even when residual intra-stent pressure gradient is considered. Physicians need to conduct multiple pullback recordings of FFR in the treatment of a diffuse/sequential lesion to obtain post-intervention FFR.

Introduction:

Fractional flow reserve (FFR) guided percutaneous coronary intervention (PCI) is associated with a favorable outcome compared with angiography guided PCI [1,2]. FFR measurement is conducted under maximum hyperemic condition induced by intracoronary or by the intravenous administration of a vasodilator, which may cause side effects including vomiting, hypotension, and arrhythmia [3,4]. Recently, resting non-hyperemic indices, including the instantaneous wave free ratio (iFR), have been developed to assess the functional severity of coronary stenosis [5]. iFR and other resting indices do not require the induction of hyperemia, and thus hyperemia-related complications are avoidable [3,4]. Another important advantage of iFR is that post-intervention iFR is predictable in a sequential or diffuse coronary lesion by the following simple equation [6,7]: $iFR_{post} = iFR_{pre} + \Delta iFR$. Prediction of post-intervention FFR is usually considered difficult in FFR due to complex hemodynamic interactions between the individual stenosis under maximum hyperemia [8,9]. Therefore, the current recommendation for a sequential or diffuse

coronary lesion is measuring FFR distally, and performing a pressure pullback under maximum hyperemia. Treatment of the most severely narrowed lesion is then determined by which of the lesions produces the largest ΔFFR[10–12].

We consider that another factor that makes post-intervention FFR prediction in a diffuse/sequential lesion difficult is the existence of an intra-stent pressure gradient after intervention. The post-intervention intra-stent pressure gradient inevitably affects the post-intervention FFR [13–16]. We hypothesized that post-intervention FFR, in a diffuse/sequential coronary lesion, is predictable if the post-intervention intra-stent FFR is considered. Thus we developed a mathematical equation to predict post-intervention FFR in diffuse/sequential lesions in consideration of the intra-stent FFR gradient. The main purpose of the present study is to validate the equation in an in-vitro circuit model and in clinical data.

Methods:

Derivation of the Equation

De Bruyne et al. described theoretic equations to predict the FFR of each

stenosis in a tandem lesion [8], but its application is limited to tandem lesions. We have mathematically generalized the equations to be applicable to a diffuse/sequential coronary lesion in a previous study (Equation A) [9].

$$FFR_{post} = \frac{P_d - P_w}{P_a - \Delta P - P_w} + \frac{P_w(P_a - \Delta P - P_d)}{P_a(P_a - \Delta P - P_w)}$$

$$= \frac{FFR_{pre}(1 - CFI) - CFI\Delta FFR}{1 - \Delta FFR - CFI} \quad (A)$$

We wanted to formulate a novel equation in which post-intervention trans-stent FFR is considered. Consider a coronary circulation model simulating the diffuse/sequential coronary lesion with a collateral circulation (Figure 1). The abbreviations were defined as follows: R_s, resistance of the target coronary stenosis; R_1, summed resistance of the proximal stenoses; R_2, summed resistance of the distal stenoses; R_{micro}, hyperemic microcirculatory resistance; R_c, resistance of the collateral circulation; P_a, aortic pressure; P_{prox}, pressure proximal to R_s; P_{dist}, pressure distal to R_s; P_d, the most distal coronary pressure; P_w, coronary wedge pressure; and P_v, central venous pressure. The pre-intervention FFR was defined as

$FFR_{pre} = (P_d - P_v)/(P_a - P_v) \fallingdotseq P_d/P_a$ because P_v was usually considered to be zero while deriving the FFR indices. Pre-intervention FFR gradient across the target lesion was defined as $\Delta FFR = (P_{prox} - P_{dist})/P_a$. The parameter calculated from $(P_w - P_v)/(P_a - P_v) \fallingdotseq P_w/P_a$ was originally named “fractional flow reserve of the collateral artery (FFR_{coll})”. Later, the name "pressure derived collateral flow index (CFI)" was used for this parameter [17]. Because the collateral flow reserve of the collateral artery is usually called pressure derived CFI in other studies, we adopted this terminology to avoid confusion. All the post-intervention parameters have been expressed by adding a prime to the pre-intervention parameters; thus, R’s indicates the resistance of the target coronary lesion after PCI and $FFR_{post} = P'_d/P_a$ and $\Delta FFR' = (P'_{prox} - P'_{dist})/P_a$ are obtained. The pressure gradient across the stenosis was proportional to the flow because the flow was assumed to be the Hagen–Poiseuille flow in this model. Thus, the coronary circulation model can be considered analogous to the electric circuit. Figure 1 also describes the electric circuit that corresponds to the coronary circulation model. Under this assumption, the FFR

indices can be expressed in terms of resistance as follows:

$$\mathrm{CFI} = \frac{R_{micro}}{R_c + R_{micro}} \quad (1)$$

$$FFR_{pre} = \frac{R_{micro}}{\left(\frac{1}{\frac{1}{R_1 + R_x + R_2} + \frac{1}{R_c}}\right) + R_{micro}} \quad (2)$$

$$\Delta\mathrm{FFR} = (1 - \mathrm{FFR}_{pre})\frac{R_x}{R_1 + R_x + R_2} \quad (3)$$

$$FFR_{post} = \frac{R_{micro}}{\left(\frac{1}{\frac{1}{R_1 + R'_x + R_2} + \frac{1}{R_c}}\right) + R_{micro}} \quad (4)$$

$$\Delta\mathrm{FFR}' = (1 - \mathrm{FFR}_{post})\frac{R'_x}{R_1 + R'_x + R_2} \quad (5)$$

By solving the above equations (1) to (5), the following Equation (B) is obtained:

$$\boldsymbol{FFR_{post} = \frac{FFR_{pre}(1 - CFI) - CFI\Delta FFR - \Delta FFR'(FFR_{pre} - CFI)}{1 - \Delta FFR - CFI}} \quad (\boldsymbol{B})$$

The detailed process of derivations of Equation B is given in the Appendix.

In-vitro experiment

The experimental system was similar to that described in our previous studies (Figure 2). It consisted of a pump, systemic circulation, coronary circulation, and 5 constrictors placed in the coronary circulation. The pump produced a pulsatile flow at 60 rpm. The pressure and flow in the coronary artery could be adjusted by a valve placed in the aorta and constrictors placed in the coronary circulation. The coronary flow was approximately 300 to 500 mL/min. The circulating fluid was a 33% glycerin and 67% water a mixture comparable to the viscosity of blood. The systemic and coronary circulations were made of silicone rubber tubes that mimic the human arterial system. The inner diameter of the coronary artery was 4 mm and the inner diameter of the aorta was 12 mm. The constrictors made variable stenoses in the coronary artery by a screw rotation movement. The constrictors names correspond to the name of the resistance in the schematic model in Figure 1. FFR measurements were conducted using three 0.014-inch pressure wires (Abbott

Vascular, Santa Clara, CA, USA), one placed in to the proximity of R_s, another placed distally to R_s, and the other placed distally to R_2.

The experiment was conducted in the following sequence. Variable degrees of coronary microcirculation and collateral circulation were randomly created by the constrictors. Variable degrees of three sequential coronary stenoses were randomly generated. Then, P_a, P_{prox}, P_{dist}, and P_d were recorded by using three pressure wires, and FFR_{pre} and ΔFFR were calculated. P_w was obtained during a temporary occlusion of the distal part of the coronary artery, and pressure derived CFI was calculated. After partially releasing the stenosis of the target stenosis (R_s), P'_{prox}, P'_{dist}, and P'_d were recorded, and then FFR_{post} and ΔFFR were calculated. The apparent FFR after partially releasing the target stenosis ($FFR_{apparent}$) was defined as $FFR_{apparent} = FFR_{pre}$ + ΔFFR, and the predicted value of FFR ($FFR_{predicted}$) was calculated using Equation A. The adjusted value of FFR considering the residual pressure gradient across the target stenosis ($FFR_{adjusted}$) was calculated using Equation B. $FFR_{apparent}$, $FFR_{predicted}$, and $FFR_{adjusted}$ were compared with FFR_{post}.

Clinical data analysis

Consecutive patients who underwent elective coronary intervention for diffuse/sequential coronary lesions in Gifu Heart Center between March 2017 and March 2018 were included in the study. The inclusion criteria required all physiological parameters including FFR_{pre}, ΔFFR, CFI, FFR_{post}, and ΔFFR' to be obtained. The data in this study consisted of 67 coronary diffuse/sequential lesions from 67 patients. As all data were retrospectively collected from the patients' records, the requirement of written informed consents was waived. The study protocol was developed in accordance with the Declaration of Helsinki and was approved by the institutional ethics committee.

Coronary angiography and pressure wire assessments of coronary stenoses were conducted using the conventional approach. Briefly, the patients were instructed not to consume caffeine 12 hours before the procedure, and PCI was performed through the radial approach using a 6 or 7 Fr system. Intracoronary nitrates (300 ug) were administered in all patients before pressure wires (OptoWire;

Opsens, Quebec, Canada) were introduced. Equalization was performed 1 to 2 mm distal to the guiding catheter. The distal position of the pressure wire was documented by angiography. Angioplasty was performed using second-generation drug-eluting stents, which were all optimized using imaging devices, such as intravascular ultrasound (IVUS) and optical coherence tomography (OCT). Maximum hyperemia was induced by intravenous administration of adenosine. The pull-back recordings were conducted during maximum hyperemia before and after PCI, and FFR_{pre}, ΔFFR, FFR_{post}, and ΔFFR' were obtained. Wedge pressure was recorded as the coronary pressure distal to the occluding balloon at 30s after the balloon occlusion, and pressure derived CFI was also obtained for all patients. Like in the in-vitro experiment, $FFR_{apparent}$, $FFR_{predicted}$, and $FFR_{adjusted}$ were calculated from FFR_{pre}, CFI, ΔFFR, and ΔFFR', and compared with FFR_{post}. It is well-known that ΔFFR' is obtained after PCI, and the coronary wedge pressure is not usually measured in real-world clinical practice. Equation B cannot be applied in the clinical practice in this form. Thus, we calculated ΔFFR'/mm defined as ΔFFR' by total stent

length (mm) and estimated ΔFFR' calculated as ΔFFR'/mm multiplied by the implanted stent length ($\Delta FFR'_{estimated}$). The estimated value of CFI ($CFI_{estimated}$) was obtained using the average value of CFI from this study. $FFR_{fixed\text{-}adjusted}$ was calculated by using $\Delta FFR'_{estimated}$ and $CFI_{estimated}$ in Equation B. $FFR_{fixed\text{-}adjusted}$ was compared with $FFR_{adjusted}$.

Statistics

$FFR_{apparent}$, $FFR_{predicted}$, and $FFR_{adjusted}$ were compared with FFR_{post} using linear regression analysis and the Bland-Altman plot in the in-vitro experiment and clinical data analysis. The absolute differences of $FFR_{apparent}$, $FFR_{predicted}$, and $FFR_{adjusted}$ to FFR_{post} were compared using a paired t-test for the in-vitro experiment and in the clinical data analysis. The correlation coefficient and Bland-Altman plot of $FFR_{fixed\text{-}adjusted}$ to FFR_{post} were calculated, and the absolute difference of $FFR_{fixed\text{-}adjusted}$ to FFR_{post} was compared with that of $FFR_{adjusted}$ to FFR_{post} in the clinical data analysis. All continuous variables were presented as mean ± standard deviation unless otherwise stated. A two-sided p-value < 0.05 was considered statistically

significant in this study.

Results:

In-vitro experiment

In the in-vitro experiment, the procedures were repeated for 50 times with changing degrees of each stenosis. Fifty different sets of pressure data were obtained in the in-vitro experiment. FFR_{pre}, CFI, and ΔFFR were 0.60 ± 0.08, 0.29 ± 0.08, 0.17 ± 0.06, respectively. After partially releasing the target stenosis, ΔFFR' and FFR_{post} were 0.05 ± 0.02 and 0.67 ± 0.08. $FFR_{apparent}$, $FFR_{predicted}$, and $FFR_{adjusted}$ were 0.78 ± 0.08, 0.71 ± 0.10, and 0.68 ± 0.09. The correlation coefficients of $FFR_{apparent}$, $FFR_{predicted}$, and $FFR_{adjusted}$ were 0.94, 0.99, and 0.99 (Figure 3). The absolute differences of $FFR_{apparent}$, $FFR_{predicted}$, and $FFR_{adjusted}$ to FFR_{post} were 0.11± 0.03, 0.04 ± 0.02, and 0.008 ± 0.006 ($p < 0.001$, paired t-test). Equation B predicted the post-intervention FFR with a 1.3 ± 1.0% error. The results indicated that Equation B perfectly predicted post intervention FFR of diffuse/sequential coronary lesions when considering the residual FFR gradient in the in-vitro experiment.

Clinical data analysis

Sixty-seven coronary diffuse/sequential lesions from 67 patients were analyzed. Patients' demographics are summarized in Table 1. Briefly, the average age was 69.1 ± 9.0 years old, and 48 patients (71.8%) were of male gender. Clinical presentations included 64 patients (95.5%) with stable angina and 3 patients (4.5%) with unstable angina. Non-ST segment elevation myocardial infarction (NSTEMI) and STEMI patients were not included in the study. Lesions and procedure characteristics are listed in Table 2. The location of the lesions was 48 lesions (71.6%) in the left anterior descending artery (LAD), 7 lesions (10.4%) in the left circumflex artery (LCX), and 12 lesions (17.9%) in the right coronary artery (RCA). All lesions were de novo coronary lesions. Stenosis diameter of the target lesion was 54.9 ± 12.2%, reference vessel diameter was 2.91 ± 0.52 mm, lesion length was 23.4 ± 9.0 mm, and the minimum lumen diameter was 1.30 ± 0.35 mm obtained by quantitative coronary angiography (QCA). The pre-procedural intravenous adenosine induced FFR (FFR_{pre}), ΔFFR of the target lesion, and CFI were 0.68 ± 0.11,

0.17 ± 0.10, and 0.23 ± 0.11. All target lesions were treated by implanting the second-generation drug-eluting stent without any complications. The procedure time was 92.9 ± 31.1 min and the contrast volume was 99.9 ± 40.6. The total number of implanted stents was 1.2 ± 0.4, and the total stent length was 29.9 ± 13.0. In post-procedural QCA, the reference diameter was 3.15 ± 0.45 mm, the minimum stent diameter was 3.00 ± 0.45, and the diameter stenosis was 5.8 ± 9.9%. The post-procedural adenosine induced FFR (FFR_{post}) was 0.81 ± 0.07, ΔFFR of the stented lesion (ΔFFR') was 0.04 ± 0.03, ΔFFR'/mm was 0.0015 ± 0.0013. $FFR_{apparent}$, $FFR_{predicted}$, and $FFR_{adjusted}$ were calculated from the obtained data and were 0.91 ± 0.05, 0.87 ± 0.07, and 0.83 ± 0.08, respectively. The correlation coefficients of $FFR_{apparent}$, $FFR_{predicted}$, and $FFR_{adjusted}$ were 0.18, 0.30, and 0.41 ($p < 0.001$, Figure 4). The absolute differences of $FFR_{apparent}$, $FFR_{predicted}$, and $FFR_{adjusted}$ to FFR_{post} were 0.11± 0.06, 0.08 ± 0.06, and 0.06 ± 0.05 ($p < 0.001$, paired t-test). Equation B was used to calculate the post-intervention FFR with an 8.0 ± 7.0% error.

When the average value of CFI of 0.17 and ΔFFR'/mm of 0.0015 were

applied to Equation B, $FFR_{fixed\text{-}adjusted}$ was obtained. $FFR_{fixed\text{-}adjusted}$ was 0.83 ± 0.07, and the correlation coefficient of $FFR_{fixed\text{-}adjusted}$ to FFR_{post} was 0.28 ($p < 0.001$, Figure 5). The absolute difference of $FFR_{fixed\text{-}adjusted}$ to FFR_{post} was 0.06 ±0.06, which was not significantly different from $FFR_{adjusted}$ to FFR_{post} ($p = 0.6420$, paired t-test). Equation B predicted the post-intervention FFR with an 8.0 ± 7.2% error.

These results indicated that the accuracy of post-procedural FFR improved by taking the residual intra-stent FFR gradient into account and the application of fixed value of CFI and intra-stent FFR gradient did not significantly lower the accuracy of the post-procedural FFR prediction. However, the prediction error of approximately 8% is considered too large for clinical practice use.

Discussion:

The main findings of the present study were: 1) the development of a novel equation which predicts the post-intervention FFR in diffuse/sequential coronary lesions, 2) the novel equation perfectly predicted post-intervention FFR of diffuse/sequential coronary lesions in the in-vitro model of coronary circulation, 3)

in the clinical data analysis, prediction accuracy of post-intervention FFR in diffuse/sequential coronary lesions improved by taking the residual intra-stent FFR gradient into account 4) the application of a fixed value of CFI and intra-stent FFR gradient did not significantly lower the accuracy of post-procedural FFR prediction, 5) however, the prediction error in post-procedural FFR is considered too large to be used in clinical practice.

Previous studies have shown that PCI for stable angina is only beneficial in patients with significant myocardial ischemia [18,19]. Although FFR has been regarded as the gold standard index for the invasive assessment of physiological severity of coronary stenosis, the world wide use of FFR remains low at around 5 – 10% of all PCIs [20]. The reason for the low utilization of FFR includes the need for hyperemic agents administration, which is time consuming and may cause unpleasant complications [3,4]. Recently, resting indices including iFR have been developed to assess the functional severity of coronary stenosis. iFR is calculated by the distal coronary pressure divided by aortic pressure during the wave-free period

under resting condition. During the wave-free period, resistance in the cardiac cycle is considered to be minimal and constant. Following the results of two large randomized trials [3,4], the current European guideline has updated iFR-guided revascularization for stable angina to class I [21]. With the success of iFR, other resting indices, including the resting full-cycle ratio (RFR) and the diastolic pressure ratio (dPR) have been introduced [21,22]. The main advantage of these resting indices over FFR is that they do not require the induction of hyperemia, thus hyperemia-related complications are avoidable. Another advantage is that post-intervention indices are predictable because resting coronary flow is maintained constant due to autoregulation of the coronary circulation. Kikuta et al. described that iFR pullback predicted the physiological outcome of PCI with a high degree of accuracy [6,7].

On the other hand, predicting post-intervention FFR is considered difficult in diffuse/sequential coronary stenoses because complicated hemodynamic interactions exist between individual coronary stenosis. De Bruyne et al. described

theoretic equations to predict FFR of each stenosis in a tandem lesion [8], but its application was limited in a tandem lesion. Thus we have developed an equation which can be used in a diffuse/sequential coronary lesion (Equation A) [9]. However, the calculation requires coronary wedge pressure measurements, which makes the application of the equation in clinical practice difficult. Therefore, when using FFR to evaluate a sequential or diffuse coronary lesion, pullback curve of the pressure wire under maximum hyperemia is used to detect the target lesion with the largest ΔFFR. After stenting the target lesion, repeat measurement of pullback recordings of FFR is conducted[10–12]. The concept of this strategy was named as "the rule of big delta" by Park et al. [11].

We consider that the existence of intra-stent pressure gradient after intervention makes the prediction even more difficult [13–16]. In the present study, we developed an equation which predicts the post-intervention FFR in the diffuse/sequential coronary lesion in consideration with the residual intra-stent FFR gradient (Equation B). Equation B predicted the post-intervention FFR with a

1.3 ± 1.0% error in the in-vitro experiment. This study results indicate that the equation was almost perfect for predicting the post-intervention FFR in the in-vitro coronary circulation. However, the prediction error was 8.0 ± 7.2% in the clinical data analysis, which was considered too large to be used in clinical practice. The results indicate that physicians need to conduct multiple pullback recordings of FFR in the treatment of a diffuse/sequential lesion based on "the rule of big delta".

Several reasons are proposed for the large prediction error which was observed in the clinical data analysis while the error was minimal in the in-vitro study. First, keeping a steady state of maximal hyperemia is mandatory during a pressure wire pullback for the assessment of diffuse/serial coronary lesion, while FFR value is usually fluctuating during continuous infusion of intravenous adenosine [23,24]. Thus, the FFR pullback curve is inevitably affected by the fluctuation of maximal hyperemia, which inevitably causes a considerable error in predicting the post-intervention FFR in a diffuse/sequential coronary lesion. Second, pressure wire was coregistered with angiography visually in this analysis. The operators were

required to observe pressure wire pullback curve and angiographic information at the same time and visually coregister the 2 pieces of information, which could represent the cause of prediction error. Third, Equation B includes 4 independent variables. All these variables are influenced by many factors in vivo, including nervous system, cardiovascular humoral factor, and stimulus during the procedure. Even small errors of each variable eventually become large errors in Equation B. In post-intervention iFR prediction, the equation includes only 2 variables, which is considered a great advantage of iFR.

Study Limitations:

Several limitations exist in the present study. First, the in vitro coronary circulation model differed from the complex human coronary circulation in many ways. The model had no side branches between stenosis, and a single large collateral artery connected the donor and recipient arteries. Coronary arteries are not uniformly smooth unlike silicone tubes. These differences limit the direct

applicability of in vitro model to real world coronary physiology. Second, the clinical data analysis was retrospectively conducted; thus, the accuracy of data acquisition might be inferior to a prospective study. Third, the sample size of the present study was relatively small for both in vitro and clinical data sets. Fourth, coronary wedge pressure measurements were conducted during balloon dilatation without the continuous infusion of adenosine. Several studies reported that maximal hyperemia can be induced by balloon occlusion of the coronary artery [17,25], but the coronary occlusive hyperemia might make a small difference that could affect the prediction of post-intervention FFR in diffuse/sequential coronary stenosis.

Conclusions:

Prediction of post-intervention FFR in a diffuse/sequential lesion is only possible in an in-vitro model of coronary circulation. In clinical practice, prediction is difficult due to considerable errors even when residual intra-stent pressure gradient is considered. Physicians need to conduct multiple pullback recordings of

FFR in the treatment of a diffuse/sequential lesion, if physicians prefer FFR over resting indices.

Acknowledgements:

The authors would like to thank Ms. Sumiko Horie and Mr. Shiichi Hamaguchi for their advice regarding the in-vitro experiments. Special thanks also go to Editage (*www.editage.jp*) for English language editing.

Funding statement

The authors received no specific funding for this study.

Conflict of interest statement:

The authors have no conflicts of interest to declare.

References

1. van Nunen LX, Zimmermann FM, Tonino P a L, Barbato E, Baumbach A, Engstrøm T, Klauss V, MacCarthy P a, Manoharan G, Oldroyd KG, Ver Lee PN, van't Veer M, Fearon WF, De Bruyne B, Pijls NHJ. Fractional flow reserve versus angiography for guidance of PCI in patients with multivessel coronary artery disease (FAME): 5-year follow-up of a randomised controlled trial. *Lancet*. 2015;6736:1–8.
2. Tonino PAL, De Bruyne B, Pijls NHJ, Siebert U, Ikeno F, van' t Veer M, Klauss V, Manoharan G, Engstrøm T, Oldroyd KG, Ver Lee PN, MacCarthy PA, Fearon WF. Fractional flow reserve versus angiography for guiding percutaneous coronary intervention. *N Engl J Med*. 2009;360:213–24.
3. Götberg M, Christiansen EH, Gudmundsdottir IJ, Sandhall L, Danielewicz M, Jakobsen L, Olsson S-E, Öhagen P, Olsson H, Omerovic E, Calais F, Lindroos P, Maeng M, Tödt T, Venetsanos D, James SK, Kåregren A, Nilsson M, Carlsson J, Hauer D, Jensen J, Karlsson A-C, Panayi G, Erlinge D, Fröbert O. Instantaneous Wave-free Ratio versus Fractional Flow Reserve to Guide PCI. *N Engl J Med*. 2017:NEJMoa1616540.
4. Davies JE, Sen S, Dehbi H-M, Al-Lamee R, Petraco R, Nijjer SS, Bhindi R, Lehman SJ, Walters D, Sapontis J, Janssens L, Vrints CJ, Khashaba A, Laine M, Van Belle E, Krackhardt F, Bojara W, Going O, Härle T, Indolfi C, Niccoli G, Ribichini F, Tanaka N, Yokoi H, Takashima H, Kikuta Y, Erglis A, Vinhas H, Canas Silva P, Baptista SB, Alghamdi A, Hellig F, Koo B-K, Nam C-W, Shin E-S, Doh J-H, Brugaletta S, Alegria-Barrero E, Meuwissen M, Piek JJ, van Royen N, Sezer M, Di Mario C, Gerber RT, Malik IS, Sharp ASP, Talwar S, Tang K, Samady H, Altman J, Seto AH, Singh J, Jeremias A, Matsuo H, Kharbanda RK, Patel MR, Serruys P, Escaned J. Use of the Instantaneous Wave-free Ratio or Fractional Flow Reserve in PCI. *N Engl J Med*. 2017:NEJMoa1700445.
5. Sen S, Escaned J, Malik IS, Mikhail GW, Foale R a., Mila R, Tarkin J, Petraco R, Broyd C, Jabbour R, Sethi A, Baker CS, Bellamy M, Al-Bustami M, Hackett D, Khan M, Lefroy D, Parker KH, Hughes AD, Francis DP, Di Mario C, Mayet J, Davies JE. Development and validation of a new adenosine-independent index of stenosis severity from coronary waveintensity analysis: Results of the ADVISE (ADenosine Vasodilator Independent Stenosis Evaluation) study. *J Am Coll Cardiol*. 2012;59:1392–402.
6. Kikuta Y, Cook CM, Sharp ASP, Salinas P, Kawase Y, Shiono Y, Giavarini A, Nakayama M, De Rosa S, Sen S, Nijjer SS, Al-Lamee R, Petraco R, Malik IS, Mikhail GW, Kaprielian RR, Wijntjens GWM, Mori S, Hagikura A, Mates M,

Mizuno A, Hellig F, Lee K, Janssens L, Horie K, Mohdnazri S, Herrera R, Krackhardt F, Yamawaki M, Davies J, Takebayashi H, Keeble T, Haruta S, Ribichini F, Indolfi C, Mayet J, Francis DP, Piek JJ, Di Mario C, Escaned J, Matsuo H, Davies JE. Pre-Angioplasty Instantaneous Wave-Free Ratio Pullback Predicts Hemodynamic Outcome In Humans With Coronary Artery Disease: Primary Results of the International Multicenter iFR GRADIENT Registry. *JACC Cardiovasc Interv*. 2018;11:757–67.

7. Nijjer SS, Sen S, Petraco R, Mayet J, Francis DP, Davies JER. The Instantaneous wave-Free Ratio (iFR) pullback: A novel innovation using baseline physiology to optimise coronary angioplasty in tandem lesions. *Cardiovasc Revascularization Med*. 2015;16:167–71.
8. De Bruyne B, Pijls NHJ, Heyndrickx GR, Hodeige D, Kirkeeide R, Gould KL. Pressure-Derived Fractional Flow Reserve to Assess Serial Epicardial Stenoses : Theoretical Basis and Animal Validation. *Circulation*. 2000;101:1840–7.
9. Saito N, Matsuo H, Kawase Y, Watanabe S, Bao B, Yamamoto E, Watanabe H, Nakatsuma K, Ueno K, Kimura T. In vitro assessment of mathematically-derived fractional flow reserve in coronary lesions with more than two sequential stenoses. *J Invasive Cardiol*. 2013;25:642–9.
10. Kern MJ, Seto AH. Instantaneous Wave-Free Ratio Pressure Pullback With Virtual Percutaneous Coronary Intervention Planning: Seeing the Future of Coronary Interventions?∗. *JACC Cardiovasc Interv*. 2018;11:768–70.
11. Park S-J, Ahn J-M, Pijls NHJ, De Bruyne B, Shim EB, Kim Y-T, Kang S-J, Song H, Lee J-Y, Kim W-J, Park D-W, Lee S-W, Kim Y-H, Lee CW, Park S-W. Validation of functional state of coronary tandem lesions using computational flow dynamics. *Am J Cardiol*. 2012;110:1578–84.
12. Matsuo H, Kawase Y. FFR and iFR guided percutaneous coronary intervention. *Cardiovasc Interv Ther*. 2016:4–14.
13. Tanaka N, Pijls NHJ, Yamashita J, Kimura Y, Ogawa M, Murata N, Sakoda K, Hoshino K, Hokama Y, Yamashina A. Analysis of suboptimal stent deployment using intravascular ultrasound and coronary pressure pullback measurement. *J Cardiol*. 2017;69:613–8.
14. Van't Veer M, Pijls NHJ, Aarnoudse W, Koolen JJ, Van De Vosse FN. Evaluation of the haemodynamic characteristics of drug-eluting stents at implantation and at follow-up. *Eur Heart J*. 2006;27:1811–7.
15. Leesar MA, Satran A, Yalamanchili V, Helmy T, Abdul-Waheed M, Wongpraparut N. The impact of fractional flow reserve measurement on clinical outcomes after transradial coronary stenting. *EuroIntervention*. 2011;7:917–23.

16. Matsuo A, Shimoo S, Takamatsu K, Tsuji Y, Kyodo A, Mera K, Koide M, Isodono K, Tsubakimoto Y, Sakatani T, Inoue K, Fujita H. Visualization of the improvement of myocardial perfusion after coronary intervention using motorized fractional flow reserve pullback curve. *Cardiovasc Interv Ther*. 2018;33:99–108.
17. Seiler C. The human coronary collateral circulation. *Heart*. 2003;89:1352–7.
18. Erne P, Schoenenberger AW, Burckhardt D, Zuber M, Kiowski W, Buser PT, Dubach P, Resink TJ, Pfisterer M. Effects of Percutaneous Coronary Interventions in Silent Ischemia. *JAMA*. 2007;297:1985–91.
19. Shaw LJ, Berman DS, Maron DJ, Mancini GBJ, Hayes SW, Hartigan PM, Weintraub WS, O'Rourke RA, Dada M, Spertus JA, Chaitman BR, Friedman J, Slomka P, Heller G V., Germano G, Gosselin G, Berger P, Kostuk WJ, Schwartz RG, Knudtson M, Veledar E, Bates ER, McCallister B, Teo KK, Boden WE. Optimal medical therapy with or without percutaneous coronary intervention to reduce ischemic burden: results from the Clinical Outcomes Utilizing Revascularization and Aggressive Drug Evaluation (COURAGE) trial nuclear substudy. *Circulation*. 2008;117:1283–91.
20. Lee JM, Choi KH, Park J, Hwang D, Rhee T, Kim J, Park J, Kim HY, Jung HW, Song Y Bin, Hahn J, Hospital NN, Korea S, Korea S, Hospital U, Korea S, Korea S. Physiologic and Clinical Assessment of Resting Physiologic Indices : Resting Full - Cycle Ratio , Diastolic Pressure - Ratio , and Instantaneous Wave - Free Ratio n.d.
21. Neumann F-J, Sousa-Uva M, Ahlsson A, Alfonso F, Banning AP, Benedetto U, Byrne RA, Collet J-P, Falk V, Head SJ, Jüni P, Kastrati A, Koller A, Kristensen SD, Niebauer J, Richter DJ, Seferović PM, Sibbing D, Stefanini GG, Windecker S, Yadav R, Zembala MO, Wijns W, Glineur D, Aboyans V, Achenbach S, Agewall S, Andreotti F, Barbato E, Baumbach A, Brophy J, Bueno H, Calvert PA, Capodanno D, Davierwala PM, Delgado V, Dudek D, Freemantle N, Funck-Brentano C, Gaemperli O, Gielen S, Gilard M, Gorenek B, Haasenritter J, Haude M, Ibanez B, Iung B, Jeppsson A, Katritsis D, Knuuti J, Kolh P, Leite-Moreira A, Lund LH, Maisano F, Mehilli J, Metzler B, Montalescot G, Pagano D, Petronio AS, Piepoli MF, Popescu BA, Sádaba R, Shlyakhto E, Silber S, Simpson IA, Sparv D, Tavilla G, Thiele H, Tousek P, Van Belle E, Vranckx P, Witkowski A, Zamorano JL, Roffi M, Windecker S, Aboyans V, Agewall S, Barbato E, Bueno H, Coca A, Collet J-P, Coman IM, Dean V, Delgado V, Fitzsimons D, Gaemperli O, Hindricks G, Iung B, Jüni P, Katus HA, Knuuti J, Lancellotti P, Leclercq C, McDonagh TA, Piepoli MF, Ponikowski P, Richter DJ, Roffi M, Shlyakhto E, Sousa-Uva M, Simpson IA, Zamorano JL, Pagano D, Freemantle N, Sousa-Uva M, Chettibi M, Sisakian H, Metzler B, İbrahimov F,

Stelmashok VI, Postadzhiyan A, Skoric B, Eftychiou C, Kala P, Terkelsen CJ, Magdy A, Eha J, Niemelä M, Kedev S, Motreff P, Aladashvili A, Mehilli J, Kanakakis I-G, Becker D, Gudnason T, Peace A, Romeo F, Bajraktari G, Kerimkulova A, Rudzītis A, Ghazzal Z, Kibarskis A, Pereira B, Xuereb RG, Hofma SH, Steigen TK, Witkowski A, de Oliveira EI, Mot S, Duplyakov D, Zavatta M, Beleslin B, Kovar F, Bunc M, Ojeda S, Witt N, Jeger R, Addad F, Akdemir R, Parkhomenko A, Henderson R. 2018 ESC/EACTS Guidelines on myocardial revascularization. *Eur Heart J*. 2018:1–96.

22. Dattilo PB, Prasad A, Honeycutt E, Wang TY, Messenger JC. Contemporary patterns of fractional flow reserve and intravascular ultrasound use among patients undergoing percutaneous coronary intervention in the United States: Insights from the national cardiovascular data registry. *J Am Coll Cardiol*. 2012;60:2337–9.
23. Toth GG, Johnson NP, Jeremias A, Pellicano M, Vranckx P, Fearon WF, Barbato E, Kern MJ, Pijls NHJ, De Bruyne B. Standardization of Fractional Flow Reserve Measurements. *J Am Coll Cardiol*. 2016;68:742–53.
24. Matsumura M, Johnson NP, Fearon WF, Mintz GS, Stone GW, Oldroyd KG, De Bruyne B, Pijls NHJ, Maehara A, Jeremias A. Accuracy of Fractional Flow Reserve Measurements in Clinical Practice: Observations From a Core Laboratory Analysis. *JACC Cardiovasc Interv*. 2017;10:1392–401.
25. Kawase Y, Omori H, Kawasaki M, Tanigaki T, Hirata T, Okamoto S, Ota H, Kikuchi J, Okubo M, Kamiya H, Hirakawa A, Suzuki T, Matsuo H. Postocclusional Hyperemia for Fractional Flow Reserve after Percutaneous Coronary Intervention. *Circ Cardiovasc Interv*. 2017;10:1–6.

Table

Table 1. Baseline clinical characteristics of 67 patients

Variables	Value
Age (years)	69.1 ±9.0
Male gender, n (%)	48 (71.6%)
Height (cm)	160.8 ± 10.3
Body Weight (kg)	66.2 ± 15.1
Diabetes mellitus, n (%)	34 (51.5%)
Hypertension, n (%)	46 (70.0%)
Dyslipidemia, n (%)	40 (61%)
Smoker, n (%)	9 (13.6%)
Hemodialysis, n (%)	5 (7.5%)
Previous myocardial infarction, n (%)	13 (19.4%)
Left ventricular ejection fraction, %	62.5 ± 10.7
Stable angina	64 (95.5%)
Unstable angina	3 (4.5%)

Table 2. Procedural data in 67 sequential coronary lesions

Variable	Value
Lesion location, LAD, LCX, RCA	48 (71.6%), 7 (10.4%), 12 (17.9%)
Pre-FFR data	
Pre-FFR	0.68 ± 0.11
Collateral flow index (=Pw/Pa)	0.17 ± 0.10
ΔFFR of the target lesion	0.23 ± 0.11
Pre-QCA data	
Lesion length, mm	23.4 ± 9.0
Pre-reference diameter, mm	2.91 ± 0.52
Pre-minimum lumen diameter, mm	1.30 ± 0.35
Pre-%DS, %	54.9 ± 12.2
Procedural data	
Implanted stent number	1.2 ± 0.4
Total stent length, mm	29.9 ± 13.0
Procedure time, min	92.9 ± 31.1
Contrast volume, cc	99.9 ± 40.6
Post-FFR data	
Post-FFR	0.81 ± 0.07
Post-ΔFFR of the target lesion	0.04 ± 0.03
ΔFFR/mm, mm	0.0015 ± 0.0013
Post-QCA data	
Post-reference diameter, mm	3.15 ± 0.45
Pre-minimum lumen diameter, mm	3.00 ± 0.45
Post-%DS, %	5.8 ± 9.9

Figure Legends

Figure 1. Schematic model representing the coronary circulation with a sequential lesion and a collateral circulation. (A) Before coronary intervention. The resistance of the target lesion is expressed as R_s. (B) After coronary intervention. The resistance of target lesion changes to R'_s.

Figure 2. In vitro experimental system. (A) The simulation system comprising a pump as well as systemic and coronary circulation. (B) Three pressure wires are placed in the coronary circulation: one placed proximally to the target stenosis (black arrow), another placed distally to the target stenosis (blue arrow), and the last one placed in the most distal point of the coronary circulation (red arrow).

Figure 3. Results of the in-vitro experiment. (A-C) Linear regression and Bland-Altman plots. The dotted line is the line of identity. (A) $FFR_{apparent}$ compared with FFR_{post}. (B) $FFR_{predicted}$ compared with FFR_{post}. (C) $FFR_{adjusted}$ compared with FFR_{post}. (D) The absolute differences to FFR_{post}. A - the absolute difference of $FFR_{apparent}$ to FFR_{post}. B - the absolute difference of $FFR_{predicted}$ to FFR_{post}. C - the absolute difference

of $FFR_{adjusted}$ to FFR_{post}.

Figure 4. Results of the clinical data analyses. (A-C) Linear regression and Bland-Altman plots. The dotted line is the line of identity. (A) $FFR_{apparent}$ compared with FFR_{post}. (B) $FFR_{predicted}$ compared with FFR_{post}. (C) $FFR_{adjusted}$ compared with FFR_{post}. (D) The absolute differences to FFR_{post}. A, the absolute difference of $FFR_{apparent}$ to FFR_{post}. B, the absolute difference of $FFR_{predicted}$ to FFR_{post}. C, the absolute difference of $FFR_{adjusted}$ to FFR_{post}.

Figure 5. Estimated FFR value using fixed value of CFI and ΔFFR in clinical data analyses. (A) Linear regression and Bland-Altman plots. (B) The absolute differences. A - the absolute difference of $FFR_{adjusted}$ to FFR_{post}. B - the absolute difference of $FFR_{fixed\text{-}adjusted}$ to FFR_{post}.

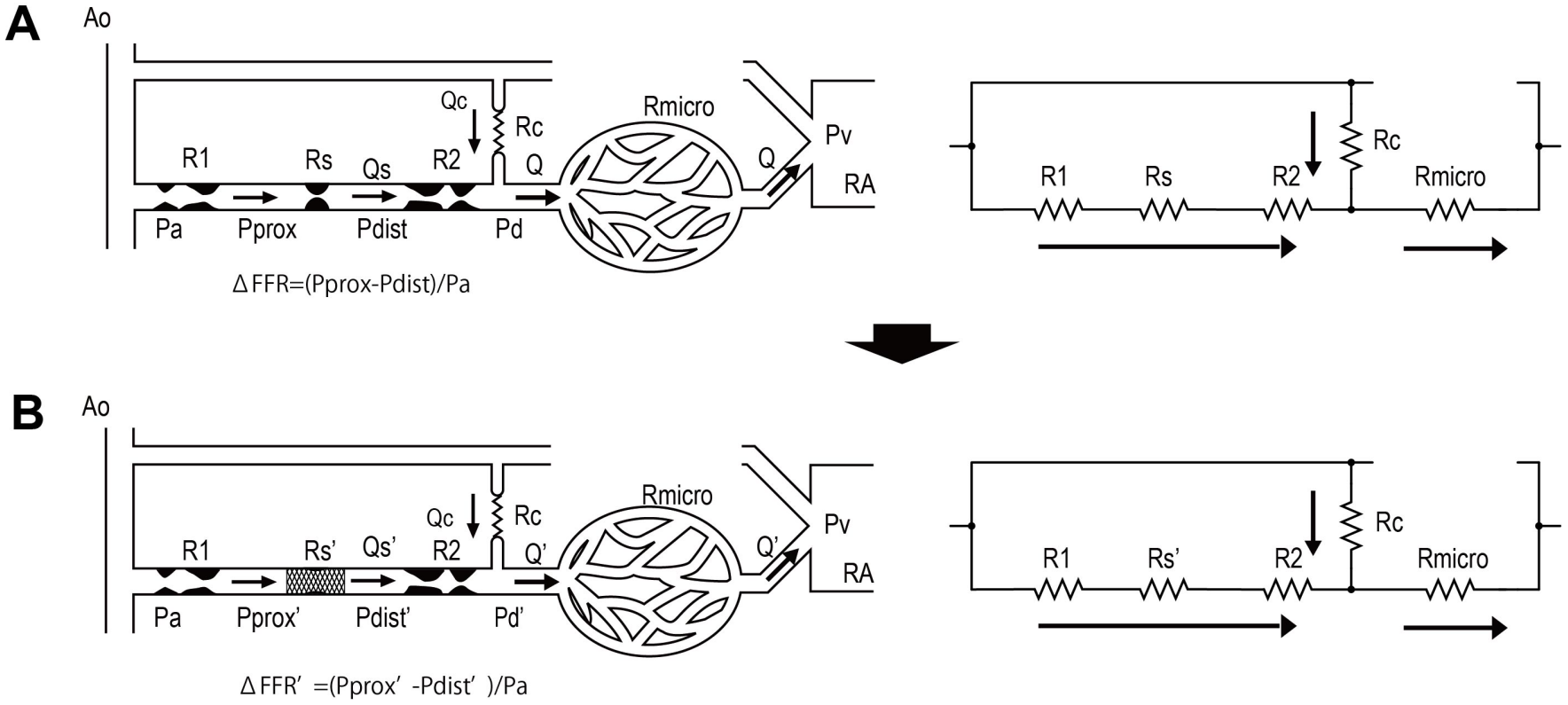

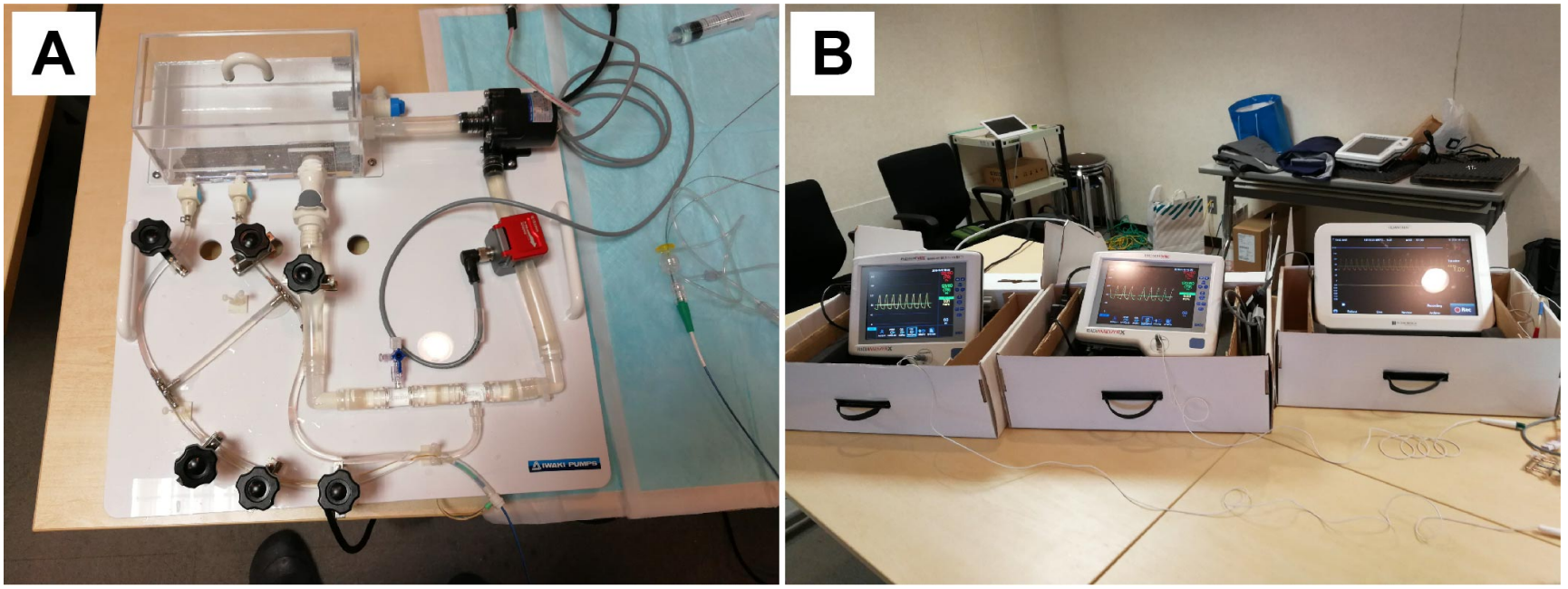

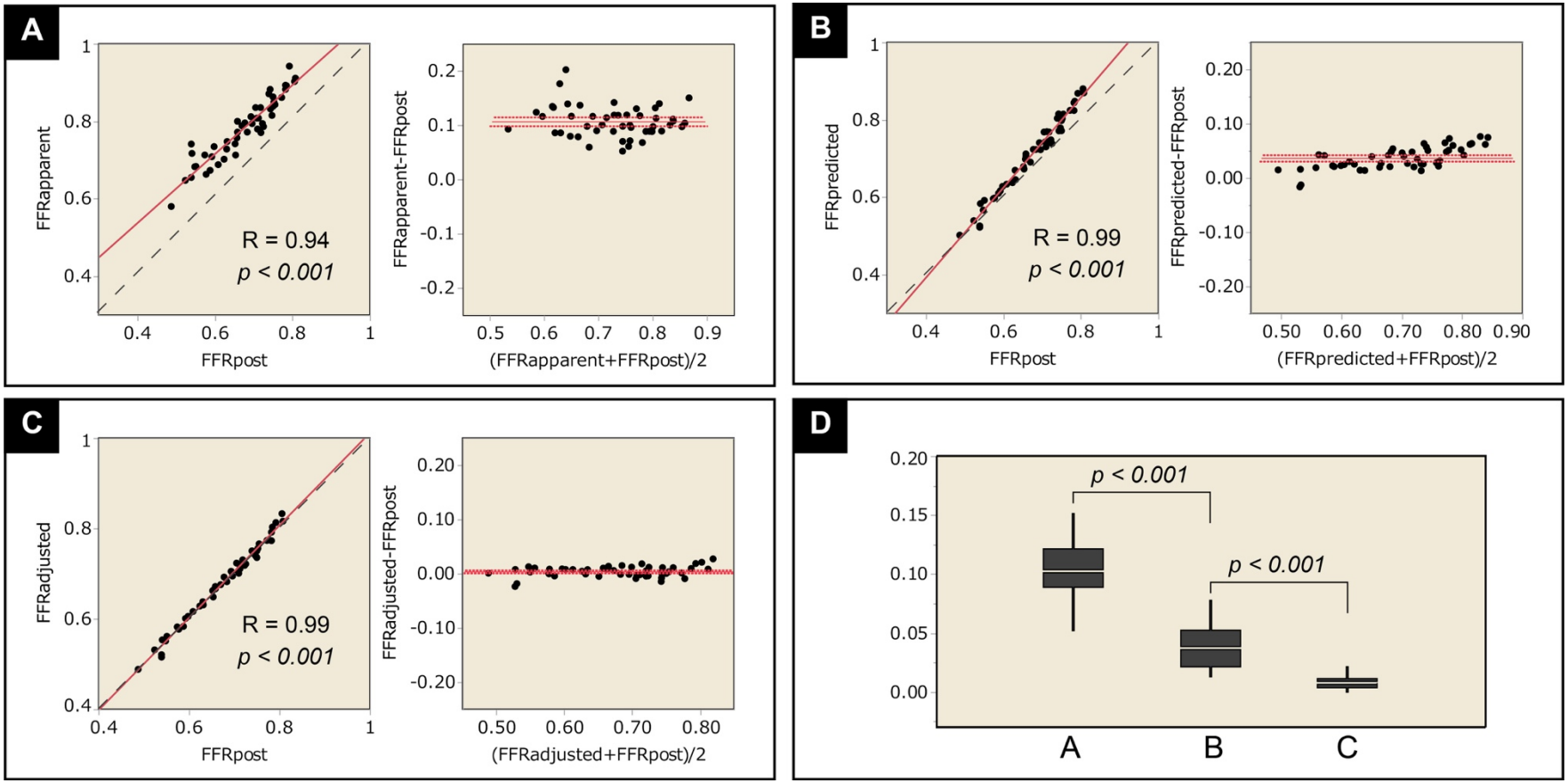

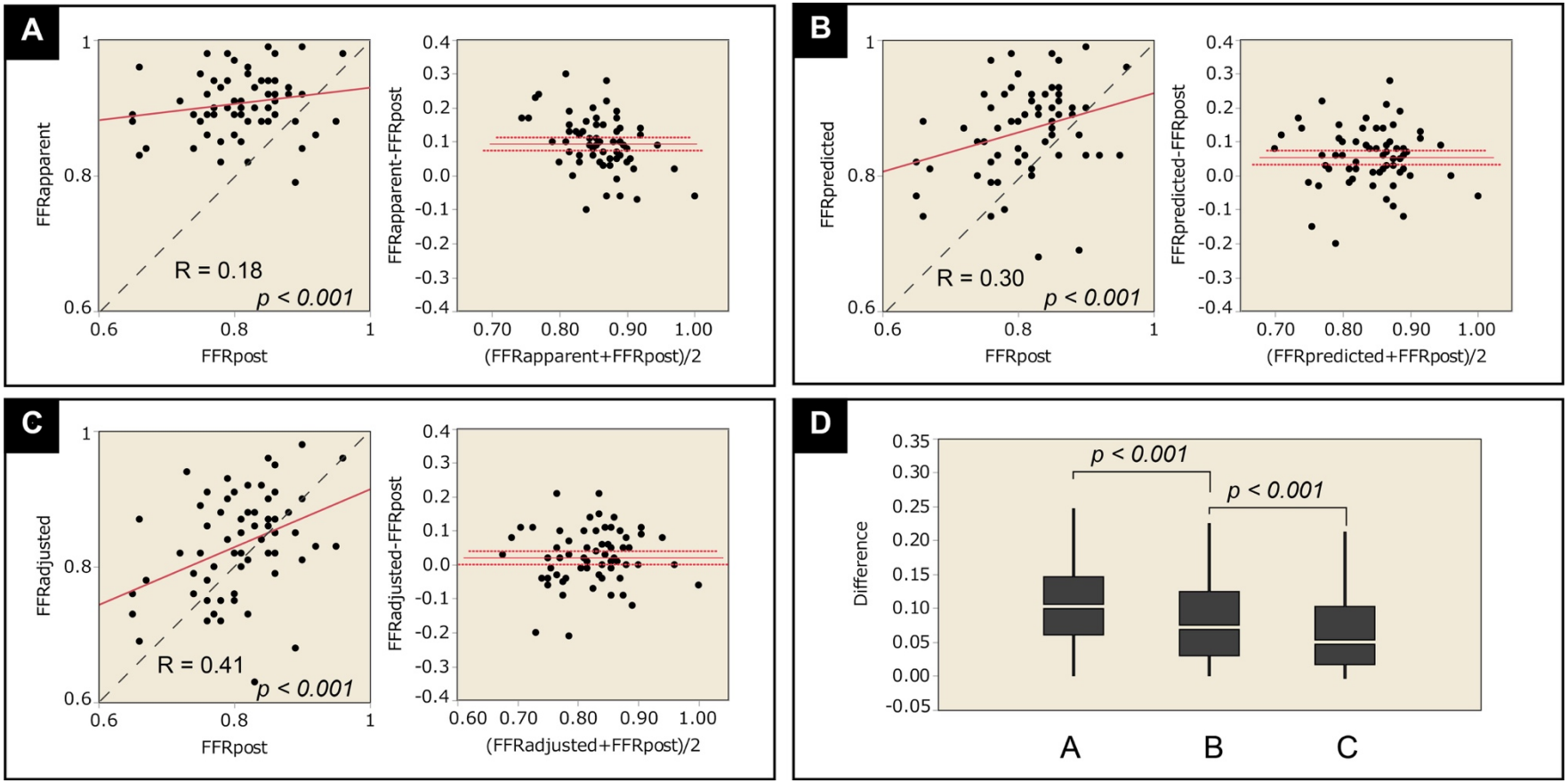

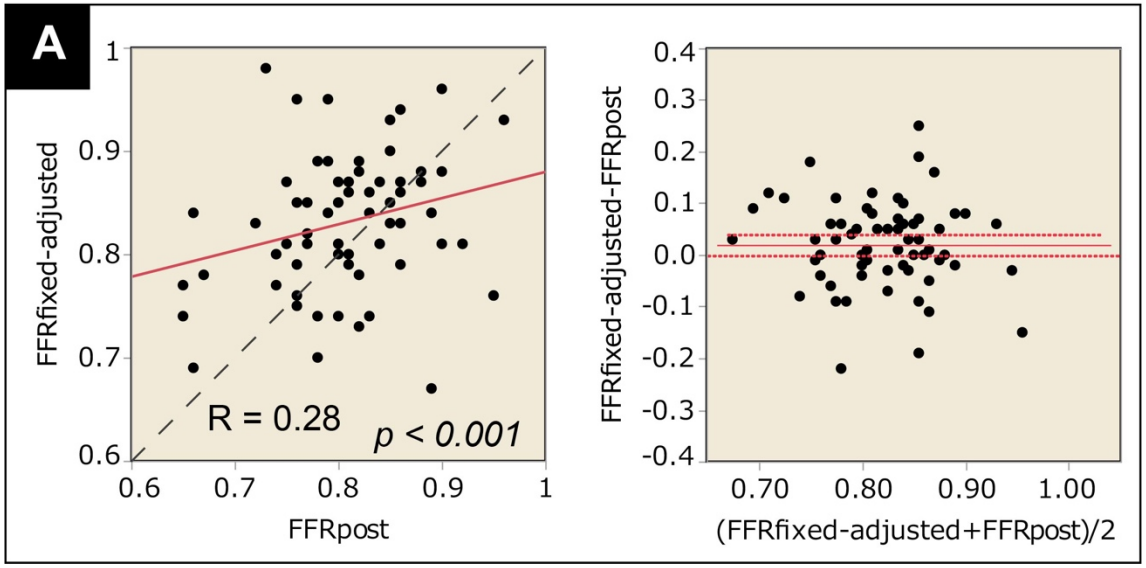

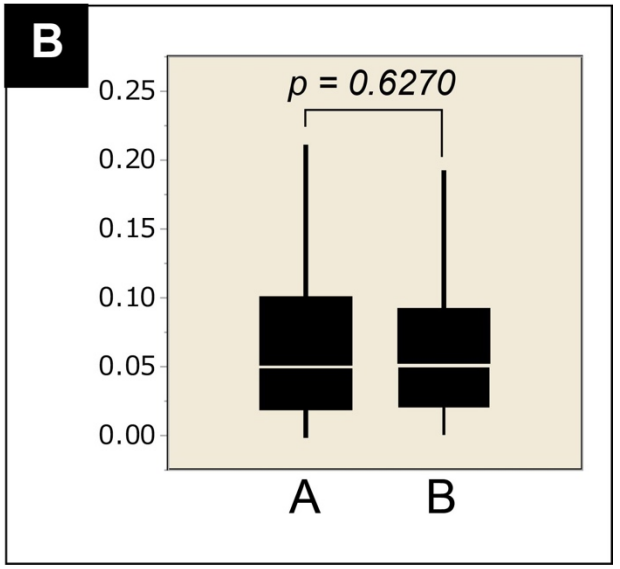

Appendix

Derivation of Equations A and B

In this appendix, the derivations of Equations (A) and (B) are presented. Consider a coronary circulation model that has sequential coronary stenosis (Figure 1 in the main text). All of the terminology is the same as that in the main text. When P_v is considered 0, the following equations are obtained: $FFR_{pre} = P_d/P_a$, $FFR_{post} = P'_d/P_a$, $CFI = P_w/P_a$, $\Delta FFR = (P_{prox} - P_{dist})/P_a$, and $\Delta FFR' = (P'_{prox} - P'_{dist})/P_a$. All calculations are done in the assumption that the pressure drop across a stenosis is proportional to the flow. Under this assumption, the electric circuit can be considered an analog of the fluid circulation and the pressure ratio can be expressed in terms of resistance. Note that the inverse of the equivalent resistance of two or more resistors connected in parallel is the algebraic sum of the inverses of the individual resistances. The following equations are obtained:

$$\mathrm{CFI} = \frac{R_{micro}}{R_c + R_{micro}} \quad (1)$$

$$FFR_{pre} = \frac{R_{micro}}{\left(\frac{1}{\frac{1}{R_1 + R_x + R_2} + \frac{1}{R_c}}\right) + R_{micro}} \quad (2)$$

$$\Delta\mathrm{FFR} = (1 - \mathrm{FFR}_{pre})\frac{R_x}{R_1 + R_x + R_2} \quad (3)$$

$$FFR_{post} = \frac{R_{micro}}{\left(\frac{1}{\frac{1}{R_1 + R'_x + R_2} + \frac{1}{R_c}}\right) + R_{micro}} \quad (4)$$

$$\Delta\mathrm{FFR}' = (1 - \mathrm{FFR}_{post})\frac{R'_x}{R_1 + R'_x + R_2} \quad (5)$$

By solving the above equations (1) to (4), R_{micro}, R_c, R_x and R'_x are presented using CFI, FFR_{pre}, ΔFFR, $\Delta FFR'$, R_1 and R_2:

$$R_{micro} = \frac{(R_1 + R_2)\left(FFR_{pre} - CFI\right)}{(1 - CFI)\left(1 - (FFR_{pre} + \Delta FFR)\right)} \quad (6)$$

$$R_x = \frac{(R_1 + R_2)\Delta FFR}{\left(1 - (FFR_{pre} + \Delta FFR)\right)} \quad (7)$$

$$R_c = \frac{(R_1 + R_2)\left(FFR_{pre} - CFI\right)}{CFI\left(1 - (FFR_{pre} + \Delta FFR)\right)} \quad (8)$$

$$R'_x = \frac{(R_1 + R_2)\Delta FFR'}{\left(1 - (FFR_{post} + \Delta FFR')\right)} \quad (9)$$

By substituting equations (6) to (9) into equation (5), the following equation (B) is obtained:

$$FFR_{post} = \frac{FFR_{pre}(1 - CFI) - CFI\Delta FFR - \Delta FFR'(FFR_{pre} - CFI)}{1 - \Delta FFR - CFI} \quad (B)$$

Equation B calculates the post-intervention FFR with residual pressure gradient across the stent. When there is no residual pressure gradients across the stent, ΔFFR' equals to 0, then the following equation (A) is obtained:

$$FFR_{post} = \frac{FFR_{pre}(1 - CFI) - CFI\Delta FFR}{1 - \Delta FFR - CFI} \quad (A)$$

Equation A calculates the post-intervention FFR when no residual intra-stent pressure gradients are existed.

AsiaIntervention
Official Journal of the Asian Pacific Society of Interventional Cardiology
(APSIC) and the Interventional Cardiology Foundation of India (ICFI)
www.asiaintervention.org

Title: **Acute Embolization of MitraClip Rescued by Snaring.**

Authors: Ningyan Wong, MBBS, MRCP, M.Med; See Hooi Ewe, MBBS, MRCP, PhD; Wei Chieh Jack Tan, MBBS, MRCP, M Med, FAMS, ACSM, FAsCC, FAPSIC, FESC, FACC, MBA; Khung Keong Yeo, MBBS, FAMS, FACC, FSCAI, ABIM

Manuscript number: AIJ-D-19-00009

Manuscript submission date: 23 February 2019

Revisions received: 15 June 2019, 7 July 2019, 16 March 2020

Accepted date: 11 June 2020

Acute Embolization of MitraClip Rescued by Snaring

Ningyan Wong [1], MBBS, MRCP, M.Med; See Hooi Ewe [1], MBBS, MRCP, PhD; Wei Chieh Jack Tan [1], MBBS, MRCP, M Med, FAMS, ACSM, FAsCC, FAPSIC, FESC, FACC, MBA; Khung Keong Yeo [1], MBBS, FAMS, FACC, FSCAI, ABIM

1. Department of Cardiology, National Heart Centre Singapore

Running Title: Snaring of dislodged MitraClip

Corresponding Author
Name: Wong Ningyan
Address: National Heart Centre Singapore, 5 Hospital Drive, Singapore 169609
E-mail: wong.ningyan@singhealth.com.sg

Conflicts of interest statement
Yeo Khung Keong is a speaker, consultant and proctor for Abbott Vascular (MitraClip) and reports receiving honoraria from Abbott Vascular. The other authors have no conflicts of interest to declare.

Classification:
Mitral regurgitation, Mitral valve disease, Mitral valve repair, Transesophageal echocardiogram, Miscellaneous

Funding:
None

First author photo:

Abstract

Percutaneous edge-to-edge repair of the mitral valve with the MitraClip system is a safe and effective treatment option for patients with severe degenerative mitral regurgitation who are at prohibitive surgical risk. However, although uncommon, complications do happen and one of which is device embolization. We describe a case of complete dislodgement of MitraClip that occurred periprocedurally and how this can be rescued percutaneously using a snare.

Abbreviations

MR mitral regurgitation
TEE transesophageal echocardiogram
LA left atrium

Introduction

Transcatheter mitral valve repair with the MitraClip (Abbott Vascular, Abbott Park, Illinois, USA) system is a treatment option for patients with severe degenerative mitral regurgitation (MR) at prohibitive surgical risk. Earlier trials had demonstrated its excellent safety profile, but complications, can happen. We describe a case of periprocedural complete dislodgement of the MitraClip and how it was successfully rescued percutaneously with a snare, followed by its retrieval through a surgical cutdown of the common femoral vein access.

Methods

An 83-year-old Chinese gentleman with stage 3 chronic kidney disease, idiopathic thrombocytopenic purpura and anemia of chronic disease presented with recurrent heart failure from severe MR. Transesophageal echocardiogram (TEE) showed Barlow's

disease – bileaflet mitral valve prolapse involving A2/P2, A3/P3, with predominant prolapse of the A3/P3 segments and a small ruptured chord at the tip of the posteromedial segment (Figure 1), resulting in severe eccentric MR. After a Heart Team discussion, in view of increased age and multiple co-morbidities, he was deemed to be at high surgical risk (EuroSCORE II and STS scores for mortality were 7.3% and 22.1%, respectively). He was hence offered percutaneous repair of the mitral valve with the MitraClip system.

The 1st clip was deployed at the A3/P3 segments. Although this reduced the MR severity from 4+ to 3+, it was still substantial lateral to the clip. A decision was made to deploy a 2nd clip. Prior to clip release, the anterior and posterior leaflet grasps were imaged with adequate tissue seen within the clip. After releasing the lock line, the 2nd clip detached immediately from the posterior leaflet but remained attached to the anterior leaflet. At this time, the team decided to deploy the clip and rescue the situation with a 3rd clip lateral to the 2nd clip to stabilize it. However, after the deployment pin was released, the entire clip was detached from the mitral valve and held in the left atrium (LA) by the gripper line (Figure 2). Decision was made to snare the clip with bailout surgery as an option. First, the guide catheter was withdrawn into the right atrium to reduce the risk of air embolism. A 0.035" wire was placed into the LA via the same transseptal hole. Initially the 9-15mm EN Snare (Merit Medical Systems, Inc. South Jordan, Utah, USA) was used but failed to grasp the clip. This was changed to a 25mm Amplatz GooseNeck snare (ev3, Plymouth, Minnesota, USA) via an 8F guide and we were successful in snaring it. The clip was pulled back across the inter-atrial septum and down into the femoral vein (Figure 3). A surgical cutdown to the common femoral vein was performed to retrieve the clip (Figure 4).

The mitral valve was reassessed and there were no signs of new torn chords or flail segments. There was residual moderate to severe MR (Figure 5). At this time, given the circumstances and that there was no worsening of MR, a decision was made to stop.

Results

He was discharged well 4 days after the procedure. The patient clinically improved to New York Heart Association Class I with no further heart failure exacerbation. His follow up echocardiogram at 1-month, 6- month and 1-year showed stable residual moderate to severe MR.

Discussion

Clip detachment is a potential complication of using the MitraClip system. Single leaflet detachment occurs more commonly but complete detachment and embolization is exceedingly rare with only a few cases reported to date[1-5]. MitraClip operators must be familiar with handling this complication.

The mechanism of early periprocedural clip detachment is usually due to inadequate leaflet capture or insertion. In our case, despite what appeared to be adequate grasping of both leaflets, there was early detachment of initially the posterior leaflet, and subsequently the anterior leaflet. Other possibilities include tearing of leaflet, grasping of chordae instead of leaflet and slippage of the leaflet from the clip and grippers. In this case, leaflet tearing was unlikely as there was no worsening of MR or visible torn leaflets. Our clinical suspicion is that while we had grasped the leaflets, there was probably insufficient capture resulting in subsequent slippage and embolization.

The MitraClip gripper line acts as a final fail-safe mechanism in the event of a completely detached clip. Because the clip was still attached to the gripper line, it

prevented complete embolization of the device and could thus be rescued with a snare. We used a 0.035" wire to ensure access to the LA and via the wire we were able to deliver the snare. The EN Snare shape was not suitable in this case as it was difficult to get the 'flower' shaped snare to grasp the embolized clip. On the other hand, it was easier to get the GooseNeck snare distal to the clip and by pulling back against the catheter, we were able to close the snare and capture the clip. Another possibility was to pull both ends of the gripper line in an attempt to retrieve the clip. However, we felt that this method will not give us adequate control to pull the clip across the interatrial septum and into the guiding catheter. Secondly, there was a risk of losing the clip completely if the nitinol gripper line stretches and break.

Limitations

None

Conclusion

In conclusion, adequate leaflet insertion into each clip arm is essential. In event that complete clip dislodgement occurs, it is crucial not to lose the gripper line as it can function as a final safety mechanism to prevent systemic embolization. Snaring allows for a percutaneous avenue to rescue the dislodged clip.

Impact on daily practice

Clip embolization is a potential complication of using the MitraClip system and this can happen periprocedurally. Snaring is a percutaneous option to rescue the dislodged clip and MitraClip operators must be familiar with handling this complication.

Conflicts of interest statement

Yeo Khung Keong is a speaker, consultant and proctor for Abbott Vascular (MitraClip) and reports receiving honoraria from Abbott Vascular. The other authors have no conflicts of interest to declare.

References

1. Chitsaz S, Jumean M, Dayah T, Rajagopal K, Kar B. Late MitraClip Embolization: A New Cause of ST-Segment-Elevation Myocardial Infarction. *Circ Cardiovasc Interv.* 2016;9.
2. Bilge M, Alsancak Y, Ali S, Duran M, Bicer H. An extremely rare but possible complication of MitraClip: embolization of clip during follow-up. *Anatol J Cardiol.* 2016;16:636-8.
3. Seeburger J, Raschpichler M, Lurz P, Noack T, Ender J, Misfeld M. Late device embolization after transcatheter mitral valve edge-to-edge repair. *Eur Heart J.* 2017;38:1260.
4. Alozie A, Westphal B, Kische S, Kaminski A, Paranskaya L, Bozdag-Turan I, Ortak J, Schubert J, Steinhoff G, Ince H. Surgical revision after percutaneous mitral valve repair by edge-to-edge device: when the strategy fails in the highest risk surgical population. *Eur J Cardiothorac Sur.* 2014;46:55-60
5. Pasala TKR, Safi LM, Jelnin V, Ruiz CE. Catching a "MitraFly". *JACC Cardiovasc Interv*. 2018 Jun 25;11:1201-1203.

Figures:

- Figure 1 – Transesophageal echocardiogram (TEE) images (A, B) of prolapsed segments A2/P2, A3/P3 with predominant prolapse of A3/P3 and a small ruptured chord at the tip of the posteromedial segment (red arrow). Severe mitral
-

regurgitation (MR) in the (C) apical 4-chamber and the (D) left ventricular outflow tract (LVOT) view.

- Figure 2 – Fluoroscopic images showing (A, B) complete detachment of the 2nd MitraClip (white arrows) after deployment but held within the left atrium by the gripper line. TEE images of the dislodged MitraClip (red arrows) in the (C) LVOT view and (D) the enface 3D view where it is held above the mitral valve by the gripper line.
- Figure 3 – Fluoroscopic images showing (A) an unsuccessful attempt to snare the MitraClip with the EN Snare. (B) The GooseNeck snare was successful in snaring the clip. Clip was (C) pulled across the interatrial septum and (D) to the common femoral vein.
- Figure 4 - Photographic images (A, B) of the MitraClip removed from the patient, with the GooseNeck snare still attached to one of the clip arms.
- Figure 5 – TEE images of residual moderate to severe MR in the (A) intercommissural view and the (B) LVOT view, with just a single MitraClip deployed. There was no evidence of torn leaflets seen.

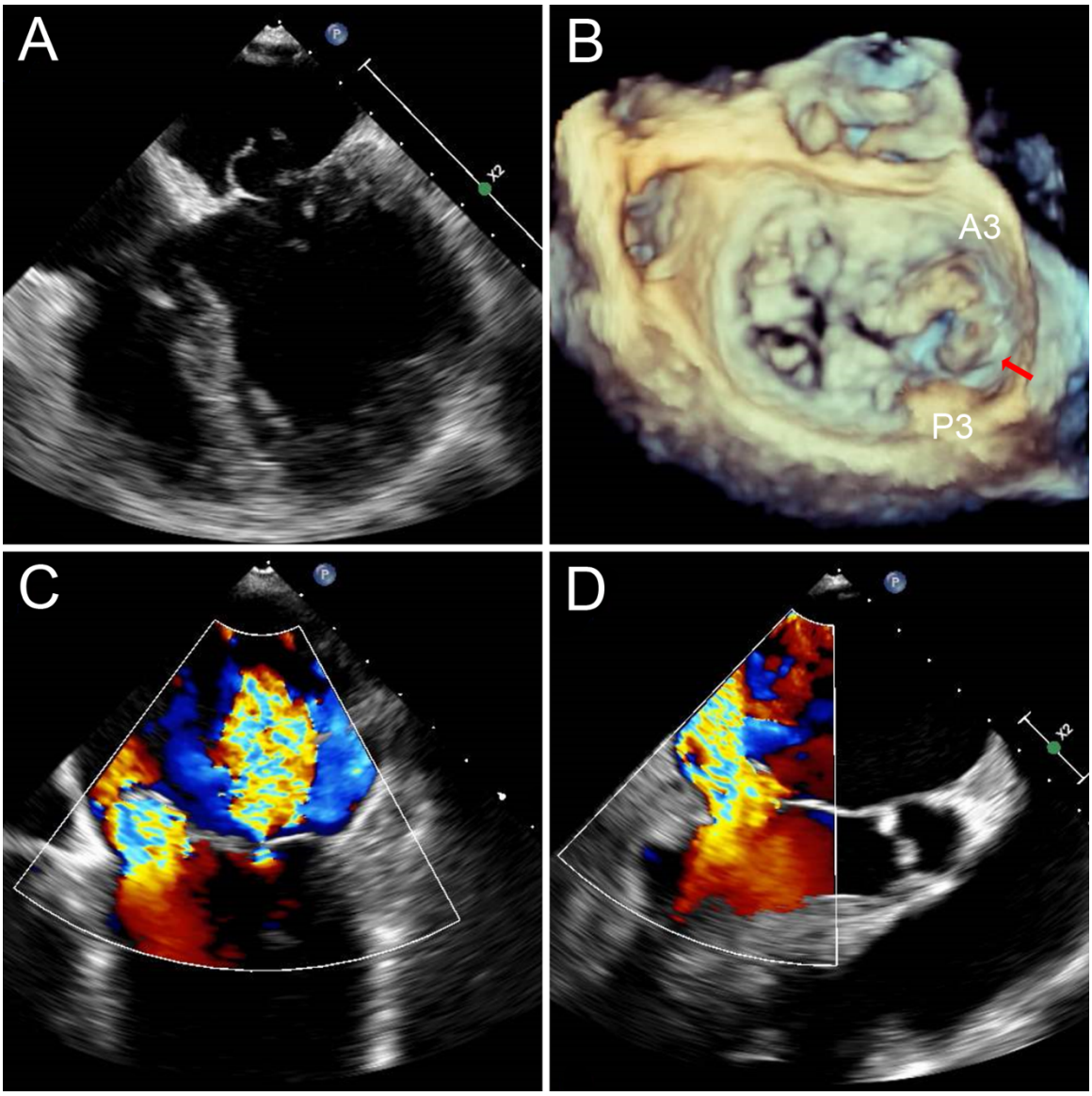

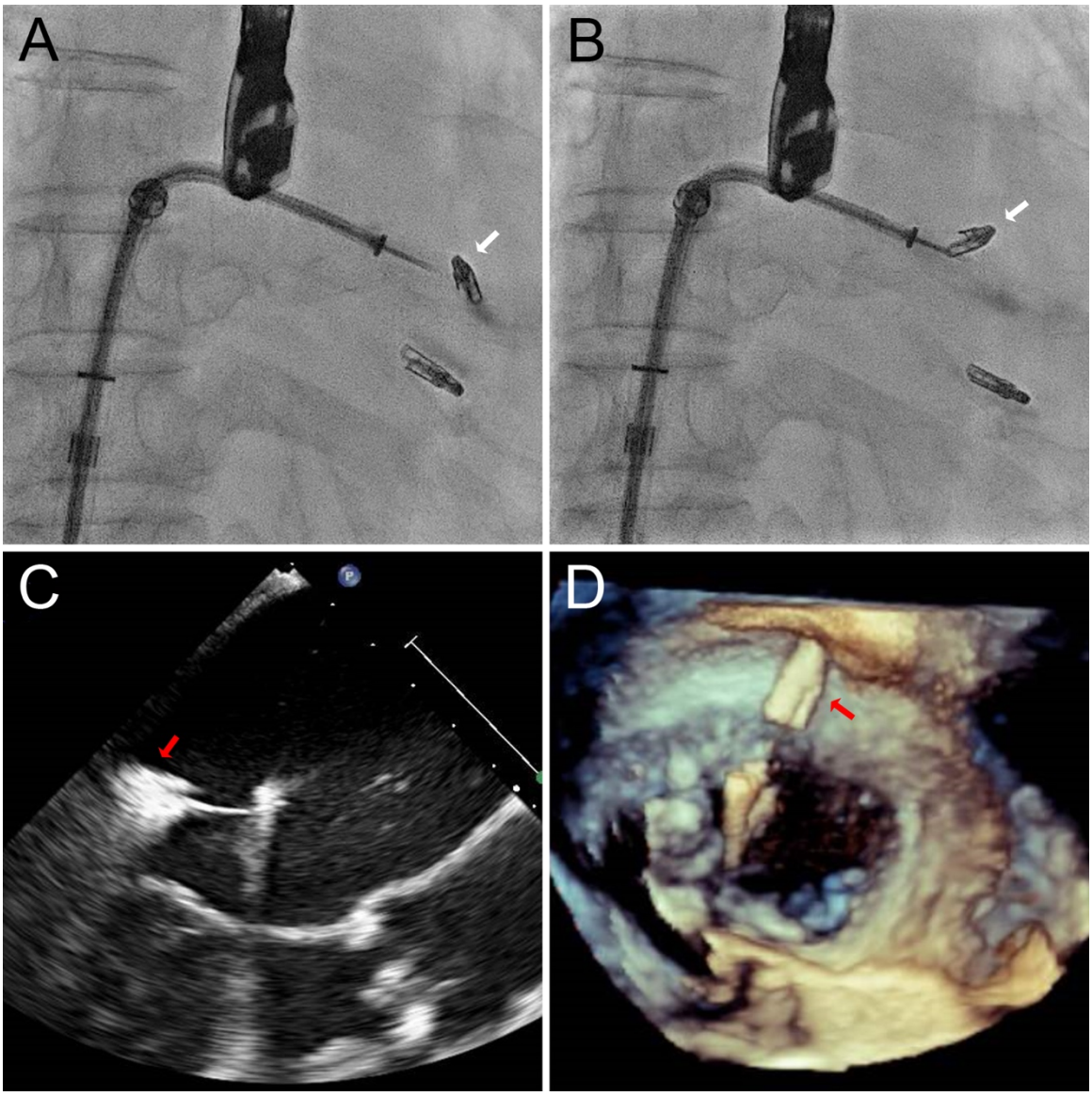

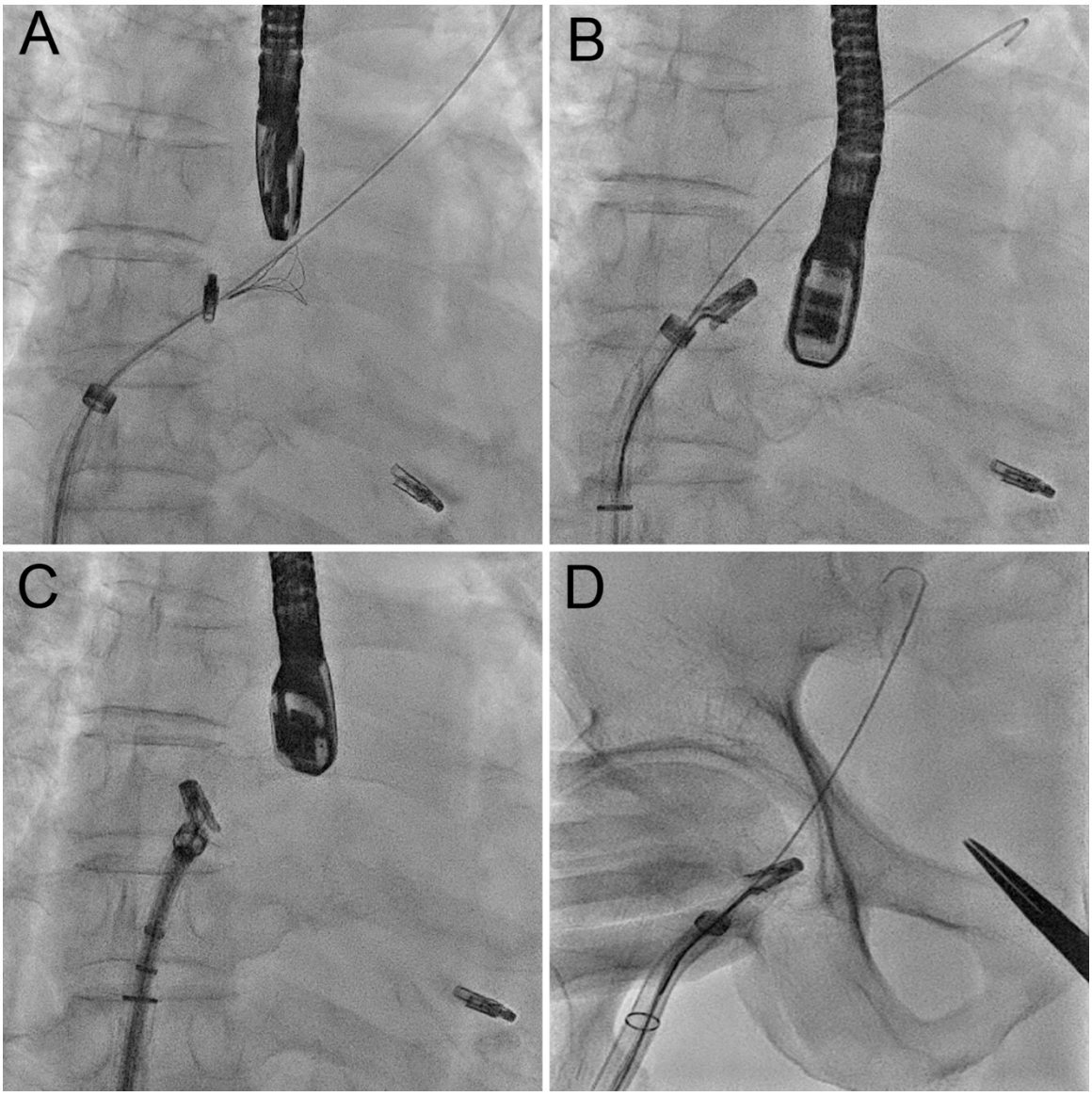

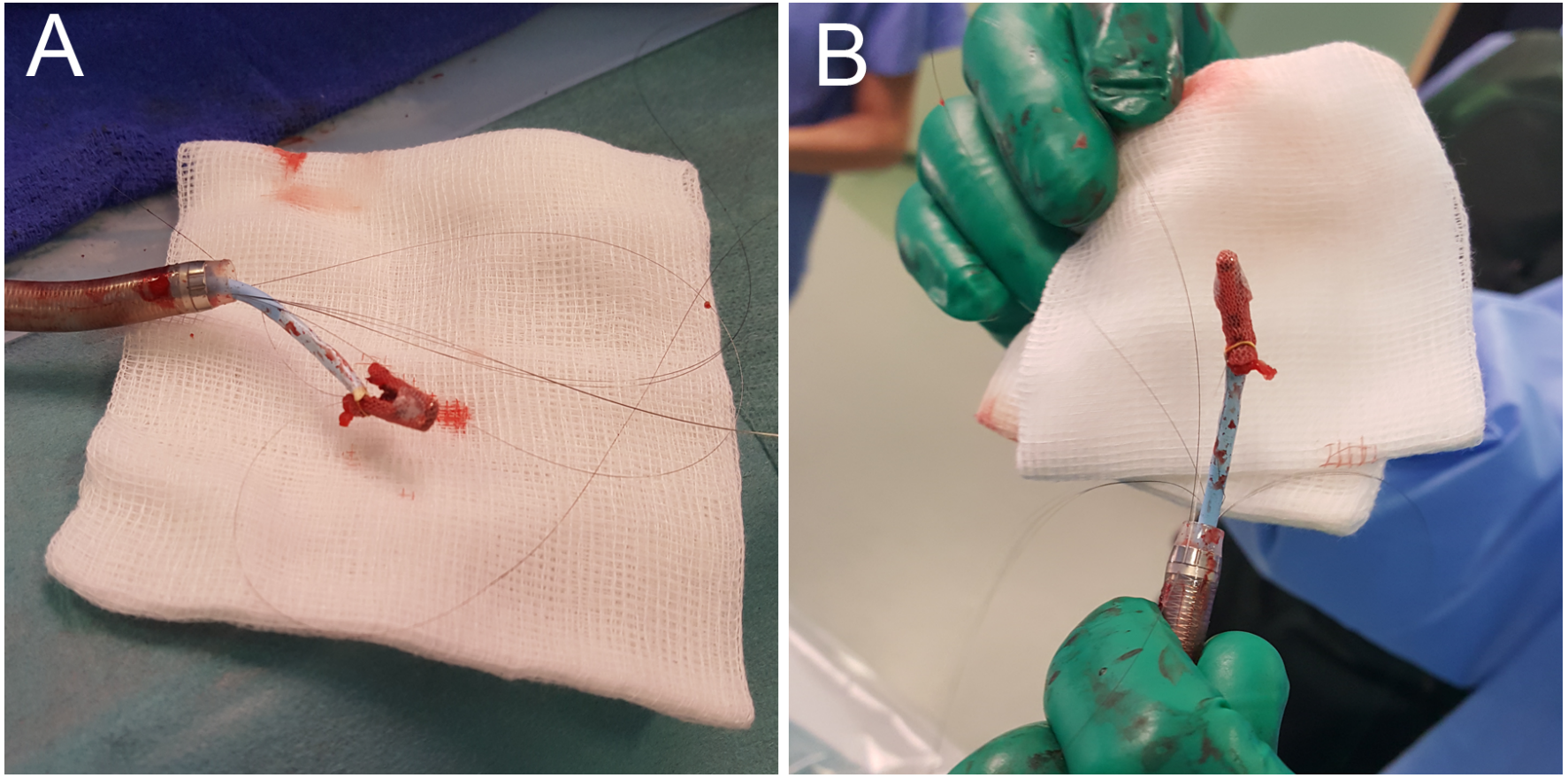

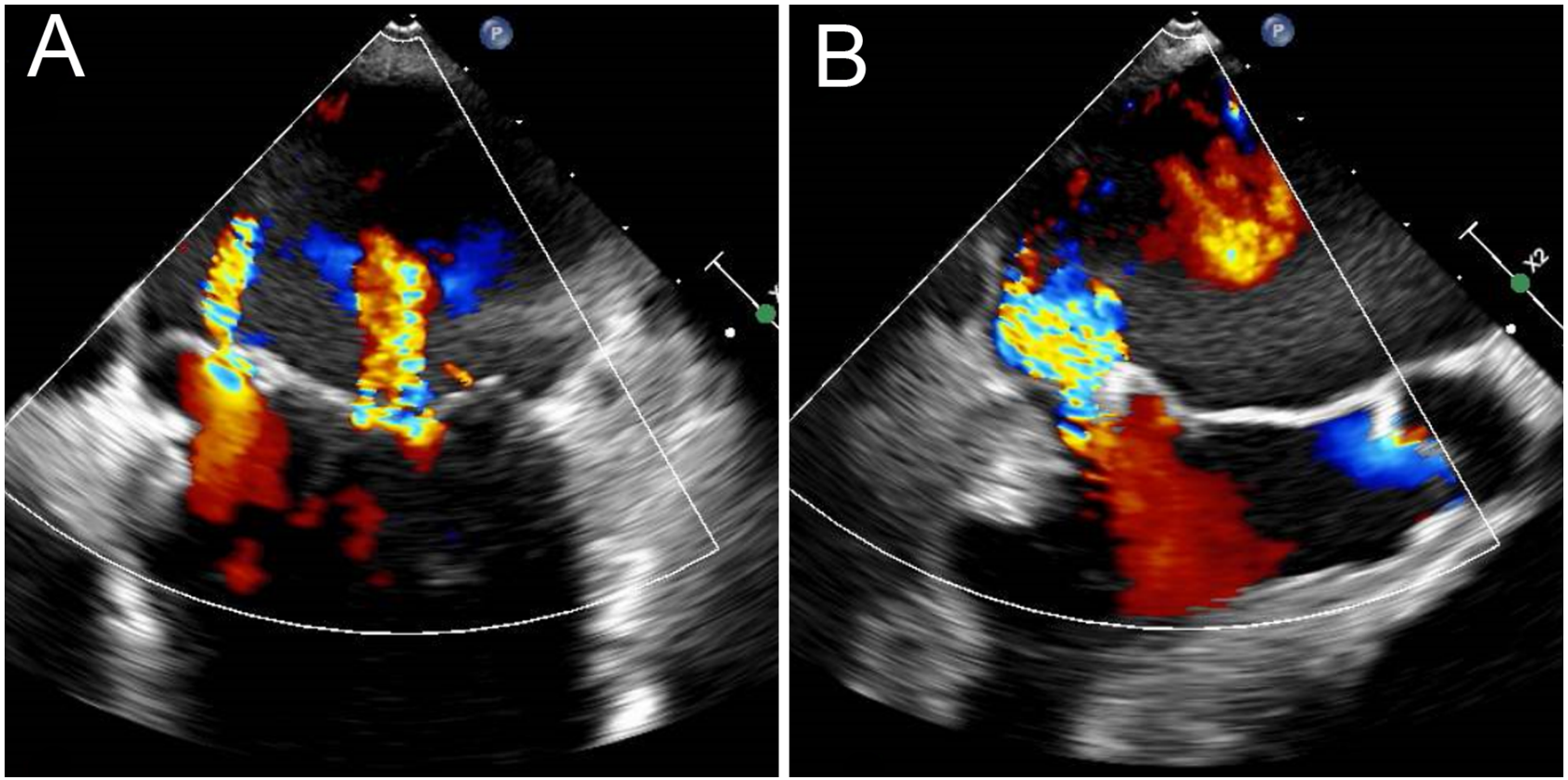

AsiaIntervention

Official Journal of the Asian Pacific Society of Interventional Cardiology

(APSIC) and the Interventional Cardiology Foundation of India (ICFI)

www.asiaintervention.org

Title: Vascular Plug device implantation for bailout treatment of severe mitral regurgitation after unsuccessful edge to edge repair.

Authors: Michael P. Chrissoheris, M.D; Afrodite Tzifa, M.D; Antonios Halapas, M.D; Konstantinos Spargias, M.D

Manuscript number: AIJ-D-19-00027

Manuscript submission date: 22 June 2019

Revisions received: 22 September 2019, 4 February 2020, 6 June 2020

Accepted date: 10 June 2020

Vascular Plug device implantation for bailout treatment of severe mitral regurgitation after unsuccessful edge to edge repair.

Michael P. Chrissoheris[1], MD; Afrodite Tzifa[2], MD; Antonios Halapas[1], MD; Konstantinos Spargias[1], MD

[1] Department of Transcatheter Heart Valves, HYGEIA Hospital Athens Greece

[2] Department of Pediatrics and Adult Congenital Heart Disease, MITERA Hospital Athens Greece

Short Running Title: Vascular plug after mitral edge to edge repair

DESIGNATED CORRESPONDING AUTHOR

Michael P. Chrissoheris, MD

Department of Transcatheter Heart Valves, HYGEIA Hospital

9 Erythrou Stavrou Street

Marousi 15123, GREECE

E-mail: mchrissoheris@hotmail.com

CONFLICT OF INTEREST: The authors have no conflicts of interest to declare.

KEYWORDS:
Mitral regurgitation; Mitral valve repair; Specific closure device / technique; Transoesophageal Echocardiogram

ABBREVIATIONS

MR: Mitral regurgitation

3D-TEE: Three dimensional transesophageal echocardiography

E2E: Edge to edge

AVP: Amplatz Vascular Plug

ASD: Atrial septal defect

Relapse of severe mitral regurgitation after transcatheter edge to edge (E2E) repair is caused by annular dilatation, leaflet tear or leaflet detachment[1]. Commonly, repeat E2E repair is performed but results may be suboptimal. The possibility of further repair with use of vascular plugs or septal occluders has been suggested as bail out in difficult "no option" situations[2, 3].

A 63-year-old male with end-stage renal failure on haemodialysis and prior open-heart surgery was referred for symptomatic relapse of severe functional ischemic mitral regurgitation 24 months after successful repair with two MitraClips. Three-dimensional transesophageal echocardiography (3D-TEE) demonstrated a tear of the posterior leaflet insertion on the medial clip, resulting in loss of edge to edge approximation and severe regurgitation (Figure 1A and 1B, Online Video 1,2).

Heart team discussion led to the decision for a repeat E2E repair and a third MitraClip was implanted medial to the failed device (Figure 1C, Online Video 3). However, despite appropriate positioning and leaflet capture, severe mitral regurgitation persisted from the area between the clips (Figure 1D). In addition, significant iatrogenic right to left shunting at the interatrial septum resulted in refractory hypoxemia. After multidisciplinary discussions, it was decided to proceed with closure of the mitral regurgitant orifice with use of a vascular plug, and of the atrial septal defect with an occluder device (both procedures in same setting three days later). Following re-entry into the left atrium, a steerable guide catheter was advanced within the mitral regurgitant orifice and an Amplatz Vascular Plug (AVP) II 16mm (size based on 3D multiplanar reconstructions of the mitral regurgitant jet vena contracta measured at 13x8mm, Supplementary Figure 1) was implanted successfully resulting in modest reduction in regurgitation (Figure 1E, 1F, 1G 1H, Online Movies 5,6,7) without stenosis (mean gradient 3.0mmHg, Supplementary Figure 2). Before exiting the left atrium, an Amplatz Septal Occluder (8mm) was deployed mitigating the interatrial shunt. Postoperatively, there was marked improvement in oxygenation and hemodynamics allowing transfer out of the intensive care for further treatment of medical comorbidities.

Figure 1.
1A 3D-TEE of the mitral valve with two MitraClips in place. There was partial tear of the posterior leaflet insertion into the medial device (arrow)
1B Severe mitral regurgitation from the area between the clips
1C Implantation of a third MitraClip medially to the failed device
1D After release, severe mitral regurgitation reappeared between the devices
1E-H Deployment of a 16mm AVP-II device in the regurgitant orifice seen from superior (**1E)**, anterior (**1F**) and posterior side (**1G**) with modest reduction in mitral regurgitation severity (**1H**).

References

1. Kreidel F, Frerker C, Schlüter M, Alessandrini H, Thielsen T, Geidel S, Schäfer U and Kuck K-H. Repeat MitraClip Therapy for Significant Recurrent Mitral Regurgitation in High Surgical Risk Patients. *Impact of Loss of Leaflet Insertion*. 2015;8:1480-1489.
2. Kubo S, Cox JM, Mizutani Y, Uberoi A, Chakravarty T, Nakajima Y, Hussaini A, Tat E, Makar M and Kar S. Transcatheter Procedure for Residual Mitral Regurgitation After MitraClip Implantation Using Amplatzer Duct Occluder II. *JACC: Cardiovascular Interventions*. 2016;9:1280-1288.
3. Taramasso M, Alessandrini H, Kuwata S, Biasco L, Nietlispach F, Gaemperli O, Zuber M, Linka A, Pedrazzini G, Kreidel F, Frerker C, Kuck K-H and Maisano F. Multicenter Experience With Treatment of Residual Mitral Regurgitation After MitraClip Implantation Using Amplatzer Closure Device. *Mid-Term Results*. 2017;10:966-970.

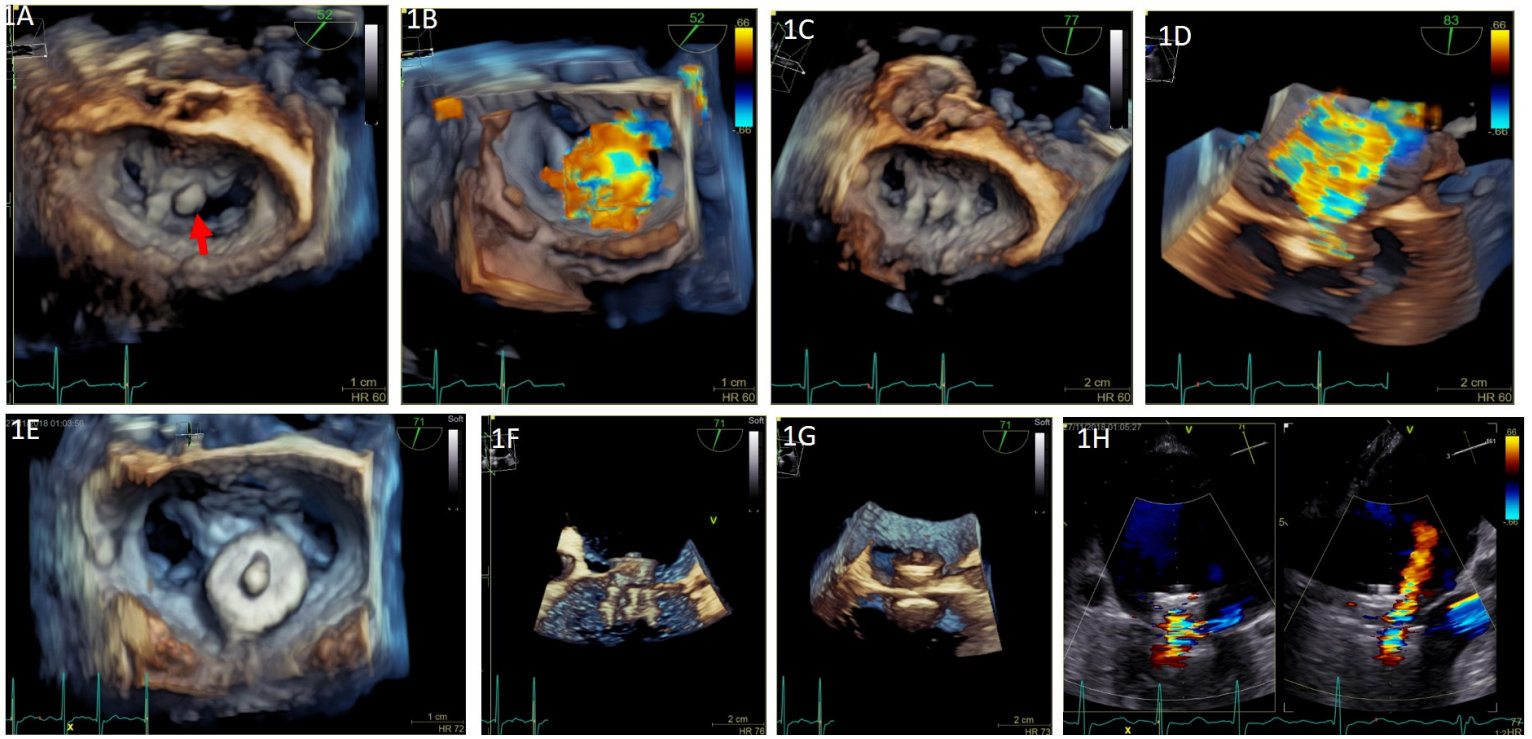

Supplementary Material

Supplementary Figure 1: Multiplanar reconstruction of the regurgitant mitral orifice

Supplementary Figure 2: Mean transmitral gradient post vascular plug implantation

Supplementary Figure 1:

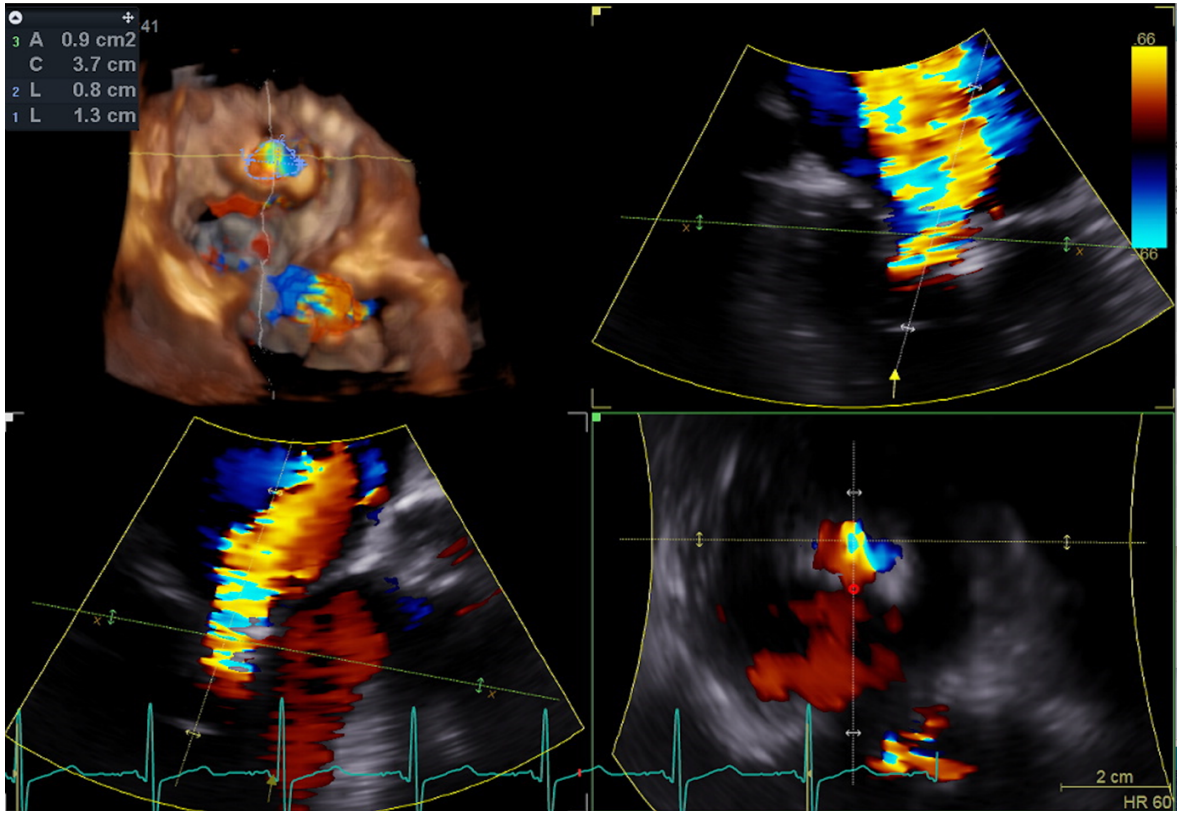

Supplementary Figure 2:

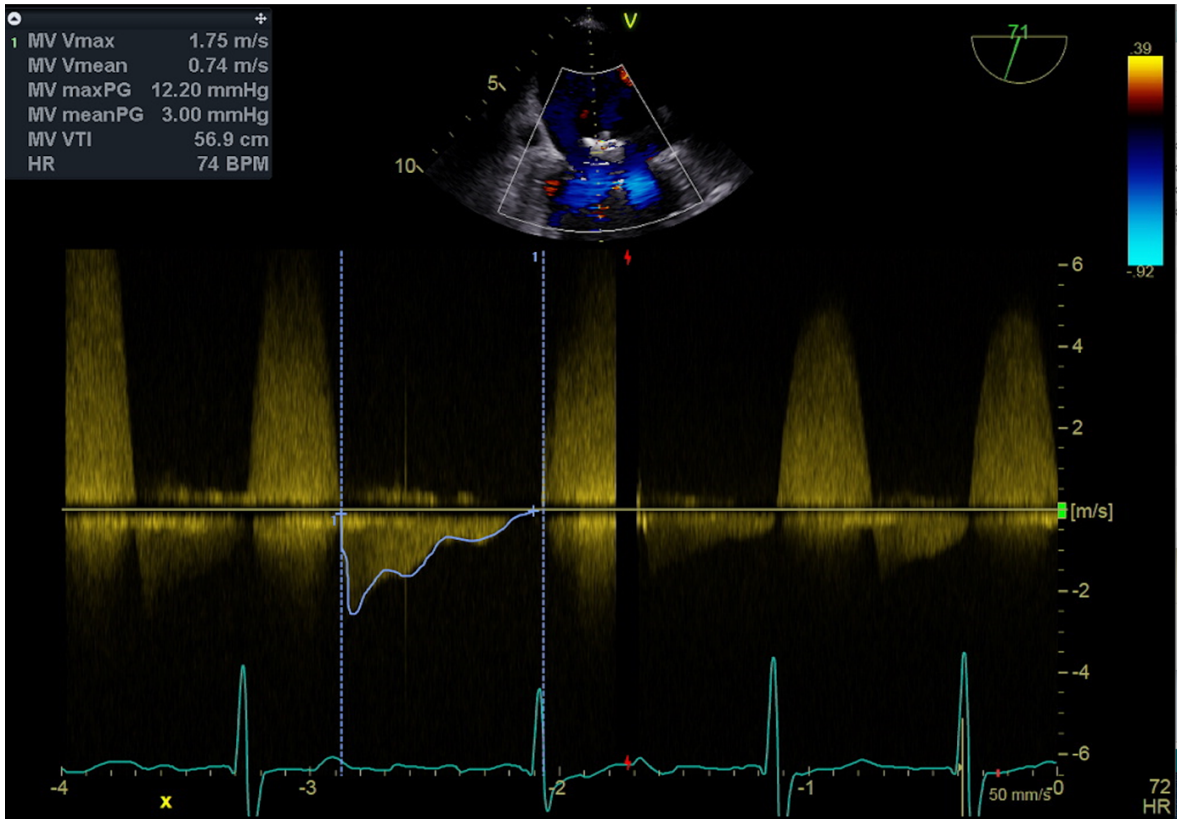

AsiaIntervention
Official Journal of the Asian Pacific Society of Interventional Cardiology
(APSIC) and the Interventional Cardiology Foundation of India (ICFI)
www.asiaintervention.org

Title: **Comparison of percutaneous MitraClip versus mitral valve surgery for severe mitral regurgitation: a meta-analysis.**

Authors: Tom Kai Ming Wang, MBCHB, FRACP, M.D(res); Andrew Chatfield, MBCHB; Michael Tzu Min Wang, MBCHB; Peter Ruygrok, MBCHB, FRACP, M.D(res)

Manuscript number: AIJ-D-19-00036

Manuscript submission date: 16 December 2019

Revisions received: 13 May 2020

Accepted date: 10 July 2020

Comparison of percutaneous MitraClip versus mitral valve surgery for severe mitral regurgitation: a meta-analysis

Tom Kai Ming Wang, MBCHB, FRACP, MD(res)[1,2]

Andrew Chatfield, MBCHB[1]

Michael Tzu Min Wang, MBCHB[1]

Peter Ruygrok, MBCHB, FRACP, MD(res)[1]

Affiliations

1. Green Lane Cardiovascular Service, Auckland City Hospital, Auckland, New Zealand

2. Department of Cardiovascular Medicine, Cleveland Clinic, Cleveland, Ohio, Unites States

Short running title: Mitraclip and mitral valve surgery meta-analysis

Corresponding Author:

Dr Tom Kai Ming Wang

Green Lane Cardiovascular Service, Auckland City Hospital

2 Grafton Road, Grafton, Auckland 1023, New Zealand

Email: TWang@adhb.govt.nz

The authors have no conflicts of interest to declare.

ABSTRACT

Aims: Mitral valve surgery (MVS) is the gold-standard treatment for severe symptomatic mitral regurgitation. Percutaneous mitral valve interventions such as Mitraclip offer another dimension to its management particularly in high risk patients. We meta-analysed the outcomes of MitraClip and MVS.

Methods and results: PubMed, MEDLINE, Embase, Cochrane and Scopus from 1980/01-2019/06 were searched for eligible studies. Data were extracted and pooled using random-effects models. After screening 959 studies and reviewing 21 full-text articles, nine studies totalling 640 Mitraclip and 531 MVS (91% valve repair) procedures. Mitraclip patients were older with more having previous cardiac surgery, coronary disease and higher EuroSCORE (all P<0.05). Pooled operative mortality were similar for Mitraclip 3% versus MVS 5%, odds ratio 0.58, 95% confidence interval (0.28-1.19), as well as at 1 year 1.09 (0.71-1.68) and 3-years 1.08 (0.72-0.163). Mitraclip patients had higher rates of early and late significant MR and more cardiovascular readmissions, while MVS had higher rates of in-hospital bleeding and pacemaker implantation (all P<0.05).

Conclusion: Mitraclip patients had higher baseline risk than MVS, but there were no significant differences in mortality short and long term. Mitraclip patients had higher rates of significant MR post-operatively and cardiovascular admissions, while MVS patients had more procedural complications.

Classifications: mitral regurgitation, mitral valve disease, mitral valve repair

ABBREVIATIONS

95%CI	95% confidence interval
MR	Mitral regurgitation
MVS	Mitral valve surgery
OR	Odds ratios
WMD	Weighted mean differences

CONDENSED ABSTRACT

This meta-analysed compared the outcomes of mitral valve surgery (MVS), the traditional gold-standard intervention for severe mitral regurgitation, and the percutaneous Mitraclip procedures. Data were pooled from nine eligible studies totalling 640 Mitraclip and 531 MVS (91% valve repair) procedures. Mitraclip patients had higher baseline risk, but similar operative, 1- and 3-year mortality. Mitraclip patients had higher rates of significant MR post-operatively and cardiovascular admissions, while MVS patients had more procedural complications. Mitraclip is therefore a valuable alternative strategy for managing severe mitral regurgitation in selected patients, especially those at high surgical risk.

INTRODUCTION

Mitral regurgitation (MR) is a common form of valvular heart disease affecting 2-12% of the general population, and the second commonest valvular indication for cardiac surgery[1-4]. The aetiology of MR is conventionally divided into primary, as a disease affecting valve leaflets, or secondary, with pathology of the mitral valve apparatus and/or left ventricle excluding valve leaflets[1,2]. This classification is important in the determination of prognosis, which is worse for secondary MR, and management strategy[6,7]. Mitral valve surgery (MVS) is the established gold standard method for treating severe primary MR with symptoms, impaired left ventricular ejection fraction, dilated left ventricular end-systolic diameter, new onset atrial fibrillation or severe pulmonary hypertension, and surgical repair is preferable to replacement where feasible[1,2]. Such efficacy of MVS has not translated to secondary MR whose management remain controversial, creating an unmet need in these and other high-risk candidates with severe MR[8,9].

Minimally invasive procedures for valvular heart disease have blossomed over the last decade, and for MR the percutaneous Mitraclip was the first readily available technology[10]. EVEREST-II was the first randomised trial comparing Mitraclip to MVS for primary MR[11]. Two further trials explored Mitraclip for secondary MR compared to medical therapy with conflicting results[12,13]. Nevertheless there remains limited randomised evidence for Mitraclip and their exact roles and

indications remain controversial. This meta-analysis compared the efficacy and safety outcomes of Mitraclip with MVS in patients with severe MR.

METHODS

Literature search:

The meta-analysis was conducted in accordance to the PRISMA guidelines. Relevant studies and abstracts, from January 1 1980 to June 30 2019, were identified through searching five electronic databases including Medline, Embase, PubMed, Cochrane Central Register for Controlled Trials (CENTRAL), and Scopus. The search terms used were "MitraClip", "percutaneous", "transcather", "catheter-based", or "endovascular"; AND "mitral regurgitation". The reference lists of retrieved articles were then screened for potentially relevant studies. Two reviewers (TW and MW) independently conducted the search and evaluated studies for inclusion. Differences were resolved by discussion and consensus.

Inclusion and exclusion criteria

Original studies comparing MitraClip and mitral valve surgery outcomes, in more than twenty adult human subjects (over 18 years of age), with significant mitral regurgitation, were eligible for inclusion. Mortality outcomes for both Mitraclip and MVS had to be reported. Both randomised trials and observational studies were included, and reviews were excluded. When multiple publications reported results from the same trial or cohort, data were extracted and pooled as one study.

Data extraction

Three reviewers (TKMW, AC and MTMW) independently extracted data, using standardised forms. Differences were resolved by discussion and consensus. Data were extracted on study design, patient and intervention characteristics, and mortality and morbidity outcome measures both short and long term.

Statistical analysis

Statistical analyses were performed using Review Manager Version 5.3 (Cochrane Collaboration, Oxford, England). Variables reported by two or more studies were pooled. Meta-analyses were conducted using odds ratios (OR) or weighted mean differences (WMD) with 95% confidence intervals (95%CI), some presented as Forrest Plots. Random effect modelling was utilised, to account for potential variation in methodology and participant characteristics between studies. Heterogeneity of studies and publication bias were assessed using I^2 test and Funnel Plots for each outcome pooled, and no significant heterogeneity or evidence of publication bias were found for all outcomes. All tests were two tailed and $p<0.05$ was considered significant.

RESULTS

There were 959 articles were identified from the literature search. Following abstract review and exclusion of 938 unrelated or duplicate articles, the full-text

of 21 articles were evaluated. Six of these studies did not report both treatment modalities of interest, and six were duplicate trials, leaving nine studies meeting the inclusion criteria selected for subsequent analysis[11, 14-22]. The study design of included studies are summarised in table 1. There was one randomised trial and eight retrospective observational cohort studies, totalling 1,171 patients (640 Mitraclips and 531 MVS), followed-up for 6-60 months.

Patient characteristics for both treatment arms of these studies are shown in table 2. In the MVS arm, 485 (91%) were mitral valve repairs. Mitraclip patients were older, had higher proportion with previous cardiac surgery, coronary artery disease, and logistic EuroSCORE 1, while the proportion of males, New York Heart Association (NYHA) class III-IV, functional MR and left ventricular ejection fraction (LVEF) were similar.

Figure 1 illustrates the Forrest plots for pooled mortality outcomes. There were no statistically significant differences between Mitraclip and MVS for operative mortality 3% versus 5%, OR 0.58 (95%CI 0.28-1.19), P=0.14 overall in eight studies; one-year mortality 12% versus 13%, OR 1.09 (95%CI 0.71-1.68), P=0.69 in seven studies; and long-term mortality 30% versus 35%, OR 0.99 (95%CI 0.69-1.4), P=0.97 in four studies.

Pooled in-hospital complications rates are listed in table 3. Mitraclip had higher early significant MR 12% versus 1%, OR 4.6 (95%CI 1.5-14), P=0.008 in eight studies; but lower bleeding rates 10% versus 27%, OR 0.26 (95%CI 0.12-0.53),

P<0.001 in five studies; and pacemaker implantation 0% versus 17%, OR 6.64 (95%CI 3.78-11.6), P=0.01 in two studies compared to MVS respectively.

Table 4 showed pooled analysis of long term complication rates during follow-up. Mitraclip had higher rates of late significant MR 22% versus 4%, OR 0.15 (95%CI 0.09-0.26), P<0.01 in six studies and cardiovascular readmission rates 20% versus 10%, OR 2.2 (95%CI 1.0-5.0), P=0.05 in four studies with no differences in symptom improvement and re-operation.

DISCUSSION

This meta-analysis compared the outcomes of percutaneous Mitraclip and MVS for severe MR, with some important findings. In high risk patients with primary or secondary MR, Mitraclip had similar outcomes to MVS in terms of operative mortality, mortality at 1-year and beyond. Mitraclip had lower rates of peri-procedural complications of bleeding and pacemaker implantation whereas other complications such as stroke, myocardial infarction and acute kidney injury were similar. The disadvantage of Mitraclip was higher rate of significant residual MR both early and later on, as well as cardiovascular readmissions during follow-up.

Only one of the nine studies was a randomised trial (EVEREST-II)[10,14], and the other eight observational studies contributed to the discrepancies in baseline characteristics between Mitraclip and MVS candidates[15-22]. Mitraclip patients having higher baseline risk, with older age, higher proportion with previous

cardiac surgery, coronary artery disease and higher EuroSCORE seen across studies was not surprising as Mitraclip introduced as a potential alternative for patients who are at either high or prohibitive risk for MVS[1,2]. This is because there is a wealth of experience for MVS as an effective strategy in low and intermediate risk MR candidates with low operative mortality rates around 3% overall and good durability[1,23]. The corollary of this is that had we found Mitraclip patients had slightly worse outcomes than MVS, then it would be difficult to discern whether this was due to higher baseline risk or that Mitraclip was truly inferior to MVS.

Despite the aforementioned differences at baseline, there were no differences in mortality outcomes between the two modalities. The pooled operative mortality rate of 3-5% is acceptable in this selectively higher risk cohort and similar compared to all-comers undergoing either procedure for severe MR[23]. Operative mortality is an important safety measure and long-term survival illustrates efficacy for valvular procedures. These results are especially reassuring for the Mitraclip cohort, which although having higher baseline risk than MVS had similar mortality rates to MVS. This highlights the utility of Mitraclip in high risk candidates warranting intervention, including those with ischaemic and functional MR and/or cardiomyopathy. Of note the original EuroSCORE which estimates operative mortality after cardiac surgery reported in these studies grossly over-estimated that of Mitraclip 23% versus 3%, and to a lesser extent MVS 11% versus 5%[24]. Although the more contemporary EuroSCORE II and STS Scores were not routinely reported, they fit better with contemporary outcomes[25-27]. They can assist patient selection for Mitraclip after determining

which patients are high risk for MVS. Unlike for MVS however, caution needs to be taken when applying these scores directly to Mitraclip due to over-estimation and modest discriminative ability[28].

Although procedural failure rates were relatively low, the main shortcomings of mitraclip are the high rates of residual MR, and possibly durability, short and long term being significantly worse than MVS. This finding was consistent across all studies[10-13-21]. Residual MR especially moderate or severe is to be avoided as it is associated with worse clinical outcomes[19,29]. Although this did not translate to statistically higher rates of reoperation during follow-up, this could've been because many of these high risk candidates at baseline would be ineligible or too high a risk for a reintervention. Whereas there are many MVS techniques to restrict residual MR, Mitraclip which mimics the Alfieri edge to edge surgical technique by clipping the two mitral valve leaflets together creating two small MV orifice does not have the same capability[9]. Notably, most of the eligible studies in our meta-analysis used the earlier generation Mitraclip device and about half started enrolling patients before 2008 when the technique was in its infancy. With increasing experience over time, the reported early residual MR rate has reduced to approximately 5% in the COAPT trial and contemporary registries[13,30]. Furthermore, a number of other percutaneous mitral valve intervention techniques are being developed and in active clinical trials to try and overcome these shortcomings, including mitral annuloplasty, chordal replacement, mid-leaflet attachment to each side of small spacer (PASCAL system), ventricle remodelling and valve replacement[31-34]. Their reported rates of significant early MR are similarly at <5%.

Other peri-procedural complications were either similar (stroke, myocardial infarction and acute kidney injury) or higher for MVS (bleeding and pacemaker implantation). These are similar to other comparisons between percutaneous or minimally invasive approaches in cardiology such as in the treatment of aortic stenosis[35,36]. The notable difference is pacemaker implantation where there is similar moderate risk for aortic or mitral valve surgery[37]. The proximity of the bioprosthetic aortic valve implanted by the transcatheter approach to the atrio-ventricular node increase the risk of heart block requiring pacemakers at a rate comparable to valve surgery[35,36], whereas the landing zone for Mitraclip is distant to the conduction system hence a low risk of pacemaker implantation (0% in our meta-analysis). Of some concern for Mitraclip however is the higher rate of cardiovascular readmission during follow-up than MVS in the pooled analysis, despite similar NYHA status. This is another important efficacy measure especially with many of these patients having heart failure admissions, likely in part due to greater residual MR and probably higher filling pressures for Mitraclip. The hope is that with further experience and advances in percutaneous mitral valve techniques, this too may be reduced to similar rates as MVS.

Secondary MR deserves a special mention as the optimal interventional strategy remains controversial[1,2]. In our meta-analysis secondary MR made up the majority at 66-74% of both arms, though higher proportion with coronary artery disease for Mitraclip than MVS patients, with no differences in mortality endpoints. Despite this, even for MVS there is no definite benefit over medical therapy alone or in addition to coronary surgery in this setting[1,2,8,9]. Two recent randomised trials specifically compared Mitraclip with medical therapy for secondary MR with

heart failure, with conflicting results[12,13]. The MITRA-FR trial found no difference with Mitraclip or medical therapy alone in terms of death and heart failure hospitalisation[12], whereas COAPT found significant reduction in both endpoints in favour of Mitraclip[13]. The COAPT trial was larger with longer follow-up, had higher heart failure biomarker level and more severe MR that was disproportionate to the underlying cardiomyopathy's remodelling of the left ventricle as compared with the MITRA-FR trial, which may explain in part the discrepancy in their findings[38]. These sicker patients with secondary MR, both functional and ischaemic, are likely those to be targeted to benefit from Mitraclip intervention.

Limitations

This meta-analysis has some limitations. The majority of studies were observational with inherent biases in patient selection and different baseline risk profiles which as described earlier influences the interpretation of the findings. There was also heterogeneity in study design including patient inclusion, aetiology of MR, intervention strategy and type and timing of characteristics endpoints. Despite pooling 9 studies, the overall sample size is moderate at best for determining differences in endpoints especially ones which occur rarely or are infrequently reported. Comparison with a non-interventional medical approach was not assessed. Some important endpoints such as quality of life were not reported. Follow-up was also limited to at most 5 years. Longer term durability and outcomes of Mitraclip compared to MVS remains an important unknown especially if Mitraclip are being introduced to treat lower risk and/or younger candidates in the future. Finally, the eligible studies were between 2011-2017 and

may not fully capture the contemporary experience, because the focus of more recent studies of Mitraclip are either single-armed registries or comparisons with medical therapy for secondary MR or other percutaneous techniques, rather than MVS.

Conclusion

Patients with severe MR had similar mortality early and late after Mitraclip compared to MVS, despite higher baseline risk for Mitraclip candidates. The main disadvantage for Mitraclip is residual post-procedural MR short and long term and cardiovascular readmissions, whereas MVS had more periprocedural complications of bleeding and pacemaker implantation. A multidisciplinary and individualised approach with sound clinical judgement is required for deciding the optimal treatment modality for high risk severe MR patients.

Impact on daily practice: This meta-analysis of 9 studies and 1171 patients showed that although percutaneous Mitraclip patients have higher baseline risk than mitral valve surgery patients, mortality early, at 1- and 3-years were similar. MItraclip had higher rates of residual post-procedural MR and cardiovascular readmissions, but lower risk of periprocedural complications especially bleeding and pacemaker implantation. Mitraclip should be considered as an alternative to mitral valve surgery particularly high-risk candidates.

ACKNOWLEDGEMENTS: None

FUNDING: None

REFERENCES

1. Baumgartner H, Falk V, Bax JJ, De Bonis M, Hamm C, Holm PJ, Iung B, Lancellotti P, Lansac E, Rodriguez Muñoz D, Rosenhek R, Sjögren J, Tornos Mas P, Vahanian A, Walther T, Wendler O, Windecker S, Zamorano JL; ESC Scientific Document Group. 2017 ESC/EACTS Guidelines for the management of valvular heart disease. Eur Heart J. 2017;38:2739-2791.

2. Nishimura RA, Otto CM, Bonow RO, Carabello BA, Erwin JP 3rd, Guyton RA, O'Gara PT, Ruiz CE, Skubas NJ, Sorajja P, Sundt TM 3rd, Thomas JD. 2014 AHA/ACC guideline for the management of patients with valvular heart disease: a report of the American College of Cardiology/American Heart Association Task Force on Practice Guidelines. J Am Coll Cardiol. 2014;63:e57–185

3. Jones EC, Devereux RB, Roman MJ, Liu JE, Fishman D, Lee ET, Welty TK, Fabsitz RR, Howard BV. Prevalence and correlates of mitral regurgitation in a population-based sample (the Strong Heart Study). Am J Cardiol. 2001;87:298-304.

4. Iung B, Baron G, Butchart EG, Delahaye F, Gohlke-Barwolf C, Levang OW, Tornos P, Vanoverschelde JL, Vermeer F, Boersma E, Ravaud P, Vahanian A. A prospective survey of patients with valvular heart disease in Europe: the Euro Heart Survey on Valvular Heart Disease. Eur Heart J. 2003;24:1231–1243.

5. Nkomo VT, Gardin JM, Skelton TN, Gottdiener JS, Scott CG, Enriquez-Sarano M. Burden of valvular heart diseases: a population-based study. Lancet. 2006; 368: 1005-11

6. Grigioni F, Enriquez-Sarano M, Zehr KJ, Bailey KR, Tajik AJ. Ischemic mitral regurgitation: long-term outcome and prognostic implications with quantitative Doppler assessment. Circulation. 2001;103:1759–1764.

7. De Bonis M, Al-Attar N, Antunes M, Borger M, Casselman F, Falk V, Folliguet T, Iung B, Lancellotti P, Lentini S, Maisano F, Messika-Zeitoun D, Muneretto C, Pibarot

P, Pierard L, Punjabi P, Rosenhek R, Suwalski P, Vahanian A, Wendler O, Prendergast B. Surgical and interventional management of mitral valve regurgitation: a position statement from the European Society of Cardiology Working Groups on Cardiovascular Surgery and Valvular Heart Disease. Eur Heart J. 2016;37:133–139.

8. Acker MA, Parides MK, Perrault LP, Moskowitz AJ, Gelijns AC, Voisine P, Smith PK, Hung JW, Blackstone EH, Puskas JD, Argenziano M, Gammie JS, Mack M, Ascheim DD, Bagiella E, Moquete EG, Ferguson TB, Horvath KA, Geller NL, Miller MA, Woo YJ, D'Alessandro DA, Ailawadi G, Dagenais F, Gardner TJ, O'Gara PT, Michler RE, Kron IL; CTSN. Mitral valve repair versus replacement for severe ischaemic regurgitation. N Engl J Med. 2014:370:23-32.

9. Smith PK, Puskas JD, Ascheim DD, Voisine P, Gelijns AC, Moskowitz AJ, Hung JW, Parides MK, Ailawadi G, Perrault LP, Acker MA, Argenziano M, Thourani V, Gammie JS, Miller MA, Pagé P, Overbey JR, Bagiella E, Dagenais F, Blackstone EH, Kron IL, Goldstein DJ, Rose EA, Moquete EG, Jeffries N, Gardner TJ, O'Gara PT, Alexander JH, Michler RE; Cardiothoracic Surgical Trials Network Investigators. Surgical treatment of moderate ischemic mitral regurgitation. N Engl J Med. 2014;371:2178-88.

10. Maisano F, La Canna G, Colombo A, Alfieri O. The evolution from surgery to percutaneous mitral valve interventions: the role of the edge-to-edge technique. J Am Coll Cardiol. 2011;58:2174-82.

11. Feldman T, Foster E, Glower DD, Kar S, Rinaldi MJ, Fail PS, Smalling RW, Siegel R, Rose GA, Engeron E, Loghin C, Trento A, Skipper ER, Fudge T, Letsou GV, Massaro JM, Mauri L; EVEREST II Investigators. Percutaneous repair or surgery for mitral regurgitation. N Engl J Med. 2011;364:1395-406.

12. Obadia JF, Messika-Zeitoun D, Leurent G, Iung B, Bonnet G, Piriou N, Lefèvre T, Piot C, Rouleau F, Carrié D, Nejjari M, Ohlmann P, Leclercq F, Saint Etienne C, Teiger E, Leroux L, Karam N, Michel N, Gilard M, Donal E, Trochu JN, Cormier B, Armoiry X, Boutitie F, Maucort-Boulch D, Barnel C, Samson G, Guerin P, Vahanian A, Mewton N; MITRA-FR Investigators.

Percutaneous Repair or Medical Treatment for Secondary Mitral Regurgitation. N Engl J Med. 2018;379:2297-2306.

13. Stone GW, Abraham WT, Kar S, Lim DS, Mishell JM, Whisenant B, Grayburn PA, Rinaldi M, Kapadia SR, Rajagopal V, Sarembock IJ, Brieke A, Marx SO, Cohen DJ, Weissman NJ, Mack MJ; COAPT Investigators. Transcatheter Mitral-Valve Repair in Patients with Heart Failure. Lindenfeld J, N Engl J Med. 2018;379:2307-2318.

14. Feldman T, Kar S, Elmariah S, Smart SC, Trento A, Siegel RJ, Apruzzese P, Fail P, Rinaldi MJ, Smalling RW, Hermiller JB, Heimansohn D, Gray WA, Grayburn PA, Mack MJ, Lim DS, Ailawadi G, Herrmann HC, Acker MA, Silvestry FE, Foster E, Wang A, Glower DD, Mauri L; EVEREST II Investigators. Randomized Comparison of Percutaneous Repair and Surgery for Mitral Regurgitation: 5-Year Results of EVEREST II. J Am Coll Cardiol. 2015;66:2844-2854.

15. Taramasso M, Denti P, Buzzatti N, De Bonis M, La Canna G, Colombo A, Alfieri O, Maisano F. Mitraclip therapy and surgical mitral repair in patients with moderate to severe left ventricular failure causing functional mitral regurgitation: a single-centre experience. Eur J Cardiothorac Surg.. 2012;42:920-6.

16. Conradi L, Treede H, Rudolph V, Graumüller P, Lubos E, Baldus S, Blankenberg S, Reichenspurner H. Surgical or percutaneous mitral valve repair for secondary mitral regurgitation: comparison of patient characteristics and clinical outcomes. Eur J Cardiothorac Surg. 2013;44:490-6.

17. Paranskaya L, D'Ancona G, Bozdag-Turan I, Akin I, Kische S, Turan GR, Rehders T, Schneider H, Westphal B, Birkemeyer R, Nienaber CA, Ince H. Percutaneous vs surgical repair of mitral valve regurgitation: single institution early and midterm outcomes. Can J Cardiol. 2013;29:452-9.

18. Swaans MJ, Bakker AL, Alipour A, Post MC, Kelder JC, de Kroon TL, Eefting FD, Rensing BJ, Van der Heyden JA. Survival of transcatheter mitral valve repair compared with surgical and conservative treatment in high-surgical-risk patients. JACC Cardiovasc Interv. 2014;7:875-81.

19. Buzzatti N, Maisano F, Latib A, Taramasso M, Denti P, La Canna G, Colombo A, Alfieri O. Comparison of outcomes of percutaneous MitraClip versus surgical repair or replacement for degenerative mitral regurgitation in octogenarians. Am J Cardiol. 2015;115:487-92.

20. De Bonis M, Taramasso M, Lapenna E, Denti P, La Canna G, Buzzatti N, Pappalardo F, Di Giannuario G, Cioni M, Giacomini A, Alfieri O. MitraClip therapy and surgical edge-to-edge repair in patients with severe left ventricular dysfunction and secondary mitral regurgitation: mid-term results of a single-centre experience. Eur J Cardiothorac Surg. 2016;49:255-62.

21. Ondrus T, Bartunek J, Vanderheyden M, Stockman B, Kotrc M, Van Praet F, Van Camp G, Lecomte P, Mo Y, Penicka M. Minimally invasive mitral valve repair for functional mitral regurgitation in severe heart failure: MitraClip versus minimally invasive surgical approach. Interact Cardiovasc Thorac Surg. 2016;23:784-789.

22. Alozie A, Paranskaya L, Westphal B, Kaminski A, Sherif M, Sindt M, Kische S, Schubert J, Diedrich D, Ince H, Steinhoff G, Öner A. Clinical outcomes of conventional surgery versus MitraClip® therapy for moderate to severe symptomatic mitral valve regurgitation in the elderly population: an institutional experience. BMC Cardiovasc Disord. 2017;17:85.

23. Badhwar V, Rankin JS, He X, Jacobs JP, Gammie JS, Furnary AP, Fazzalari FL, Han J, O'Brien SM, Shahian DM. The Society of Thoracic Surgeons Mitral Repair/Replacement Composite Score: A Report of The Society of Thoracic Surgeons Quality Measurement Task Force. Ann Thorac Surg. 2016;101:2265-71.

24. Roques F, Michel P, Goldstone AR, Nashef SA. The logistic EuroSCORE. Eur Heart J. 2003;24:881-2.

25. Nashef SA, Roques F, Sharples LD, Nilsson J, Smith C, Goldstone AR, Lockowandt U. EuroSCORE II. Eur J Cardiothorac Surg. 2012;41:734-44.

26. O'Brien SM, Shahian DM, Filardo G, Ferraris VA, Haan CK, Rich JB, Normand SL, DeLong ER, Shewan CM, Dokholyan RS, Peterson ED, Edwards FH, Anderson RP; Society of Thoracic Surgeons Quality Measurement Task Force. The Society of Thoracic Surgeons 2008 cardiac surgery risk models: part 2--isolated valve surgery. Ann Thorac Surg. 2009;88:S23-42.

27. Wang TK, Harmos S, Gamble GD, Ramanathan T, Ruygrok PN. Performance of contemporary surgical risk scores for mitral valve surgery. J Card Surg. 2017;32:172-176.

28. Adamo M, Capodanno D, Cannata S, Giannini C, Laudisa ML, Barbanti M, Curello S, Immè S, Maffeo D, Grasso C, Bedogni F, Petronio AS, Ettori F, Tamburino C; GRASP-IT Investigators. Comparison of three contemporary surgical scores for predicting all-cause mortality of patients undergoing percutaneous mitral valve repair with the MitraClip system (from the multicenter GRASP-IT registry). Am J Cardiol. 2015;115:107-12.

29. Kaneko H, Neuss M, Weissenborn J, Butter C.Impact of residual mitral regurgitation after MitraClip implantation. Int J Cardiol. 2017;227:813-819.

Buzzatti N, De Bonis M, Denti P, Barili F, Schiavi D, Di Giannuario G, La Canna G, Alfieri O. What is a "good" result after transcatheter mitral repair? Impact of 2+ residual mitral regurgitation. J Thorac Cardiovasc Surg. 2016;151:88-96

30. Chhatriwalla AK, Vemulapalli S, Holmes DR Jr, Dai D, Li Z, Ailawadi G, Glower D, Kar S, Mack MJ, Rymer J, Kosinski AS, Sorajja P. Institutional Experience With Transcatheter Mitral Valve Repair and Clinical Outcomes: Insights From the TVT Registry. JACC Cardiovasc Interv. 2019;12:1342-1352.

31. Siminiak T, Wu JC, Haude M, Hoppe UC, Sadowski J, Lipiecki J, Fajadet J, Shah AM, Feldman T, Kaye DM, Goldberg SL, Levy WC, Solomon SD, Reuter DG. Treatment of functional mitral regurgitation by percutaneous annuloplasty: results of the TITAN Trial. Eur J Heart Fail. 2012;14:931-8.

32. Praz F, Spargias K, Chrissoheris M, Büllesfeld L, Nickenig G, Deuschl F, Schueler R, Fam NP, Moss R, Makar M, Boone R, Edwards J, Moschovitis A, Kar S, Webb J, Schäfer U, Feldman T, Windecker S. Compassionate use of the PASCAL transcatheter mitral valve repair system for patients with severe mitral regurgitation: a multicentre, prospective, observational, first-in-man study. Lancet. 2017;390:773-780.

33. Muller DWM, Farivar RS, Jansz P, Bae R, Walters D, Clarke A, Grayburn PA, Stoler RC, Dahle G, Rein KA, Shaw M, Scalia GM, Guerrero M, Pearson P, Kapadia S, Gillinov M, Pichard A, Corso P, Popma J, Chuang M, Blanke P, Leipsic J, Sorajja P, Tendyne Global Feasibility Trial Investigators. Transcatheter Mitral Valve Replacement for Patients With Symptomatic Mitral Regurgitation: A Global Feasibility Trial. J Am Coll Cardiol. 2017;69:381-391.

34. Takagi H, Hari Y, Kawai N, Kuno T, Ando T; ALICE (All-Literature Investigation of Cardiovascular Evidence) Group. Transcatheter mitral valve replacement for mitral regurgitation-A meta-analysis. J Card Surg. 2018;33:827-835.

35. Smith CR, Leon MB, Mack MJ, Miller DC, Moses JW, Svensson LG, Tuzcu EM, Webb JG, Fontana GP, Makkar RR, Williams M, Dewey T, Kapadia S, Babaliaros V, Thourani VH, Corso P, Pichard AD, Bavaria JE, Herrmann HC, Akin JJ, Anderson WN, Wang D, Pocock SJ; PARTNER Trial Investigators. Transcatheter versus surgical aortic-valve replacement in high-risk patients. N Engl J Med. 2011;364:2187-98.

36. Leon MB, Smith CR, Mack MJ, Makkar RR, Svensson LG, Kodali SK, Thourani VH, Tuzcu EM, Miller DC, Herrmann HC, Doshi D, Cohen DJ, Pichard AD, Kapadia S, Dewey T, Babaliaros V, Szeto WY, Williams MR, Kereiakes D, Zajarias A, Greason KL, Whisenant BK, Hodson RW, Moses JW, Trento A, Brown DL, Fearon WF, Pibarot P, Hahn RT, Jaber WA, Anderson WN, Alu MC, Webb JG; PARTNER 2 Investigators. Transcatheter or Surgical Aortic-Valve Replacement in Intermediate-Risk Patients. N Engl J Med. 2016;374:1609-20.

37. Leyva F, Qiu T, McNulty D, Evison F, Marshall H, Gasparini M. Long-term requirement for pacemaker implantation after cardiac valve replacement surgery. Heart Rhythm. 2017;14:529-534.

38. Grayburn PA, Sannino A, Packer M.Proportionate and Disproportionate Functional Mitral Regurgitation: A New Conceptual Framework That Reconciles the Results of the MITRA-FR and COAPT Trials. JACC Cardiovasc Imaging. 2019;12:353-362.

Table 1: Design of included studies.

Author/Year	Country	Time of procedures	Centre	Study design	Total	Follow-up (months)
Feldman 2011[11]+2015[14]	United States/Canada	Sep 2005-Nov 2008	37	Randomised trial	279 - 184, 95	60
Taramasso 2012[15]	Italy	Mar 2000-Apr 2011	1	Retrospective Cohort	143 - 52, 91	8.5, 18
Conradi 2013[16]	Germany	Mar 2002-June 2010	1	Retrospective Cohort	171 - 95, 76	6
Paranskaya 2013[17]	Germany	Apr 2010-Dec 2011	1	Retrospective Cohort	50 - 24, 26	12
Swaans 2014[18]	Netherlands	Jan 2009-Apr 2013	1	Retrospective Cohort	192 - 139, 53	20, 32
Buzzatti 2014[19]	Switzerland	Sep 2008-Apr 2014	1	Retrospective Cohort	60 - 25, 35	22, 30
De Bonis 2015[20]	Italy	1999-2006 and 2008-2011	1	Retrospective Cohort	120 - 55, 65	48
Ondrus 2016[21]	Belgium	1997 onwards	1	Retrospective Cohort	72 - 24, 48	34, 30
Alozie 2017[22]	Germany	Oct 2008-Oct 2014	1	Retrospective Cohort	84 - 42, 42	9, 25

Total (9 studies)					**1,171 (640, 531)**	

X, Y=corresponding are numbers, means or medians for Mitraclip and mitral valve surgery respectively when reported.

Table 2: Patient characteristics of included studies.

Author/Year	Age (years)	Male (%)	Previous cardiac surgery (%)	Coronary artery disease (%)	Functional MR (%)	NYHA 3-4 (%)	LVEF (%)	EuroSCORE I (%)
Feldman 2011[11]+2015[14]	67, 66	63%, 66%	21%, 19%	47%, 46%	27%, 27%	52%, 47%	60%, 61%	-, -
Taramasso 2012[15]	68, 65	83% ,77%	23%, 10%	71%, 48%	100%, 100%	85%, 67%	28%, 39%	22%, 10%
Conradi 2013[16]	72, 65	64%, 45%	46%, 11%	53%, 29%	86%, 96%	98%, 88%	36%, 42%	34%, 10%
Paranskaya 2013[17]	80, 63	42%, 65%	8%, 0%	58%, 23%	33%, 27%	88%, 96%	58%, 59%	12%, 4%
Swaans 2014[18]	75, 70	68%, 51%	42%, 17%	64%, 53%	77%, 59%	89%, 89%	37%, 44%	24%, 14%
Buzzatti 2014[19]	85, 82	-, -	12%, 6%	28%, 20%	100%, 100%	68%, 37%	60%, 61%	19%, 8%
De Bonis 2015[20]	68, 63	84%, 69%	24%, 6%	73%, 66%	100%, 100%	82%, 86%	28%, 29%	19%, 11%

Ondrus 2016[21]	75, 76	75%, 56%	63%, 31%	62%, 74%	100%, 100%	88%, 92%	31%, 30%	18%, 14%
Alozie 2017[22]	82, 82	57%, 45%	17%, 17%	88%, 44%	50%, 41%	89%, 81%	48%, 53%	11%, 12%
Pooled characteristics	72, 69	67%, 61%	30%, 14%	70%, 46%	66%, 74%	78%, 74%	44%, 45%	23%, 11%
P-value	<0.001	0.05	<0.001	<0.001	0.63	0.09	0.05	<0.001

MR=mitral regurgitation, NYHA=New York Heart Association, LVEF=left ventricular ejection fraction. X, Y=corresponding are numbers (means or medians) or percentages for Mitraclip and mitral valve surgery respectively when reported.

Table 3: Pooled in-hospital morbidity outcomes.

In-hospital outcome	Studies	Mitralclip (%)	Mitral valve surgery (%)	OR or WMD	95% confidence interval	P-value
Procedural failure (%)	8	4%	2%	1.9	0.71-4.8	0.21
Neurological event (%)	8	0.8%	3%	0.47	0.17-1.3	0.15
Myocardial infarction (%)	6	0.2%	0.5%	0.65	0.10-4.2	0.66
Bleeding (%)	5	10%	27%	0.26	0.12-0.53	<0.001
Acute kidney injury (%)	6	7%	17%	0.50	0.19-1.4	0.17
Pacemaker implantation (%)	2	0%	17%	0.07	0.01-0.57	0.01
Length of hospital stay (days)	7	10	11	-2.2	-6.9 - +2.5	0.36
Early MR (%)	8	12%	1%	4.5	1.5-14	0.008

MR=significant at least moderate mitral regurgitation, OR=odds ratio, WMD=weighted mean difference

Table 4: Pooled morbidity outcomes during follow-up.

Outcome during follow-up	Studies	Mitralclip (%)	Mitral valve surgery (%)	OR	95% confidence interval	P-value
Late significant MR (%)	6	22%	4%	6.6	3.8-12	<0.001
Re-operation (%)	3	6%	3%	2.1	0.8-5.4	0.12
Cardiovascular readmission (%)	4	20%	10%	2.2	1.0-5.0	0.05
Reduction in NYHA 3-4 (%)	7	60%	55%	1.4	0.96-2.00	0.08

MR=significant at least moderate mitral regurgitation, NYHA=New York Heart Association, OR=odds ratio.

Figure 1: Forest plot of pooled odds ratios comparing Mitraclip and MVS for mortality a) operative, b) 1 year and c) 3 years

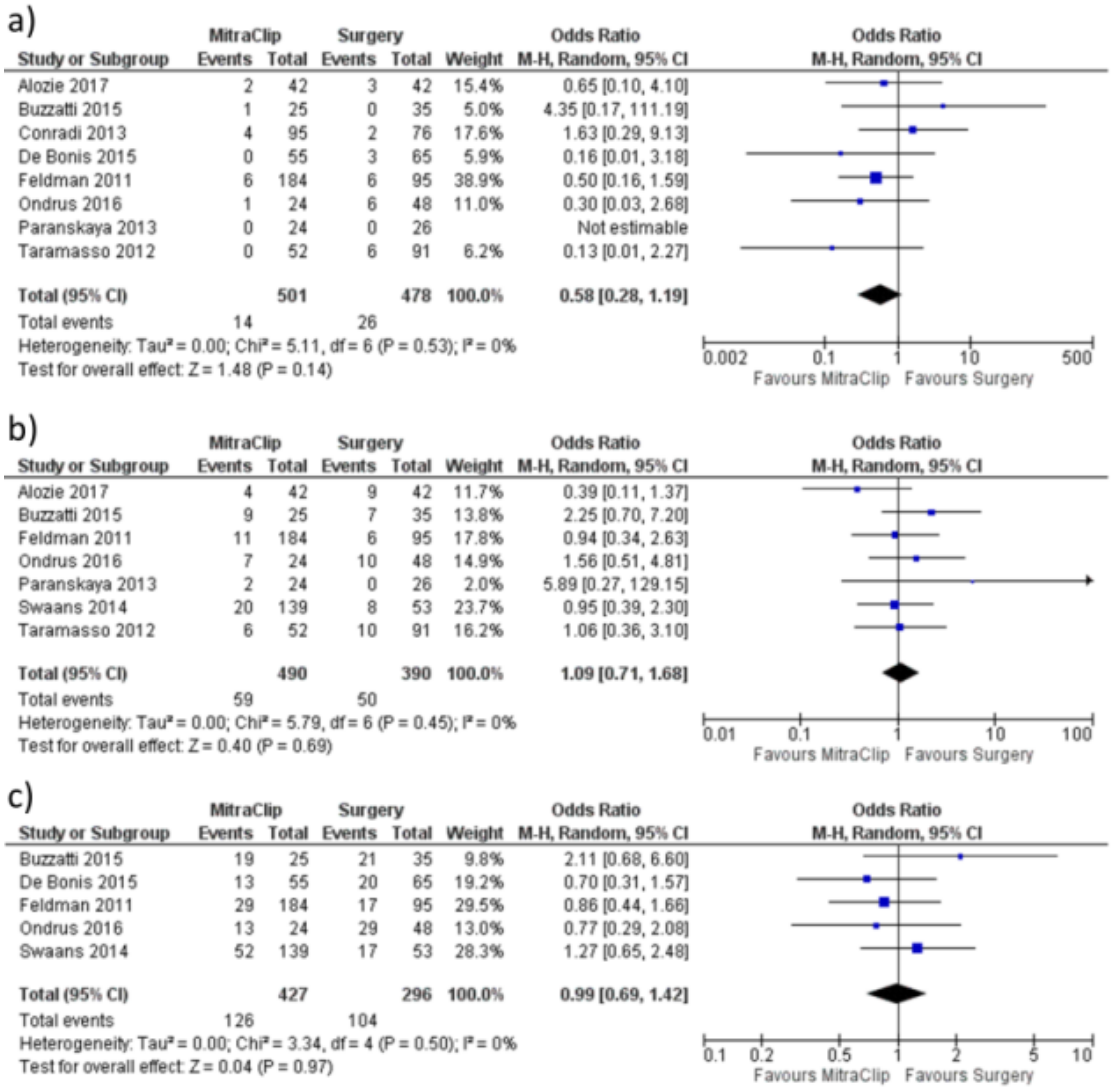

AsiaIntervention

Official Journal of the Asian Pacific Society of Interventional Cardiology

(APSIC) and the Interventional Cardiology Foundation of India (ICFI)

www.asiaintervention.org

Title: **From Reverse CART to Antegrade Wire Access - a guide to externalization, tip-in, rendezvous, and snaring from the APCTO Club.**

Authors: Eugene B Wu, M.D; Hsien-Li Kao, M.D; Sidney Lo, M.D; Soo Teik Lim, M.D; Lei Ge, M.D; Ji-Yan Chen, M.D; Jie Qian, M.D; Seung-Whan Lee, M.D, PhD; Scott A Harding, M.D; Etsuo Tsuchikane, M.D, PhD

Manuscript number: AIJ-D-19-00031

Manuscript submission date: 04 June 2019

Revisions received: 20 February 2020, 16 May 2020

Accepted date: 10 July 2020

From Reverse CART to Antegrade Wire Access - a guide to externalization, tip-in, rendezvous, and snaring from the APCTO Club.

Eugene B Wu1, MD, Hsien-Li Kao2, MD, Sidney Lo3, MD, Soo Teik Lim4, MD, Lei Ge5, MD, Ji-Yan Chen6, MD, Jie Qian7, MD, Seung-Whan Lee8, MD, PhD, Scott A Harding9, MD, Etsuo Tsuchikane10, MD PhD.

1 Prince of Wales Hospital, Hong Kong.
2 National Taiwan University Hospital, Taipei, Taiwan.
3 Liverpool Hospital, Sydney, Australia. Sidney.
4 National Heart Centre, Singapore.
5 Shanghai Zhongshan Hospital, Shanghai, China.
6 Guangdong General Hospital, Guangdong, China.
7 Beijing Fuwai Hospital, Beijing, China.
8 Asan Medical Centre, Seoul, Korea.
9 Wellington Hospital, Wellington, New Zealand.
10 Toyohashi Heart Centre, Toyohashi, Aichi, Japan.

Short title: Reverse CART to antegrade access.

Key words: Chronic coronary total occlusion; Undilatable lesion; Miscellaneous

Conflicts of interests: Dr. Harding has received speaking and consultancy fees from Boston Scientific, Medtronic, Bio-Excel, and Asahi Intecc. Dr. Wu has received proctoring fees from Boston Scientific, Abbott Vascular, and research grant from Orbus Neich and Asahi Intecc. Dr. Lo has received speaking and proctoring honoraria from Bio-Excel. Dr. Lim has received research grant/travel support or speaker honorarium from Orbus Neich, Asahi Intecc, Terumo, Biosensors, Biotronik, Abbott Vascular, Aluimedica, Boston Scientific, and Keneka. Dr. Tsuchikane is a consultant for Boston Scientific, Asahi Intecc, kaneka, and Nipro. All other authors have reported that they have no relationships relevant to the contents of this paper to disclose.

Address for Correspondence: Dr Eugene B Wu, Department of Medicine and Therapeutics, Prince of Wales Hospital, Ngan Shing Street, Shatin, Hong Kong.
email: cto.demon@gmail.com

Abstract.

We, the Asia Pacific Chronic Total Occlusion (APCTO) club, provide a review to address this gap between reverse controlled antegrade and retrograde subintimal tracking (CART) and antegrade wire access. We describe the usual method for externalization wire. We then address how to deal with failure to wire the proximal part of the Chronic Total Occlusion (CTO) vessel or the guiding catheter. After successful antegrade guiding wiring, we address the problem of failing to cross the CTO body with the retrograde microcatheter and we recommend the use of retrograde small balloon, reversion to traditional CART, retrograde knuckle wiring into the subintimal space and antegrade scratch and go and external cap crush. We also propose rendezvous type tip in and describe the way to do this to overcome the problem. In conclusion, we reviewed and made recommendations for methods to gain antegrade wire access after successful reverse CART. We have addressed each failure mode in detail covering the different options, balancing risks and success rates. Our recommendations focus upon safety first and ease of use. We hope this work will help all retrograde operators to further improve their safety, efficacy, and success rates of their retrograde procedures.

Abbreviations:
APCTO – Asia Pacific Chronic Total Occlusion Club.
CART – controlled antegrade and retrograde subintimal tracking.
CTO – Chronic Total Occlusion.
PCI – percutaneous coronary intervention.
GC – guiding catheter
MC – microcatheter.
LAD – Left Anterior Descending artery.
PDA – Posterior Descending Artery.
RCA – right coronary artery.
IVUS – intravascular ultrasound.

Introduction.

The retrograde approach for CTO has adopted two major changes since its original description more than a decade ago [1,2]. First, the introduction of the Corsair (Asahi Intecc, Aichi, Japan) microcatheter in 2009 [3] transformed the cumbersome small balloon septal channel dilatation technique into a simple single microcatheter/channel dilator method for channel crossing. This led to the inevitable dominance of reverse controlled antegrade and retrograde tracking (Rev-CART) as the go to technique for achieving CTO segment crossing. Secondly, the widespread availability of the Gaia wire series (Asahi Intecc, Nagoya, Aichii, Japan) since 2012 improved retrograde wire control markedly, leading to the subsequent development of the more efficient “Directed Rev CART” [4]. Since then, the retrograde approach has reached a plateau in its development with widespread global adoption [5,6,7,8,9,10,11], and a significant improvement of overall success in CTO percutaneous coronary intervention (PCI) [5,8,10,11,12,13]. The retrograde approach had been incorporated into the hybrid algorithm [14,15], and the group has published step-by-step guide [16,17]. Along with the landmark work of Wu et al [18], most of the procedural details

of retrograde CTO PCI have been described. However, a more update version is required in view of the recent technical and device advancement.
Our group: the Asian Pacific Chronic Total Occlusion Club (APCTO), a group of 10 highly experienced retrograde operators, have published recently an overall algorithm for CTO intervention [19], a comprehensive retrograde algorithm [20], and a state-of-the-art guide to CTO wiring [21]. However, we noticed that there has been scarcely any publication describing what to do after successful retrograde wire crossing. This particular gap between successful Rev-CART and establishment of an antegrade wire access involves a wide array of techniques that are not well describe in the literature. Although we often think that successful reverse CART guarantees successful procedure, but this is not necessarily true. These rarely used techniques are important in certain subsets of patients: those where the retrograde microcatheter cannot pass the CTO, those with tortuous proximal vessel anatomy, and rarely the ipsilateral single guiding retrograde percutaneous coronary intervention (PCI). Familiarity with these techniques and using them safely is an important part of the armory of the CTO interventionists. The aim of this present work, therefore, is to review and describe these techniques in comprehensive detail, providing useful expert instructions to retrograde operators worldwide.

1. Default wire externalization.

This is recommended in the majority of retrograde CTO cases.

1.1 Wiring into and anchoring inside the antegrade guiding.

Once the retrograde wire enters the proximal true lumen following successful Rev-CART, it should be further advanced into the antegrade guiding catheter (GC). A trapping balloon is then inflated inside the antegrade GC to anchor the retrograde wire. This provides strong wire support for the retrograde microcatheter (MC) to be pushed across the CTO body into the antegrade GC. Once the retrograde MC is securely inside the antegrade GC, we can deflate the trapping balloon and replace the retrograde wire with an externalization wire such as RG3 wire (Asahi) or Viperwire (Cardiovascular systems Inc, St Paul MN, USA).

1.2 Anchoring the MC.

Some operators prefer to push the trapping balloon forward and inflate it to anchor the retrograde MC in the antegrade GC before exchanging the guide wires. There are two advantages for this practice: 1) the balloon will anchor and stabilize the retrograde MC during exchange, and 2) the inflated balloon will prevent back bleeding during disconnection of the antegrade hemostatic valve/connector while completing wire externalization.

1.3 Passing through the antegrade hemostatic valve/connector.

The operator should push the externalization wire until the wire tip is about to emerge from the antegrade GC hub, judged and estimated by the remaining wire length, under fluoroscopic guidance. Then, the operator should put a wire introducer through the antegrade hemostatic valve/connector in parallel to the anchor balloon (figure 1a), and disconnect the connector (figure 1b). The retrograde externalization wire should then be pushed forward out of the hub of the antegrade GC (figure 1c), and the wire tip is brought into the tip of the wire introducer (figure 1d). Finally, the hemostatic valve/connector should be reconnected to the GC, with both the trapping balloon and wire introducer still in place (figure 1e). The wire introducer is

then removed, and the externalization wire may be used to deliver devices antegradely (figure 1f). The above-described wire externalization should be used as default whenever possible in retrograde approach.

1.4 When to continue on externalized wire and when to switch to antegrade wire?

Once we have externalized a wire, we have a choice to either work on the externalized wire or to put a MC or dual lumen catheter over the externalized wire and place a second antegrade wire. Although the default position is to use the externalized wire as a working wire as it provides better support for tracking devices, in some cases, the option of switch to antegrade wire is preferable.
If we need to stent beyond where the retrograde channel enters the CTO vessel due to distal disease, then it is preferable to switch to antegrade wire. This usually occurs in the Left anterior descending artery (LAD) where the Posterior descending artery (PDA) septal channel often enters the mid LAD with significant disease in distal LAD that requires stenting. In this case, using a dual lumen catheter to deliver a second wire into the septal channel and then pulling back this wire to wire the true LAD is the best method. We must remove the externalized wire before stenting to avoid wire trapping. Other reasons to switch to antegrade wire include the retrograde channel entering near the distal CTO cap or the need to protect a side branch distal to the retrograde channel entry site.

However, sometimes, this default method of wire externalization fails and we now turn to addressing these problems.

2. Failure to access proximal vessel lumen with retrograde wire.

The operator may fail to manipulate retrograde wire through the proximal vessel lumen despite successful Rev CART achieving proximal vessel true lumen position of the retrograde wire. This is almost always due to migration the retrograde wire tip back into intraplaque or subintimal space in the proximal vessel. It occurs more frequently when the proximal vessel is significantly diseased and tortuous, when balloon angioplasty had been performed in the proximal vessel segment, and when a high penetration force retrograde wire is used for Rev CART.
In this scenario, we recommend the use of guide extension, as described by Mozid et al [22]. A guide extension catheter such as GuideLiner (Teleflex, Wayne, Pennsylvania, USA) or Guidezilla (Boston Scientific, Mass, USA) should be advanced into the proximal vessel to the point where the retrograde wire is in true lumen, and the retrograde wire may be manipulated easily into the guide extension. A 2.5 or 3.0 mm balloon inflation is sometimes needed to dilate the proximal vessel and facilitate guide extension catheter delivery. The use of guide extension catheter is almost always successful in these cases.

3. Failure to manipulate the retrograde wire into the antegrade GC.

3.1 Tips and tricks for wiring into antegrade GC.

There are certain tricks to increase the efficiency of wiring into the antegrade GC with the retrograde wire. We have to recognize that manipulation of the antegrade GC is far more important than manipulation of the retrograde wire. The operator should ensure that the antegrade GC is coaxial with the coronary artery. For example, in Right coronary artery (RCA)

CTO, often the antegrade GC is pointing towards the anterior wall of the right coronary ostium. Therefore, applying clockwise rotation to the GC in right anterior oblique view will enhance its coaxiality with the right coronary ostium and facilitate retrograde wring into the antegrade GC. The operator should push the retrograde wire forward and observe its trajectory, and then manipulate the antegrade GC to cover the expected area that the retrograde wire will travel to [23]. Simultaneous manipulation of retrograde wire and antegrade GC may also be very helpful. However, certain unfavorable anatomy may require the use guide extension catheter. Inserting a guide extension catheter into the proximal part of the CTO vessel makes wiring into the antegrade system much easier, since it will always be coaxial to the vessel course.

3.2 Change the retrograde wire.

If operator failed all the above methods to wire into the antegrade GC, it is usually due to the difficulty of controlling of a stiff high penetration force retrograde wire. We recommend the operator to switch the retrograde wire to a more controllable slippery soft wire, such as Sion Black (Asahi Intecc). To do this, we need to push the retrograde MC across the CTO body into the proximal true lumen of the CTO vessel. The first step is to push the retrograde guide wire as far up the aorta as possible (figure 2a), ideally passing arch into the descending aorta. The bend at the arch will provide extra support to this wire and allow us to track the MC across. If this failed, we can consider using an antegrade balloon to trap and anchor the retrograde wire inside the proximal part of the CTO vessel (figure 2b).

If this too failed, we should exchange the retrograde MC for a new low profile rotational channel dilator type MC, such as the Turnpike LP (Teleflex) or Corsair pro XS (Asahi Intecc), which will often be able to cross the CTO body (figure 2c). Once the retrograde MC has passed through the CTO body, we can exchange the retrograde high penetration force wire with a controllable soft wire to wire the antegrade GC or guide extension catheter (figure 2d) and complete the externalization (figure 2e), and stenting (figure 2f).

When all the above techniques are used properly in a stepwise fashion, the antegrade GC wiring will be successful in the majority of retrograde CTOs. However, there are still occasional cases where retrograde wire snaring, as originally described by Otsuka et al [24], is required.

3.3 Our position on retrograde wire snaring.

We regard snaring of the retrograde wire as a last resort, to be considered only after all other methods have been exhausted. We emphasize the small but inherently real risk associated with snaring, as Fang et al [25] have pointed out. These issues included: 1) the danger of failure to release the snared retrograde wire inside the antegrade GC, and 2) failure to remove the snared retrograde wire from the retrograde MC due to an excessive bend created by the snaring. Although previous authors have suggested several methods to rectify these situations, these methods are not always reliable [26]. There is also a small but unavoidable risk of stroke, with the possible plaque embolism during snare manipulation in the aorta. We, the APCTO club group, recommend hereafter a safety first method of retrograde wire snaring.
3.4 Safety first method of retrograde wire snaring.

When the operator decides to start retrograde wire snaring, the retrograde wire should already be in the descending aorta, as a consequence of prior attempt to push the retrograde MC across CTO body for wire switch to a soft controllable wire. The 3-lobed EN snare (Merit

Medical System, Utah, USA) is the easiest to use to catch the wire but we recommend using a "homemade" snare with guiding extension catheter and monorail balloon [27,28]. The advantages of homemade snare are that the size of the snare loop can be easily increased to as large as needed [29] by pushing the wire forward (figure 3a) and also when the snare has pulled the retrograde wire back into the guiding catheter (figure 3b), release of the retrograde wire can easily be done simply by deflating the balloon. Since there is no connected loop once the balloon is deflated, the retrograde wire can almost always be released. Then an anchoring balloon can be placed to anchor the retrograde wire inside the antegrade GC allowing the retrograde MC to pass (figure 3c). We should aim to snare the floppy tip of the retrograde wire in the descending aorta or the arch. Snaring in the ascending aorta closer to the coronary ostium may increase the embolic stroke risk. After catching the retrograde wire, if we are using a more robust snare such as EN snare, we should first try pushing the retrograde MC across the CTO body into the aorta while pulling on the snare as anchor. Then the snared retrograde wire is released in the descending aorta and exchange it with a new soft controllable wire to wire into the guiding GC again. This will remove the risk of locking the snare with the trapped retrograde wire inside antegrade GC.
If we cannot push the retrograde MC across the CTO body despite snare anchoring, or if we are using a homemade snare, we may try pulling the snared retrograde wire into the antegrade GC. The retrograde MC is then tracked into the GC before the snare is released, and then the retrograde wire may be exchanged to an externalization wire. The risk of failing to release a soft hydrophilic wire from a snare is considered low, but still possible. If we cannot release the 190 cm retrograde wire from snare, we should push the snare and wire back into the aorta and try release again. We can also use a balloon inside the antegrade GC to anchor the wire tip, facilitating the release of the snare. We should never, however, try to pull the whole 190 cm wire through the retrograde channel into the antegrade GC. This is because the proximal end of wire is very stiff and un-coated, and may get stuck in a tortuous retrograde channel with the MC as a unit.
The alternative is to exchange the retrograde wire to RG3 wire, and start snaring its tip at the level of contralateral common iliac artery. This reduces the risk of embolism, and snaring in a smaller vessel such as the Iliac is often easier. If we failed to release the snare on RG3, we can always pull it's snared distal tip out from the contralateral access. With its 300cm exchange length, the proximal end will still be controlled outside of the retrograde GC. We do not, however, recommend wiring through the coronary with RG3, as its 3g tip load and poor torquability can create dissection in diseased proximal vessel easily.

4. Rendezvous techniques.

4.1 The Rendezvous technique.

Rendezvous technique refers to using the antegrade or retrograde wire to wire into or "meet" (in French "rendezvous") the opposite MC. The early descriptions of this technique [30,31] involves wiring the antegrade wire into the retrograde MC. Tip-in is also a kind of rendezvous technique. In tip in, the retrograde wire is wired into an antegrade MC, either in the GC [32] or in the coronary artery [33]. These techniques are used less frequently nowadays, with the availability of low profile MCs and algorithmic intravascular ultrasound (IVUS) usage in Rev-CART.

The advantages of rendezvous are: 1) rapid establishment of antegrade wire track [32] without the need for externalization wire, and 2) to bail out the situation when retrograde MC fail to cross the CTO body [33].

4.2 The role of rendezvous techniques in contemporary retrograde CTO PCI.

Much of the issues requiring original rendezvous techniques [30-33] are no longer relevant, with application of IVUS-guided Rev-CART, low profile MCs and RG3 or Viper wires, and guide extension catheters. However, there are a few conditions that may still mandate rendezvous techniques in the current era of retrograde CTO PCI: 1) failure to cross the CTO body with the retrograde MC, 2) inadequate length of retrograde MC to reach the antegrade system, and 3) the need to quickly establish antegrade track. 4) Single guiding catheter ipsilateral channel retrograde CTO PCI.

4.3 Failure to cross the CTO with retrograde MC.

Despite trapping balloon anchoring the retrograde wire in the antegrade GC, we may still fail to push the retrograde MC across the CTO body. Rendezvous techniques may be helpful, but alternative solutions may also include: 1) balloon dilatation of the CTO from the retrograde direction, 2) reverting to traditional CART [20], 3) antegrade "external cap crush" by inflating a balloon in the subintimal space parallel to the CTO segment to weaken it [34], and 4) re-cross the CTO body in a different subintimal path using retrograde knuckle wiring. These alternatives are time consuming and cumbersome, therefore in the face of these cumbersome options, rendezvous technique remains a valid choice.

4.4 Failure to reach the antegrade system.

With the provision of short (85 or 90cm) GC and guide extension catheters, failure of the retrograde MC to reach the antegrade system due to length issue is rare. However, sometimes final retrograde channel used may be different and significantly longer than the pre-procedural planning and we may need rendezvous. Extensive calcification and tortuosity of the proximal vessel segment may also prevent antegrade guide extension catheter delivery and unexpected lengthy vascular route, especially in tall patients, may prohibit the use of short GC to reach the coronary ostium. Rendezvous is a solution in these scenarios.

4.5 Need to rapidly establish antegrade track.

When a dominant collateral channel is used for retrograde approach, significant ischemia and hemodynamic instability may occur. Proper antegrade preparation before collateral channel tracking and expedited Rev-CART are helpful in this case. Rendezvous technique facilitates rapid establishment of antegrade wire track which minimizes the ischemia induced by the retrograde devices occupying the collateral channel.
Donor artery complications such as thrombosis and channel perforations may also interrupt our retrograde CTO PCI. Rapid establishment of antegrade wire track may be mandatory, so that further salvage procedures such as thrombus aspiration or embolization for hemostasis can be performed.

4.6 Ipsilateral channel collateral retrograde CTO PCI with single guiding catheter.

Although we usually recommend ping-pong guiding catheter technique when dealing with ipsilateral collateral retrograde CTO PCI, there are instances where we might end up doing a retrograde through single GC. If access is impossible, or if we began with single GC for antegrade CTO PCI but decided to try a difficult retrograde channel with low success rate, we might forego a second femoral puncture on anticoagulation for a brief try of the channel

through the single GC. Sometimes, we face an easy retrograde with ipsilateral collateral and we might attempt it through single GC. In all these cases, rendezvous is essential as we cannot trap the retrograde wire with balloon anchoring in the GC and we often cannot push the retrograde MC through the CTO lesion. This remains a valid reason for rendezvous.

5. Tips and tricks for rendezvous techniques.

5.1 Position of rendezvous.

The easiest position to achieve rendezvous is at the level of the secondary bend of the antegrade GC. The tips of the MC and wire will both lean against the outer curvature of the catheter, therefore, it is will be easy to advance the wire into the MC at this level (figure 4a).

5.2 Rapid switching to antegrade.

After tip-in, the retrograde wire should be advanced as far as possible into the antegrade MC. A torque device is then locked firmly on the remaining end of the wire against the retrograde MC hub (figure 4b) to prevent loss of wire control. The antegrade MC now can be pushed, meeting the retrograde MC tip, continuously across the CTO segment [32].

5.3 When MC cannot cross the CTO body after rendezvous.

If the indication for rendezvous is the inability to pass the retrograde MC through the CTO body, then we need to maximize the antegrade MC's penetrative power to cross the CTO. In these cases we should start with the maximal back up and most powerful MC. When we suspect that the MC cannot cross the CTO body, we should change to a strong back-up support antegrade GC, engage a guide extension catheter, or use anchor balloon in a side branch. Special penetrative MC, such as Turnpike Gold (Teleflex) or Turnpike spiral (Teleflex) may also help. Applying continuous negative suction to the antegrade penetrative MC (figure 4c) may pull the retrograde wire inside indirectly, and increase the penetrative force of the antegrade MC.

5.4 RotaWire exchange technique.

If all the above described in 5.3 were tried and the antegrade MC still failed to cross, and the reminding distance between the antegrade and retrograde MCs is short, we can attempt advancing an antegrade rotablator wire into retrograde MC. The retrograde wire is withdrawn to the tip of the antegrade MC, then a RotaWire (Boston Scientific) is placed into the antegrade MC until its tip is in contact with the retrograde wire tip. The retrograde wire is then pulled back a short distance gradually, with the antegrade RotaWire advanced to follow closely (figure 4d). This will allow the RotaWire to tract the void of the removed retrograde wire, and achieve wire exchange. Once the RotaWire is across the CTO body and entered into distal vessel (figure 4e), subsequent rotation atherectomy can be carried out to complete the CTO intervention (figure 4f).

5.5 Comparison of methods to overcome tough CTO segment when MC passage is difficult.

There are several options to overcome this problem when retrograde wire crossed the CTO but the MC cannot cross. Continuing aggressive pushing on the retrograde MC can lead to rupture of the retrograde channel or retrograde MC tip deformation, both results in the loss of

retrograde access. Exchanging the retrograde MC for a small balloon to dilate the lesion is also associated with risks of channel injury. Giving up the original wire position and performing retrograde knuckle wiring across CTO segment via subintimal space, or conversion to traditional CART [20], are both time consuming and does not guarantee success. External cap crush carries the risk of proximal vessel injury, hematoma extension, and perforation. Therefore, well-executed tip-in type rendezvous followed by dedicated penetrative antegrade MC is probably the most reasonable option [33]. Antegrade RotaWire change is also relatively simple and with low risk.

6. Conclusions.

Technical success of CTO PCI is usually very high after successful Rev-CART. However, operator may still be unable to establish antegrade wire access, resulting in final failure. This gap is not well covered in the previous literature.
We, the APCTO club, have provided a review and recommendations for methods to achieve antegrade wire access after successful Rev-CART. We have addressed every failure mode in detail, covering different options and their risks. Our recommendations focus upon safety first, and then ease of use. We hope this work will help all retrograde operators to further improve their procedures.

Funding Statement: There are no financial grants or donations in relation to this work.

References.

1. Surmely JF, Tsuchikane E, Katoh O, Nashida Y, Nakayama M, Nakamura S, Oida A, Hattori E, Suzuki T. New concept for CTO recanalization using controlled antegrade and retrograde subintimal tracking: the CART technique. J Invasive Cardiol. 2006;18:334–338.

2. Surmely JF, Katoh O, Tsuchikane E, Nasu K, Suzuki T. Coronary septal collaterals as an access for the retrograde approach in the percutaneous treatment of coronary chronic total occlusions. Catheter Cardiovasc Interv. 2007;69:826–832. doi: 10.1002/ccd.20816.

3. Tsuchikane E, Katoh O, Kimura M, Nasu K, Kinoshita Y, Suzuki T. The first clinical experience with a novel catheter for collateral channel tracking in retrograde approach for chronic coronary total occlusions. JACC Cardiovasc Interv. 2010;3:165-71.

4. Matsuno S, Tsuchikane E, Harding SA, Wu EB, Kao HL, Brilakis ES, Masahyekhi K, Werner GS. Overview and Proposed Terminology for the Reverse Controlled Antegrade and Retrograde Tracking (reverse CART) Techniques. EuroIntervention. 2018 May 20;14(1):94-101. doi: 10.4244/EIJ-D-17-00867.

5. Galassi AR, Sianos G, Werner GS, Escaned J, Tomasello SD, Boukhris M, Castaing M, Büttner JH, Bufe A, Kalnins A, Spratt JC, Garbo R, Hildick-Smith D, Elhadad S, Gagnor A, Lauer B, Bryniarski L, Christiansen EH, Thuesen L, Meyer-Geßner M, Goktekin O, Carlino M, Louvard Y, Lefèvre T, Lismanis A, Gelev VL, Serra A, Marzà F, Di Mario C, Reifart N on behalf of the Euro CTO Club. Retrograde recanalization of chronic total occlusions in Europe: Procedural, in-hospital, and long-term outcomes from the multicenter ERCTO registry. J Am Coll Cardiol 2015;65:2388-400.

6. Karmpaliotis D, Michael TT, Brilakis ES, Papayannis AC, Tran DL, Kirkland BL, Lembo N, Kalynych A, Carlson H, Banerjee S, Lombardi W, Kandzari DE. Retrograde coronary chronic total occlusion revascularization: procedural and in-hospital outcomes from a multicenter registry in the United States. JACC Cardiovasc Interv. 2012;5:1273–1279. doi: 10.1016/j.jcin.2012.06.025.

7. Michael TT, Mogabgab O, Alomar M, Kotsia A, Christopoulos G, Rangan BV, Abdullah S, Grodin J, Banerjee S, Brilakis ES. Long-term outcomes of successful chronic total occlusion percutaneous coronary interventions using the antegrade and retrograde approach. J Interv Cardiol. 2014;27:465–471. doi: 10.1111/joic.12149.

8. Karmpaliotis D, Karatasakis A, Alaswad K, Jaffer FA, Yeh RW, Wyman RM, Lombardi WL, Grantham JA, Kandzari DE, Lembo NJ, Doing A, Patel M, Bahadorani JN, Moses JW, Kirtane AJ, Parikh M, Ali ZA, Kalra S, Nguyen-Trong PK, Danek BA, Karacsonyi J, Rangan BV, Roesle MK, Thompson CA, Banerjee S, Brilakis ES. Outcomes with the use of the retrograde approach for coronary chronic total occlusion interventions in a contemporary multicentreUS registry. Circ Cardiovasc Interv 2016;9:e003434 doi:10.1161/CIRCINTERVENTIONS.115.003434.

9. Rinfret S, Joyal D, Nguyen CM, Bagur R, Hui W, Leung R, Larose E, Love MP, Mansour S. Retrograde recanalization of chronic total occlusions from the transradial approach; early Canadian experience. Catheter Cardiovasc Interv. 2011;78:366–374. doi: 10.1002/ccd.23140.

10. Huang Z, Ma D, Zhang B, Folson AA, Lin J, Wu K, Liao H, Zhong Z. Epicardial collateral channel for retrograded recanalization of chronic total occlusion percutaneous coronary intervention: predictors of failure and procedural outcome. J Interv Cardiol 2017; doi: 10.1111/joic.12441.

11. Lee CK, Chen YH, Lin MS, Yeh CF, Hung CS, Kao HL, Huang CC. Retrograde approach is as effective and safe as antegrade approach in contemporary percutaneous coronary intervention for chronic total occlusion: A Taiwan single-center registry study. Acta Cardiol Sin 2017;33:20-17.

12. Maeremans J, Walsh S, Knaapen P, Spratt JC, Avran A, Hanratty CG, Faurie B, Agostoni P, Bressollette E, Kayaert P, Bagnall AJ, Egred M, Smith D, Chase A, McEntegart MB, Smith WH, Harcombe A, Kelly P, Irving J, Smith EJ, Strange JW, Dens J. The hybrid algorithm for treating chronic total occlusions in Europe. The RECHARGE registry. J Am Coll Cardiol 2016;68: doi: 10.1016/j.jacc.2016.07.034

13. Wu EB, Tsuchikane E, Lei G, Harding S, Lo S, Lim ST, Chen JY, Lee SW, Qian J, Kao HL, Yan BPY. Retrograde Versus Antegrade Approach for Coronary Chronic Total Occlusion in an Algorithm-Driven Contemporary Asia-Pacific Multicenter Registry: Comparison of Outcomes. Heart Lung Circ 2019 doi.org/10.1016/j.hlc.2019.05.188.

14. Thompson CA. The hybrid approach for percutaneous revascularization of coronary chronic total occlusions. Interv Cardiol Clin 2012;1:349-353.

15. Brilakis ES, Grantham JA, Rinfret S, Wyman RM, Burke MN, Karmpaliotis D, Lembo N, Pershad A, Kandzari DE, Buller CE, DeMartini T, Lombardi WL, Thompson CA. A percutaneous treatment algorithm for crossing coronary chronic total occlusions. J Am Coll Cardiol Intv 2012;5:367-79.

16. Joyal D, Thompson CA, Grantham JA, Buller CE, Rinfret S. Retrograde technique for recanalization of chronic total occlusions: a step-by-step approach. JACC Cardiovasc Interv. 2012;5: 1-11.

17. Brilakis ES, Grantham JA, Thompson CA, DeMartini TJ, Prasad A, Sandhu GS, Banerjee S, Lombardi WL. The retrograde approach to coronary artery chronic total occlusions: a practical approach. Catheter Cardiovasc Interv. 2012;79:3-19.

18. Wu EB, Chan WW, Yu CM. Retrograde chronic total occlusion intervention: tips and tricks. Catheter Cardiovasc Interv. 2008; 72:806-14.

19. Harding SA, Wu EB, Lo S, Lim ST, Ge L, Chen JY, Qian J, Lee SW, Kao HL, Tsuchikane E . A new algorithm for crossing chronic total occlusions from the Asia Pacific Chronic Total Occlusion Club. J Am Coll Cardiol Intv 2017;10:2135-2143.

20. Wu EB, Tsuchikane E, Lo S, Lim ST, Ge L, Chen JY, Qian J, Lee SW, Harding SA, Kao HL. Retrograde algorithm for chronic total occlusion from the Asia Pacific Chronic Total Occlusion club. Asian Intervention Journal 2018;4:98-107.

21. Wu EB, Tsuchikane E, Lo S, Lim ST, Ge L, Chen JY, Qian J, Lee SW, Kao HL, Harding SA. "Chronic Total Occlusion Wiring: A State-of-the-Art Guide From the Asia Pacific Chronic Total Occlusion Club." *Heart, lung & circulation* (2019)doi:10.1016/j.hlc.2019.04.004.

22. Mozid AM, Davies JR, Spratt JC. The utility of a guideliner catheter in retrograde percutaneous coronary intervention of a chronic total occlusion with reverse CART - the "capture" technique. Catheter Cardiovasc Intv 2014;83:929-32.

23. Online Data Supplement - Pushing retrograde wire and noting its position and then manipulating the ipsilateral ping-pong guide to the position of the retrograde wire path and successful wiring of the antegrade guiding catheter.

24. Otsuka Y, Kataoka Y, Fukuoka T. Snaring the retrograde wire in the aortic root for chronic total occlusion after Bentall operation in a patient with Bechet's disease. J Invasive Cardiol 2009;21(7):E137-40.

25. Fang HY, Lee WC, Fang CY, Wu CJ. Application of a snare technique in retrograde chronic total occlusion percutaneous coronary intervention- a step by step practical approach and an observational study. Medicine (Baltimore) 2016;95(41):e5129.

26. Wu EB, Tsuchikane E. The inherent catastrophic traps in retrograde CTO PCI. Catheter Cardiovasc Interv. 2018;91:1101-9.

27. Kensuke Y, Sumitsuji S, Kaneda H, Siegrist PT, Okayama K, Ide S, Mizote I, Kumada M, Kuroda T, Tachibana K, Sakata Y, Nanto S. "A Novel Homemade Snare, Safe, Economical and Size-adjustable." *EuroIntervention* 2015;10:1307-10.

28. https://www.youtube.com/watch?v=wJ0if-5OEfM.

29. Online data supplement- Illustrating the ability of the home made snare to increase its loop size by pushing on the wire.

30. Kim MH, Yu LH, Mitsudo K. A new retrograde wiring technique for chronic total occlusion. Catheter Cardiovasc Interv 2010;75:117-119.

31. Muramatsu T, Tsukahara R, Ito Y. "Rendezvous in coronary" technique with the retrograde approach for chronic total occlusion. J Invasive Cardiol 2010;22(9):E179-82.

32. Funatsu A, Kobayashi T, Nakamura S. Use of the kissing microcatheter technique to exchange a retrograde wire for an antegrade wire in the retrograde approach to intervention in chronic total occlusion. J Invasive Cardiol 2010;22(5):E74-7.

33. Vo MN, Ravandi A, Brilakis ES. "Tip-in" technique for retrograde chronic total occlusion revascularization. J Invasive Cardiol 2015;27(5):E62-4.

34. Vo MN, Ravandi A, Grantham JA. Subintimal space plaque modification for "Balloon-uncrossable" Chronic total occlusions. *J Inv Cardiology*. 2014;26:E133-136.

Figures.

Figure 1. Passing the externalisation wire through the antegrade Y connector. 1a. Insertion of wire introducer in parallel to the anchor balloon shaft through the antegrade Y connector. 1b. Disconnected Y connector now pulled back over the anchor balloon. 1c. Retrograde wire pushed out of antegrade guiding hub. 1d. Putting the externalisation wire into the wire introducer. 1e. Y connector brought near to guiding hub for reconnection. 1f. Removal of wire introduced to allow passage of devices.

Figure 2. Initial steps to deal with failing to wire the antegrade guiding catheter. 2a. Pushing the retrograde wire far into aorta. 2b Using proximal vessel anchor balloon. 2c. Switching for new low profile rotational retrograde MC. 2d. Switching to soft wire to wire guiding. 2e. Successful externalization. 2f. Good final results.

Figure 3. Homemade snare. 3a. Homemade snare pushed to large size. 3b. Snared retrograde wire. 3c. Anchored retrograde wire, MC passed.

Figure 4. Rendezvous and tip in. 4a. Best bending position of the antegrade guide to do tip in. 4b. Locking torque device on retrograde side of wire after tip in. 4c. Applying negative pressure to improve wire tracking. 4d. Antegrade rota wire tracking retrograde microcatheter tip in technique. 4e. Successful antegrade rota wire passage to distal true lumen. 4f. 1.25 mm burr to CTO lesion.

1a.

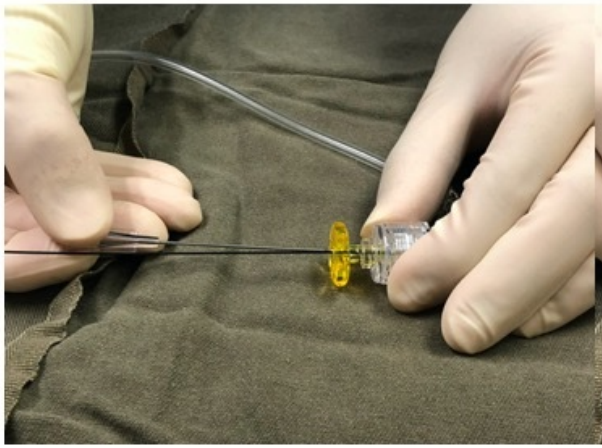

1b

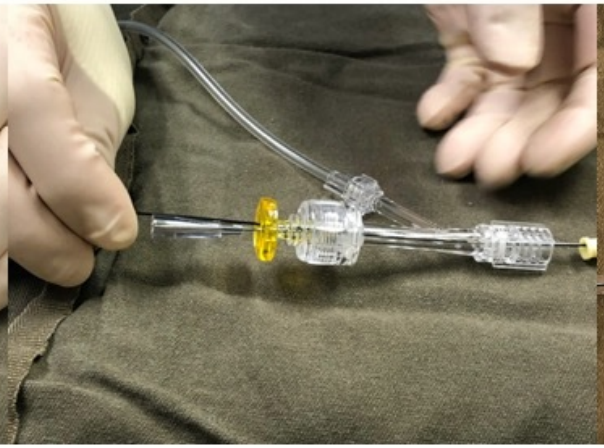

1c.

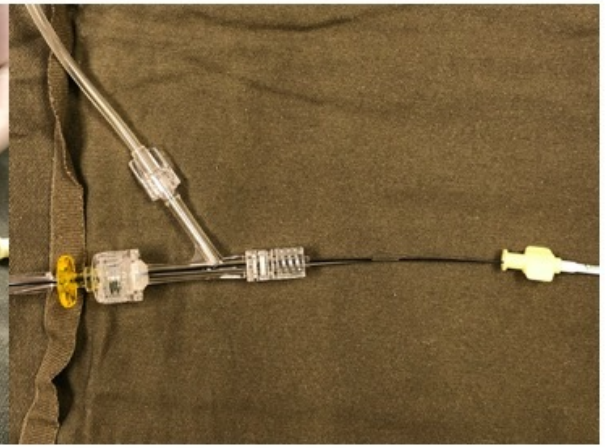

1d

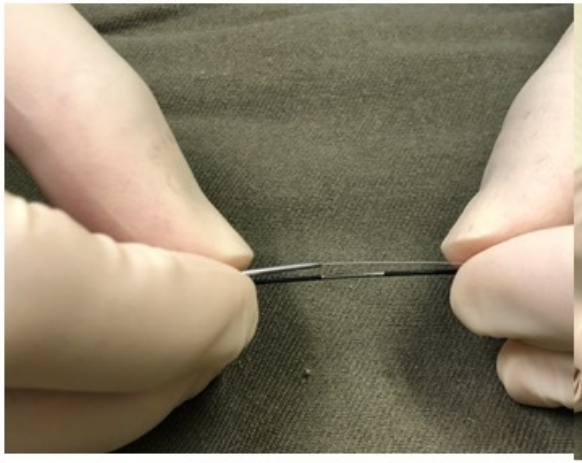

1e

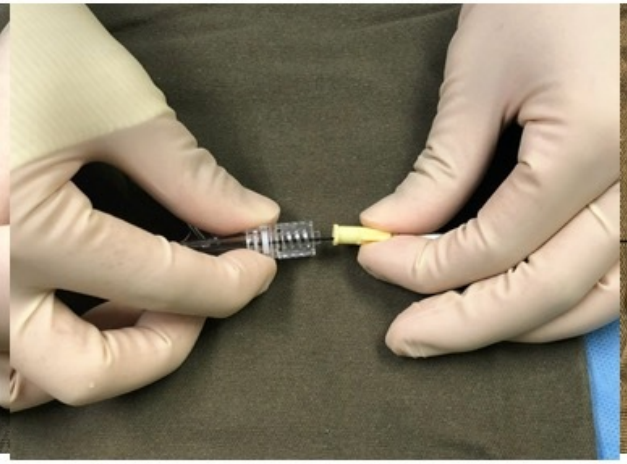

1f

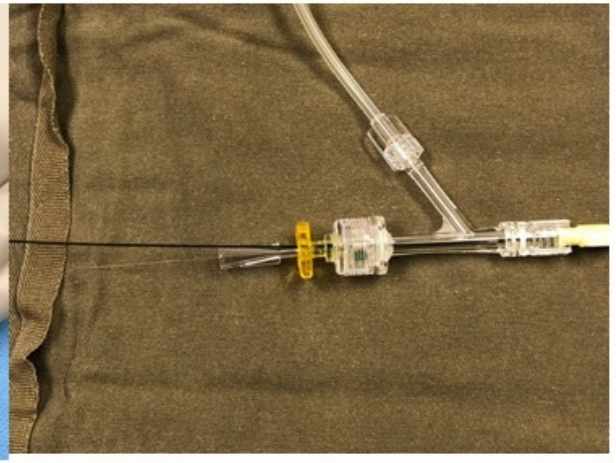

2a.

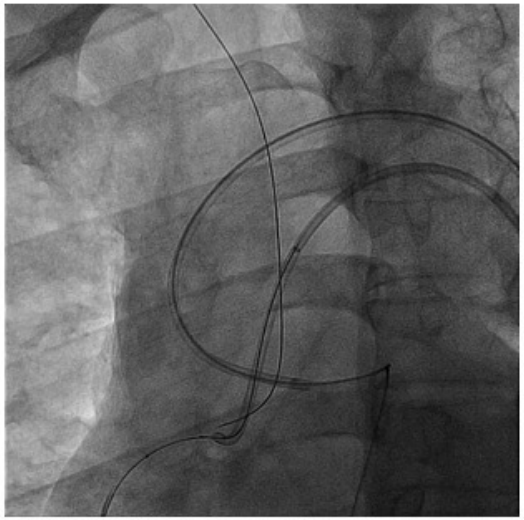

2b.

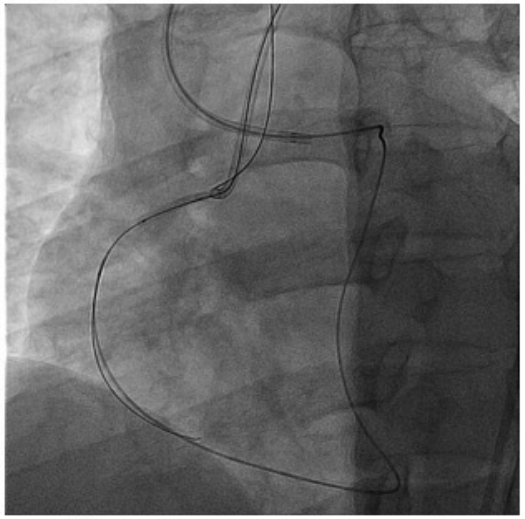

2c.

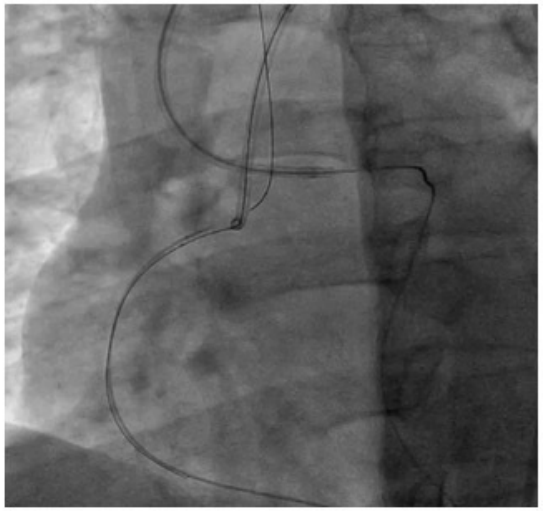

2d.

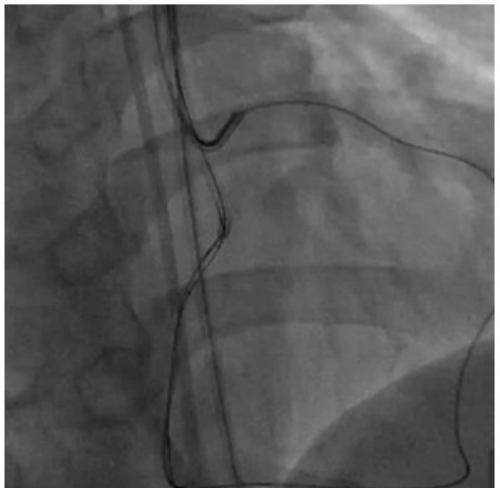

2e.

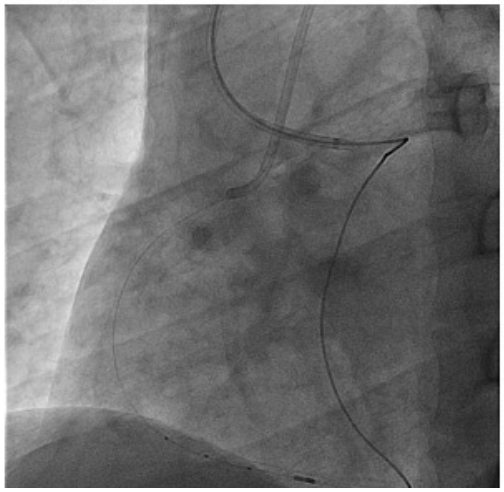

2f.

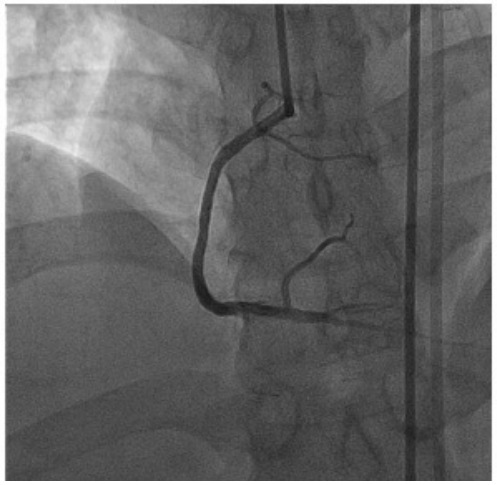

Fig 3a.

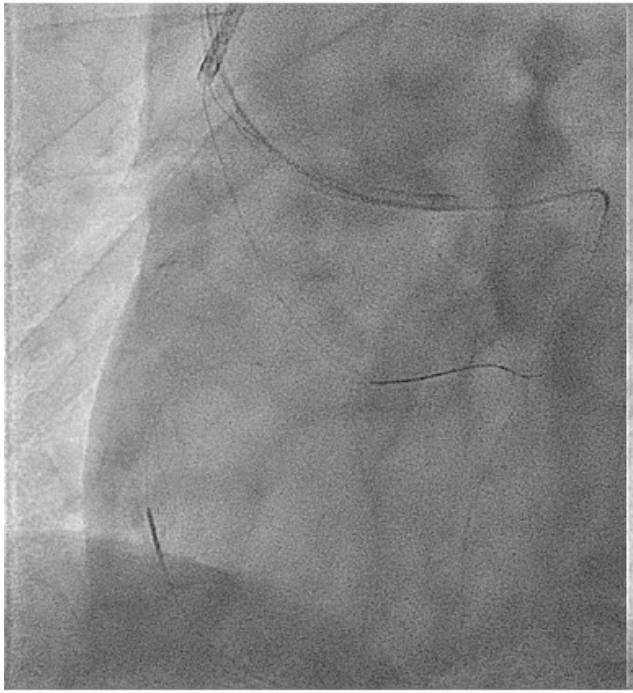

Fig 3b.

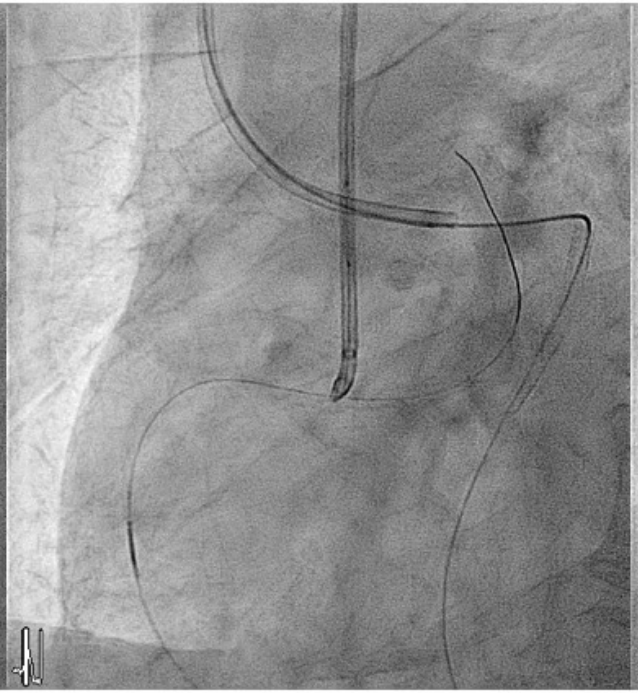

Fig 3c.

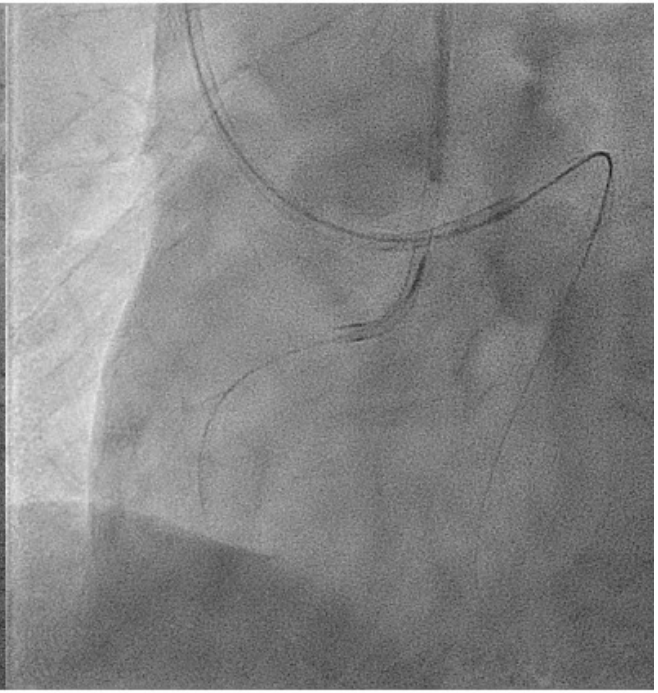

4a.

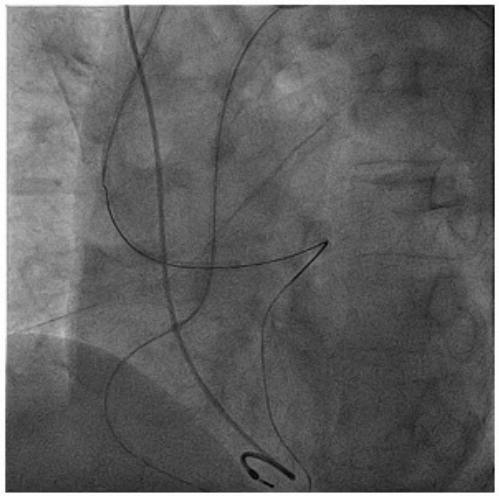

4b.

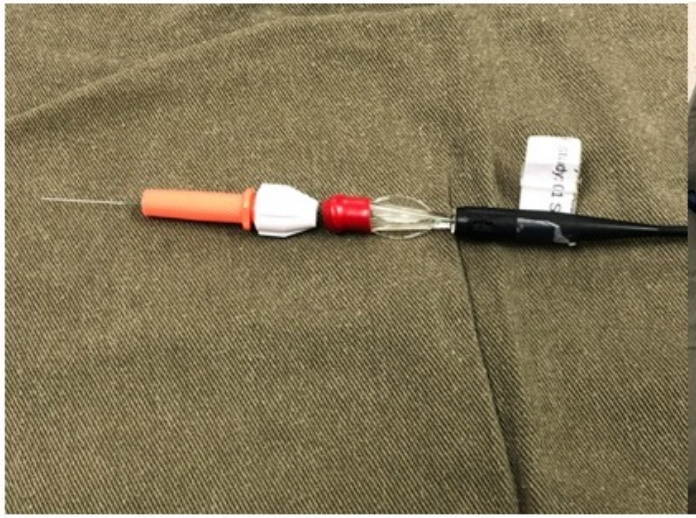

4c

4d

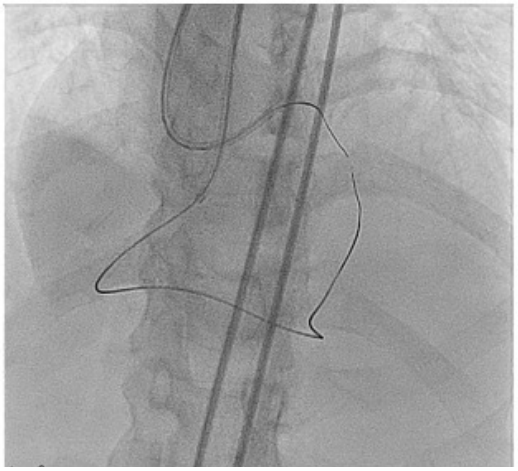

4e

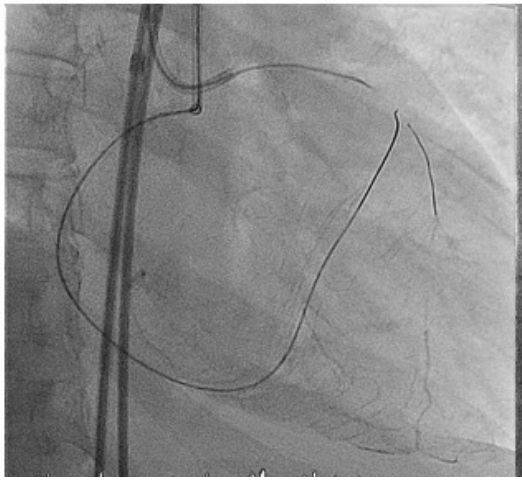

4f.

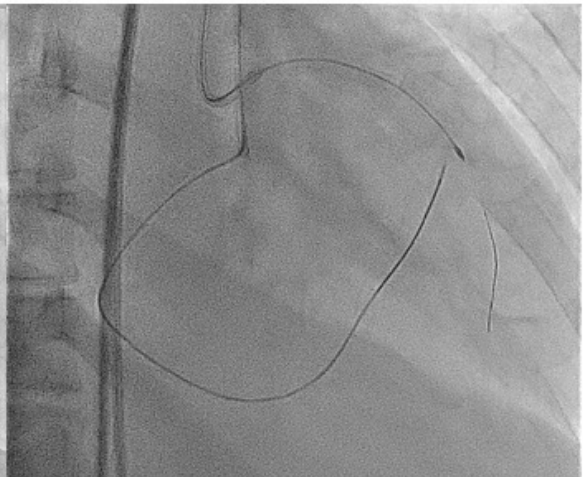

AsiaIntervention

Official Journal of the Asian Pacific Society of Interventional Cardiology

(APSIC) and the Interventional Cardiology Foundation of India (ICFI)

www.asiaintervention.org

Title: **Evaluation of a portable assembly catheter simulator using a 3D-printed heart model for percutaneous transvenous mitral commissurotomy in developing countries.**

Authors: Xiaoyang Song, M.D; Naritatsu Saito, M.D; Yoshimasa Nagata, Afzalur Rahman, M.D; Martin M Murage, M.D; Farhana Ahmed, M.D; Mohammad Arifur Rahman, M.D; Tariq Ahmed Chowdhury, M.D; Bernard Muriuki Gitura, M.D; Christine Awuor Yuko- Jowi, M.D; Peter Muriithi Nyamu, M.D; Takeshi Kimura, M.D; Kanji Inoue, M.D

Manuscript number: AIJ-D-19-00013

Manuscript submission date: 25 March 2019

Revisions received: 30 April 2020

Accepted date: 10 July 2020

Evaluation of a portable assembly catheter simulator using a 3D-printed heart model for percutaneous transvenous mitral commissurotomy in developing countries

Xiaoyang Song MD[1], Naritatsu Saito MD[1], Yoshimasa Nagata[2], Afzalur Rahman MD[3], Martin M Murage MD[4], Farhana Ahmed MD[3], Mohammad Arifur Rahman MD[3], Tariq Ahmed Chowdhury MD[3], Bernard Muriuki Gitura MD[4], Christine Awuor Yuko- Jowi MD[4], Peter Muriithi Nyamu MD[4], Takeshi Kimura MD[1], Kanji Inoue MD[2]

1 Department of Cardiovascular Medicine, Graduate School of Medicine, Kyoto University, Kyoto, Japan

2 PTMC institute, Kyoto, Japan

3 National Institute of Cardiovascular Disease, Dhaka, Bangladesh

4 Kenyatta National Hospital, Nairobi, Kenya

Short running title: Catheter simulator for PTMC

Address for correspondence:

Naritastu Saito, MD

Department of Cardiovascular Medicine, Kyoto University Graduate School of Medicine,

54 Kawahara-cho, Shogoin, Sakyo-ku, Kyoto, 606-8507, Japan

E-mail: naritatu@kuhp.kyoto-u.ac.jp

Classifications

Balloon valvuloplasty, Mitral stenosis, Mitral valvuloplasty, Training and education

Abbreviations

PTMC: Percutaneous Transvenous Mitral Commissurotomy, CT: Computed tomography, RHD: Rheumatic Heart Disease, NICVD: National Institute of Cardiovascular Diseases, KNH: Kenyatta National Hospital, JICA: Japan International Cooperation Agency

Abstract

Introduction:

We developed a catheter simulator for percutaneous transvenous mitral commissurotomy (PTMC) based on the data from a patient with mitral valve stenosis.

The simulator has the following characteristics: 1) the simulator is portable and easy to assemble and disassemble, 2) the cardiac portion is created using a 3D-printer based on patient computed tomography data, 3) the simulator uses a foot-operated water pump to create pulsatile flow, and 4) the fossa ovalis in the atrial septum of the heart model is made of thin polyurethane membrane and is interchangeable. We aimed to assess the effectiveness of this novel simulator for training in PTMC using the Inoue balloon in developing countries.

Methods and Results:

We used this simulator for training in the National Institute of Cardiovascular Diseases in Bangladesh (13 physicians), and in Kenyatta National Hospital in Kenya (11 physicians). The effectiveness of training was evaluated by questionnaire and the procedure time in simulation.

The questionnaire obtained from the trainees showed that realism of the model scored 4.7 ± 0.5, utility of pulsatile flow scored 4.7 ± 0.5, simulator utility scored 4.9 ± 0.3, and the effect of training on PTMC performance scored 4.9 ± 0.5. The procedure time in simulation was shortened from 30.0 ± 12.6 min (first time), to 23.4 ± 11.9 min (second time) and to 20.4 ± 11.1 min (third time) ($p < 0.01$).

Conclusions:

The novel portable assembly catheter simulator using a 3D-printed heart model for PTMC received positive comments and improved the skills of trainees.

Condensed abstract

We developed a 3D-printed catheter simulator for percutaneous transvenous mitral commissurotomy (PTMC) based on the computed tomography data from a patient with mitral valve stenosis. We used this simulator for training in the National Institute of Cardiovascular Diseases in Bangladesh (13 physicians), and in Kenyatta National Hospital in Kenya (11 physicians). The procedure time in simulation was shortened by repeating the practice. The novel portable assembly catheter simulator using a 3D-printed heart model for PTMC received positive comments and improved the skills of trainees.

Introduction:

Rheumatic fever is a leading cause of valvular heart disease, especially in developing countries with large populations and poor public health quality, and rheumatic heart disease (RHD) is a major public health problem[1,2]. Therefore, there is a need for skilled cardiologists, and especially interventionists, to treat rheumatic valvular disease. However, there is often a shortage of skilled physicians,

and the training of qualified medical teams is hindered by socioeconomic factors[3]. In light of these factors, teams from other countries have directly assisted local surgeons, and the effort has achieved considerable success[3,4]. However, the number of patients who benefit from this approach is limited. Training a local heart team is a reasonable solution. Teaching catheter intervention technique is a challenge, and simulation-based training is reportedly effective. However, quantitative assessment of simulation-based training has not been reported. We developed a novel catheter simulator for training of percutaneous transvenous mitral commissurotomy (PTMC). The purpose of the present study was to assess the effectiveness of this novel simulator for training PTMC using the Inoue balloon in a developing country.

Methods:

The simulator consisted of a water tank (length 500 mm, width 385 mm, depth 170 mm), a heart model, a rubber tube representing the inferior vena cava and femoral vein, and a foot-operated water pump (Figure 1). The heart model was constructed with a 3D printer (crossEffect Inc., Kyoto, Japan) using polyurethane resin based on patient computed tomography (CT) data. The cardiac portion of the simulator was translucent, and the right and left ventricle were omitted to better visualize the catheter movement. The fossa ovalis in the atrial septum of the heart

model was made of thin polyurethane membrane and was interchangeable. The simulator used a foot pump to create physiological pulsatile flow. The pump drew water from the water tank and discharged water into the left atrium. The suction tube was connected to a translucent cup. By covering the mitral annulus with the translucent cap, a pulsatile flow that sucked the Inoue balloon catheter into the translucent cap was made (Figure 2). Utilizing the flow to navigate the Inoue balloon catheter into the left ventricle is an important technique in PTMC. Physicians can practice this technique in this simulator.

The effectiveness of the simulation was evaluated by conducting questionnaire surveys after the simulation and measuring the change in procedure time. In the questionnaire, the participants rated the realism and training potential of the simulator on a Likert scale from 1 (poor) to 5 (excellent) (Figure 3). The procedure time (min) was defined as the time from insertion of the 7-Fr sheath to passage of the Inoue balloon into the left ventricle. We used the procedure time as an objective index to evaluate trainee improvement. This training program aimed at transferring knowledge and developing skills in local heart teams.

Statistics:

Statistical analyses were performed using JMP 14 Pro (SAS Institute Inc, Cary, NC, USA) software. Continuous variables were presented as mean ± standard deviation. A 2-sided p-value of <0.05 was considered statistically significant.

Results:

The simulator-based training was conducted in the National Institute of Cardiovascular Diseases (NICVD), Bangladesh (13 physicians in 5 days from November 4-8, 2018). The training was also conducted in Kenyatta National Hospital (KNH), Kenya (11 physicians in 5 days from December 1-5, 2019). The average age of training participants was 45.1 ± 6.7 years old (NICVD: 45.1 ± 6.7, KNH: 49.3 ± 6.9), the average years of experience as physicians was 20.1 ± 7.0 (NICVD: 17.1 ± 4.3, KNH: 23.6 ± 8.1), and the average years of experience as interventional cardiologists was 7.1 ± 5.2 (NICVD: 5.8 ± 2.9, KNH: 8.7 ± 6.8). 22 out of 24 physicians (91.7%) had experience in PTMC mainly as assistants (NICVD: 13/13 (100%), KNH: 9/11 (81.8%)), and 8 (62%) had experience in PTMC using the Inoue balloon (NICVD: 8/13 (61.5%), KNH: 3/11 (27.2%)). Only 4 out of 24 physicians (16.7%) had experienced simulation-based training for other catheter intervention procedures (NICVD: 2/13 (15.4%), KNH: 2/11 (18.1%)).

The questionnaires completed by all the trainees after the course showed that: realism of the model scored 4.7 ± 0.5 (NICVD: 4.8 ± 0.4, KNH: 4.3 ± 0.8), utility of pulsatile flow scored 4.7 ± 0.6 (NICVD: 5 (all participants scored 5), KNH: 4.5 ± 0.5), simulator utility scored 4.9 ± 0.3 (NICVD: 4.8 ± 0.4, KNH: 4.9 ± 0.3), and the effect of training on PTMC performance scored 4.9 ± 0.4 (NICVD: 4.9 ± 0.3, KNH: 4.8

± 0.6). The procedure time in the simulation was shortened from 30.0 ± 12.6 min in the first time (NICVD: 31.5 ± 10.9, KNH: 27.5 ± 15.6), to 23.4 ± 11.9 min in the second time (NICVD: 26.1 ± 10.4, KNH: 20.1 ± 13.6), and 20.4 ± 11.1 min in third time (NICVD: 20.8 ± 10.8, KNH: 19.9 ± 12.3) (Figure 4, $p < 0.01$, paired t-test). The procedure time in simulation was not recorded in 3 trainees in KNH.

Discussion:

The main findings of the present study were that: (1) a novel portable assembly catheter simulator using a 3D-printed heart model with a foot pump to create pulsatile flow for PTMC was effective for training; (2) the simulator was highly rated by the participants as close to actual treatment; and (3) the training shortened the procedure time in simulation.

Mitral valve stenosis is a common valvular sequela of acute rheumatic fever. There are nearly 33 million people with RHD globally, contributing to approximately 275 000 deaths every year. RHD is still a major problem in developing countries. PTMC, also known as percutaneous mitral balloon valvotomy, is the first choice of treatment for symptomatic patients with rheumatic mitral valve stenosis. PTMC using the Inoue balloon was first developed by Inoue in 1982[5]. As with other interventional procedures, there is a certain learning curve for mastering PTMC technique using the Inoue balloon catheter, and teaching catheter intervention

technique is a challenge. Simulation-based training has now been widely accepted as an important tool for procedural training and is seen as an important future development for interventional cardiology training programs worldwide. The novel simulator presented in this paper does not require a power supply, it can be used with a small amount of water, and it is portable and easy to assemble within 1 h. We developed this simulator for use in developing countries with limited power and water supplies.

The training program also included observation and performance of PTMC in actual patients. During the training period, a total of 25 patients underwent PTMC (NICVD: 13 patients, NKH 12 patients) where the Inoue balloon catheter was used by Dr. Inoue himself or by the training participants under the supervision of Dr. Inoue (Figure 5).

Limitations:

The present study has several important limitations. First, evaluation of the simulation was done by a questionnaire, which is subjective and may have poor reproducibility. Second, most participants had already carried out PTMC using other balloon procedures, which could have influenced the study results. Third, the 3D-printed heart models used in this study were created from patients with typical mitral stenosis, but the variation in heart morphology is much greater in real patients.

Funding statement:

The training in Bangladesh was conducted as part of an international program supported by the Ministry of Health, Labour and Welfare, Japan, and the training in Kenya was conducted as part of an international program supported by Japan International Cooperation Agency (JICA). All authors have no conflict of interest to declare.

Acknowledgements:

We thank Mr. Atsushi Yamazaki for his commitment and the trustworthy collaboration for this project. We would like to thank the NICVD and KNH staff who cooperated in this training. We also acknowledge the generous support of the Ministry of Health, Labour and Welfare in Japan, and JICA.

Conclusions:

A novel assembly catheter simulator using a 3D-printed heart model with a foot pump to create pulsatile flow for PTMC is useful for training physicians in developing countries.

Impact on daily practice:

A novel portable assembly catheter simulator using a 3D-printed heart model with a foot pump to create pulsatile flow was developed. The simulator can be used with a small amount of water, and it is portable and easy to assemble. This simulator will be utilized in many developing countries for training of complex catheter procedures.

References:

1. Watkins DA, Johnson CO, Colquhoun SM, Karthikeyan G, Beaton A, Bukhman G, Forouzanfar MH, Longenecker CT, Mayosi BM, Mensah GA, Nascimento BR, Ribeiro ALP, Sable CA, Steer AC, Naghavi M, Mokdad AH, Murray CJL, Vos T, Carapetis JR, Roth GA. Global, Regional, and National Burden of Rheumatic Heart Disease, 1990-2015. *N Engl J Med*. 2017;377:713–22.

2. Marijon E, Mirabel M, Celermajer D, Jouven X. Rheumatic heart disease. *Lancet*. 2012;379:953–64.

3. Tefera E, Qureshi SA, Bermudez-Cañete R. Successful training of self-sufficient interventional paediatric cardiology team in a sub-Saharan setting: A multicentre collaborative model. *Cardiol Young*. 2015;25:874–8.

4. Zühlke L, Karthikeyan G, Engel ME, Rangarajan S, Mackie P, Cupido-Katya Mauff B, Islam S, Daniels R, Francis V, Ogendo S, Gitura B, Mondo C, Okello E, Lwabi P, Al-Kebsi MM, Hugo-Hamman C, Sheta SS, Haileamlak A, Daniel W, Goshu DY, Abdissa SG, Desta AG, Shasho BA, Begna DM, Elsayed A, Ibrahim AS, Musuku J, Bode-Thomas F, Yilgwan CC, Amusa GA, Ige O, Okeahialam B, Sutton C, Misra R, Abul Fadl A, Kennedy N, Damasceno A, Sani MU, Ogah OS, Elhassan TOHM, Mocumbi AO, Adeoye AM, Mntla P, Ojji D, Mucumbitsi J, Teo K, Yusuf S, Mayosi BM. Clinical Outcomes in 3343 Children and Adults with Rheumatic Heart Disease from 14 Low-and Middle-Income Countries: Two-

Year Follow-Up of the Global Rheumatic Heart Disease Registry (the REMEDY Study). *Circulation*. 2016;134:1456–66.

5. Inoue K, Owaki T, Nakamura T, Kitamura F, Miyamoto N. Clinical application of transvenous mitral commissurotomy by a new balloon catheter. *J Thorac Cardiovasc Surg*. 1984;87:394–402.

Figures Legends:

Figure 1. Percutaneous transvenous mitral commissurotomy simulator using a 3D-printed heart model. A, Design of the heart model (frontal view). The right and left ventricle are omitted to better visualize the catheter movement. B, The cardiac portion is created using a 3D-printer based on patient computed tomography data. The the fossa ovalis in the atrial septum is made of interchangeable thin polyurethane membrane; C, Overall view of the simulator; D, simulator packed in a water tank.

Figure 2. The translucent cap of the suction tube covering the mitral annulus. The suction tube is connected to a foot pump creating pulsatile flow that sucks the Inoue balloon catheter into the translucent cap.

Figure 3. Questionnaire for assessing efficacy of catheter simulator training.

Figure 4. Change in simulation procedure time during training. The procedure time in the simulation was shortened from 30.0 ± 12.6 min in the first time to 23.4 ± 11.9 min in the second time, and 20.4 ± 11.1 min in third time. The blue marker indicates the procedure time of each participant in National Institute of Cardiovascular Disease in Bangladesh, and the red marker indicates the procedure time of each

participant in Kenyatta National Hospital in Kenya. Note that the procedure time in simulation was not recorded in 3 trainees in KNH.

Figure 5. Simulation training and observation and education in an actual percutaneous transvenous mitral commissurotomy (PTMC). A, Simulation training in National Institute of Cardiovascular Disease (NICVD). B, Actual PTMC in NICVD. C, Simulation training in Kenyatta National Hospital (KNH). D, Actual PTMC in KNH.

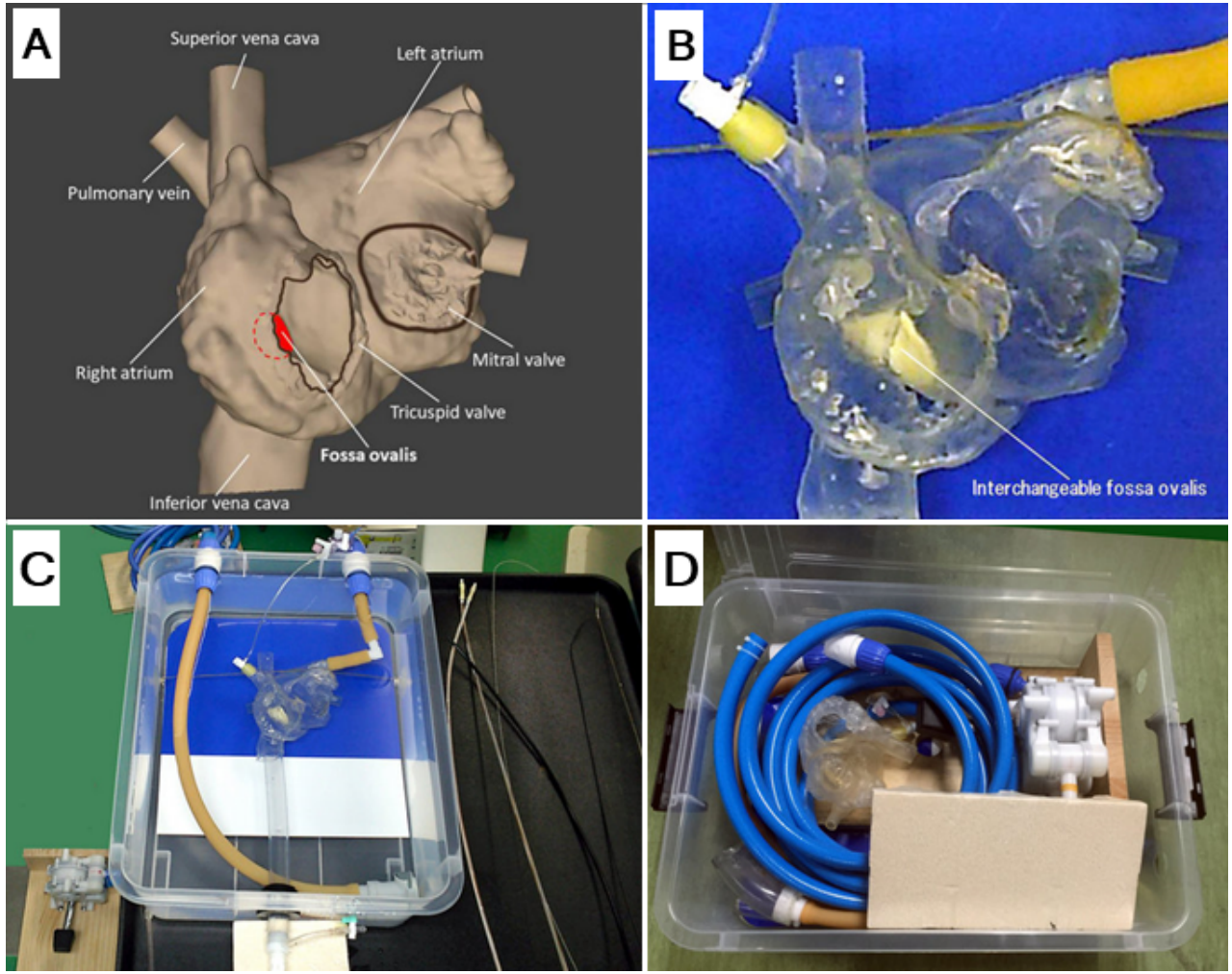

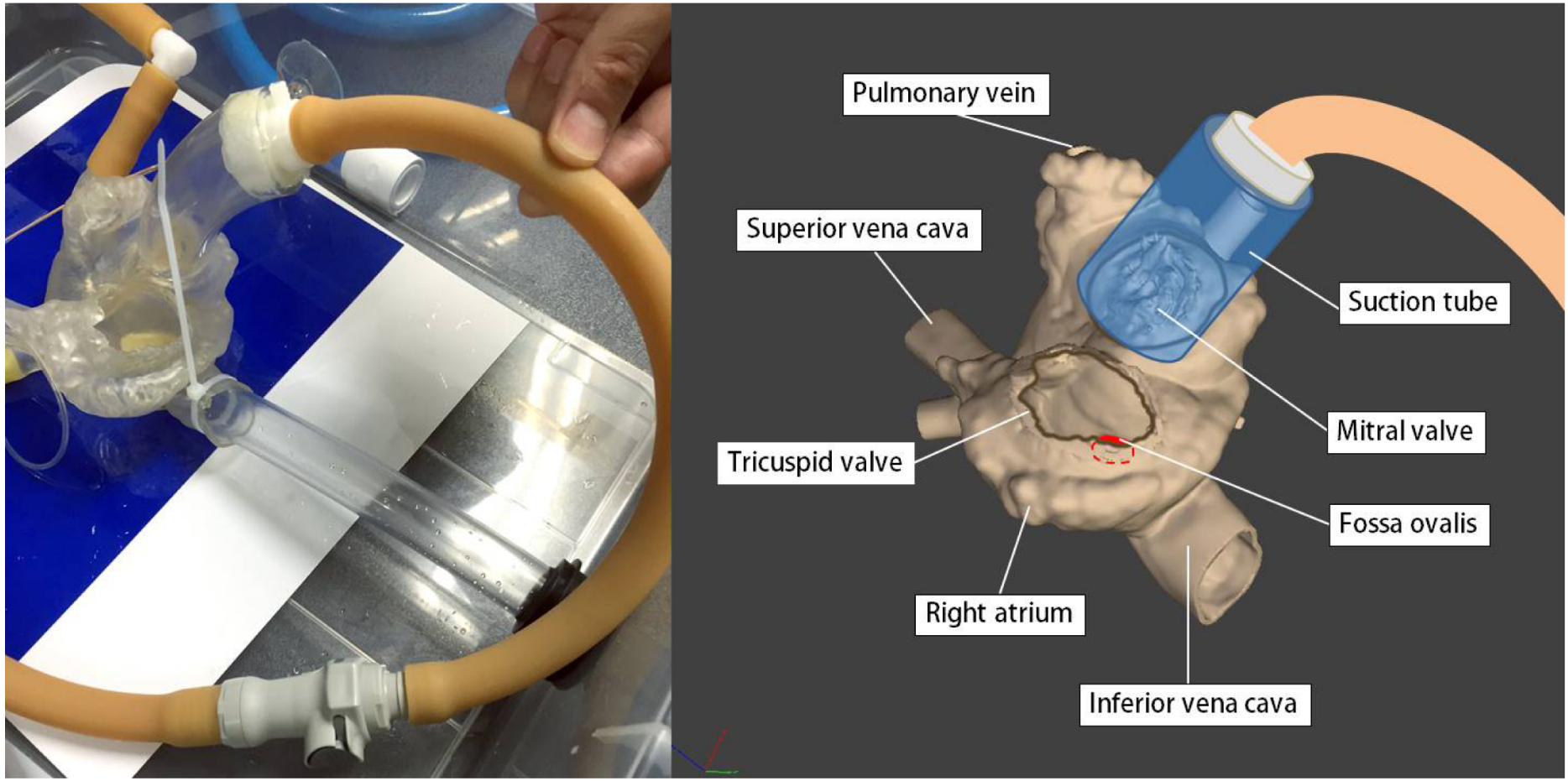

Evaluation of PTMC simulator using foot pump for producing pulsatile flow

■■■, 20XX

Questionnaire

Name:_____ Age:___years

How many years have you worked as a medical doctor?	_____years
How many years have you worked as an interventional cardiologist?	_____years
Have you ever experienced PTMC?	Yes / No
Have you experienced PTMC using the Inoue balloon catheter?	Yes / No
Have you ever experienced the simulation-based training?	Yes / No

Realism of the model

1	2	3	4	5
Not Realistic				Realistic

Do you think that pulsatile flow is necessary for PTMC simulation?

1	2	3	4	5
Disagree				Agree

This model is useful to practice the real case on the simulator, prior to performing the real PTMC procedure.

1	2	3	4	5
Disagree				Agree

Does this simulation-based training change your PTMC practice pattern?

1	2	3	4	5
No				Yes

Simulation Time

Procedure time (1st):	_____min
Procedure time (2nd):	_____min
Procedure time (3rd):	_____min

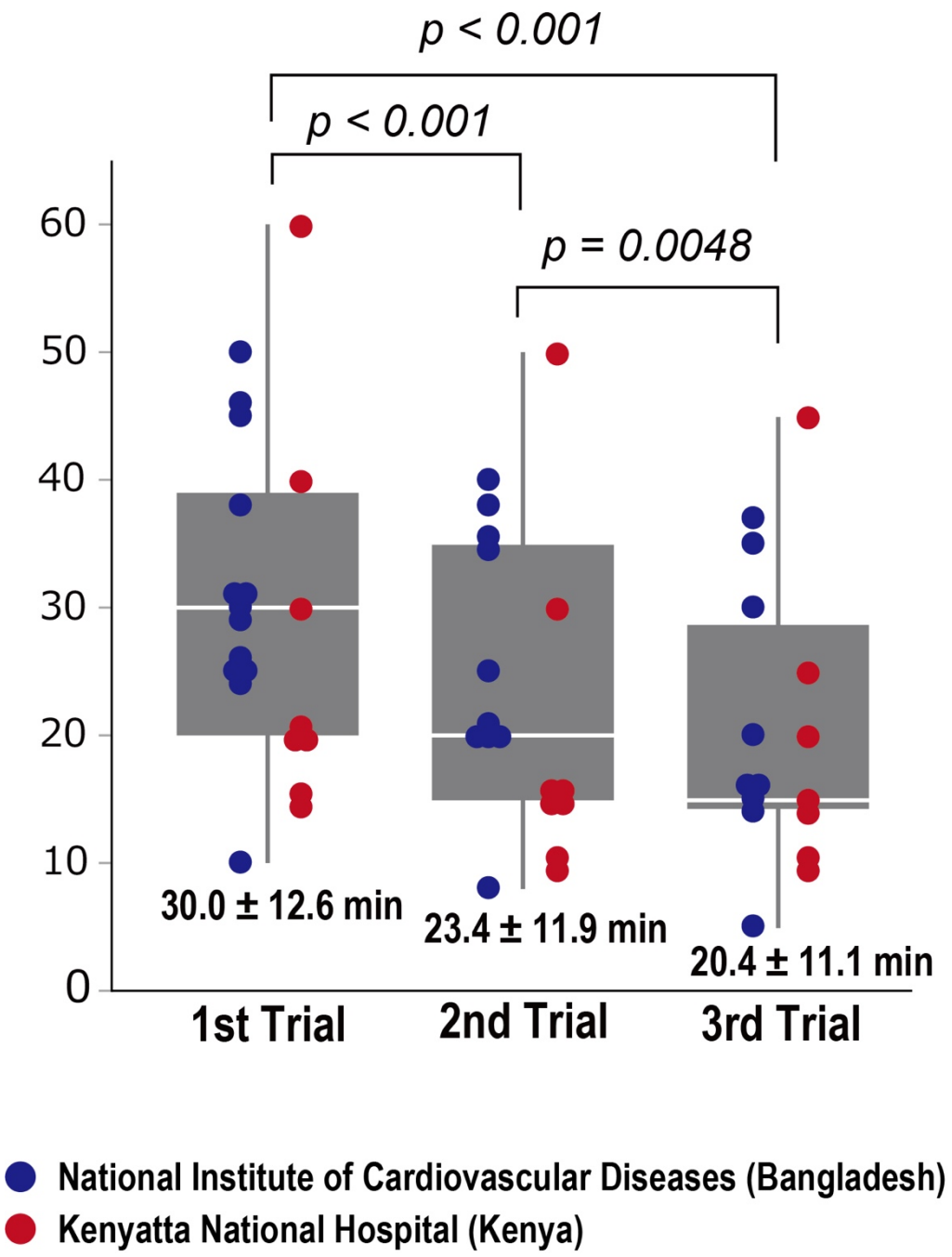

AsiaIntervention

Official Journal of the Asian Pacific Society of Interventional Cardiology

(APSIC) and the Interventional Cardiology Foundation of India (ICFI)

www.asiaintervention.org

Title: **Direct Stenting Disaster; Bailed out by Intra-vascular Lithotripsy.**

Authors: Sandeep Basavarajaiah, M.D, MRCP, FESC; Kaeng Lee , M.D, MRCP;

Gurbir Bhatia, M.D, MRCP; Michael Pitt , M.D, MRCP

Manuscript number: AIJ-D-20-00001

Manuscript submission date: 27 December 2019

Revisions received: 30 April 2020

Accepted date: 10 July 2020

Direct Stenting Disaster; Bailed out by Intra-vascular Lithotripsy

Sandeep Basavarajaiah [1] MD, MRCP, FESC, Kaeng Lee [1] MD, MRCP,

Gurbir Bhatia [1] MD, MRCP Michael Pitt [1] MD, MRCP

[1] Heartlands hospital, University hospitals Birmingham, Birmingham UK

Short running title: Direct stenting disaster

Address for correspondence:

Sandeep Basavarajaiah

Heartlands Hospital

Birmingham, UK B9 5SS

Email: sandeep270478@gmail.com

Conflicts of interest: None

Keywords: ACS / NSTE-ACS; Calcified stenosis; Undilatable lesion

58-year old lady with acute coronary syndrome had significant lesion in the mid-segment of LAD, which appeared smooth on the angiogram. **(Figure 1 -Fig1)**. The operator directly stented the lesion (3.0x38-mm DES) without pre-dilatation that resulted in focal area of significant under-expansion **(Figure 1-Fig2)**, which failed to expand despite using 3.0 high-pressure non-compliant balloon inflated to 35 atm. **(Figure 1-Fig3-4)** The IVUS demonstrated fibro-calcific nature of the lesion that resisted stent expansion and the MSA was 3.5 mm^2. **(Figure 1-Fig5)** Although, intra-vascular lithotripsy (IVL) is used before stent deployment in calcified un-dilatable lesions, there are no reports of its use in recently deployed stent. We felt it was relatively safe to use IVL over larger-diameter high-pressure balloons that risked perforation. A 3.0 mm IVL balloon adequately expand the stent **(Figure 1-Fig6)** and achieved excellent final result **(Figure 1-Fig7)**. Patient was discharged 24-hours later and she remains free of any clinical events at 12-months. Although there appears to be a theoretical risk of polymer and drug disruption with IVL in a recently deployed stent, but in our case, we felt that it was the safest option over high pressure balloons and we have not seen any adverse clinical outcomes at 12-months. This case reinforces the message that no lesion should be stented directly without pre-dilatation even if it appears smooth and non-calcific on the angiogram.

Figure legends for Figure 1

- **Fig1:** Significant lesion in the mid-segment of LAD
- **Fig2:** Direct stenting resulting in a focal area of significant under-expansion
- **Fig3-4:** Failed attempt to optimise the stent with high-pressure non-compliant balloon
- **Fig-5:** IVUS showing fibro-calcific lesion at the site of under-expanded stent
- **Fig6:** IVL assisted post-dilatation
- **Fig-7:** Final result with better expanded stent

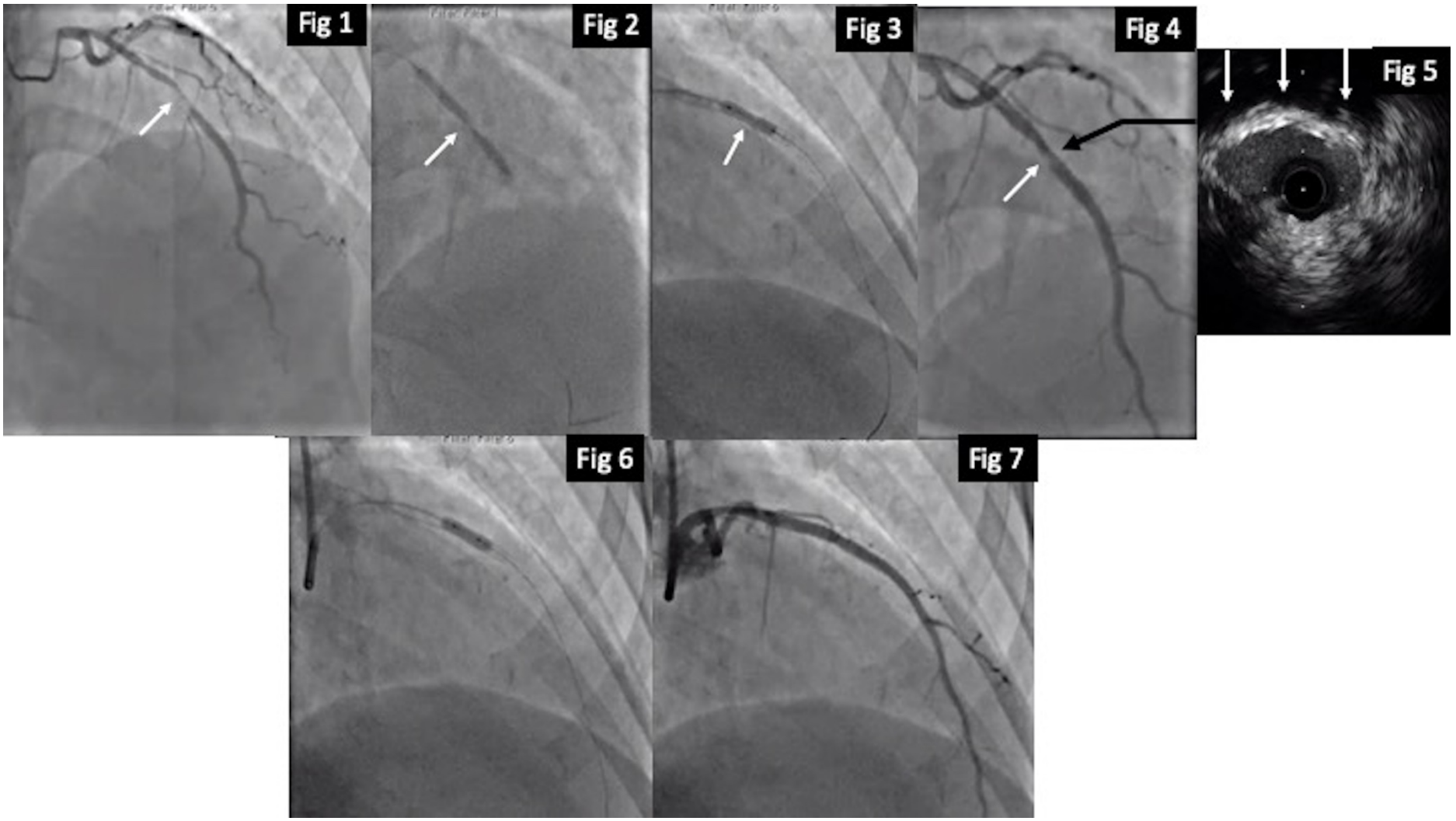

AsiaIntervention
Official Journal of the Asian Pacific Society of Interventional Cardiology
(APSIC) and the Interventional Cardiology Foundation of India (ICFI)
www.asiaintervention.org

Title: Usefulness of sheathless guiding catheter in patients with upper extremities vascular anomalies.

Authors: Cristina Aurigemma, M.D, PhD; Osama Shoeib, M.D, PhD; Francesco Burzotta, M.D, PhD; Maria Leone Antonio, M.D, PhD, Giampaolo Niccoli, M.D, PhD; Italo Porto, M.D, PhD; Giulio Russo, Verdirosi Diana, Carlo Trani, M.D

Manuscript number: AIJ-D-19-00024

Manuscript submission date: 8 June 2019

Revisions received: 9 November 2019, 24 April 2020, 14 June 2020

Accepted date: 10 July 2020

USEFULNESS OF SHEATHLESS GUIDING CATHETER IN PATIENTS WITH UPPER EXTREMITIES VASCULAR ANOMALIES

Aurigemma Cristina[1*MD,PhD], Shoeib Osama[3* MD,PhD], Burzotta Francesco[1,2 MD,PhD], Leone Antonio Maria[1 MD,PhD], Niccoli Giampaolo[1,2 MD,PhD], Porto Italo[1 MD,PhD], Russo Giulio[1], Diana Verdirosi [1], Trani Carlo[1,2 MD]

[1]*Institute of Cardiology, Fondazione Policlinico Universitario A. Gemelli IRCSS, Rome, Italy*

[2]*Institute of Cardiology Università cattolica del Sacro Cuore, Rome, Italy*

[3] *on behalf of absence from Cardiology department, Tanta University, Tanta, Egypt.*

**the two authors have equally contributed to this manuscript so they are considered as two first authors*

Short Title: sheathless catheter in upper vascular anomalies

Keywords: radial, access site, coronary artery disease.

DISCLOSURES

Dr. Burzotta discloses to have been involved in advisory board meetings or having received speaker's fees from Abbott, Abiomed, Medtronic and Biotronic. Dr. Trani discloses to have been involved in advisory board meetings or having received speaker's fees from Abbott, Abiomed, Medtronic and Biotronic. Dr. Aurigemma has been involved in advisory board activities or having received speaker's fees from Abbott, Abiomed, Medtronic and Biotronic. Dr. Leone has received speaker's fees from Abbott, Abiomed and Bracco. Dr. Porto has been involved in advisory board activities or having received speaker's fees from Abbott, Abiomed and Biotronic.

Corresponding author:
Francesco Burzotta, MD, PhD
Institute of Cardiology, Catholic University of the Sacred Heart
L.go A. Gemelli 1, 00168 Rome, Italy
francesco.burzotta@unicatt.it

Abstract

Aims. Transradial approach (TRA) reduces hospitalization and access-site complications compared to transfemoral approach. Nevertheless, the TRA technical failure is significantly higher compared to transfemoral approach failure. Such higher failure rate of TRA is due to a series of factors. In particular, a wide range of anatomic vascular variants may be present in patients undergoing TRA procedures hindering procedural success.

Methods and Results. In our retrospective observational study, including 1.596 consecutive patients with upper limb vascular anomalies underwent TRA between January 2006 and July 2015, we evaluate the usefulness of the sheathless guiding catheter system (SG) compared to conventional guiding catheter (CG). The primary study end-point was the "procedure success" defined as successful transradial procedure (selective cannulation of both coronary ostium in diagnostic procedure and successful stent delivery in intervention procedures) without access change. All procedures were successful in SG, instead only 1.274 (86%) procedures were successfully performed in CG (P=0.0001). At multivariable analysis, age (p=0.001) and sheathless catheter use (P=0.001) were independent predictor of procedures success.

Conclusions. The sheathless GC is a safe and useful system not only in small radial but also in presence of upper vascular anomalies and it can be used in PCI and diagnostic procedures.

Condensed abstract

The TRA approach the rate of technical failure is significantly higher compared to transfemoral approach. A series of factors are responsible in particular a wide range of anatomic vascular variants. In our retrospective observational study, including 1.596 consecutive patients with upper limb vascular anomalies underwent TRA, we evaluate the usefulness of the sheathless guiding catheter system (SG) compared to conventional guiding catheter (CG) in procedure success. At multivariable analysis sheathless catheter use (P=0.001) were independent predictor of procedures success. The sheathless GC is a safe and useful system not only in small radial but also in presence of upper vascular anomalies.

List of abbrevations

AV arteriovenous

GC guiding catheter

PCI percutaneous coronary intervention

TRA trans radial approach

TFA trans femoral approach

Introduction:

Transradial approach (TRA) for coronary diagnostic and interventional procedures reduces hospitalization and access-site complications compared to transfemoral approach (1-2). Therefore, TRA is now increasingly adopted not only for coronary diagnostic and interventional procedures but also for peripheral interventions (3–8). Nevertheless, the TRA technical failure is significantly higher than that reported in transfemoral approach (2). Radial artery spasm and anatomic variants either of brachioradial and of axillo subclavian anonymous arterial axis or of the aortic arch influence the TRA technical procedures success. Device development improves to overcome these TRA limitations. Indeed a sheathless guiding catheter system (Asahi Intecc, Aichi, Japan), which does not require an introducer, is developed in order to allow a gain in inner diameter and the hydrophilic coating, which covers the whole length of the sheathless device, reduces frictional forces, radial artery spasm and hindering in anatomic variants navigation (**Figure 1**) (9).

In the present study we retrospectively evaluate the usefulness of the sheathless guiding catheter system in patients with upper arm vascular anomalies.

Materials and Methods

Study design

We conducted a retrospective observational study including consecutive patients with upper arm vascular anomalies who underwent TRA procedures between January 2006 and July 2017 in a single tertiary high-volume centre (1100 percutaneous coronary intervention per year). Clinical and procedural characteristics were prospectively collected for each patient and entered a dedicated catheterization laboratory database (Estensa, Esaote, Genoa, Italy)

that had been previously proven to help assessing the role of Euroscore I and II in PCI (10,11) and safety of transradial approach (12).

Trans-Radial Approach Technique and Vascular Anatomic Variants Classification

The TRA was used in presence of a normal Allen test or, if abnormal, of a normal Barbeau test (based on oximetry and plethysmography) (13). Patients on dialysis, with previous coronary artery surgery using both internal mammary arteries, or in cardiogenic shock were excluded to the study. The catheterization of radial artery was performed with an arterial puncture kit (with plastic cannula and hydrophilic wire) and long (25 cm) hydrophilic sheath (Radifocus, Terumo, Japan). A 5 or 6 French sheath was used in diagnostic procedures, a 6 French sheath in coronary interventions. In diagnostic procedures, 5.000 IU heparin bolus was administered through the sheath; in interventional procedures, weight-adjusted heparin (100 IU/kg) bolus was administered and was eventually followed by intravenous heparin boluses to maintain activated clotting time between 250 and 300 sec. A routinely administration of vasodilator drugs were not performed and nitrates only were used in the case of radial artery spasm. Retrograde arterial angiography was effected (from the cannula, from the sheath or from the catheter) anytime difficulty was encountered during wire or catheter advancement/manipulation. The upper arm vascular anomalies were classified according to ABC operative classification (14) (**Figure 2**):

• Group A: radial-brachial arterial axis;

• Group B: axillary-subclavian-anonymous axis;

• Group C: aortic arch.

When an anatomic variant was recognized by angiography, some tricks, as previously provided (15), or the sheathless guiding catheters (GC) system were used to try to overcome

the technical problems and complete the TRA procedure. The sheathless GC has a hydrophilic coating covering its whole length and a central dilator allowing smooth insertion into small and/or spastic radial arteries. The sheathless GC and central dilator were advanced over a 0.035" guide wire to the ascending aorta. The central dilator and the 0.035"guide wire were subsequently withdrawn a few centimetres from the ostium in order to allow safe intubation of the coronary artery. Because of its stiffness, extreme care had to be taken not to advance the central dilator close to the aortic valve. The decision to use the sheathless GC, instead the conventional catheter, and the selection of a specific shape were left to the interventional cardiologist's discretion.

Clinical/angiographic data recordings, need of crossover to other approaches and reason for access crossover were prospectively recorded in a dedicated catheterization laboratory database (Estensa, Esaote, Genoa, Italy).

Study End-points

The primary study end-point was the "procedure success" defined as successful transradial procedure (selective cannulation of both coronary ostium in diagnostic procedure and successful stent delivery in intervention procedures) without access change. Secondary end points were procedural time, amount of contrast, radiation amount, the use of additional techniques to complete the procedure (guiding catheter extension or buddy wire to increase the guiding catheter support) and incidence of vascular complication (pseudoaneurysm, AV fistula, dissection, minor and major hematoma, compartmental syndrome, perforation, occlusion).

Statistical analysis

Continuous variables were reported as mean ± standard deviation and compared with analysis of variance (Student's *t* test). Categorical variables were expressed as frequencies and compared with $\chi 2$ test. Normality of data was determined using the D'Agostino-Pearsons test and verified using histogram plots. A two-sided P value of 0.05 was considered significant in Student's *t* test. one-sided P value of 0.05 was considered significant in $\chi 2$ test. Multivariable analysis to assess independent predictors of the primary procedural end-point was performed using a backward elimination model which included the baseline clinical and anatomical variation as well as the type of catheter used to complete the procedure. Statistical analyses were conducted using SPSS v.18 (SPSS, Chicago, IL, USA).

Results

Out of 31.032 consecutive patients underwent TRA at our center during study period, 1.596 (5%) patients had an upper arm vascular anomalies (**Figure 3**). Sheathless GC was systematically used in 112 patients (7%), in 2 patients it was used after failure of conventional diagnostic catheter) and constituted the SHEATHLESS group (SG), while the remaining 1.482 (93%) patients, in whom the conventional catheters were used, constituted the CONTROL group (CG). In 30 patients of SG (27%) and in 257 patients of CG (17%) only diagnostic procedure was performed.

The baseline patient's clinical characteristics are reported in Table 1 showing some differences in cardiovascular risk factors and cardiac clinical presentation between the two groups. In particular, female gender and hypertension was more common in SG compared to CG (66% vs 47%, P value 0.001 and 81% vs 61%, P value 0.001, respectively). Moreover the acute coronary syndromes, either ST elevation myocardial infarction (STEMI) or non ST

elevation myocardial infarction (NSTEMI), were clinical presentation more frequent in SG compared to CG (STEMI: 14% vs 4%, P value 0.001, NSTEMI: 26% vs 17%, P value 0.006).

The incidence of upper arm vascular anomalies in the two study groups is reported in Table 2. The high origin radial artery was more frequent vascular anomaly in SG compared to CG (46% vs 31%, p value 0.001), instead in CG the incidence of radial tortuosity was more common compared to SG (39% vs 27%, P value 0.009). The percutaneous coronary interventions (PCI) were more frequent performed in SG group compared to CG (72% vs 17%, P value 0.001) (Table 1).

Procedural outcomes

Procedural failure occurred in 212 (13%) patients. Radial artery loop 360° and brachial artery tortuosity were anatomic variations more frequent in failed procedures (P=0.001 and P=0.01, respectively) (Table 2).

The procedure success was significantly different between the two study groups, in particular all procedures were successful in 112 SG (the 2 patients, in which sheathless CG was used after conventional catheter failure, was exclude from procedural outcomes analysis), instead only 1.274 procedures were successfully performed in CG (100% vs 86% CG; P=0.0001). The procedure success was also significantly higher in SG compared to CG in PCI procedures and in PCI sub-analysis on conventional guiding catheter size.

At multivariable analysis, age (p=0.001) and sheathless catheter use (P=0.001) were independent predictor of procedures success.

Procedure duration, fluoroscopic time and amount of contrast media were significant increase in SG compared to CG (Table 3). Instead in a subanalysis of PCI procedures dose area product (DAP) and amount of contrast media were significant lower in SG compared to CG (Table 3). In the PCI procedures the sub-analysis according to conventional guiding

catheter size has demonstrated a lower DAP and amount contrast media in SG compared to 6F CG, instead only the procedure success was different between SG and 5F CG (Table 4).

Discussion

The TRA is associated to a relevant reduction of hospitalization and vascular complications (1-2). However the average technical failure of TRA in coronary procedures is 5.8% (2) and it is significantly higher than that reported in transfemoral approach. The TRA is associated with a number of difficulties such as catheter friction attributable to the small diameter or occurrence of spasm and anatomical variations which should be navigated to reach the ascending aorta. Limitations such as small radial artery size or the occurrence of spasm may be resolved using hydrophilic catheters for TRA procedures. Indeed Koga S et al have demonstrated that the use of hydrophilic catheters reduce radial artery spasm upon insertion, manipulation, and withdrawal of the catheter compared with non hydrofilic catheters. The sheathless guiding catheter system, a sheathless guiding catheter (GC) (Asahi Intecc, Aichi, Japan), which does not require an introducer and with a hydrophilic coating on whole length, allows the TRA in patients with small radial arteries reducing frictional forces, discomfort and pain-induced radial artery spasm (9). Youn et al. have demonstrated the feasibility of sheathless GC during PCI procedures in patients with small radial artery size (diameter < 2.3 mm) with a procedural success rate comparable to that of transfemoral PCI, in addition to reduced bleeding and vascular complication rates (17). Recently the sheathless guiding catheters are also proven a safe, effective method for complex PCI via TRA in small radial arteries without catheter-related complications (18). The gain in inner diameter of the sheathless guiding catheter system, as well as the hydrophilic coating, allows the use of small radial as vascular approach in complex PCI and can also reduce the risk of radial artery

occlusion. This complication occurs on average in 5-12 % of patients undergoing TRA procedures and several studies have demonstrated that a Ratio Sheath to Artery> 1 is independent predictor of radial artery occlusion (19). The sheathless catheter system allows a catheter downsize, indeed the external diameter of a 6.5-F (2.16 mm) sheathless GC is smaller than that of a conventional 5-F GC and, similarly, the external diameter of a 7.5-F (2.49 mm) sheathless GC is smaller than that of a 6-F GC (2.7 mm) (Figure 1).

A previous study have demonstrated that the TRA failure was more frequent associated with upper arm vascular anomalies (15.6%) than with radial artery spasm (0.7%). In the presence of documented variants the cause of TRA failure was unsuccessful advancement of catheters into the radial/brachial artery and ascending aorta (20). Our data confirmed that in a high volume center the procedure failure of TRA is associated with radial loop 360° and brachial tortuosity. This retrospective study has also demonstrated that the sheathless system may be used to resolve the difficult navigation to reach the ascending aorta in presence of upper arm vascular anomalies. Indeed in our study the use of sheathless GC is associated with a higher incidence of procedure success compared to conventional catheter. Nevertheless the use of sheathless GC is associated with a higher procedure duration, fluoroscopic time and amount of contrast media in all (diagnostic and interventional) study procedures. The sheathless GC was used in diagnostic procedures after the evidence of upper limb vascular anomalies and the manipulation of guiding catheter might be more complex compared to conventional diagnostic catheter. However the use of the sheathless GC is associated with a higher procedural success rate. In a sub analysis of PCI procedures the use of sheathless system is associated with a lower dose area product (DAP) and amount of contrast media. In PCI procedures the procedural success advantage of sheathless GC is independent of conventional guiding catheter size. Therefore the usefulness and safety of sheathless GC has

been demonstrated in resolving the difficult navigation to reach the ascending aorta in presence of upper arm vascular anomalies not only for PCI procedures but also for diagnostic procedures.

Previous experiences have demonstrated that sheathless GC allows effective cannulation of the ostium, but it is not as efficient as conventional catheters in terms of support. In our study the incidence of the use of additional techniques to complete the procedures, such as guiding catheter extension or buddy wire to increase the guiding catheter support, is not different between SG and CG. Probably the good selection of the most suitable catheter shape might have helped in order to obtain the best possible support.

The TRA is associated to a relevant reduction of vascular complications and that this reduction may limit in some patients, for instance those with ST-elevation myocardial infarction patients, major clinical adverse events (2, 21). In our study the incidence of vascular complications is not different between the SG and CG. However the incidence of female gender with small radial artery and the incidence of unstable clinical presentation were more frequent in SG group compared to CG group. This selection bias of non randomized study might be underestimated the beneficial effects of sheathless GC on vascular complications.

Limitations

This is a non-randomized, observational study, the results of which may have been affected by a selection bias. In particular in the study the decision to use the sheathless GC, instead the conventional catheter was left to the interventional cardiologist's discretion after the evidence of an upper limb vascular anomalies. However, although the use of this device was at the discretion of each operator, it became increasingly and almost automatically used in

particular upper arm anomalies such as the high origin radial artery. In 2 diagnostic procedures the sheathless GC was used after a failure of conventional catheter. In all diagnostic procedures and in all PCI procedures of the SG group the sheathless GC was intended to be systematically used.

Conclusions

The TRA for coronary diagnostic and interventional procedures is known to shorten hospitalization and dramatically reduce access-site complications. On such bases, TRA is now increasingly adopted in coronary and peripheral interventions. Nevertheless, the TRA technical failure is significantly higher than that reported in transfemoral approach. Such higher failure rate of TRA is due to a series of factors. In particular, a wide range of anatomic variants either of the brachioradial and of the axillo-subclavian-anonymous arterial axis or of the aortic arch may be present in patients undergoing TRA procedures hindering procedural success. Our study has demonstrated that the sheathless GC system is a safe and useful method not only in small radial but also in presence of upper vascular anomalies and it can be used in PCI and diagnostic procedures.

Impact on daily practice

- Transradial approach (TRA) for diagnostic and interventional procedures reduces hospitalization and access-site complications compared to transfemoral approach. Nevertheless, the TRA failure is significantly higher compared to transfemoral approach.
- Radial artery spasm and upper vascular anatomic variants influence the TRA technical procedures success.

- Device development improves to overcome these TRA limitations. A sheathless guiding catheter system (SGC), which does not require an introducer, is developed in order to allow a gain in inner diameter and the hydrophilic coating, reduces frictional forces, radial artery spasm and hindering in anatomic variants navigation. Indeed the sheathless guiding catheter system is a safe and useful system not only in small radial but also in presence of upper vascular anomalies.
- The major advantages of the sheathless guiding catheter system are in PCI procedures but it can also be advantageous in diagnostic procedures only in terms of procedural success.

Funding statement

Nothing to declare

Reference

1. Agostoni P, Biondi-Zoccai GG, de Benedictis ML, Rigattieri S, Turri M, Anselmi M, Vassanelli C, Zardini P, Louvard Y, Hamon M. Radial versus femoral approach for percutaneous coronary diagnostic and interventional procedures; systematic overview and meta-analysis of randomized trials. J Am Coll Cardiol 2004;44:349–56.

2. Jolly SS, Amlani S, Hamon M, Yusuf S, Mehta SR. Radial versus femoral access for coronary angiography or intervention and the impact on major bleeding and ischemic events: a systematic review and meta-analysis of randomized trials. Am Heart J 2009;157:132–40.

3. Hildick-Smith DJ, Ludman PF, Lowe MD, Stephens NG, Harcombe AA, Walsh JT, Stone DL, Shapiro LM, Schofield PM, Petch MC. Comparison of radial versus brachial approaches for diagnostic coronary angiography when the femoral approach is contraindicated. Am J Cardiol 1998;81:770–2.

4. Sciahbasi A, Romagnoli E, Trani C, Burzotta F, Pendenza G, Tommasino A, Leone AM, Niccoli G, Porto I, Penco M, Lioy E. Evaluation of the "learning Curve" for left and right radial approach during percutaneous coronary procedures. American Journal of Cardiology 2011;108:185-188.

5. Burzotta F, Trani C, Hamon M, Amoroso G, Kiemeneij F. Transradial approach for coronary angiography and interventions in patients with coronary bypass grafts: tips and tricks. Catheter Cardiovasc Interv 2008;72:263–72.

6. Trani C, Tomassino A, Burzotta F. Transradial renal stenting: why and how. Catheter Cardiovasc Interv. 2009;74:951-6

7. Trani C, Burzotta F, Tomassino A, Giammarinaro M. Transradial approach to treat superficial artery in-stent restenosis. Catheter Cardiovasc Interv 2009;74:267–72.

8. Trani C, Burzotta F, Coroleu GF. Transradial carotid artery stenting with proximal embolic protection. Catheter Cardiovasc Interv 2009;74:494-498–272.

9. Mamas M, D'Souza S, Hendry C, Ali R, Iles-Smith H, Palmer K, El-Omar M, Fath-Ordoubadi F, Neyses L, Fraser DG. Use of the sheathless guide catheter during routine transradial percutaneous coronary intervention: a feasibility study. Catheter Cardiovasc Interv. 2010;75:596-602.

10. Romagnoli E, Burzotta F, Trani C, Siviglia M, Biondi-Zoccai GG, Niccoli G, Leone AM, Porto I, Mazzari MA, Mongiardo R, Rebuzzi AG, Schiavoni G, Crea F. EuroSCORE as predictor of in-hospital mortality after percutaneous coronary intervention. Heart 2009;95:43-8.

11. Saffioti S, Coluccia V, Burzotta F, Trani C, Niccoli G, Leone AM, Aurigemma C, Crea F. Value of EuroSCORE II in predicting total and cardiac mortality in patients undergoing percutaneous coronary interventions. Am J Cardiol. 2014;113:745-6.

12. Burzotta F, Trani C, Mazzari MA, Tommasino A, Niccoli G, Porto I, Leone AM, Tinelli G, Coluccia V, De Vita M, Brancati M, Mongiardo R, Schiavoni G, Crea F. Vascular complications and access crossover in 10,676 transradial percutaneous coronary procedures. Am Heart J. 2012;163:230-8.

13. Barbeau GR, Arsenault F, Dugas L, Simard S, Larivie`re MM. Evaluation of the ulnopalmar arterial arches with pulse oximetry and plethysmography: Comparison with the Allen's test in 1010 patients Am Heart J 2004;147:489–493.

14. Burzotta F, Trani C, De Vita M, Crea F. A new operative classification of both anatomic vascular variants and physiopathologic conditions affecting transradial cardiovascular procedures. International journal of cardiology 2010;145:120-2.

15. Burzotta F, De Vita M, Trani C. How to manage difficult anatomic conditions affecting transradial approach coronary procedures? Indian Heart J 2010;62:238–244.
16. Koga S, Ikeda S, Futagawa K, Sonoda K, Yoshitake T, Miyahara Y, Kohno S. The use of a hydrophilic-coated catheter during transradial cardiac catheterization is associated with a low incidence of radial artery spasm. Int J Cardiol. 2004;96:255-8.
17. Youn YJ, Yoon J, Han SW, Lee JW, Sung JK, Ahn SG, Kim JY, Yoo BS, Lee SH, Choe KH. Feasibility of transradial coronary intervention using a sheathless guiding catheter in patients with small radial artery. Korean Circ J. 2011;41:143-148.
18. Cheaito R, Benamer H, Hovasse T, Tritar A, Hage F, Garot P, Lefèvre T, Unterseeh T, Chevalier B, Morice MC, Louvard Y. Feasibility and safety of transradial coronary interventions using a 6.5-F sheathless guiding catheter in patients with small radial arteries. Catheter Cardiovasc Interv. 2015;86:51-8.
19. Buturak A, Gorgulu S, Norgaz T, Voyvoda N, Sahingoz Y, Degirmencioglu A, Dagdelen S. The long-term incidence and predictors of radial artery occlusion following a transradial coronary procedure. Cardiol J. 2014;21:350-6.
20. Burzotta F, Brancati MF, Trani C, Tommasino A, Porto I, Niccoli G, Leone AM, Coluccia V, Di Noi P, Crea F. Impact of radial-to-aorta vascular anatomical variants on risk of failure in trans-radial coronary procedures. Catheter Cardiovasc Interv. 2012;80:298-303.
21. Jolly SS, Yusuf S, Cairns J, Xavier D, Widimsky P, Budaj A, Niemelä M, Valentin V, Lewis BS, Avezum A, Steg PG, Rao SV, Gao P, Afzal R, Joyner CD, Chrolavicius S, Mehta SR; RIVAL trial group. Radial versus femoral access for coronary angiography and intervention in patients with acute coronary syndromes (RIVAL): A randomised, parallel group, multicentre trial. Lancet 2011;377:1409–1420.

Figure Legends

Figure 1. The sheathless guiding catheter system. The sheathless guiding catheter system (Asahi Intecc, Aichi, Japan), which does not require an introducer, is developed in order to allow a gain in inner diameter**.**

Figure 2. Upper limb vascular anomalies. Many upper limb vascular anomalies are associated to transradial approach failure and are classified according to ABC operative classification. Group A radial-brachial axis: Radial tortuosity (Z shape) (A), Radial loop (360°) (B), Brachial tortuosity (C), Brachial loop (D), High radial origin (E). Group B axillary-subclavian-anonymous axis: High radial origin (E), Axillary stenosis (F), Subclavian tortuosity (G), Subclavian Lousoria (H). Group C: aortic arch: aortic elongation (J).

Figure 3. Study Flow Chart.

Table 1. Baseline characteristics of the study group.

	All population (n = 1.596)	SG (n = 114)	CG (n = 1.452)	P value
Age	72 ± 27	74 ± 11	72 ± 28	0.1
Sex (female)	772 (48%)	76 (66%)	696 (47%)	<0.001
DM	275 (17%)	26 (22%)	249 (17%)	0.06
HTN	979 (61%)	93 (81%)	886 (61%)	<0.001
History of peripheral arterial disease	35 (2%)	3 (3%)	32	0.4
Clinical presentation: - **STEMI** - **NSTEMI** - **CSA**	68 (4%) 271 (17%) 594 (37%)	16 (14%) 30 (26%) 43 (37%)	52 (4%) 241 (17%) 551 (38%)	<0.001 0.006 0.4
Previous PCI	262 (16%)	23 (20%)	239 (16%)	0.1
Previous CABG	139 (9%)	10 (9%)	129 (9%)	0.5
Diagnostic procedure	1.230 (77%)	31 (27%)	1.199 (81%)	0.001
PCI	339 (21%)	82 (72 %)	257 (17%)	0.001
Peripheral intervention	27 (2%)	1 (1%)	26 (2%)	0.7

DM: diabetes mellitus; HTN: Hypertension; STEMI: ST elevation myocardial infarction; NSTEMI: non-ST elevation myocardial infarction; CSA: chronic stable angina; PCI: percutaneous coronary intervention; CABG: coronary artery bypass graft

Table 2. Upper vascular anomalies in the two study groups and in successful and failed procedures

	SG (n = 114)	CG (n = 1.482)	P value	Procedural success (n = 1.384)	Procedural failure (n = 212)	P value
A group	97 (85%)	1.171	0.1	1.098 (97%)	170 (80%)	0.8
Radial stenosis or	5 (4%)	(79%)	0.8	52 (4%)	13 (6%)	0.1
atherosclerosis	2 (2%)	60 (4%)	0.2	8 (0.5%)	4 (2%)	0.06
Radial occlusion	53 (46%)	10 (0.6%)	0.001	445 (32%)	66 (31%)	0.8
Remnant radial artery	31 (27%)	458 (31%)	0.009	545 (39%)	70 (33%)	0.08
Radial tortuosity > 45 degree	15 (12%)	584 (39%)	0.6	129 (9%)	59 (28%)	0.0001
Radial loop 360°	2 (2%)	173 (12%)	1	30 (2%)	6 (3%)	0.4
Brachial loop	10 (9%)	34 (2%)	1	139 (10%)	10 (5%)	0.01
Brachial tortuosity		139 (9%)				
B group	21 (18%)	362 (24%)	0.1	325 (23%)	58 (27%)	0.2
Axillary or subclavian	18 (16%)	282 (19%)	0.4	260 (19%)	40 (19%)	1
tortuosity	5 (4%)	91 (6%)	0.5	73 (5%)	23 (11%)	0.003
Axillary or subclavian stenosis						
or occlusion						
C group	1 (0.8%)	44 (3%)	0.3	39 (3%)	6 (3%)	1
Lusoria	1 (0.8%)	36 (2 %)	0.5	34 (2%)	3 (1%)	0.4
Aortic elongation	0	8 (0.5%)	1	5 (0.3%)	3 (1%)	0.07

Table 3. Study endpoints in the two study groups and in PCI subgroups

	SG (n = 112)	**CG (n = 1482)**	**P value**	**PCI SG (n = 82)**	**PCI CG (n = 257)**	**P value**
Procedure success (%)	112 (100%)	1.274 (86%)	0.0001	82 (100%)	221 (85.9%)	0.001
Procedure duration (min)	81 ± 34	60 ± 32	0.001	87 ± 39	87 ± 37	0.8
Fluoroscopic time (min)	20 ± 13	13 ± 9	0.001	21 ± 15	21 ± 11	0.7
Total DAP	55.985 ± 70.320	97.770 ± 92.872	0.001	60.686 ± 74.907	129.765 ± 122.395	0.001
Contrast media (ml)	220 ± 109	160 ± 101	0.001	236 ± 111	265 ± 105	0.03
Vascular complication	2 (1.7%)	47 (3%)	0.5	1 (1%)	9 (3%)	0.4
Need for a Buddy wire	4 (3.5%)	8 (0.5%)	0.4	4 (4.8%)	8 (3.1%)	0.4
Need for a guiding catheter extension	3 (2.6%)	3 (0.2%)	0.1	3 (3.6%)	3 (1.2%)	0.1

DAP: dose area product

Table 4. Study endpoints in the sheathless and 6F and 5F guiding catheter groups in PCI procedures.

	PCI SG 6.5 and 7.5F (n = 82)	PCI CG 6F (n = 247)	P value*	PCI CG 5F (n = 12)	P value§
Procedure success (%)	82 (100%)	213 (86.2%)	0.001	8(66.6%)	0.001
Procedure duration (min)	87 ± 39	87 ± 37	0.9	75 ± 35	0.3
Fluoroscopic time (min)	21 ± 15	21 ± 11	0.9	16.5 ± 8.3	0.3
Total DAP	60.686 ± 74.907	132.975 ± 122.893	0.001	30.277 ± 25.264	0.3
Contrast media (ml)	236 ± 111	268 ± 105	0.02	210 ± 80	0.4
Vascular complication	1 (1%)	8 (3.2%)	1	1 (8.3%)	0.3
Need for a Buddy wire	4 (4.8%)	8 (3.2%)	0.5	0 (0%)	1
Need for a guiding catheter extension	3 (3.6%)	3 (1.2%)	0.1	0 (0%)	1

DAP: dose area product;*p value for sheathless group vs Conventional Guiding Catheter 6F;
§ p value for sheathless group vs Conventional Guiding Catheter 5F

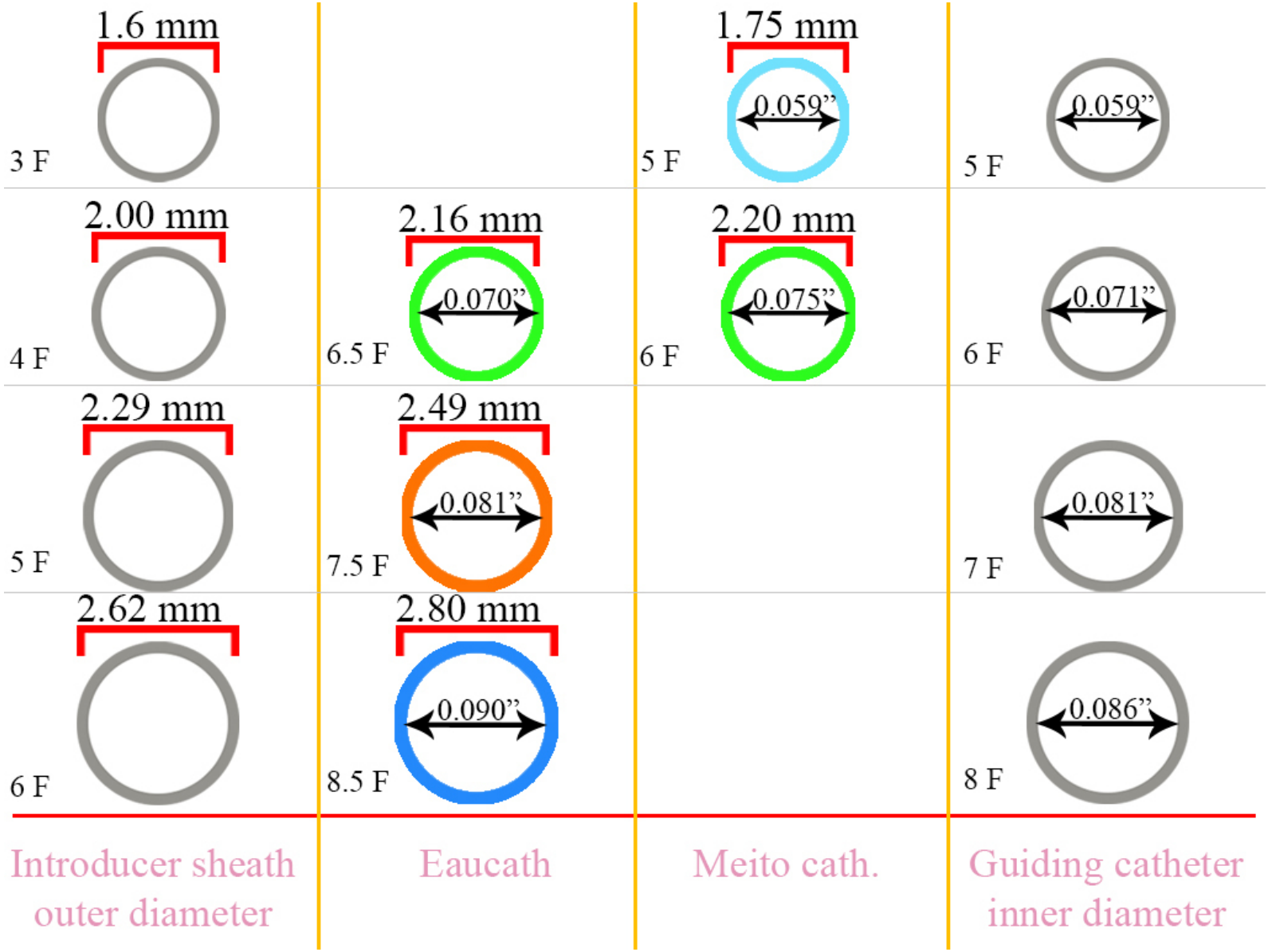

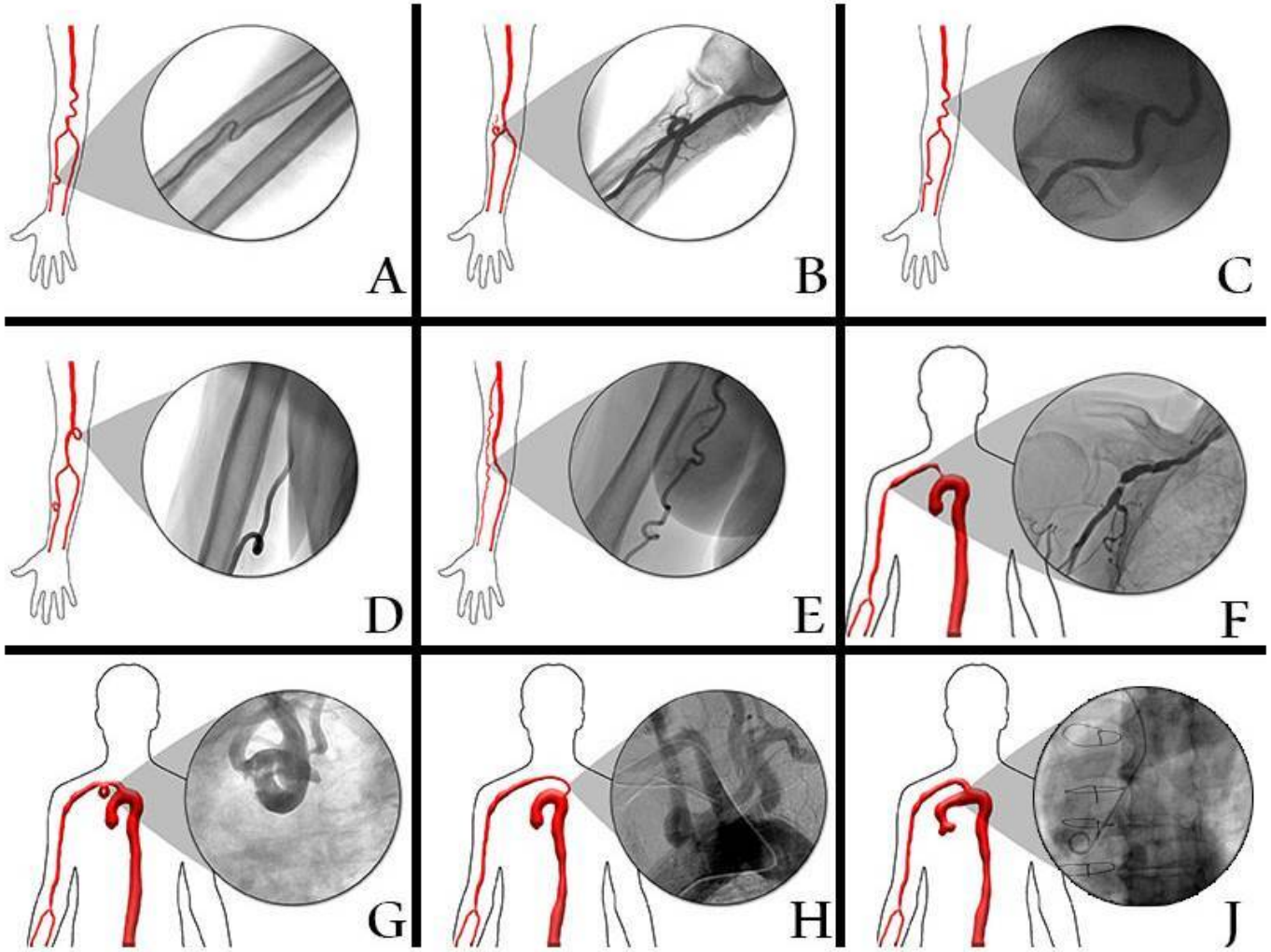

Figure 2. Upper limb vascular anomalies.

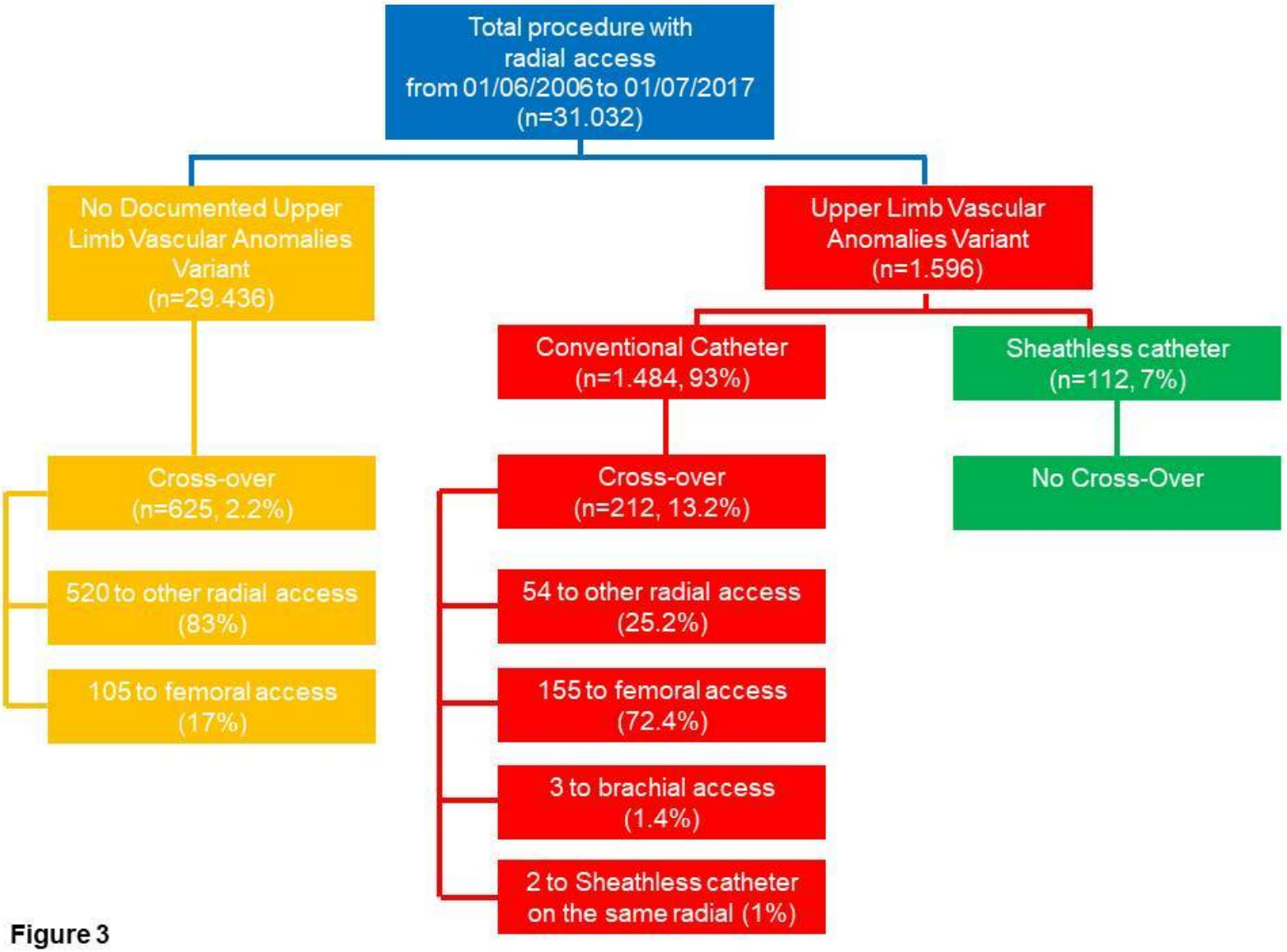

Figure 3

AsiaIntervention

Official Journal of the Asian Pacific Society of Interventional Cardiology

(APSIC) and the Interventional Cardiology Foundation of India (ICFI)

www.asiaintervention.org

Title: **Knuckle wire technique in percutaneous coronary intervention of chronic total occlusion.**

Authors: Sharath Reddy A, M.D, DM, FSCAI, FACC, FAHA; Ajith Ananthakrishna Pillai, M.D, DM; Bharath Reddy, M.D, DM; Venkat Rao, M.D, DM; Aparajita Deshpande, Pharm.D

Manuscript number: AIJ-D-19-00028

Manuscript submission date: 11 July 2019

Revisions received: 17 October 2019, 12 March 2020, 24 June 2020

Accepted date: 10 July 2020

Title: Knuckle wire technique in percutaneous coronary intervention of chronic total occlusion

Authors and affiliations:

Dr Sharath Reddy A[1*],MD, DM, FSCAI, FACC, FAHA; Dr Ajith Ananthakrishna Pillai[2], MD, DM; Dr Bharath Reddy[1], MD, DM; Dr Venkat Rao[1], MD, DM; Dr Aparajita Deshpande[3], Pharm. D.

[1]Department of Cardiology, Medicover Hospitals, Madhapur, Hyderabad 500081, Telangana. India.

[2]Department of Cardiology, JIPMER, Dhanvantri Nagar, Gorimedu 605006, Puducherry. India.

[3]Department of Research, Medicover Hospitals, Madhapur, Hyderabad 500081, Telangana. India.

Short running title: Knuckle wire technique

Corresponding author:

Dr Sharath Reddy A, Department of Cardiology, MedicoverHospitals, Madhapur, Hyderabad 500081, Telangana. India.Email: drsr.research@gmail.com,

Abstract

In percutaneous coronary intervention, knuckle wire technique is one of the approaches to cross the long and ambiguous course of the occluded segment. However, this technique is generally used as a last alternative, when all other techniques fail. Although knuckle wiring expedites chronic total occlusion crossing,it can also complicate the percutaneous coronary intervention strategy irreversibly. Therefore, understanding the various aspects of knuckle wire technique is a prerequisite in a chronic total occlusion setting. The authors herein intend to describe in detail the knuckle wire technique and its safe and effective approach in various chronic total occlusion wiring strategies, while befitting to the scope of a mainstream interventionist.

Classification: Multiple vessel disease; Bifurcation; Calcified stenosis; Chronic coronary total occlusion; Intravascular ultrasound; Other technique

List of abbreviations

STAR: Subintimal tracking and re-entry

CTO: Chronic total occlusion

CART: Controlled antegrade and retrograde tracking

BASE: Balloon-assisted subintimal entry

PCI: Percutaneous coronary intervention

IVUS: Intravascular ultrasound

Introduction

Knuckle wire designed for subintimal angioplasty, originated in the peripheral circulation, having been first described in 1989 in percutaneous intervention for femoropopliteal occlusions. The original subintimal tracking and re-entry (STAR) technique with knuckle wire was attempted by Colombo in coronary occlusion (1). It involves creating a cleavage in the subintimal plane by advancing a hydrophilic wire with a J-loop configuration to allow a blunt dissection between the anatomical planes of the vessel using the principle of differential longitudinal and tangential resistance (Figure 1)(2, 3). In STAR, the knuckle wire is used both for subintimal entry and to continue dissection to re-enter into the true lumen at bends in the vessel or branch points; however, re-entry to the true lumen is quite unpredictable and not controllable. Therefore, in contemporary chronic total occlusion (CTO) intervention scenario (Figure 2), knuckle wire is used mostly as a last resort only to create subintimal dissection and re-entry is assisted by CrossBoss–Stingray, controlled antegrade and retrograde tracking (CART), or reverse CART (4, 5). The knuckle technique when performed antegrade or retrograde helps in long occlusions, especially with calcification to maintain the guidewire position in subintimal space within the vessel architecture (6-9).

How Knuckle Works: Principle of differential resistance

Knuckling works based on the principle of differential resistance by subintimal space and media/adventitia tissue. The resistance offered by the subintimal space, i.e. longitudinal resistance, is less than the resistance presented by media/adventitia, which is the tangential/radial resistance. Therefore, when the knuckle is advanced, it moves down the subintimal low-resistance plane, rather than splitting-out through media/adventitia (Figure 3). As long as the knuckle width is within the size of the vessel, it remains in subintimal space. If the width of knuckle exceeds beyond the size of the vessel, it may cut through the media and perforate the vessel.

Technique

1. **Wires and Tip Shaping**

Polymer jacket hydrophilic wires with lower tip gram weight, such as Fielder XT series (Asahi Intecc, Japan), Sion Black (Asahi Intecc, Japan), and Pilot series (Abbott Vascular, USA) are best suited for knuckle wiring. To create a knuckle, the wire must loop on itself such that the leading edge is usually the junction between the stiff shaft and the floppy distal segment [Figure 4 (B)]. The knuckle loop can be initiated by pre-shaping the wire tip as an "umbrella handle" and by applying forward pressure on the wire, once it is within the CTO [Figure 4 (A)]. To avoid knot formation while forming a knuckle, the wire should not be rotated in any way. The advancement of knuckle wire should always be done within an over the wire support microcatheter. This adds in controlling the knuckle width and length. Further, the microcatheter aids in wire exchange if the wire gets trapped in a calcified subintimal tissue or gets broken. The microcatheter also helps in exchanging to a stiffer wire for true lumen re-entry once the knuckle crosses the CTO length. Once knuckle is formed, further advancement of knuckle should be done keeping microcatheter close to the tip of the knuckle(10). Otherwise, the knuckle may shift onto stiff portion of wire leading to the wider knuckle, which may split open the vessel [Figure

4(C)]. If knuckling is done to avoid entry into side branches, tip shaping is performed with a wide knuckle. The angiographic representation of tip shaping is as shown in Figure 5.

2. **Where to start knuckle?**

Knuckle within CTO segment

Generally, it is not possible to enter the subintimal space without penetrating the proximal CTO cap first with a stiff wire or disrupted by other means (11, 12). Further, this allows the entry of microcatheter into the CTO body, through which a polymer jacketed wire is introduced (Figure 6). Knuckling inside the lesion does not allow the subintimal space to get exposed to systemic pressure, as entry is too narrow. Penetrating the proximal cap with angiographic or intravascular ultrasound (IVUS) guidance should be done initially if possible and knuckle technique to be used if the antegrade wire escalation fails or when the antegrade wire gets trapped in the plaque (13). In the "long plus" type of CTO (i.e. longer CTO with added morphological complexities, such as calcification, tortuosity, and previous attempt with subintimal passage), if the antegrade technique is not progressing, knuckle technique should be used with a clear cut plan for re-entry. If the distal vessel is not accessible by retrograde channels, extreme caution should be considered to perform re-entry soon after exiting the CTO length.

Knuckle proximal to CTO

Knuckling proximal to CTO is not preferable [Figure 7 (A) and (B)] due to direct exposure of the subintimal space to systolic pressure of the aorta leading to the expansion of the subintimal space, which may complicate further steps of re-entry [Figure 7 (C) and (D)]. In such cases, measures to isolate subintimal space from the aortic pressure should be used, such as Trapliner, proximal balloon occlusion, and/or deep seating of guide.

In the presence of calcification and tortuosity, a large amount of force might be required, often utilizing measures, such as a large, deep-seated guide with microcatheter and anchor balloon (Figure 7). In cases of extreme resistance, a balloon (loaded on the knuckled wire) can be inflated in the vessel, just proximal to the occlusion, for maximal support (12, 14).

Controlling knuckle size

During knuckle wiring, it is preferable to keep the size of the knuckle as small as possible to minimize vessel trauma. Loops formed with Fielder XT (Asahi Intecc, Japan) wire tend to be smaller than those formed with Pilot 200 (Abbott Vascular, USA) wire; as the stiffness of wire increases the diameter of knuckle increases. The knuckle diameter can be controlled to some degree by adjusting the distance between the supporting microcatheter and the knuckle tip. Ultimately, however, the knuckle size is determined by the diameter of the vessel and the proximity of the microcatheter to the knuckle tip determines the degree of force applied to create the dissection plane (Figure 8) (12).

Guide catheter support for knuckle

As the formation and advancement of knuckle need a forceful push to guide wire, this mandates enough guide catheter support (15). In situations of inadequate guide support, the following techniques can be used to enhance guide support for knuckle advancement (Figures 9, 10, and 11).

1) ***Anchor balloon***
2) ***Balloon-assisted subintimal entry (BASE)/Side-BASE with knuckle in impenetrable or ambiguous proximal cap***

   Monorail balloon with a size equivalent to the main vessel (BASE) or side branch (Side BASE) lumen diameter is inflated with a microcatheter side by knuckle wire

advanced through the microcatheter. Inflated balloon facilitates subintimal entry of knuckle as well as gives good guide catheter support for knuckle advancement

3) ***Proximal over-the-wire balloon inflation with a knuckle through***

In cases where support enhancement is needed with a lack of option of side branch anchor, the over-the-wire proximal balloon inflation with a knuckle-through can be used (Figure 11).

When to use knuckle

Knuckle in CTO Percutaneous Coronary Intervention (PCI)

With the progress of wire technology, knuckle wire should NOT be a first line wiring technique in most CTO lesions (14, 15).

1. Knuckle wire canbe used when thevessel course is ambiguous angiographicallyto reveal the vessel course (Figure 12)
2. In highly calcified and tortuous long CTO, where high penetration wiring may perforate the vessel, knuckle wire can be considered (Figure 13). The angiographic representation of knuckle wire progression is as shown in Figure 14
3. Knuckle wire can be used after difficult and long retrograde channel crossing in a long CTO, where procedure time is long and the radiation limit has been nearly reached. In this situation, knuckle wire can rapidly cross the CTO body allowing completion of the case before the radiation limit is reached
4. After the failure of antegrade/retrograde wire escalation, or failure of the retrograde approach
5. Knuckle can be used in conjunction with CrossBoss (Boston Scientific, USA) to facilitate the crossing of tortuous segments (Figure 14), avoid side branch entry(Figure 15), and circumvent calcium spots stalling CrossBoss (Boston Scientific, USA;Figure 16).

6. Rarely, knuckling can be used as an initial crossing strategy (primary dissection/re-entry), provided the lesion fulfils the following characteristics (Figure 17) (16):
    a. Well-defined proximal cap
    b. ≥ 20 mm length
    c. Large calibre distal vessel
    d. No large branches within the CTO or, more importantly, at the distal cap
7. Knuckling in retrograde PCI (17) can be used in the following circumstances:
    a. Ambiguous course in CTO
    b. Tortuous CTO segment
    c. Heavy calcification

Knuckle wire v/s CrossBoss for subintimal tracking

Although, the knuckle is a faster and less expensive technique of subintimal tracking, itis not totally controllable and predictable. Re-entry can get complicated due to wider dissection [Figure 18 (A)] or intramural hematoma [Figures 18 (B) and (C)] compressing the true lumen. In contrast, CrossBoss(Boston Scientific, USA)acts like a micro knuckle with its 1 mm blunt, stainless steel tip causing highly controllable microdissection and rarely complicates re-entry into the true lumen [Figures 18 (D) and (E)]. Stent malapposition is frequently observed in knuckled areas due to deeper shelving of subintimal space [Figure 19 (A)] with knuckle; however, it is rarely seen with CrossBoss(Boston Scientific, USA) subintimal dissection. Therefore, CrossBoss(Boston Scientific, USA) with Stingray (Boston Scientific, USA)provides more controllable, quite predictable and small subintimal dissection with a high probability of successful re-entry and low possibility of the malapposed stent than knuckling [Figure 19 (B)]. The principle of minimum vessel distortion should be applied and it is preferable that the majority of

subintimal tracts be created by a CrossBoss(Boston Scientific, USA) catheter rather than a knuckle, where possible (5-7).

Re-entry after knuckle

The initial description of knuckle in coronary CTO PCI was STAR, in which, knuckle was used for subintimal tracking as well as re-entry into the true lumen, which is unpredictable and unsuccessful in a significant number of cases. In the present day CTO practice, the knuckle is used in conjunction with CrossBoss–Stingray for more predictable re-entry (2, 15, 18, 19). Stingray (Boston Scientific, USA) is a modified hydrophilic coated balloon with a flat profile. It has dual lumen with 180˚ opposed and offsetting exit ports enabling selective guidewire re-entry.

Re-entry can also be done with mini-STAR or limited antegrade subinitmal tracking (LAST; Figure 20) (11, 20-22).

When not to perform a stand-alone knuckle wire technique

The biggest challenge for the knuckle procedure is the unpredictable re-entry, which can be avoided by careful case selection. Presence of good interventional collaterals and access to retrograde gear is always a big advantage in knuckle technique as this ensures the safety of the distal vessel if the knuckle does not create the desired result.

1. When the proximal/distal cap is over a major bifurcation point
2. Ambiguous CTO entry cap, when cap penetration is not possible with Coronary angiography/IVUS guidance
3. When the CTO body involves a significant side branch
4. When there is a diffuse distal disease, which may preclude a predictable re-entry

Conclusion

Knuckle wire technique in its conventional form or in the various fine-tuned modifications that provides “controlled knuckle”, adds to the success ofCTO intervention

in ambiguous vessel course and long length occlusions. Often it comes as a last resort when intervention is neither progressing antegradely or retrogradely due to impenetrable plaque or ambiguous course. In contemporary CTO PCI scenario, antegrade knuckling is predominantly used to facilitate CrossBoss advancement and further re-entry with Stingray.However, the technique requires a thorough understanding of the CTO anatomy and orientation of the subintimal space created. A clear cut strategy to protect the distal territoryfrom subintimal hematoma isof paramount importance while performing this procedure.

Conflicts of interest

The authors of the study declare no conflicts of interest.

Funding statement

The authors received no financial support for the research, authorship, and/or publication of this article.

Conflict of Interest Statement

Dr. Reddy A has nothing to disclose.

Dr. Ananthakrishna Pillai has nothing to disclose.

Dr. Reddy has nothing to disclose.

Dr. Rao has nothing to disclose.

Dr. Deshpande has nothing to disclose.

References

1. Colombo A, Mikhail GW, Michev I, Iakovou I, Airoldi F, Chieffo A, Rogacka R, Carlino M, Montorfano M, Sangiorgi G, Corvaja N. Treating chronic total occlusions using subintimal tracking and re-entry: the STAR technique. *Catheter Cardiovasc Interv*. 2005;64:407-11.
2. Martinez-Rumayor AA, Banerjee S, Brilakis ES. Knuckle wire and stingray balloon for recrossing a coronary dissection after loss of guidewire position. *JACC Cardiovasc Interv*. 2012;5(10):e31-2.
3. Tasic M, Sreckovic MJ, Jagic N, Miloradovic V, Nikolic D. Knuckle technique guided by intravascular ultrasound for in-stent restenosis occlusion treatment. *Postępy w KardiologiiInterwencyjnej= Advances in Interventional Cardiology*. 2015;11(1):58.
4. Mishra S. Unraveling the mystique of CTO Interventions: tips and techniques of using hardware to achieve success. *Indian Heart J*. 2017;69:266-276.
5. Brilakis ES, Karmpaliotis D, Vo MN, Garcia S, Michalis L, Alaswad K, Doshi P, Lombardi WL, Banerjee S. Advances in the management of coronary chronic total occlusions. *Journal of Cardiovascular Translational Research*. 2014;7(4):426-36.
6. Harding SA, Wu EB, Lo S, Lim ST, Ge L, Chen JY, Quan J, Lee SW, Kao HL, Tsuchikane E. A new algorithm for crossing chronic total occlusions from the Asia Pacific Chronic Total Occlusion Club. *JACC: Cardiovascular Interv*. 2017;10:2135-43.
7. Rinfret S, Ybarra LF. Antegrade Chronic Total Occlusion Crossing: CrossBoss First or Last?. *JACC Cardiovasc Interv.* 2018;11(3):234-236.
8. Isawa T, Ochiai M, Munehisa M, Ootomo T. A Novel, Modified Reverse Controlled Antegrade and Retrograde Subintimal Tracking Technique for

Bypassing the Calcified Proximal Cap of Coronary Total Occlusions. *Case Reports in Cardiology*. 2017vol. 2017, Article ID 3850646, 6 pages.

9. CL Lim M. Antegrade techniques for chronic total occlusions. *Curr Cardiol Rev*. 2015;11(4):285-90.

10. Carlino M, Demir OM, Colombo A, Azzalini L. Microcatheter knuckle technique: A novel technique for negotiating the subintimal space during chronic total occlusion recanalization. *Catheter Cardiovasc Interv*. 2018 Dec 1;92(7):1256-60.

11. Dash D. Guidewire crossing techniques in coronary chronic total occlusion intervention: A to Z. *Indian Heart J*. 2016;68:410-20.

12. Wilson W, Spratt JC. Advances in procedural techniques-antegrade. *CurrCardiol Rev*. 2014;10:127-44.

13. Shaukat A, Mooney M, Burke MN, Brilakis ES. Use of chronic total occlusion percutaneous coronary intervention techniques for treating acute vessel closure. *Catheter Cardiovasc Interv*. 2018;92(7):1297-300.

14. Danek BA, Karatasakis A, Karmpaliotis D, Alaswad K, Yeh RW, Jaffer FA, Patel M, Bahadorani J, Lombardi WL, Wyman MR, Grantham JA. Use of antegrade dissection re-entry in coronary chronic total occlusion percutaneous coronary intervention in a contemporary multicenter registry. *Int J Cardiol*. 2016;214:428-37.

15. Wu EB, Tsuchikane E, Lo S, Lim ST, Ge L, Chen JY. Retrograde algorithm for chronic total occlusion from the Asia Pacific Chronic Total Occlusion club. *Asian Interv*. 2018;4:98-107.

16. Joyal D, Thompson CA, Grantham JA, Buller CE, Rinfret S. The retrograde technique for recanalization of chronic total occlusions: a step-by-step approach. *JACC Cardiovasc Interv*. 2012;5(1):1-1.

17. Brilakis ES, Badhey N, Banerjee S. "Bilateral knuckle" technique and Stingray re-entry system for retrograde chronic total occlusion intervention. *J Invasive Cardiol*. 2011;23(3):E37-9.

18. Schumacher SP, Stuijfzand WJ, Opolski MP, van Rossum AC, Nap A, Knaapen P. Percutaneous coronary intervention of chronic total occlusions: when and how to treat. *Cardiovasc Revasc Med*. 2019;20(6):513-22.

19. Tarar MN, Christakopoulos GE, Brilakis ES. Successful management of a distal vessel perforation through a single 8-French guide catheter: Combining balloon inflation for bleeding control with coil embolization. *Catheter Cardiovasc Interv*. 2015;86(3):412-6.

20. Michael TT, Papayannis AC, Banerjee S, Brilakis ES. Subintimal dissection/re-entry strategies in coronary chronic total occlusion interventions. *Circ Cardiovasc Interv*. 2012;5:729-38.

21. Maeremans J, Dens J, Spratt JC, Bagnall AJ, Stuijfzand W, Nap A, Agostoni P, Wilson W, Hanratty CG, Wilson S, Faurie B. Antegrade dissection and re-entry as part of the hybrid chronic total occlusion revascularization strategy: asubanalysis of the RECHARGE Registry (Registry of CrossBoss and Hybrid Procedures in France, the Netherlands, Belgium and United Kingdom). *Circ Cardiovasc Interv*. 2017;10:e004791.

22. Godino C, Sharp AS, Carlino M, Colombo A. Crossing CTOs—The tips, tricks, and specialist Kit that can mean the difference between success and failure. *Catheter Cardiovasc Interv*. 2009;74(7):1019-46.

Figure legends

Figure 1: J-loop configuration of wire to allow a blunt dissection

Figure 2: AP-CTO algorithm for CTO crossing

Figure 3: Differential resistance by subintimal tissue and media/adventitia tissue leads to knuckle progression in the subintimal plane

Figure 4: Wires and tip shaping (A) Umbrella handle (B) Formed knuckle (C) Large knuckle

Figure 5: Knuckle technique **(A)** A indicates knuckle in formation **(B)** Final knuckle at the junction of a soft and stiff portion of the wire, B indicates fully formed knuckle

Figure 6: Penetration of proximal cap with a stiff wire to allow the introduction of microcatheter and soft wire into CTO body

Figure 7: Knuckle proximal to CTO **(A)** Long RCA CTO with JCTO score 3 with impenetrable proximal cap, where A is Ambiguous proximal cap, B is Calcium in CTO, C is Bifurcation at CTO, D is Good distal target with a lesion length of > 30 mm **(B)** Knuckle wire done with side BASE proximal to CTO **(C)** Subintimal hematoma created after knuckling, as subintimal space is directly exposed to aortic pressures **(D)** IVUS showing subintimal hematoma (green dotted outline)

Figure 8: Controlling knuckle

Figure 9: Proximal RCA CTO—Knuckle pushed with Anchor balloon in atrial branch, where A is Anchor balloon (1.5x12 mm) and B is Knuckle with Fielder XT-R

Figure 10:BASE/Side BASE with knuckle in impenetrable or ambiguous proximal cap**Figure 11:** Knuckle formation with support of a proximal OTW inflated balloon

Figure 12: Knuckle in CTO PCI. **(A)** Proximal RCA CTO with calcium in a post CABG patient with JCTO score of 3, where A is PLVB filling from left system **(B)** Distal RCA filling up to crux in retrograde injection; course of RCA is invisible with an angle > 40, where A

is Proximal RCA CTO **(C)** Antegrade knuckle to guide and navigate retrograde wire, where A indicates antegrade knuckle guiding retrograde wire

Figure 13: Progression of knuckle wire though highly calcified and long tortuous CTO **(A)** Perforation of the vessel with the use of a stiff wire **(B)** Use of a soft wire will prevent perforation

Figure 14: Highly calcified and long tortuous CTO. **(A**) In this image we can see clear proximal cap (A), lesion length > 50 mm(B), and angulation > 40° (C); **(B)** In this image we can see good distal target with a bifurcation at the distal cap (A)

Figure 15: Knuckle used in conjunction with CrossBoss to avoid side branch entry **(A**) In this image A is CrossBoss (Boston Scientific, USA) in side-branchand B is Axis of the main vessel-RCA **(B)** Knuckle to cross side branch for CrossBoss (Boston Scientific, USA) advancement beyond branch point; A indicates CrossBoss, B indicates location of side branch, and C indicates knuckle with Pilot 150

Figure 16: Knuckle used in conjunction with CrossBoss to cross the circumvent calcium spots**(A)** CrossBoss stuck in lesion, where A indicates CrossBoss (Boston Scientific, USA) stalled by calcium in the mid-CTO **(B)** Knuckle wire to cross the calcium and CrossBoss (Boston Scientific, USA) advanced over knuckle wire, whereA indicates retracted CrossBoss, B indicates point where CrossBoss is stalled, and C indicates Fielder-FC knuckle crossed the point at which CrossBoss stalled **(C)** CrossBoss (Boston Scientific, USA) advancement till re-entry zone, where A indicates CrossBoss and B indicates Distal RCA lumen

Figure 17: Criteria to use knuckle as an initial crossing strategy

Figure 18: Knuckle wire versus CrossBoss (Boston Scientific, USA) for subintimal tracking **(A)** intravascular ultrasound (IVUS) showing subintimal space created by knuckle, where A indicates wide crescent-shaped space **(B)** Intramural hematoma (green dotted outline) created by knuckle in distal RCA **(C)** Intramural hematoma in distal

RCA—Post knuckling **(D)** IVUS showing subintimal space created by CrossBoss(Boston Scientific, USA)—small, circular space **(E)** Fluoroscopy showing wide irregular lumen in knuckled area and regular, uniform lumen in CrossBoss(Boston Scientific, USA) area, where A is area of CrossBoss advancement, B is Knuckled area of the vessel, and C is area of CrossBoss advancement

Figure 19: CrossBoss with Stingray to overcome stent malapposition**(A)** Stent malapposition at 3–6 o'clock in the knuckled arterial segment**,**where A indiciates stent strut and B indicates vessel wall **(B)** Proper stent apposition in CrossBoss (Boston Scientific, USA) arterial segment

Figure 20: CTO dissection/re-entry strategies after knuckle wiring

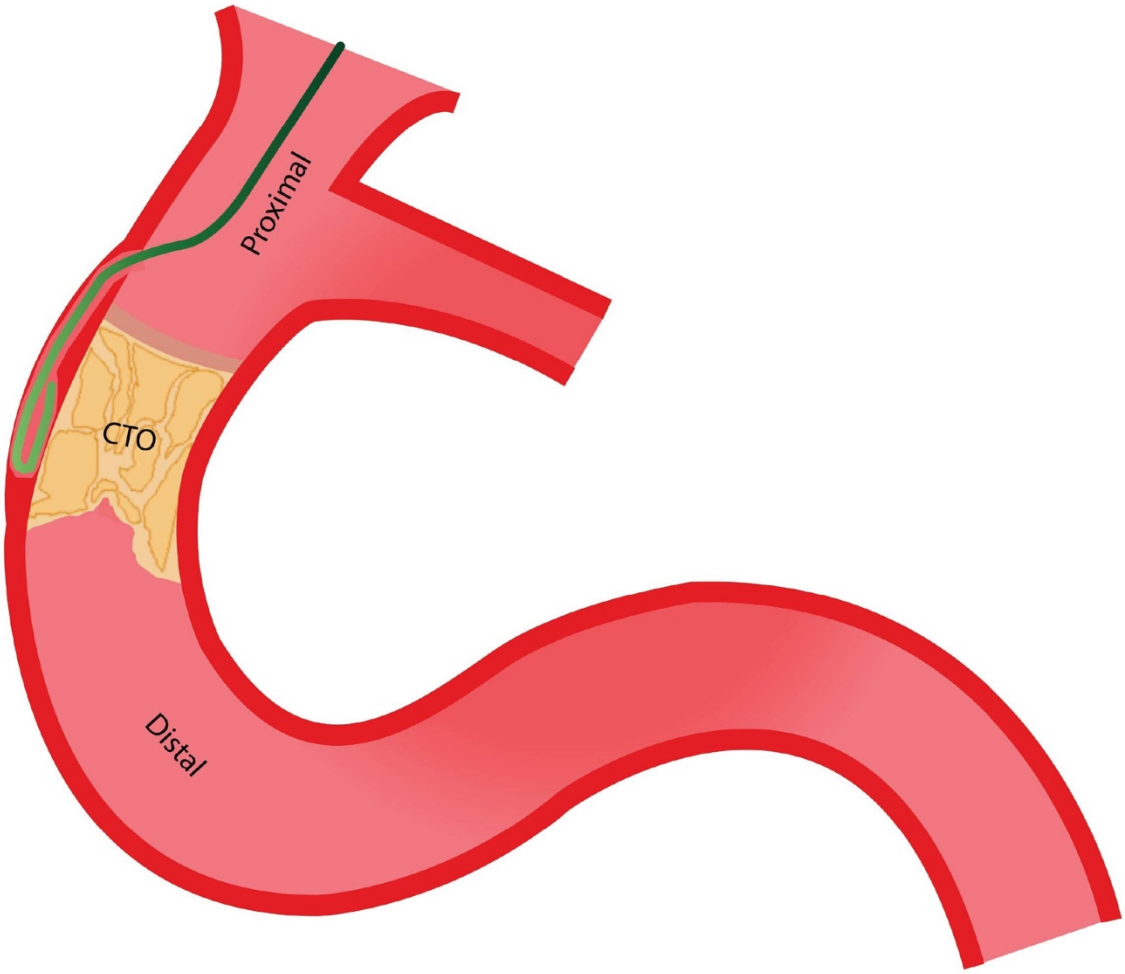

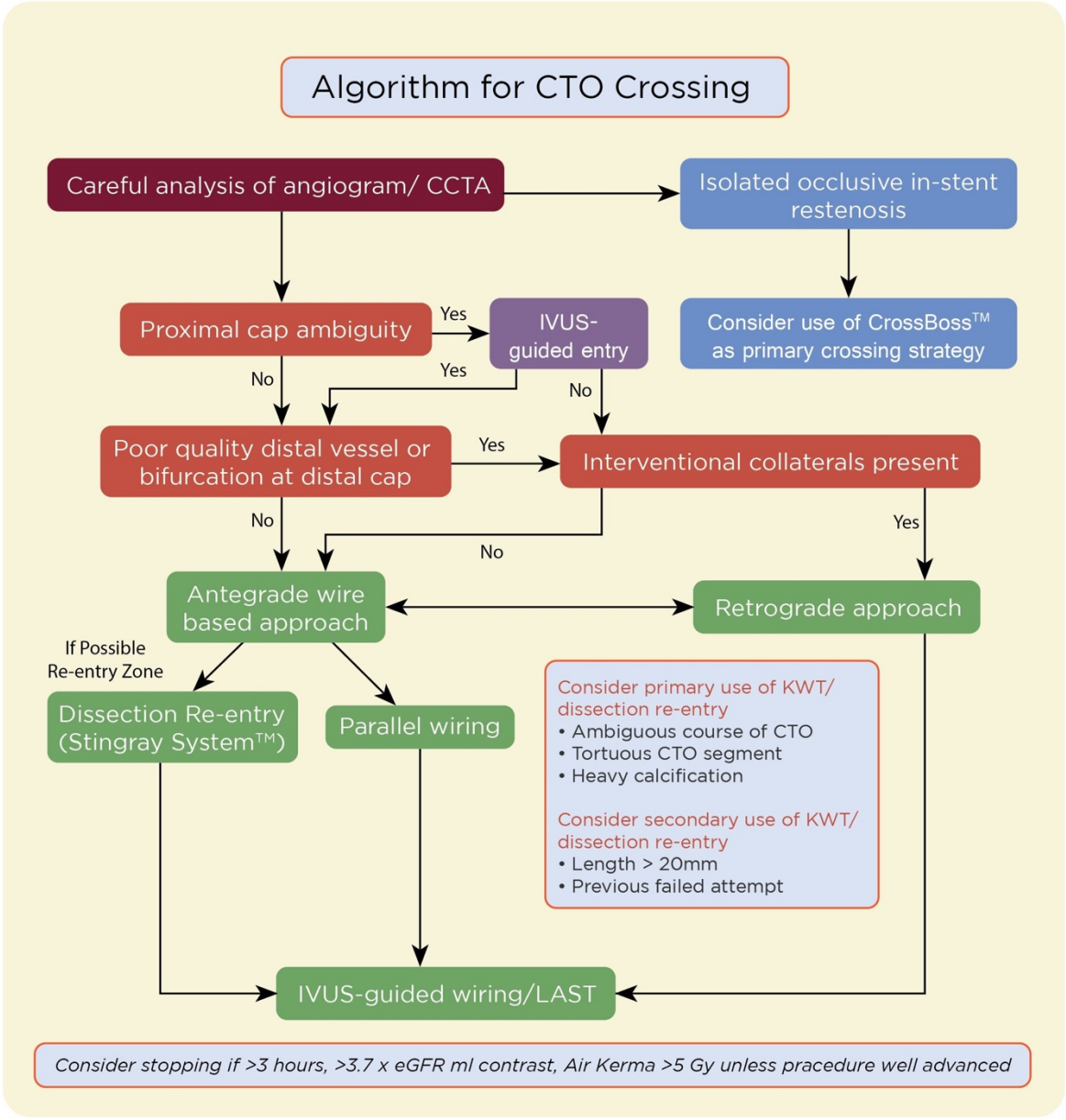

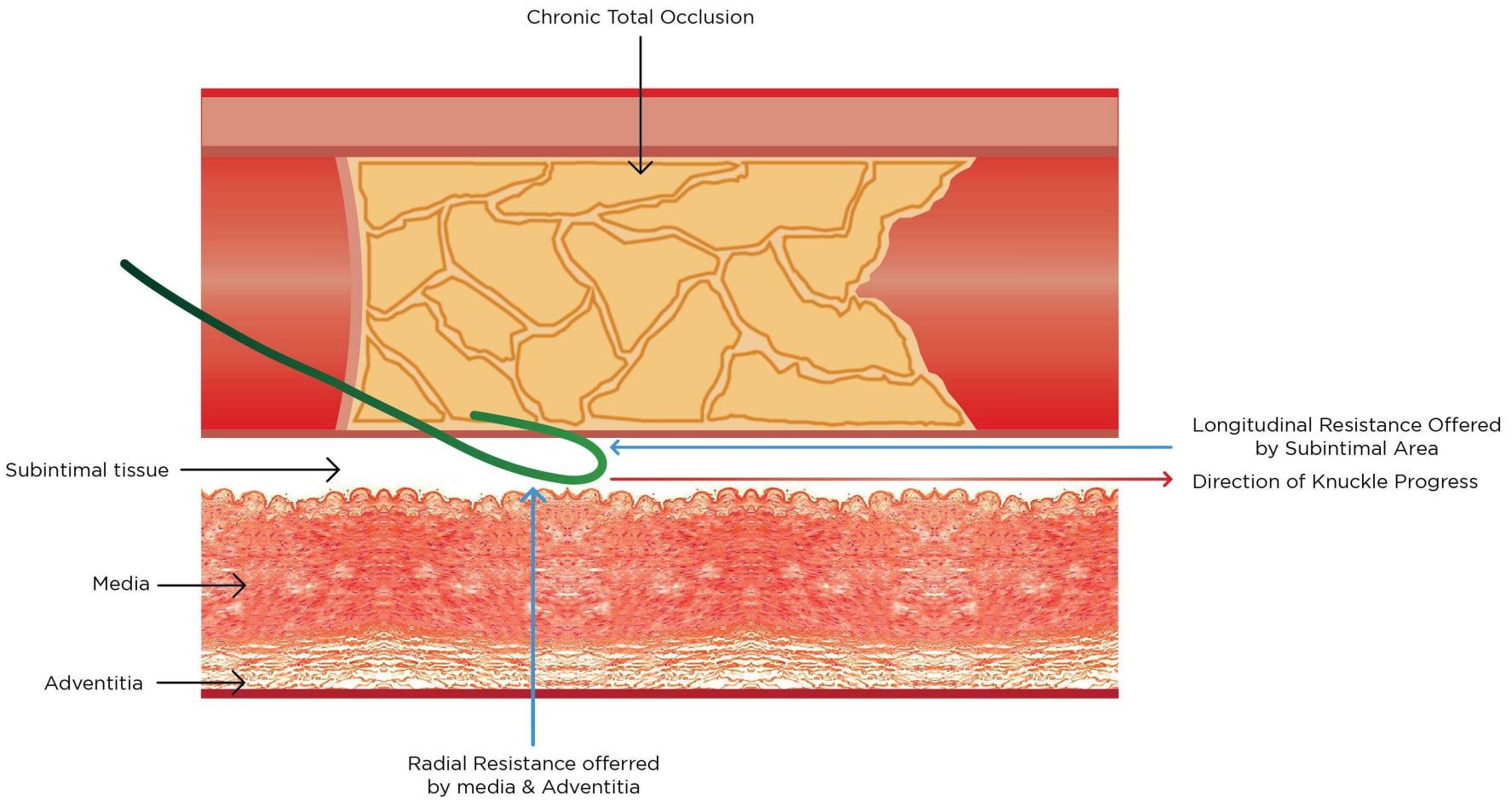

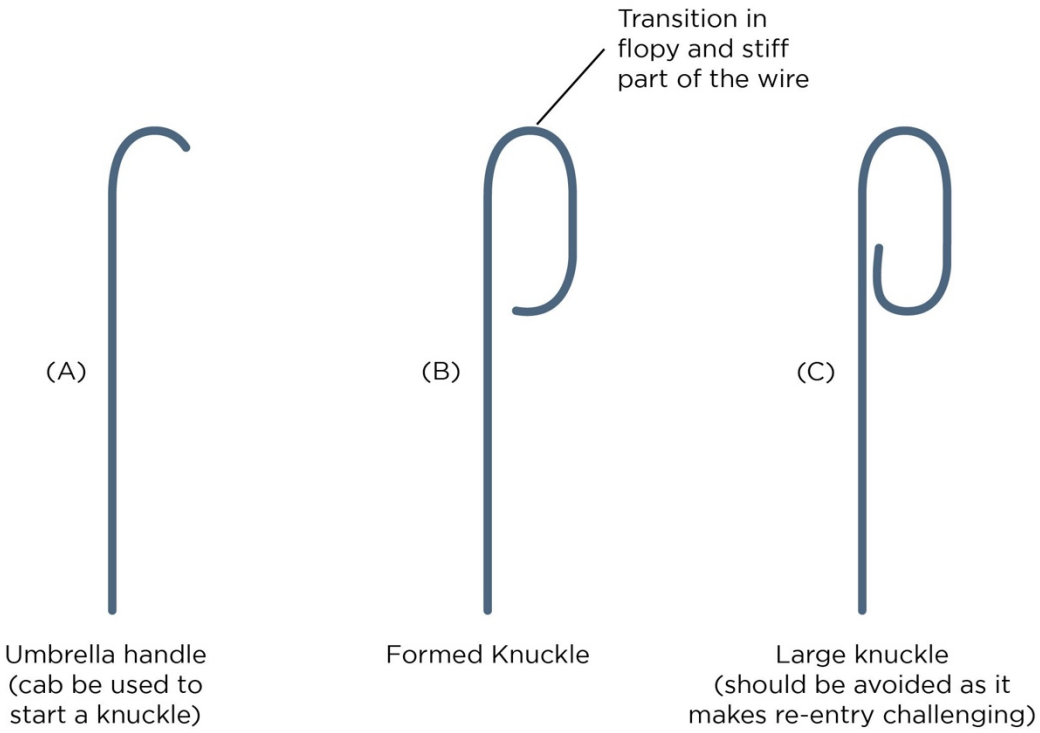

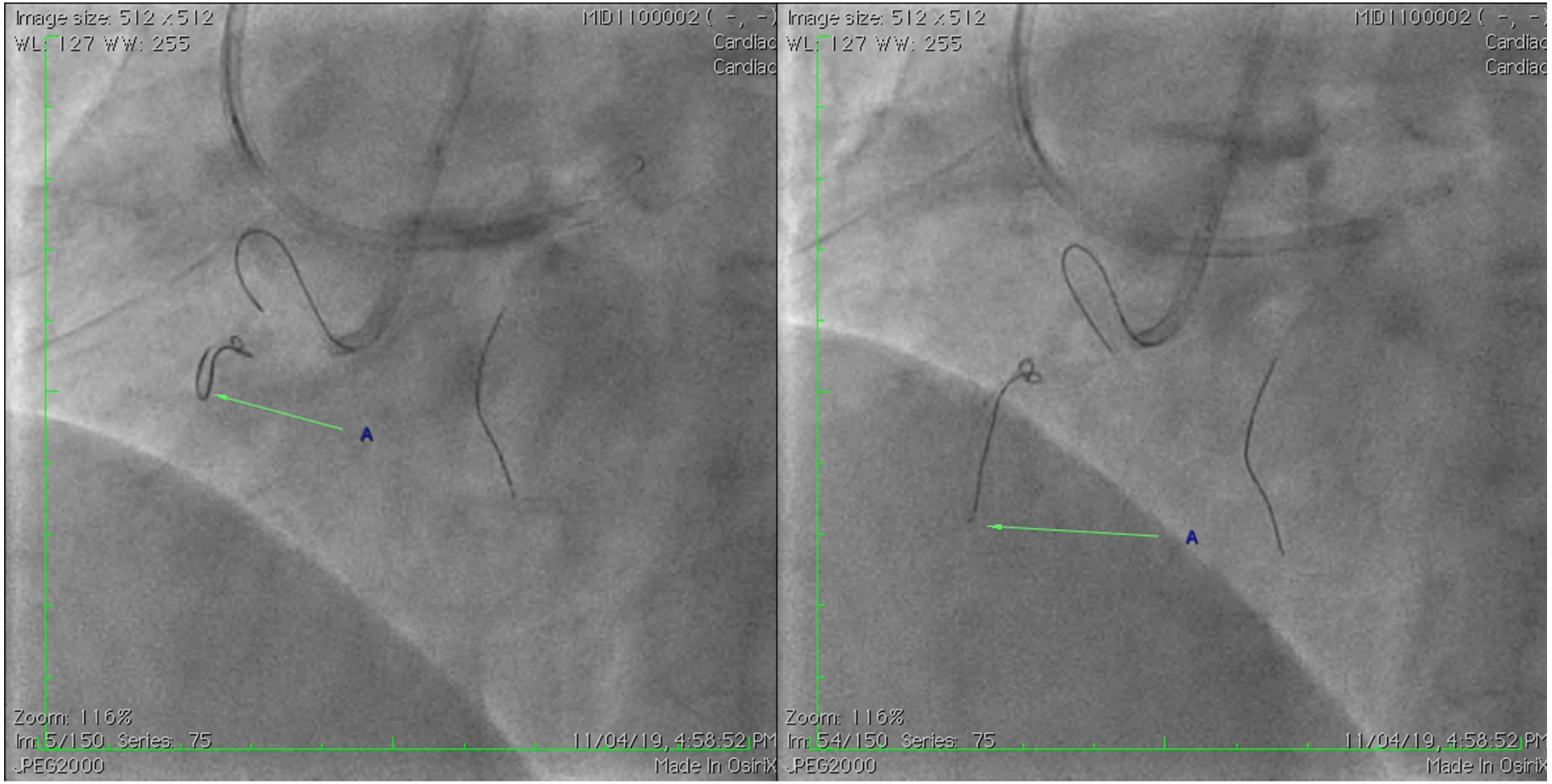

(A) (B)

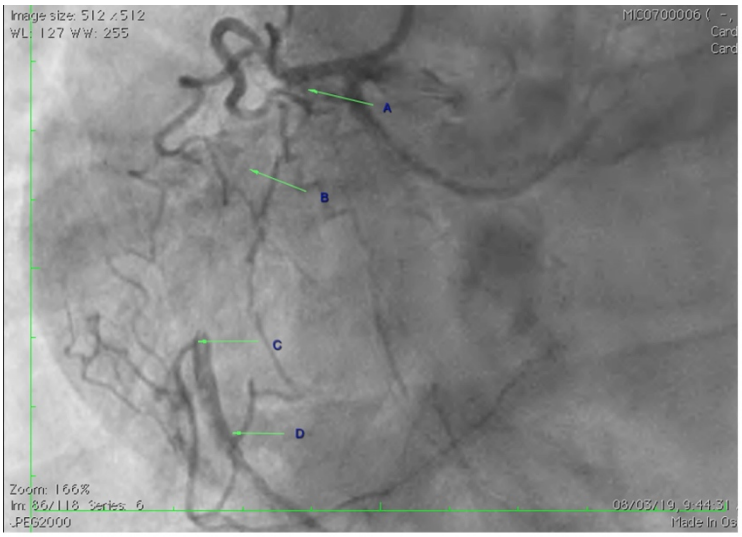

(A)

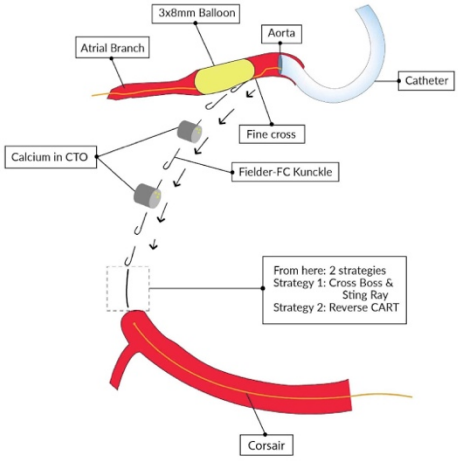

(B)

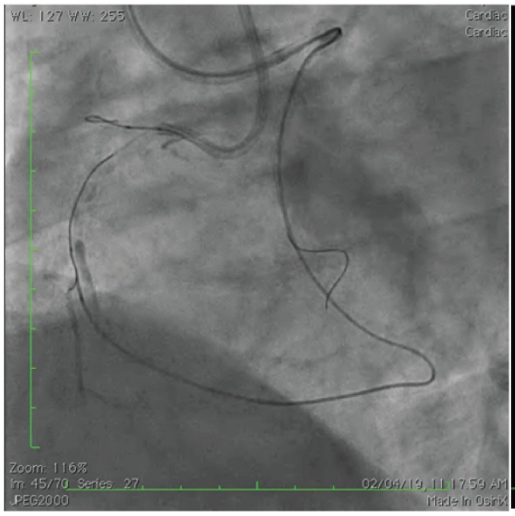

(C)

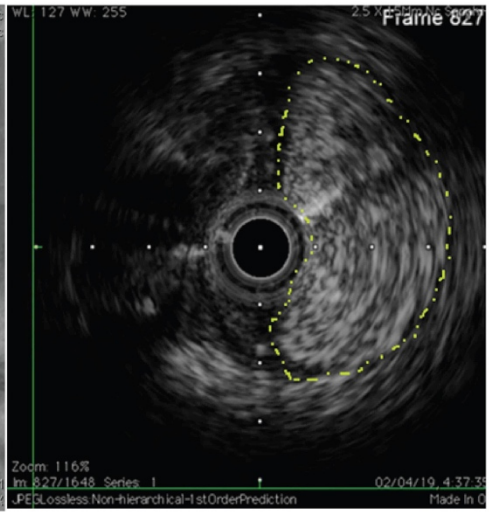

(D)

Controlling Knuckle

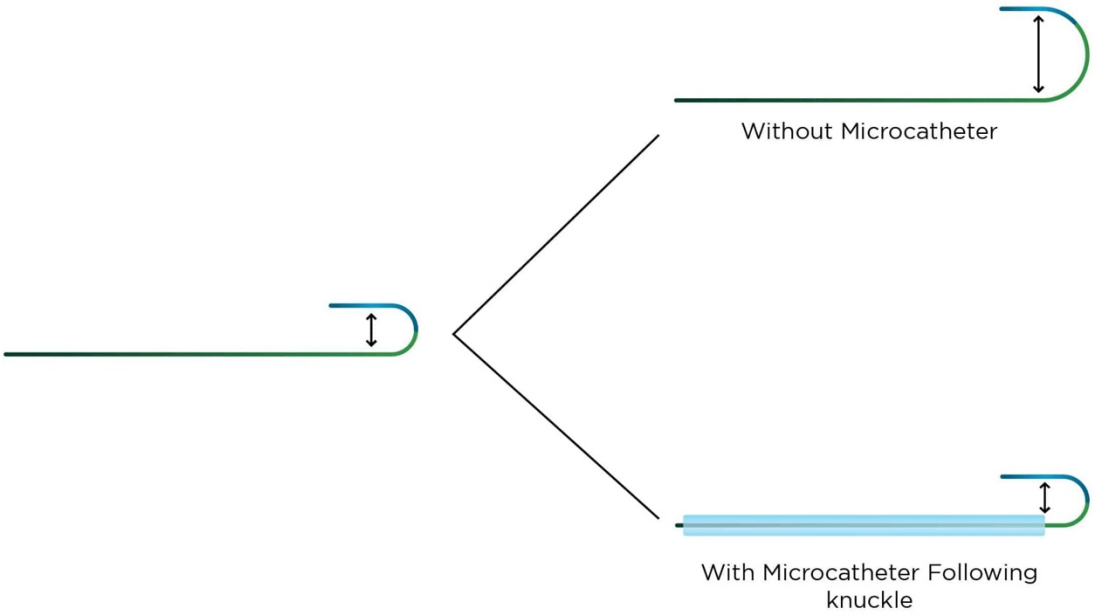

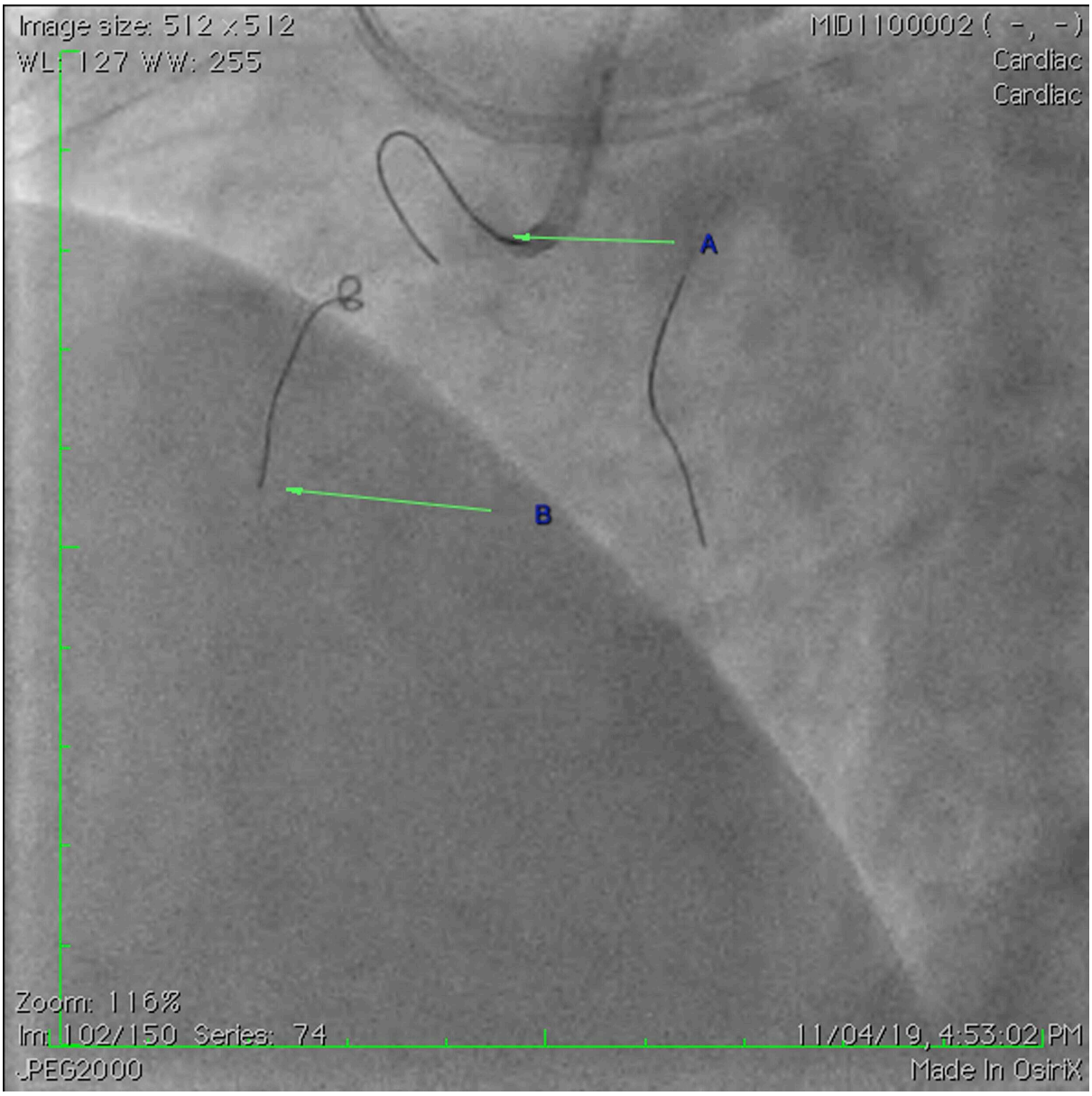

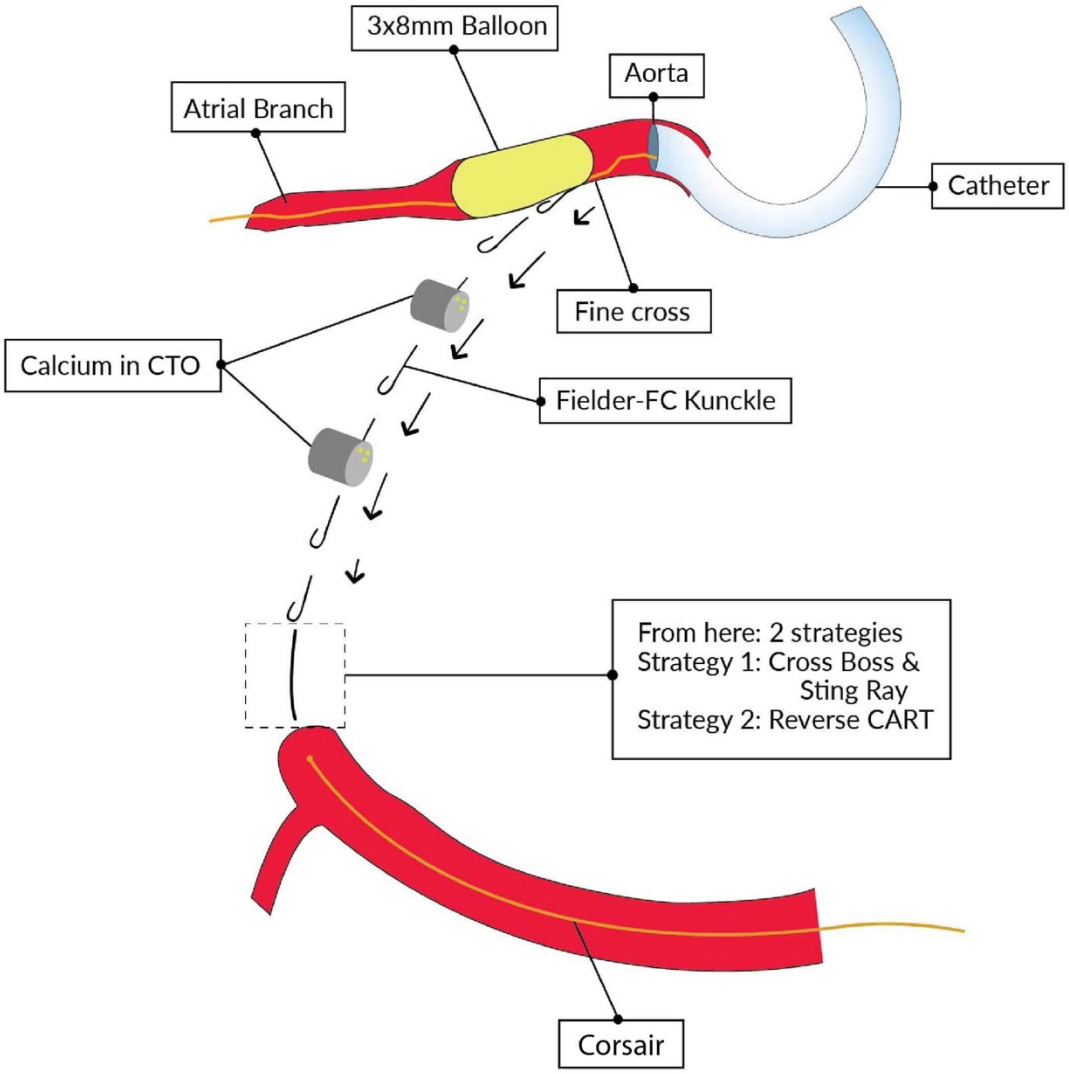

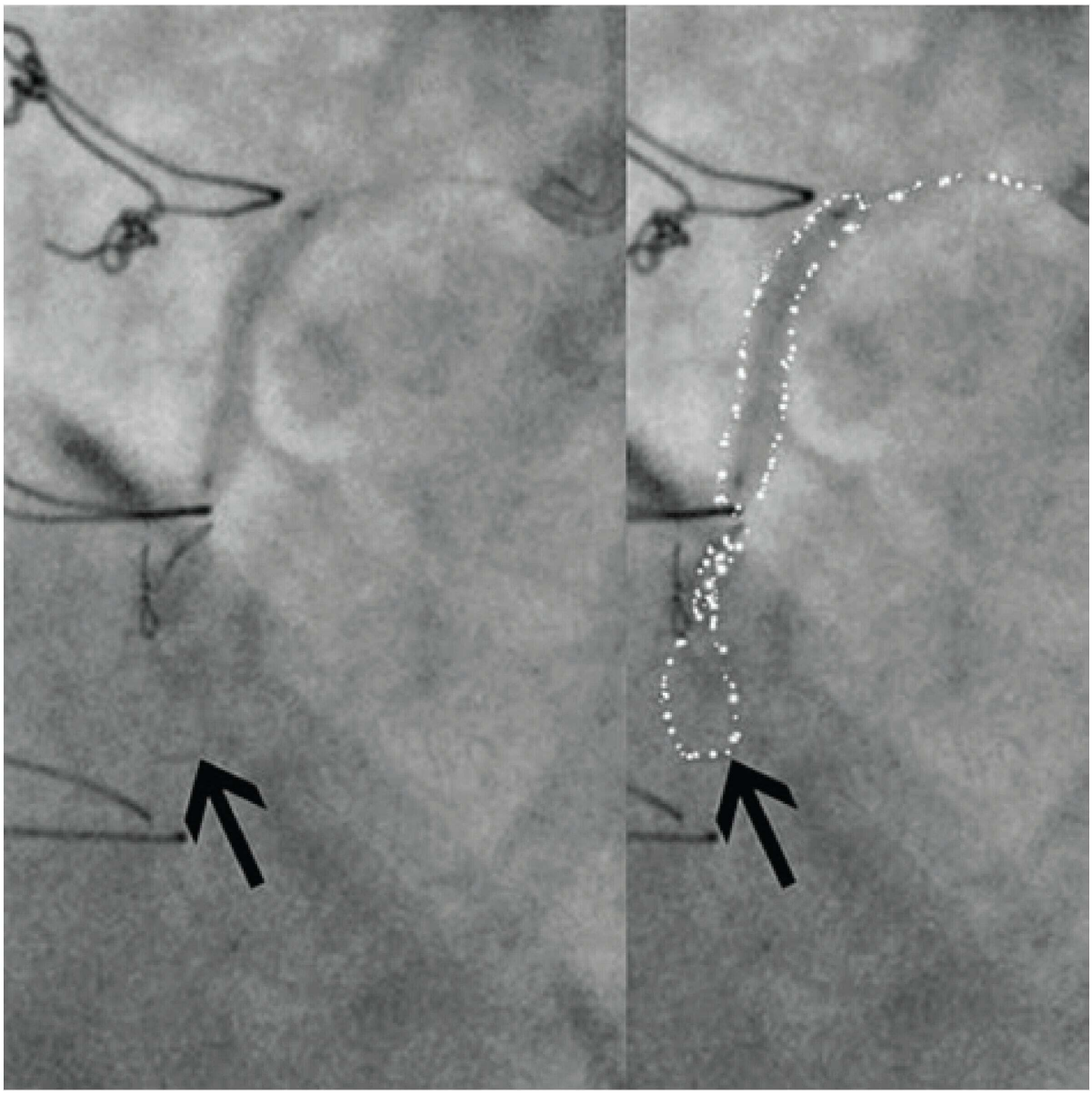

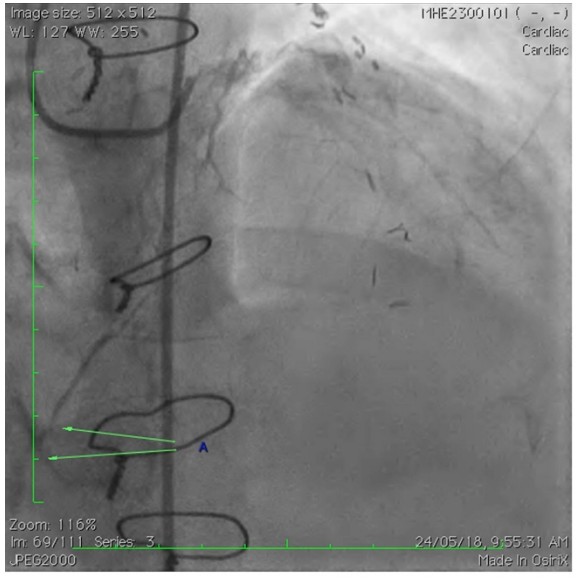

(A)

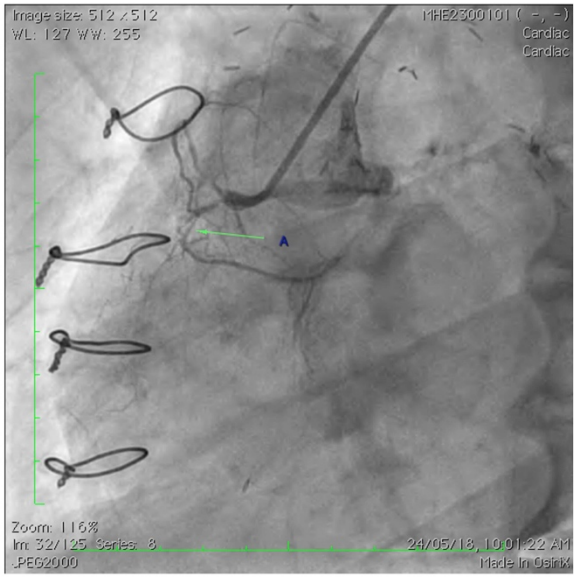

(B)

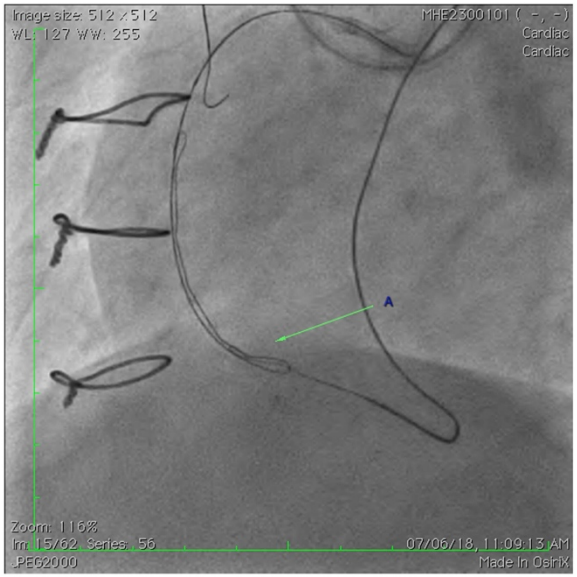

(C)

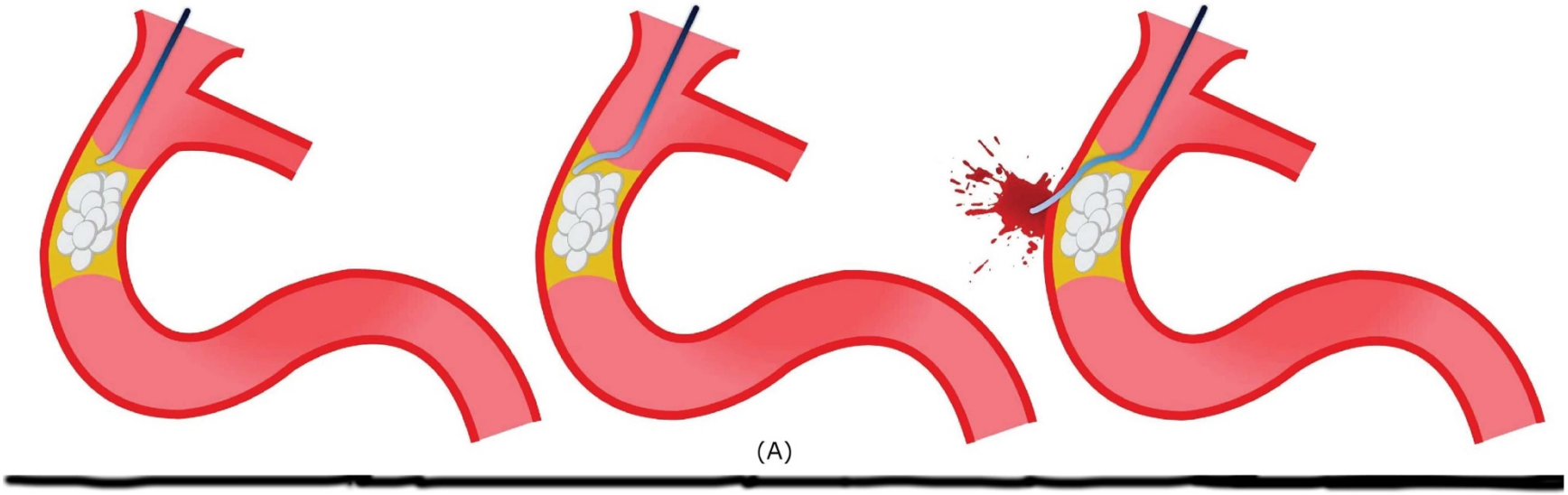

(A)

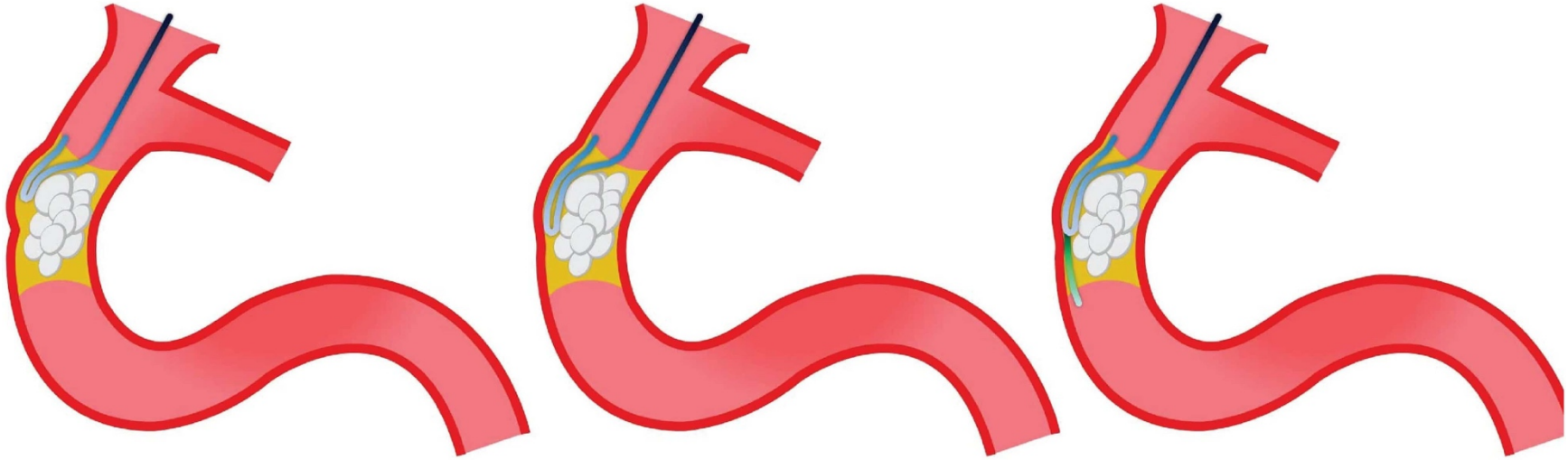

(B)

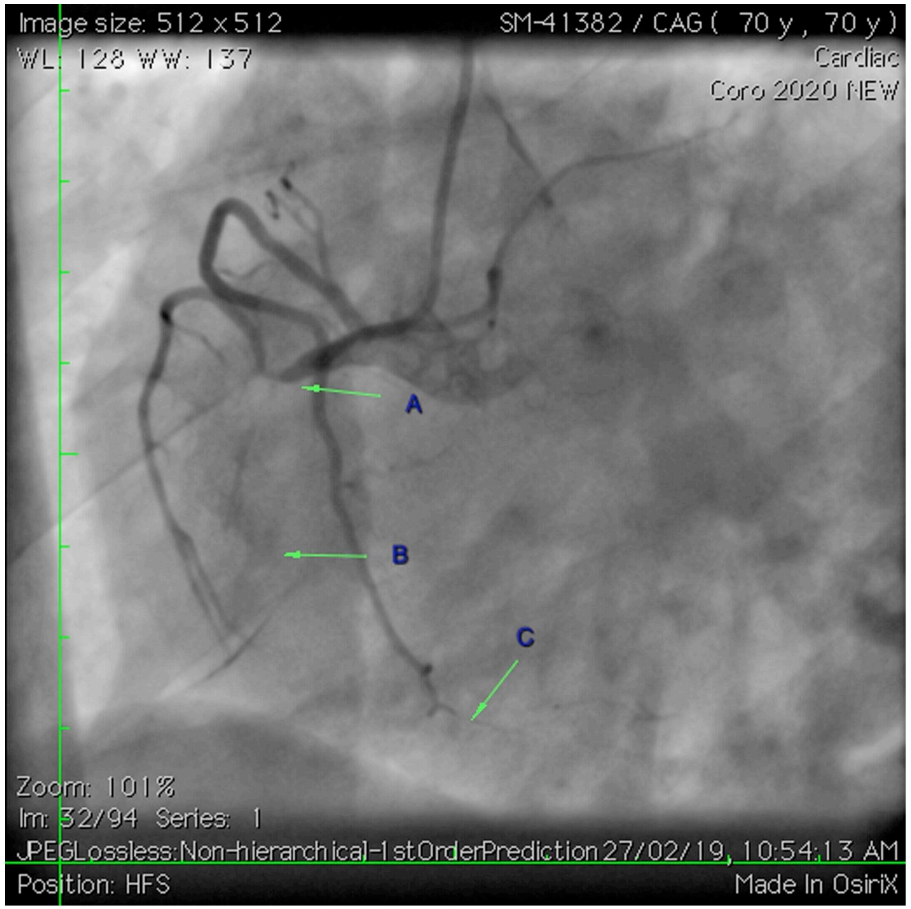

(A)

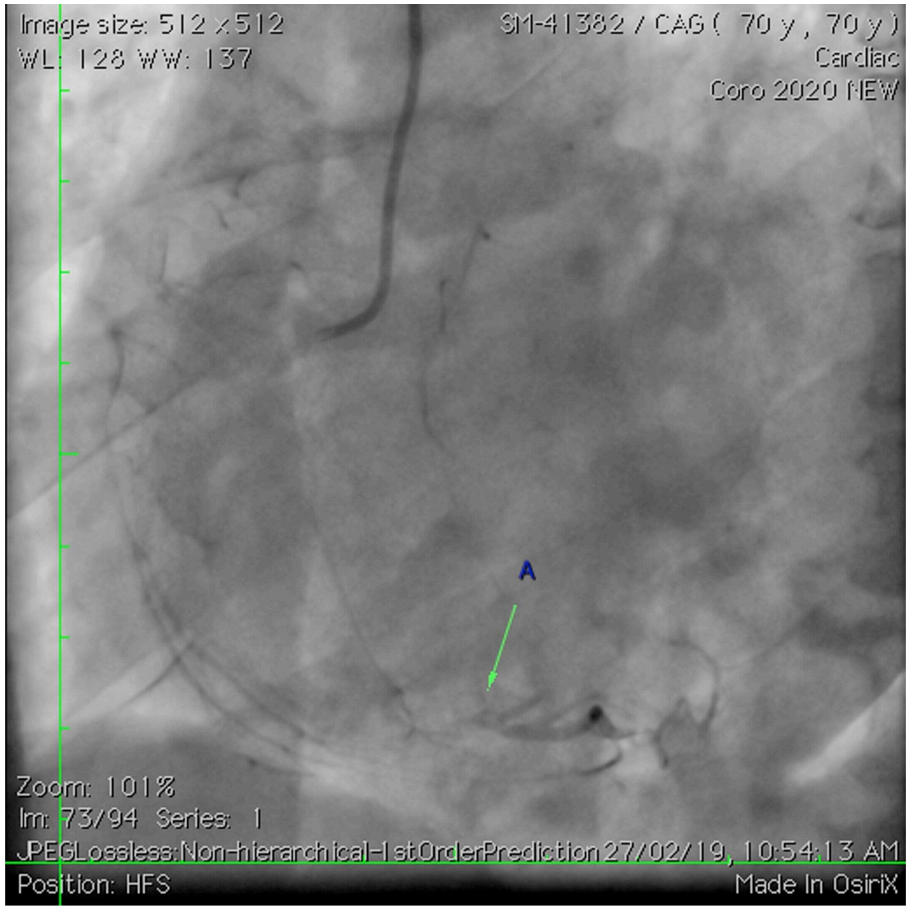

(B)

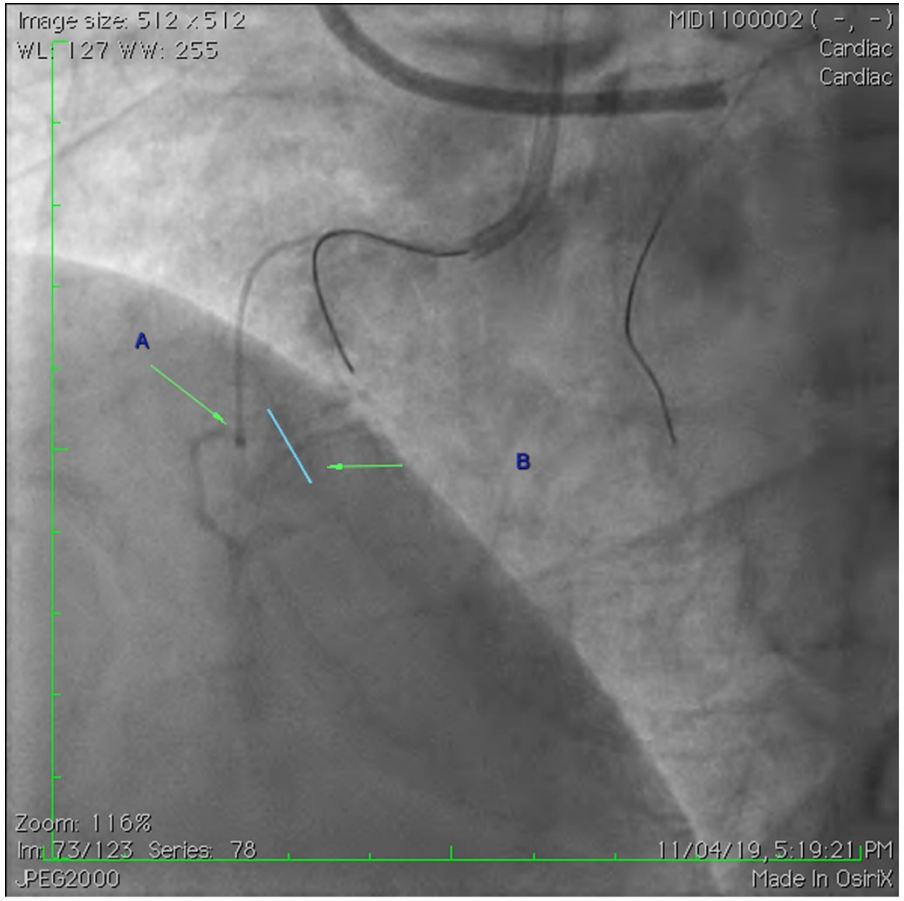

(A)

(B)

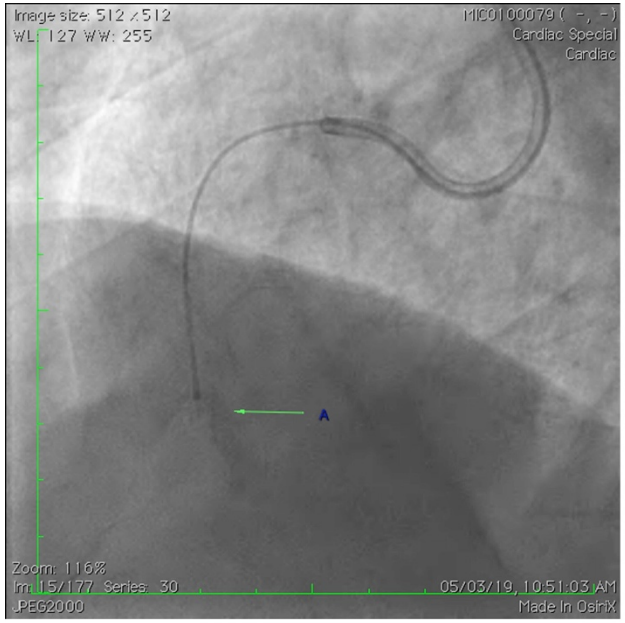

(A)

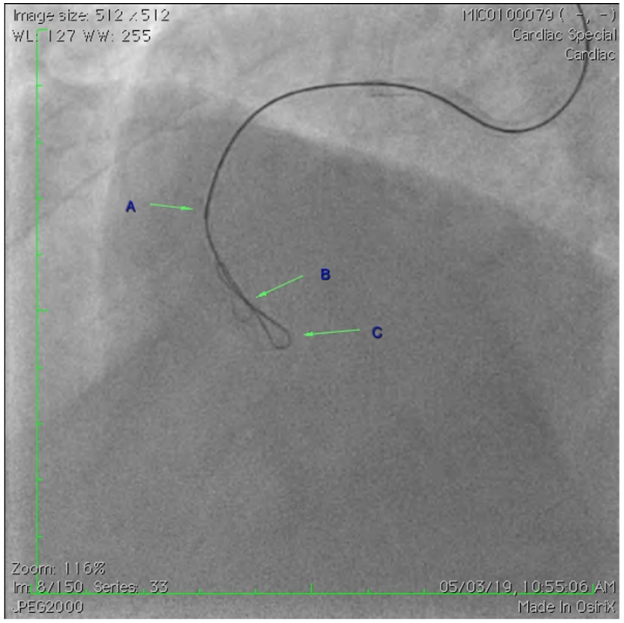

(B)

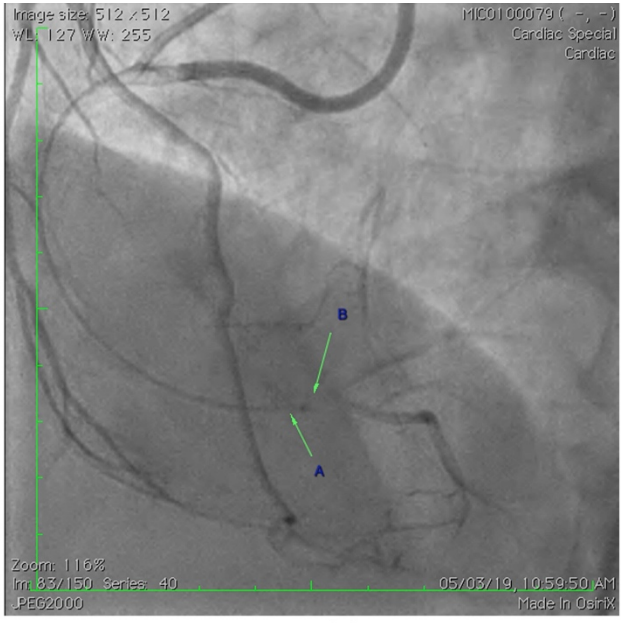

(C)

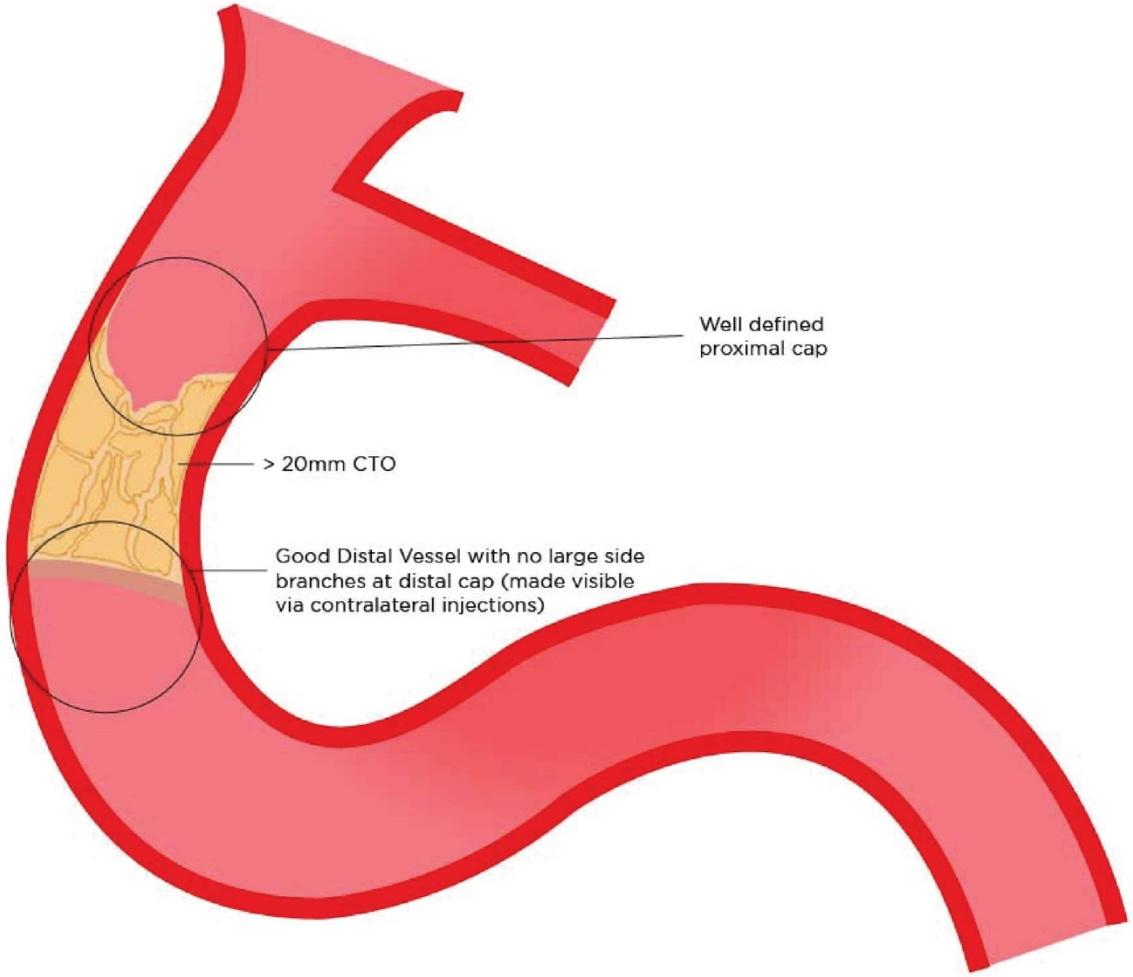

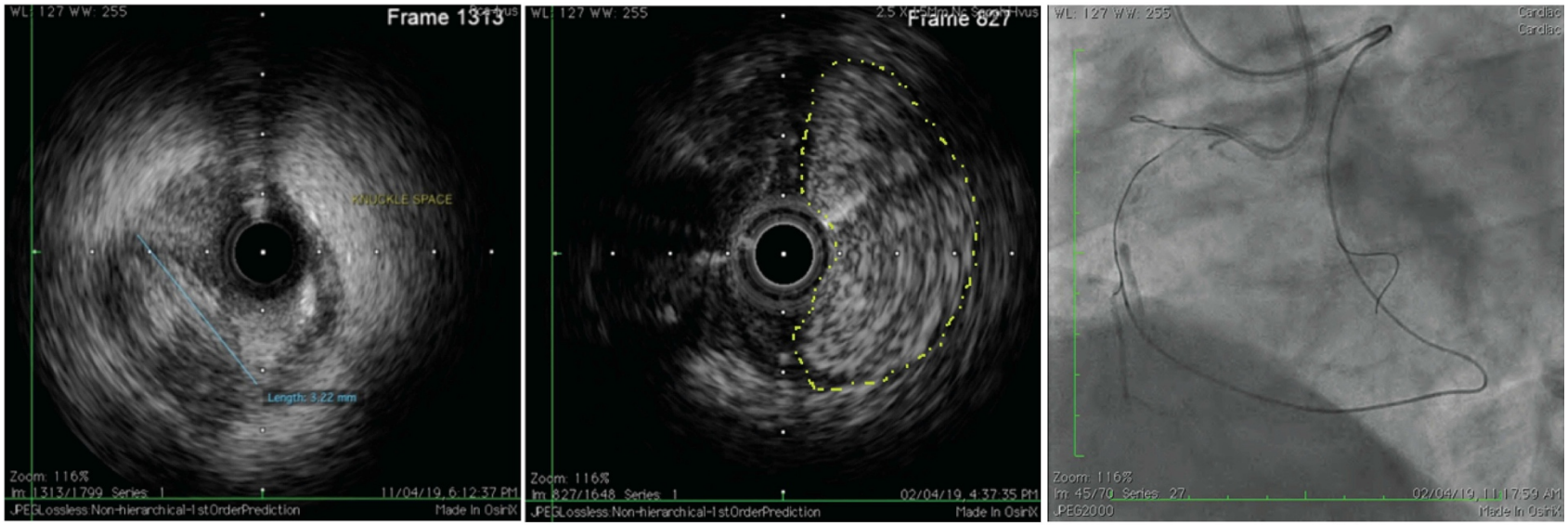

(A) (B) (C)

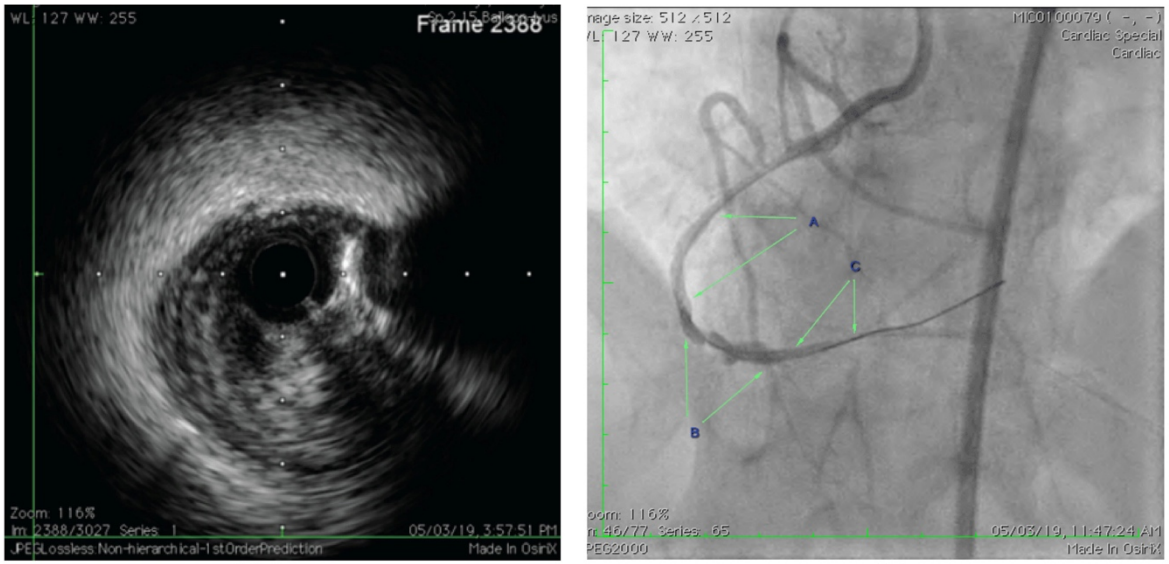

(D) (E)

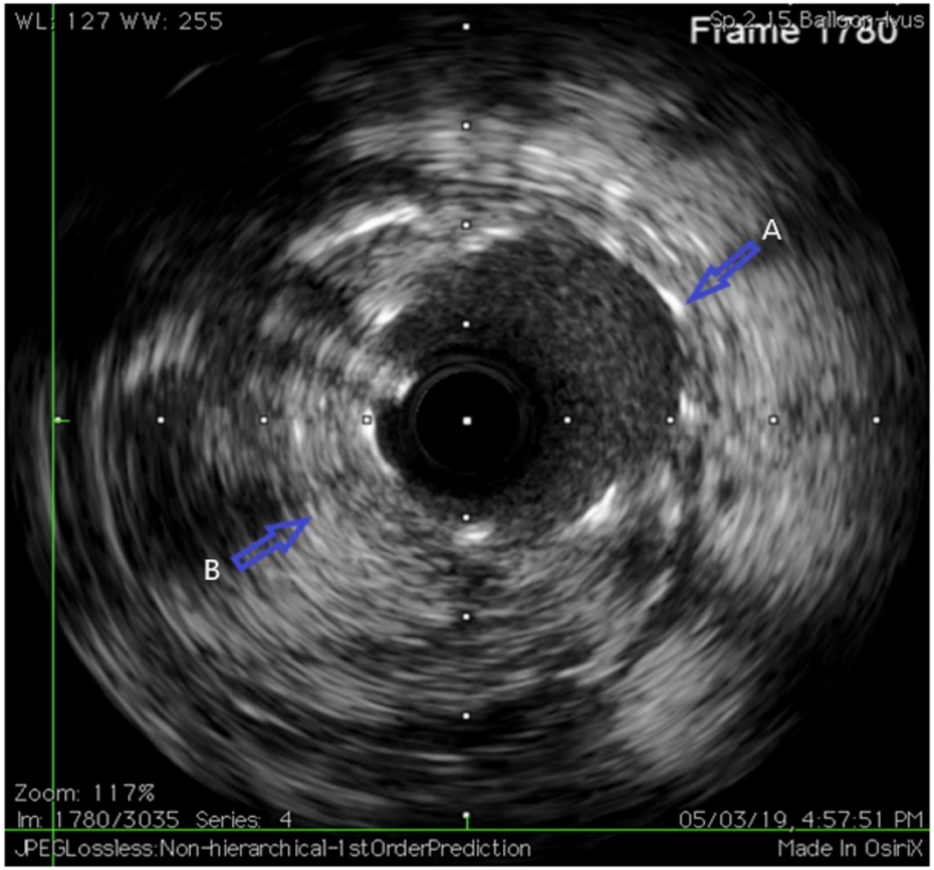

(A)

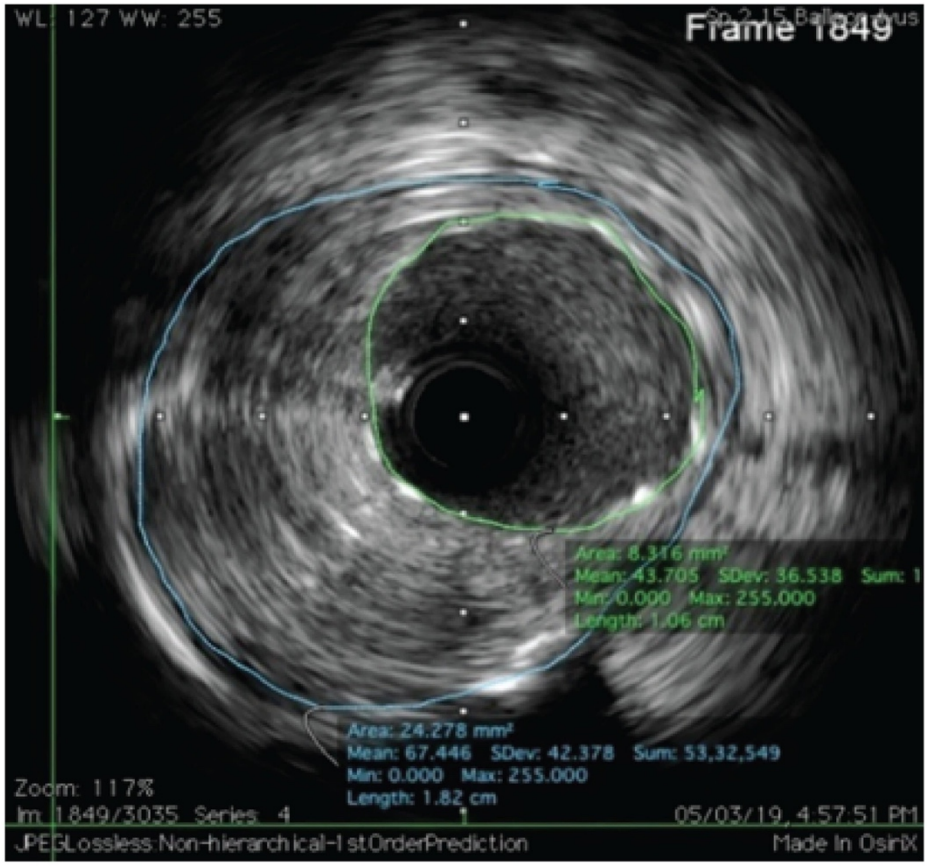

(B)

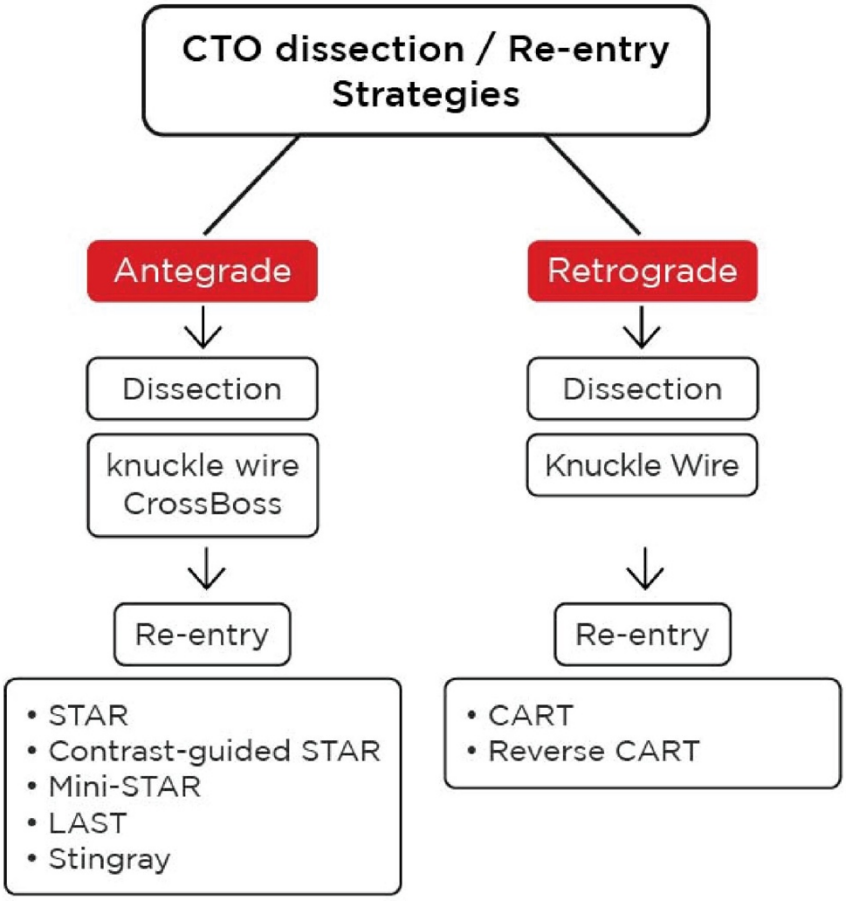

AsiaIntervention

Official Journal of the Asian Pacific Society of Interventional Cardiology

(APSIC) and the Interventional Cardiology Foundation of India (ICFI)

www.asiaintervention.org

Title: **Non Cyclic Obstruction of Aortic Disc Prosthesis: A rare case report**
ECG changes reflect coronary events in prosthetic valve cases: Probably not?

Authors: Hakim Irfan Showkat, M.D; Rekha Mishra, M.D; Sadaf Anwar, M.D; Siddharth Saxena, M.D; Sudheer Saxena, M.D

Manuscript number: AIJ-D-20-00006

Manuscript submission date: 24 January 2020

Revisions received: 14 July 2020

Accepted date: 14 July 2020

Non Cyclic Obstruction of Aortic Disc Prosthesis: A rare case report

ECG changes reflect coronary events in prosthetic valve cases: Probably not?

Hakim Irfan Showkat *[1]M.D; Rekha Mishra[1] M.D; Sadaf Anwar[2] M.D; Siddharth Saxena[3] M.D; Sudheer Saxena[4] M.D

1.National Heart Institute, New Delhi. 2. Fortis escorts hospital Faridabad, New Delhi 3.Kingsbrook Jewish medical center, New York USA. 4.Max hospital Mohali, Punjab

Conflict of interest : NONE

Short Title: Unusual Non Cyclic Obstruction of Aortic Disc Prosthesis

Funding: NONE

Consent of patients: TAKEN

Abbreviations: TTE (Transthoracic echocardiography), TEE (Transesophageal echocardiography), AR (aortic regurgitation), ECG (electrocardiogram).

Keywords: Miscellaneous; Aortic regurgitation; Mitral regurgitation; Other

Introduction

Mechanical valve dysfunction can be classified as endogenous and exogenous according to the etiology. Endogenous dysfunctions are caused by valve damage or defect, which has become extremely rare with the improvement of design, materials, manufacture and detection methods *in vitro* . Exogenous causes include inappropriate selection of prosthesis, technical issues or other complications, such as thrombosis, excessive pannus overgrowth into the prosthetic rim, excessively long knot end, residual chordae tendinae stuck in the prosthetic sewing ring, extremely long residual papillary muscles in left ventricle or calcified tissues under the prosthesis hampering leaflet mobility.

Methods

A Thirty seven year old woman underwent aortic valve replacement [21 mm medtronic hall mechanical prosthesis] for aortic valve endocarditis with severe aortic regurgitation in 1999. She was doing fairly well for these years and now this time she presented with intermittent episodes of chest discomfort, palpitation and breathlessness which used to subside after 10-15 minutes since last 5—6 days. She was admitted with initial normal ECG and 2D echoshowing normal gradients across aortic valve with normal LV and prosthetic valve function. She became symptomatic while in hospital and ECG showed sinus tachycardia with ST depression in leads I, II, III, augmented vector left (aVF) and V3-V6. Acute Coronary Syndrome was suspected as she had raised cardiac enzymes, so immediate coronary angiography was done which revealed normal coronary arteries with normal prosthetic valve opening and closing on fluoroscopy. She was stabilised and further evaluation and management was planned. Her initial international normalized ratio (INR) was 1.675 and had audible valve click. The patient developed similar complaints while in ICU and repeat ECG showed sinus tachycardia with transient ST elevation in the leads augmented vector right (aVR) and V1 and ST depression in leads I, II, III, augmented vector left (aVF) and V3-V6 , but this resolved within ten to fifteen minutes. Auscultation at that time revealed the absence of a valve click and hypotension (systolic blood pressure of 80 mmhg). The patient recovered spontaneously, and a repeat ECG showed no significant abnormalities. Patient was planned for trans-esophageal echocardiography (TEE) but when she reached TEE room, she became symptomatic and transthoracic echocardiography (TTE) during episode revealed acute severe aortic

regurgitation , moderate Mitral valve regurgitation with restricted prosthetic valve motion. (**Fig 1a**).

Results:

She was taken for surgical intervention. Intraoperative TEE was done showing high gradients. (**Fig 1b**). Pannus was found underneath the lesser orifice of the prosthetic valve (**Fig 2a/b**). Aortic prostheses was explanted and new aortic valve was replaced using size 19 mm st jude regent mechanical prosthesis. Postoperative echocardiography showed a normally functioning aortic valve, with normal gradients. Her postoperative course was uneventful, and the patient was discharged after 5 days. On follow-up, the patient is asymptomatic and normally functioning aortic prosthesis on 2D echocardiography.

Discussion: Mechanical valve dysfunction can be classified as endogenous and exogenous according to the etiology. Endogenous dysfunctions are caused by valve damage or defect, which has become extremely rare with the improvement of design, materials, manufacture and detection methods *in vitro*. Exogenous causes include inappropriate selection of prosthesis, technical issues or other complications, such as thrombosis, excessive pannus overgrowth into the prosthetic rim, excessively long knot end, residual chordae tendineae stuck in the prosthetic sewing ring, extremely long residual papillary muscles in left ventricle or calcified tissues under the prosthesis hampering leaflet mobility. The most common causes of mechanical valve dysfunction are thrombosis and pannus formation, which was present in 87.5% of patients in this series. (1) In comparison with the mitral position, intermittent prosthetic regurgitation in the aortic position is very rare. Prosthetic valve dysfunction as a result of pannus formation due to fibrous tissue ingrowth is an infrequent but a serious complication. However, the mechanism of pannus formation has not been fully described yet and hence effective preventive methods have not been developed.(2) Usually, the pannus produces a stenosis of the prosthesis due to obstruction of the LV outflow tract or restriction on the movement of the opening of the discs of the prosthetic valve.(3) In our patient AR was due to pannus underneath the lesser orifice of prosthetic valve. This impeded the normal closing of the leaflet intermittently, leading to the phasic AR. Clinical signs and auscultation may be confusing and unhelpful in the evaluation of the severity of valvular dysfunction. Murmurs may be heard in normally functioning valves whereas paravalvular regurgitation may be silent Single tilting disc prostheses are more prone to develop this condition, and it has also been linked to sub valvular non obstructing

pannus. (2,4) In addition, intermittent prosthetic aortic valve regurgitation (AVR) due to malfunction can present as severe acute ischemia from the load/perfusion mismatch or as heart failure (HF) as in our case. Given the fact that the valve may appear almost normal in between the episodes, valve malfunction may be difficult to identify.[5,6] The absence of an audible click ,repeat trans thoracic echocardiographic interrogation of the valve during the episode of hemodynamic instability will help to make correct diagnosis. And obviously management will be surgical as per the correct diagnosis.

Conclusion

An intermittent non cyclic dysfunction may not be obvious at the time of clinical examination. So under these conditions and as TEE cannot be repeated promptly everytime, trans thoracic 2-D and Doppler echocardiography should be available at any time when symptoms develop. As this may be life threatening condition TTE is the method of choice for acute patient evaluation and urgent referral for surgical management is a rule.

Impact on daily practice: We must always suspect intermittent valve dysfunction in prosthetic valve with intermittent symptoms and normal baseline transthoracic echocardiography.

References

1.Wei-Guo Ma, Bin Hou, Adiljan Abdurusul, Ding-Xu Gong, Yue Tang, Qian Chang, Jian-Ping Xu, Han-Song Sun. Dysfunction of mechanical heart valve prosthesis: experience with surgical management in 48 patients. *Journal of Thoracic Disease*. 2015;7(12):2321-2329. doi:10.3978/j.issn.2072-1439.2015.12.25.

2. Aoyagi S, Nishimi M, Tayama E, Fukunaga S, Hayashida N, Akashi H, Kawara T. Obstruction of St Jude medical valves in the aortic position: a consideration for pathogenic mechanism of prosthetic valve obstruction. Cardiovasc Surg 2002;10:339–44.

3. Toma´s Francisco Cianciulli, Marı´a Cristina Saccheri, Jorge Alberto Lax. Intermittent acute aortic regurgitation of a mechanical bileaflet aortic valve prosthesis: diagnosis and clinical implications. European Journal of Echocardiography (2009) 10, 446–449

4. Lengyel M, Vandor L. The role of thrombolysis in the management of leftsided prosthetic valve thrombosis: study of 85 cases diagnosed by transesophageal echocardiography. J Heart Valve Dis 2001;10:636–49.

5. Karagiannis SE, Karatasakis G, Spargias K, Louka L, Poldermans D, Cokkinos DV. Intermittent acute aortic valve regurgitation: a case report of a prosthetic valve dysfunction. Eur J Echocardiogr 2008;9:291-3.

6. Giroux SK, Labinaz MX, Grisoli D, Klug AP, Veinot JP, Burwash IG. Intermittent, noncyclic dysfunction of a mechanical aortic prosthesis by pannus formation. J Am Soc Echocardiogr 2010;23:107.e1-3.

Figure Legend

Fig 1a: TTE Doppler with high gradients during episode

Fig 1b: Intraoperative TEE with high gradients

Fig 2 a: Intraoperative valve with pannus,

Fig 2b: Explanted Valve with pannus

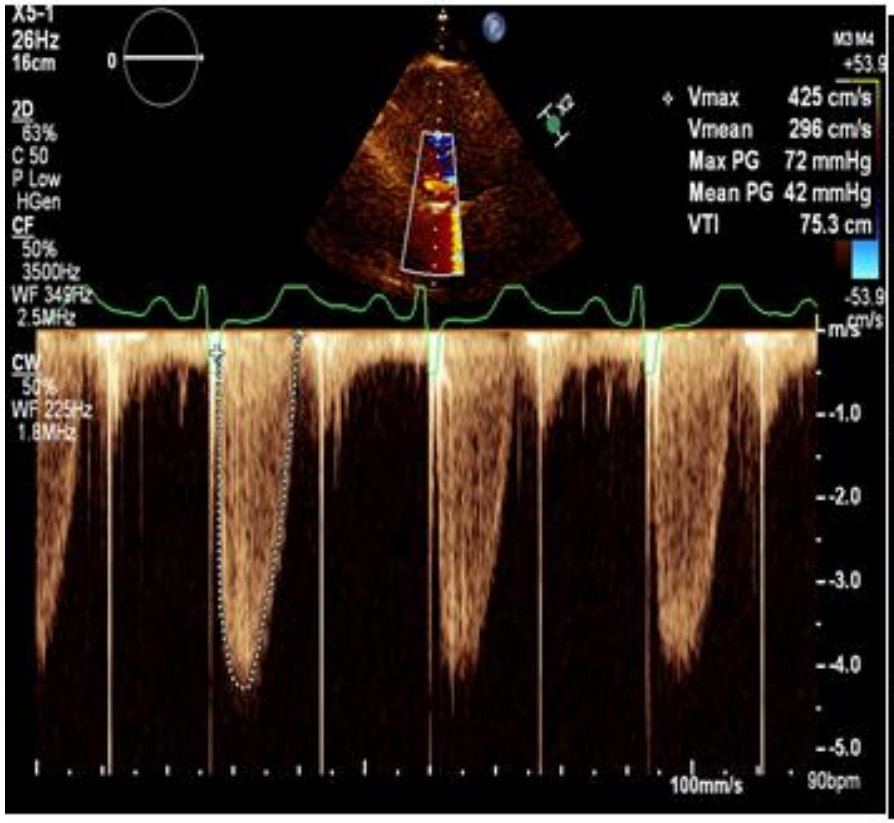

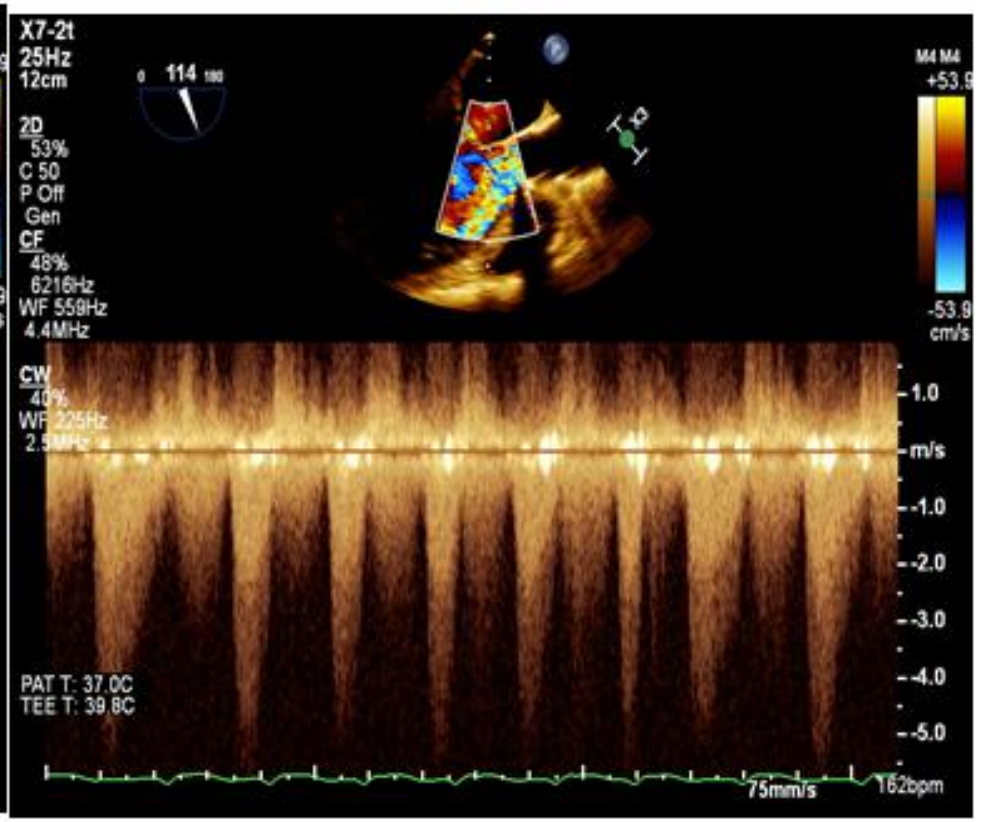

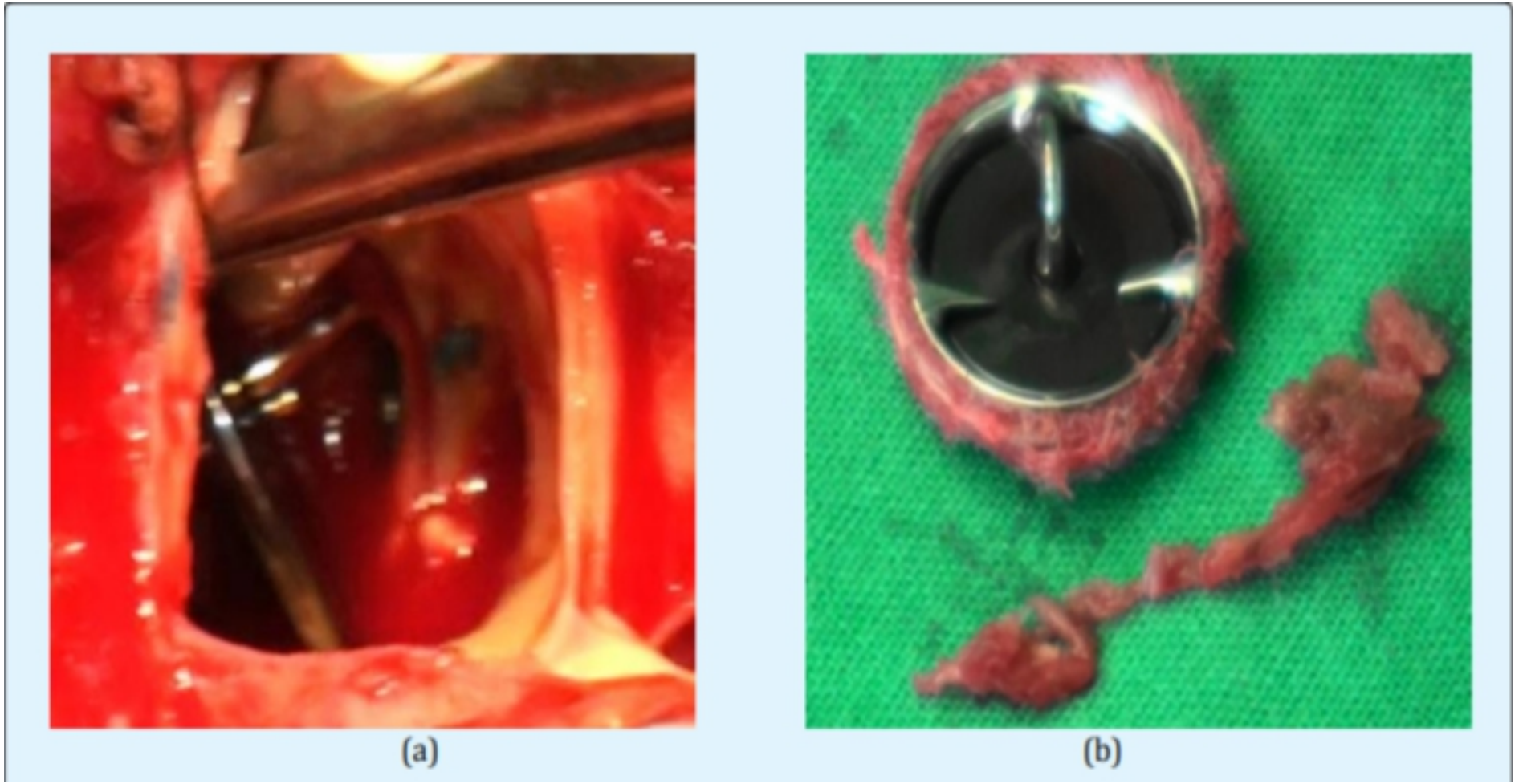

(a) (b)

AsiaIntervention
Official Journal of the Asian Pacific Society of Interventional Cardiology
(APSIC) and the Interventional Cardiology Foundation of India (ICFI)
www.asiaintervention.org

Title: Jailed Balloons For Side Branch Protection- A Review Of Techniques and Literature.

Authors: Bilal Kabeer Khan, MBBS, FCPS; Muhammad Nasir Rahman, MBBS, FCPS, FCPS; Javed Majid Tai, MBBS, FCPS, FCPS; Osman Faheem, M.D, FACC

Manuscript number: AIJ-D-19-00025

Manuscript submission date: 4 July 2019

Revisions received: 20 February 2020, 16 May 2020

Accepted date: 10 July 2020

TITLE

"Jailed Balloons For Side Branch Protection- A Review Of Techniques and Literature"

SHORT TITLE

"Jailed Balloons For Side Branch Protection"

Bilal Kabeer Khan[1], MBBS, FCPS, Muhammad Nasir Rahman[1], MBBS, FCPS, FCPS, Javed Majid Tai[1], MBBS, FCPS, FCPS, Osman Faheem[1], MD, FACC

1. Department of Medicine, Aga Khan University Hospital, Stadium road, Karachi

Conflict of interest statement: The authors have no conflicts of interest to declare

Narrative Abstract

Coronary bifurcation lesionsare commonly encountered and side branch compromise is a major complication of these bifurcation interventions. Jailing a wire in the side branch is the most common method of significant side branch protection. Jailing a balloon in the side branch is a less well known and seldom practiced strategy of side branch preservation but tends to have lower occlusion rates as compared to conventional jailed wires. Various modifications have been applied to the original jailed balloon techniquein an attempt to further improve side branch patency. Complications arising from this technique have been limited to case reports only and relates mainly to calcified vessels.

Classification: Bifurcation, Other technique, Drug-eluting stent

Abbreviations

BSKT	balloon stent kissing technique
IVUS	intravascular ultrasound
JBT	jailed balloon technique
JWT	jailed wire technique
LAD	left anterior descending artery
Diag	diagonal artery
LCx	left circumflex artery
OM	obtuse marginal artery
MB	main branch
MV	main vessel
ODFI	optical domain frequency imaging
POT	proximal optimization technique
RI	ramus intermedius
SB	side branch
TAP	T-stenting and protrusion
TLR	target lesion revascularization

Introduction

Coronary bifurcation lesions represent a challenge to the interventional cardiologist and account for up to 20 % of all lesions encountered in clinical practice and side branch compromise is a major complication of stenting these bifurcation lesions(1). Although; the subject of a lot of investigation, provisional stenting has beenproven to superior to a two stent strategy in terms of long term outcomes (2,3). Till now, a two stent strategy has been shown to be superior in complex left main lesions only (4) . The most commonly employed strategy to protect a significant side branch during provisional stenting is to jail a coronary wire in the SB which maintains side branch patency, modifies side branch angle and acts as a marker for rewiring (5,6).In the multicenter TULIPE study, absence of a jailed wire resulted in higher rates of target lesion revascularization but despite these measures the CACTUS study still reported an inability to salvage the side branch in 1.1% of cases (7,8). In an attempt to develop a superior side branch protection strategy, Burzotta,et al.in 2010; published their bench test report and first clinical experience on 'jailed balloon protection'. They proposed it as a novel technique to preserve side branch (SB) patency during provisional main vessel (MV) stenting in cases where there is a high risk of side branch compromise(9). For this article we have reviewed 107 papers that were identified through a Pub med search.

Classification of bifurcation lesions and bifurcation stenting techniques:

Numerous classifications of bifurcation lesions have been proposed; however, the European Bifurcation Club consensus document promotes a simplified classification, the Medina classification. In the Medina classification, any lesion greater 50% is considered significant. Significant lesions are denoted by "1" and insignificant lesions by "0". Lesions

are recorded in the following order: proximal main vessel, distal main vessel and side branch, These figures are separated by commas. The consensus document also endorses the MADS classification for bifurcation stenting techniques which takes into account the position of stents in the bifurcation and the order in which stenting is performed. In this classification, four distinct strategies have been described. Each of this strategy is represented by an acronym; "M" for main vessel first, "A" for main vessel across side branch first, "D" for distal vessel first and "S" for side branch first (10,11,12).

The "Conventional" Jailed Balloon Technique (JBT) :

In the original JBT (figure 1A-G) a stent was positioned in the main branch (MB) and a long semi-compliant balloon; with proximal marker extending beyond proximal marker of stent, was positioned in the side branch (SB). MB stent was deployed and SB assessed angiographically. If SB was not occluded then SB balloon was withdrawn followed by proximal optimization of stent with a short balloon. SB was subsequently rewired and kissing balloon inflation performed. In case SB was occluded then jailed balloon was inflated resulting in stent distortion and restoration of flow. The remaining steps were the same as previous including proximal optimization (POT), side branch rewiring and final kissing balloon inflation A greater occupancy of the SB ostium is proposed to ensure better side branch patency. Resistance during balloon withdrawal was deemed equivalent to that encountered during jailed wire removal and in case of more than usual resistance a low pressure inflation was recommended rather than application of force. No major MB stent mal-apposition was observed (9).

One drawback of the procedure is that it becomes quite complex when a SB gets occluded (figure 2A-H); although this happened in only a single instance. In this case the SB balloon

has to be deployed but for it to be deployed, another balloon has to be positioned in the MB to immediately correct stent distortion that results after SB balloon deployment; which would definitely make rewiring challenging if any residual distortion remains. In an attempt to correct distortion, vascular injury and edge dissections are possible. In case stenting of side branch is required, an inverted "provisional crush" technique was recommended; but it would be difficult to track a stent through MB stent with any degree of residual distortion.

"Simplified" Jailed Balloon Technique :

Singh, et al. published an independently developed simplified JBT in 2012. In this technique (figure 3) both MB and SB were wired followed by pre-dilatation of MB with semi-compliant balloon. Stent placement in MB and long semi-compliant balloon placement in SB was followedby stent deployment. If SB was patent then SB balloon was inflated at low pressures (less than 3 atmospheres), deflated and subsequently removed along with SB wire. However, if side branch was compromised; a routine balloon angioplasty was performed restoring SB flow but causing mal-apposition of MB stent. In this technique rather than using a short balloon to optimize the stent, the stent balloon itself was used to optimize stent apposition by inflation to supra-nominal pressures. No kissing balloon inflation was performed. Out of a total of 102 patients who underwent percutaneous coronary intervention using this technique, only 9 side branches had to be re-crossed with wires and only 2 required stenting (13).

This technique appears simpler, but at the same time, the use of a compliant stent balloon for proximal optimization needs to be questioned. The variable expansion profile of

compliant balloons can result in edge dissection and stent under expansion. Also, routine low pressure balloon inflation in the absence of any side branch compromise may be unnecessary. Intra-vascular ultrasound (IVUS) was performed in 74% patients (at operator's discretion) and on the basis of this 41% of lesions required further intervention. This is quite intriguing and underscores the importance of incorporating intravascular imaging while performing jailed balloon techniques. It also raises questions whether a suboptimal intervention may be performed when JBT are used without intravascular imaging. It should also be mentioned that left main bifurcation lesions were excluded.

Jailed Semi-inflated Balloon Technique:

Although results of the simplified JBT were promising, it did not completely prevent side branch occlusion (7). A further modification of this technique known as jailed semi-inflated balloon technique has been proposed to further improve side branch patency (figure 4A-C). This technique follows the same basic principles as the simplified JBT with respect to balloon length and positioning; however, the side branch balloon (sized 1:1 as per SB diameter) is simultaneously inflated at low pressures (3 atm) during MB stent deployment. As the MB stent is deployed, the proximal segment of the SB balloon is compressed and distal part is overinflated to completely occupy side branch ostium and prevent plaque shift. Final POT is performed with a short non-compliant balloon (14).

Despite a theoretical risk of balloon entrapment due to loss of profile, no cases of entrapment were encountered. Another point of concern is trauma to SB ostia from the semi-inflated balloon. This concern was shared by the authors of Jailed Semi-inflated balloon technique themselves and they proposed that SB balloon could be slightly undersized. IVUS was performed in 25% patients only and only 19% patients were found

to have mal-apposed stents. Better results on IVUS as compared to Simplified JBT could due to the use of non-compliant balloon for POT.

Ermiş et al. published their experience with this technique. Out of 82 bifurcation lesions in 64 patients (60.9% of whom had presented with acute coronary syndrome), only 5 cases of SB occlusion were reported that required intervention. Interestingly, the SB balloon was inflated to higher pressures than usual (4.8±2.0 atm) (15).

"Modified" Jailed Balloon Technique andBalloon Stent Kissing Technique:

Modified JBT is a technique that has been studied only recently; the proximal marker of the SB balloon is positioned so that it touches the MB stent (Figure 5A-C). In all other JBT the proximal marker is placed proximal to MB stent. The SB balloon diameter was selected as half of the MB stent diameter if it did not exceed SB diameter. Both balloons were then deployedsimultaneously, withdrawn and wires crossed. Final Kissing balloon inflation was performed at operator's discretion and if SB required stenting, a T-stenting and Protrusion (TAP) technique was employed (figure 5). Saito S and colleagues carried outin vitro testing with optical domain frequency imaging (OFDI) was used to determine "eccentrity index" (ratio between maximum and minimum stent diameters in main branch) and was found to be greater with conventional JBT as compared to modified JBT in proximal segment of bifurcation. No difference in eccentrity index was observed in distal segment of bifurcation. Out of 254 bifurcation lesions that were intervened by this method, 253 (99.6%) side branches showed post intervention TIMI III flow (16).

A recently published study which included 9 month follow up of patients managed with this technique; reported no adverse outcomes at 9 months. However, this study did not compare outcomes with any other technique and had a smaller sample size (17).

The “Balloon Stent Kissing Technique” technique varies slightly from modified jailed balloon technique as the balloon is placed slightly more proximally but not proximal to stent. Cohort analysis of thistechnique showed superior immediate results as compared to provisional stenting in terms of side branch patency and TIMI flow but no difference in outcomes was observed at 12 months follow up. Only true bifurcation lesions were included and complex bifurcations were excluded. Despite a theoretical risk, no cases of balloon entrapment or damage were reported with either technique(16, 18).

Jailed Stent Balloon Technique :

The jailed stent balloon technique is a dedicated two stent strategy recently published by Shpigel A, et al. It involves balloon angioplasty of both MB and SB lesions followed by stenting of the side branch first. The SB stent balloon is partially withdrawn and MB stent is deployed. This is followed by sequential redeployment of SB and then MB stent balloons to correct any deformities. Final rewiring with kissing balloon dilatation or proximal optimization (POT) is optional (figure 6A-F). Procedural success was observed in 100% of the 34 patients treated. At 2 year follow up only one patient required target lesion revascularization (TLR) and TLR/ binary stenosis occurred in 3 patients (18).

This method quotes a high success rate but the need to jail a balloon in the SB is unclear; if a stent has already been properly deployed to cover the ostium of the SB. Jailing, a stent balloon between two layers of stents also poses significant risk of entrapment.

Jailed Balloon and Corsair Trifurcation technique:

Limited to case reports, this technique integrates the jailed semi-inflated balloon technique with the “Jailed Corsair Technique” that was published in a 2017 case report by Numusawa and colleagues (20). Munakata M, et al. reported a left main trifurcation lesion (modified

Medina classification 1-1-1-0) managed with this technique. They employed a cross-stenting strategy from the left main coronary artery (LMCA) into the left anterior descending artery (LAD) while at the same time positioned a semi-inflated (3 atm) balloon in ramus intermedius (RI) and a corsair micro-catheter in left circumflex (LCx) artery. Stent was deployed jailing both balloon and micro-catheter, which were withdrawn post stent deployment. This was followed by rewiring of both RI and LCX. Kissing balloon dilatation was performed in both LAD and RI followed by LAD and LCX (21).

In our opinion, all of the jailed balloon techniques can be incorporated into a trifurcation strategy. Jailing a second device; in this case,a micro-catheter, increases the complexity of the procedure, chances of device entrapment and stent deformity. Another possibility that should be considered is inter-twining of coronary wire of the jailed balloon and micro-catheter around each other which could cause difficulty in device withdrawal.

Complications

The most dreaded complication of this technique is entrapment of the jailed balloon. This has been reported in case reports in calcified lesions despite plaque modification with rotational atherectomy. The jailed balloon was eventually withdrawn in these cases with manual traction causing deformation of stent in one case requiring correction with proximal optimization. Another significant area of concern identified by one of the case reports was that repeated balloon inflation and deflation to rescue the trapped balloon itself will cause loss of balloon profile and this loss of balloon profile may further hinder balloon withdrawal (22, 23). Although these complications are limited to case reports only and successfully managed on each occasion, inability to retrieve a balloon would be

catastrophic and surely lead to emergent surgery. Moreover, in comparison a trapped wire will definitely be easier to release and retrieve than a trapped balloon.

Discussion

The effectiveness of the JBT was demonstrated in a recent publication by Omori H. et al. where a pressure wire assessment of JBT efficacy was performed. The Pd/Pa in the SB immediately after stenting was 0.34, which increased to 0.60 after balloon removal. Although still suboptimal, it showed that a jailed balloon can secure lumen patency in the jailed SB (24).

We have summarized literature from some of the major trials on jailed balloon techniques in tables 1, 2 and 3. In terms of patient characteristics, most patients enrolled were hypertensive, non-diabetic males in their 60s and 70s without prior coronary intervention except in modified JBT trial where half of the patients had undergone prior coronary intervention. The modified JBT and BSKT group of patients also differed from the others in the fact that majority of the patients enrolled were diagnosed with stable angina whereas the other trials had enrolled predominantly acute coronary syndrome patients (table 1).The majority of the lesions intervened were LAD/Diagonal bifurcations. LM lesions had been excluded in the simplified JBT and BSKT trials. Most of the lesions intervened were classified as Medina 1,1,1. The procedure was performed predominantly with a 6Fr. Guide catheter and through a trans-radial access. A variety of stent platforms were used and had similar outcomes (table 2). IVUS when performed showed less well apposed stents with simplified JBT which may be due to the use of compliant stent balloon for optimization. The jailed semi-inflated balloon technique reported significantly more well apposed stents as it involved POT with a non-compliant balloon. In both these studies only two edge dissections

were reported. Although it would have been interesting to compare procedural times between the different techniques and to traditional wire trapping; only Cayli, et al. measured procedural times and they were reported as 16.3±4.8 minutes. Procedural success rates were 100% and only one side branch was lost with the simplified JBT. No cases of balloon damage or entrapment were reported. The role of intravascular imaging with jailed balloon techniques need to be stressed. Mal-apposition that may or may not be related to balloon jailing can be effectively identified and corrected along with any edge dissections. Table 3 summarizes these outcomes and Intravascular imaging findings (9,13,14,16,118) .It is important to highlight here that the main limitation of these techniques is the limited data. Direct comparison between various jailed balloon techniques, is not possible and in our review of literature no studies in this regard have been performed to date. However, we found 2 studies that had compared the jailed wire technique (JWT) with JBT. The first is a randomized control trial from china where 192 consecutive patient were randomized to JBT or JWT and immediate post procedural outcomes were studied. Only patients with Medina 1,1,1 lesions were enrolled. In this study SB TIMI III flow was achieved less in patients who underwent JWT vs JBT (74.6%vs.93.2%,P=0.001). Patients undergoing JWT also experienced more peri-procedural MI (11.9%vs.2.7%,P=0.008) and more SB occlusion (18.6%vs.5.4%,P=0.009). No device related complication was reported in the study (25). Results from a prospective double blinded randomized control trial involving patients with true bifurcation lesions (Medina classification 1.1.1, 1.0.1, or 0.1.1)showed lower incidence of perioperative MACE with BSKT vs. JWT (0% vs 13.6%, P=< .05). The incidence of MACE, angina and heart failure was similar on median follow up of 19.0±6.1 months. There was no difference in survival between the two groups at 24 months (BSKT 97.7%vs JWT 91.1%, P = .18). Although these

results are promising, but they may not be easily replicated. The data is limited to single centers; where the procedure would have been performed by operators who specialized in JBT (26). To show superiority, adequately powered studies with a control arm, intravascular imaging and medium to long term follow-up would be required. Thus, although the authors do not recommend the routine use of JBT in the absence of any robust data proving superiority over the JWT, there may be a potential role in selected patients.

Conclusion

Jailed balloon technique appears safe and effective at side branch preservation. However, most operators have limited to no experience of the technique. Current data is limited, single centered and in the absence of head to head trials; offers no definitive advantage over the jailed wire technique. Multi-centered randomized studies are required to directly compare the various jailed balloon techniques with each other and with the JWT.

Funding: None

Conflicts of Interest: None

References:

1. Collins N, Seidelin PH, Daly P, Ivanov J, Barolet A, Mackie K, Bui S, Schwartz L, Džavík V. Long-term outcomes after percutaneous coronary intervention of bifurcation narrowings. The American journal of cardiology. 2008 Aug 15;102(4):404-10.
2. Steigen T, Holm N, Kumsars I, Niemela M, James S, Erglis A, Kervinen K, Jensen JS, Galloe AM, Wiseth R, Gunnes P. TCT-318 Ten-year All-cause Mortality after Simple versus Complex Stenting of Coronary Artery Bifurcation Lesions in the Randomized Nordic Bifurcation Study. Journal of the American College of Cardiology. 2016 Nov 1;68(18 Supplement):B131-2.
3. Généreux P, Kumsars I, Lesiak M, Kini A, Fontos G, Slagboom T, UngiI, Metzger DC, Wykrzykowska JJ, Stella PR, Bartorelli AL. A randomized trial of a dedicated bifurcation stent versus provisional stenting in the treatment of coronary bifurcation lesions.Journal of the American College of Cardiology. 2015 Feb 17;65(6):533-43.
4. Chen SL, Zhang JJ, Han Y, Kan J, Chen L, Qiu C, Jiang T, Tao L, Zeng H, Li L, Xia Y. Double kissing crush versus provisional stenting for left main distal bifurcation lesions: DKCRUSH-V randomized trial. Journal of the American College of Cardiology. 2017 Nov 20;70(21):2605-17.
5. Louvard Y, Lefèvre T, Cherukupalli R, Tavolaro O, Loubeyre C, Dumas P, Morice MC. Favorable effect of the" jailed wire" technique when stenting bifurcation lesions. InAMERICAN JOURNAL OF CARDIOLOGY 2003 Sep 15 (Vol. 92, No. 6 A, pp. 62L-63L). 650 AVENUE OF THE AMERICAS, NEW YORK, NY 10011 USA: EXCERPTA MEDICA INC.

6. Louvard Y, Sashikand G, Lefèvre T, Garot P, Darremont O, Brunel P. Angiographic predictors of side branch occlusion during the treatment of bifurcation lesions. CathCardiovasc Int. 2005 (Abstr.Supp.)
7. Brunel P, Lefevre T, Darremont O, louvard Y. Provisional T-stenting and kissing balloon in the treatment of coronary bifurcation lesions: Results of the French multicenter "TULIPE" study. Catheterization and cardiovascular interventions. 2006 Jul;68(1):67-73.
8. Colombo A, Latib A, Airoldi F, Bramucci E, Saccà S, Violini R, Lettieri C, Zanini R, Sheiban I, Paloscia L, Grube E. Response to Letter Regarding Article,"Randomized Study of the Crush Technique Versus Provisional Side-Branch Stenting in True Coronary Bifurcations: The CACTUS (Coronary Bifurcations: Application of the Crushing Technique Using Sirolimus-Eluting Stents) Study". Circulation. 2009 Aug 25;120(8):e64-.
9. Burzotta F, Trani C, Sianos G. Jailed balloon protection: a new technique to avoid acute side-branch occlusion during provisional stenting of bifurcated lesions. Bench test report and first clinical experience.EuroIntervention: journal of EuroPCR in collaboration with the Working Group on Interventional Cardiology of the European Society of Cardiology. 2010 Feb;5(7):809-13.
10. Lassen JF, Holm NR, Banning A, Burzotta F, Lefèvre T, Chieffo A, Hildick-Smith D, Louvard Y, Stankovic G. Percutaneous coronary intervention for coronary bifurcation disease: 11th consensus document from the European Bifurcation Club. EuroIntervention. 2016 May 1;12(1):38-46.
11. Medina A, Suárez DL, Pan M. A new classification of coronary bifurcation lesions. Revista espanola de cardiologia. 2006 Feb;59(2):183.

12. Louvard Y, Thomas M, Dzavik V, Hildick-Smith D, Galassi AR, Pan M, Burzotta F, Zelizko M, Dudek D, Ludman P, Sheiban I. Classification of coronary artery bifurcation lesions and treatments: time for a consensus!. Catheterization and Cardiovascular Interventions. 2008 Feb 1;71(2):175-83.
13. Singh J, Patel Y, Depta JP, Mathews SJ, Cyrus T, Zajarias A, Kurz HI, Lasala JM, Bach RG. A Modified Provisional Stenting Approach to Coronary Bifurcation Lesions: Clinical Application of the "Jailed-Balloon Technique".Journal of interventional cardiology. 2012 Jun;25(3):289-96.
14. Çaylı M, Şeker T, Gür M, Elbasan Z, Şahin DY, Elbey MA, Çil H. A Novel-Modified Provisional Bifurcation Stenting Technique: Jailed Semi-Inflated Balloon Technique.Journal of interventional cardiology. 2015 Oct;28(5):420-9.
15. Ermiş E, Uçar H, Demirelli S, İpek E, Gür M, Çaylı M. Assessment of side branch patency using a jailed semi-inflated balloon technique with coronary bifurcation lesions. Turk KardiyolDernArs. 2018 Jul 1;46(5):340-8.
16. Saito S, Shishido K, Moriyama N, Ochiai T, Mizuno S, Yamanaka F, Sugitatsu K, Tobita K, Matsumi J, Tanaka Y, Murakami M. Modified jailed balloon technique for bifurcation lesions. Catheterization and Cardiovascular Interventions. 2018 Sep 1;92(3):E218-26.
17. Zhang W, Ji F, Yu X, Wang X. Long-term treatment effect and adverse events of a modified jailed-balloon technique for side branch protection in patients with coronary bifurcation lesions. BMC cardiovascular disorders. 2019 Dec;19(1):12.
18. Wenbo QU, Li X, Liu B. GW29-e1527" Balloon-stent kissing" technique avoid side-branch compromise for simple true bifurcation lesions. Journal of the American College of Cardiology. 2018 Oct 16;72(16 Supplement):C130.

19. Shpigel A, Sintek M, Singh J. THE JAILED STENT BALLOON TECHNIQUE: A NOVEL CORONARY BIFURCATION TECHNIQUE. Journal of the American College of Cardiology. 2018 Mar 12;71(11):A1364.
20. Numasawa Y, Sakakura K, Yamamoto K, Yamamoto S, Taniguchi Y, Fujita H, Momomura SI. A novel side branch protection technique in coronary stent implantation: jailed Corsair technique. Cardiovascular Revascularization Medicine. 2017 Jun 1;18(4):295-8.
21. Munakata M, Numasawa Y, Ishikawa S, Koyama T. A Novel Double Side Branch Protection Technique for a Left Main Trifurcation Lesion: Simultaneous Jailed Balloon and Jailed Corsair Technique. Case reports in cardiology. 2018;2018.
22. Noda T. TCTAP C-042 Entrapment of Balloon in Bifurcation Lesion PCI with Jailed Balloon Technique.Journal of the American College of Cardiology. 2018 Apr 24;71(16):S110.
23. Numasawa Y, Hitomi Y, Imaeda S, Yokokura S, Tanaka M, Tabei R, Kodaira M. Stent deformation caused by entrapment of the side branch balloon catheter during the jailed balloon protection technique for a calcified coronary bifurcation lesion: A case report and literature review. Cardiovascular Revascularization Medicine.2018 Nov 22.
24. Omori H, Kawase Y, Tanigaki T, Matsuo H. Pressure wire assessment of jailed balloon technique efficacy in a patient with complex bifurcated lesion. EuroIntervention: journal of EuroPCR in collaboration with the Working Group on Interventional Cardiology of the European Society of Cardiology. 2018 Jun 8;14(3):e316.

25. He P, Luo J, Gu M, Liu Y, Huang W, Tan N, Zhou Y, Chen J. Effect of jailed balloon technique on side branch protection in percutaneous coronary intervention for bifurcation lesions.South China Journal of Cardiology. 2013(3):1.
26. Jin Z, Song L, Zheng Z, Zhang S, Wang M. Balloon-stent kissing technique versus jailed wire technique for interventional treatment of coronary bifurcation lesions: Comparison of short-and long-term clinical outcomes. Medicine. 2019 May;98(20).

Figure Legends

Figure 1: Figure shows stepwise "conventional" jailed balloon technique if side branch is not compromised

Figure 2: Figure shows stepwise "conventional" jailed balloon technique if side branch is compromised

Figure 3: Figure shows steps of "simplified" jailed balloon technique with and without side branch compromise. Final proximal optimization is performed with stent balloon.

Figure 4: Figure shows jailed semi-inflated balloon technique. Side branch balloon is inflated at low pressures during stent deployment. Final proximal optimization is performed with short balloon.

Figure 5: Figure shows Modified jailed balloon technique. Side branch balloon is positioned so that it protrudes about 1 mm into main branch. If side branch is compromised a kissing balloon inflation or T-stenting and protrusion is performed.

Figure 6: Figure shows stepwise jailed stent balloon technique.

Table -1 Literature Review of Jailed Balloon Techniques- A Comparison of Clinical Characteristics

	Burzotta, et al.[9]	Singh, et al.[10]	Cayli, et al.[11]	Saito, et al.[13]	Wen-Bo Qu, et al.[15]
Technique	Conventional JBT	Simplified JBT	Jailed Semi inflated balloon	Modified Jailed Balloon Technique	Balloon Stent Kissing Technique
Total Patients	19	100	137	233	40
Age (n±SD/IQR)	69.0±7.3	63.1 ± 11.7	63.6± 11.7	71.5 ± 9.7	62 IQR 12
Females	7 (35%)	39 (39%)	33 (24.1%)	11 (18.3)	10 (25%)
Diabetes mellitus	8 (40%)	33 (33%)	54 (39.4%)	98 (42.1)	14 (35%)
Hypertension	-	88 (88%)	72 (52.6%)	181 (77.7%)	28 (70%)
Smoker	-	45 (45%)	52 (38.0%)	120 (51.5%)	15 (37.5%)
Dyslipidemia	-	84 (84%)	64 (46.7%)	186 (79.8%)	14 (35%)
Prior CAD	-	48 (48%)			
Prior coronary bypass graft	-	13 (13%)	19 (13.9%)	5 (2.1%)	1 (2.5%)
Prior PCI	-	13 (13%)	41 (29.9%)	114 (48.9%)	6 (15%)
Peripheral arterial disease	-	3 (7%)	-	-	-
Chronic kidney disease	-	7 (7%)	-	112 (48.1%)	1 (2.5%)
Stable angina	13 (65%)	17 (17%)	49 (35.8%)	197 (84.5%)	28 (70%)
Acute coronary syndrome	7 (35%)	68 (68%)	88 (64.2%)	36 (15.5%)	12 (30%)

Abbreviations: CAD= coronary artery disease, PCI- percutaneous coronary angioplasty, SD= standard deviation, IQR interquartile range

Table 2 Literature Review of Jailed Balloon Techniques- Angiographic and Lesion Characterisitics

	Burzotta, et al.[9]	Singh, et al.[10]	Cayli, et al.[11]	Saito, et al.[13]	Wen-Bo Qu, et al.[15]
Technique	Conventional JBT	Simplified JBT	Jailed Semi Inflated balloon	Modified JBT	BSKT
Left Main (n,%)	11 (55%)	Nil	28 (18.9%)	54 (21.3%)	Nil
LAD/ Diagonal (n,%)	7 (35%)	50 (49%)	85 (57.4%)	148 (58.3%)	27 (67.5%)
LCX/ OM (n,%)	2 (10%)	16 (16%)	26 (17.6%)	32 (12.6%)	2 (5.0%)
Medina 1,1,1 (n,%)	17 (85%)	93 (91%)	93 (62.8%)	53 (20.9%)	31 (77.5%)
Medina 0,1,1(n,%)	1 (10%)	2 (2%)	3 (2.0%)	68 (26.8%)	5 (12.5%)
Medina 1,0,1(n,%)	2 (10%)	1 (1%)	13 (8.8%)	33 (13.0%)	4 (10.0%)
Bifurcation angle (degree, n , %)	-	-	<70 102 (68.9)	<30 43 (16.9)	-
			70-90 25 (16.9)	30–60 97 (38.2)	
			>9021 (14.2)	>60 114 (44.9)	
Radial Cases(n,%)	12 (60%)	-	23 (16.8%)	213 (91.4%)	-
6 Fr.system (n,%)	20 (100%)	-	-	227 (89.4%)	-
Pre–dilation MV(n,%)	17 (85%)	-	81 (54.7%)	246 (96.9%)	-
Pre-dilation SB(n,%)	3 (15%)	-	22 (14.9%)	20 (7.9%)	-
MV stent					
BMS (n,%)	Nil	17 (17%)	Nil	Nil	Nil
Drug Eluting Stent					
Sirolimus(n,%)	1 (5%)	17 (17%)	Nil	-	-
Everolimus(n,%)	7 (35%)	53 (52%)	32 (21.6%)	125 (49.2%)	
Paclitaxel(n,%)	3 (15%)	5 (5%)	Nil	-	-
Zotarolimus(n,%)	6 (30%)	11 (11%)	35 (23.7%)	37 (14.6%)	-
Biolimus(n,%)	3 (15%)	Nil	81 (54.7%)	3 (1.2%)	-
Ultimaster(n,%)	Nil	Nil	Nil	64 (25.2%)	-
Synergy(n,%)	Nil	Nil	Nil	25 (9.8%)	-
MV stent diameter (mm± SD)	3.5±0.5	-	2.9±0.3	3.2 ± 0.4	-
MV stent length (mm± SD)	22.6±5.2	-	24.0.±6.8	24.4 ± 6.7	-
POT (n,%)	10 (50%)	Nil	137 (100%)	40 (100%)	
KBI (n,%)	20 (100%)	7 (7%) as rescue	3 (2.0 %) – Final Kissing Balloon	183 (72.1%)	7 (17.5%) as rescue
SB Stenting (n,%)	10 (53%)	2 (2%)	3 (2.0%)	31 (12.2%)	0 (0%)
SB stent diameter (mm± SD)	3.2±0.4	-	-	2.6 ± 0.3	-
SB stent length (mm± SD)	16.6±5.4	-	-	15.4 ± 7.0	-

Abbreviations :BMS = bare metal stent, KBI= kissing balloon inflation,LAD= Left anterior descending artery, LCx= Left circumflex artery, MV= main vessel, OM= obtuse marginal artery, POT= proximal optimization technique, SB= Side branch, SD = standard deviation

Table 3- Literature Review of Jailed Balloon Techniques- Intracoronary Imaging and Outcomes					
	Burzotta, et al.[9]	Singh, et al.[10]	Cayli, et al.[11]	Saito, et al.[13]	Wen-Bo Qu, et al.[15]
Technique	Conventional JBT	Simplified JBT	Jailed Semi inflated balloon	Modified Jailed Balloon Technique	Balloon Stent Kissing Technique
Intracoronary Imaging (n,%)	No	IVUS 75 (74%)	IVUS 37 (25%)	IVUS234 (92.1) OCT 12 4.7) OFDI2 (0.8)	No
Well-apposed stent without complication(n,%)	-	44 (59%)	29 (78.4%)	-	-
Stent underexpansion(n,%)	-	23 (31%)	6 (16.2%)	-	-
Edge dissection (n,%)	-	2 (3%)	2 (5.4%) Proximal	-	-
Stent fracture (n,%)	-	0 (0%)	0 (0%)	-	-
Stent struts distortion(n,%)	-	1 (1%)	0 (0%)	-	-
IVUS finding prompting further intervention(n,%)	-	31 (41%)	-	-	-
Plaque shift(n,%)	-	4 (5%)	-	-	-
Malapposition(n,%)	-	1 (1%)	-	-	-
Procedure Time(minutes)	-	-	16.3±4.8	-	-
Outcomes	-	-	-	-	-
Procedural success (n,%)	20 (100%)	102 (100%)	148 (100 %)	254 (100 %)	40 (100 %)
TIMI 3 flow after procedure(n,%)	-	MV 102 (100%) SB101 (99%)	MV 148(100%) SB148 (100%)	MV 253 (99.6)	MV 40 (100%) SB 37 (92.5%)
PeriproceduralMI(n,%)	-	1 (1%)	0 (0%)	0 (0%)	-
Dissection - Edge (n,%)	-	4 (4%)	7 (4.8%)	-	-
Dissection- Side branch(n,%)	-	-	4 (2.7)	-	-
Side branch loss (n,%)	0 (0%)	1 (1%)	0 (0%)	0 (0%)	-
Jailed-balloon or wire entrapment(n,%)	0 (0%)	0 (0%)	0 (0%)	0 (0%)	0 (0%)

Jailed-balloon rupture (n,%)	0 (0%)	0 (0%)	0 (0%)	0 (0%)	0 (0%)

Abbreviations: MV= main vessel, OCT= Optical coherence tomography, SB= Side branch, OFDI= optical frequency domain imaging

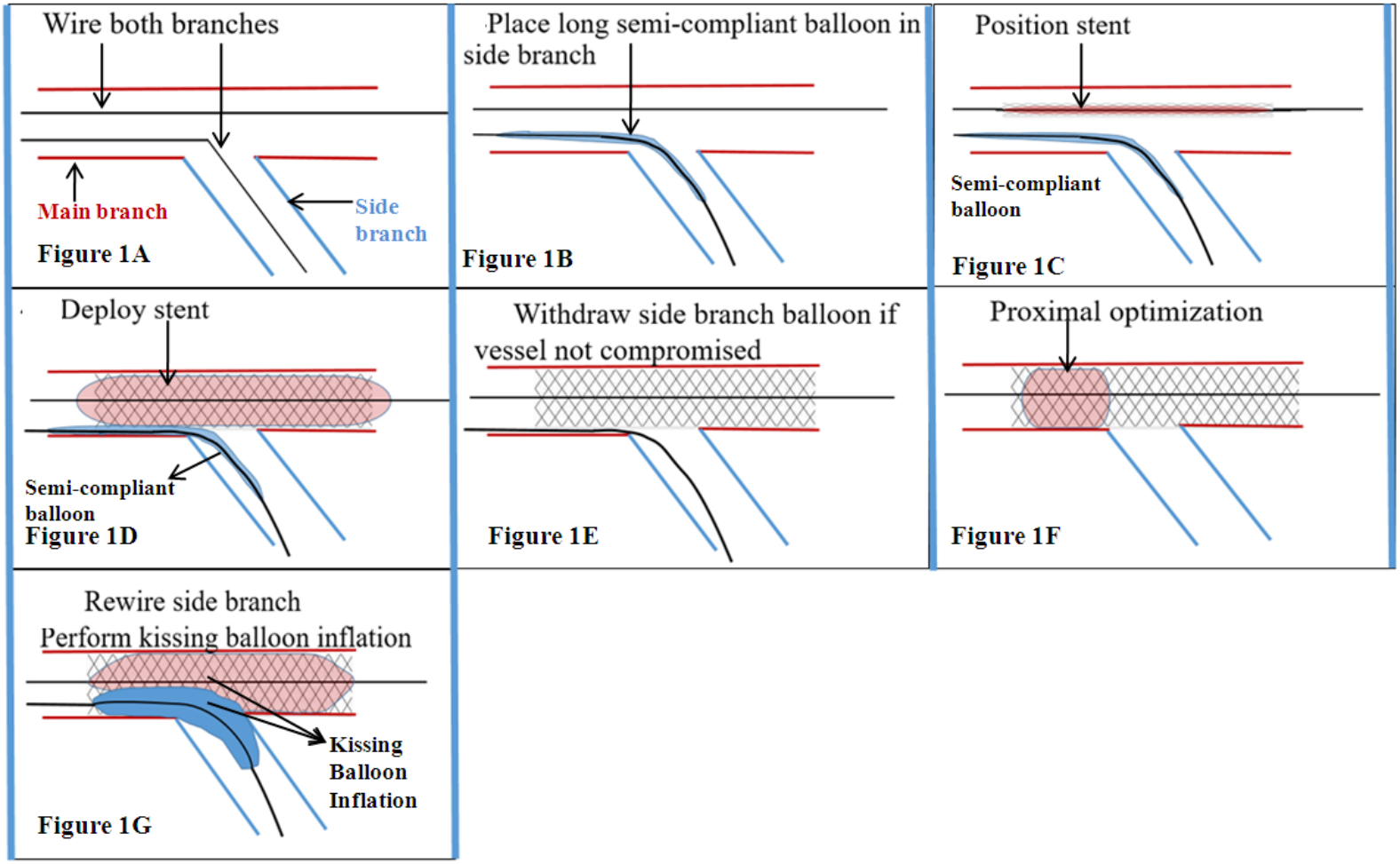

Figure 1A-G Step-wise "Conventional" Jailed Balloon Technique without side branch compromise

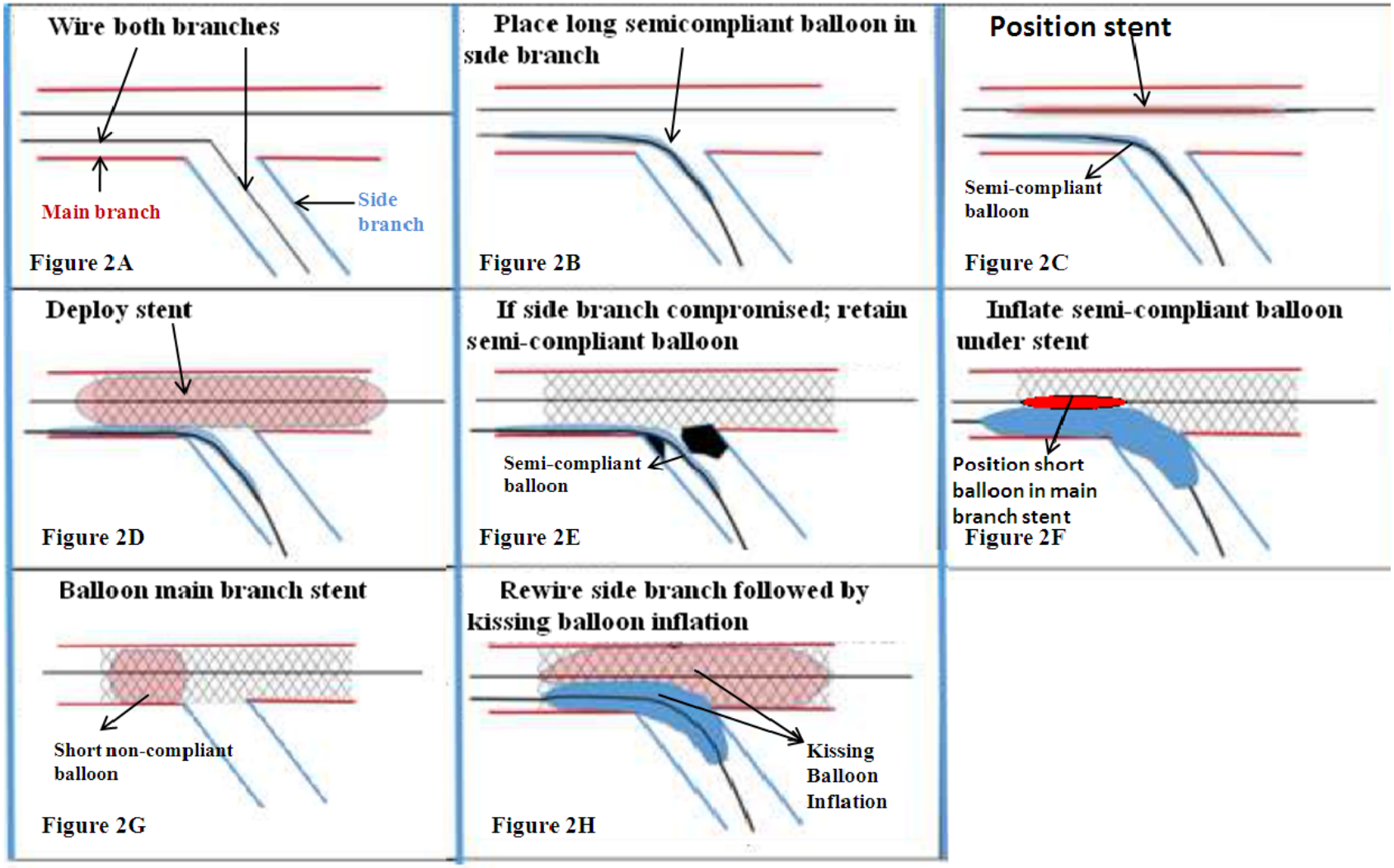

Figure 2A-H Step-wise "Conventional" Jailed Balloon Technique with side branch compromise

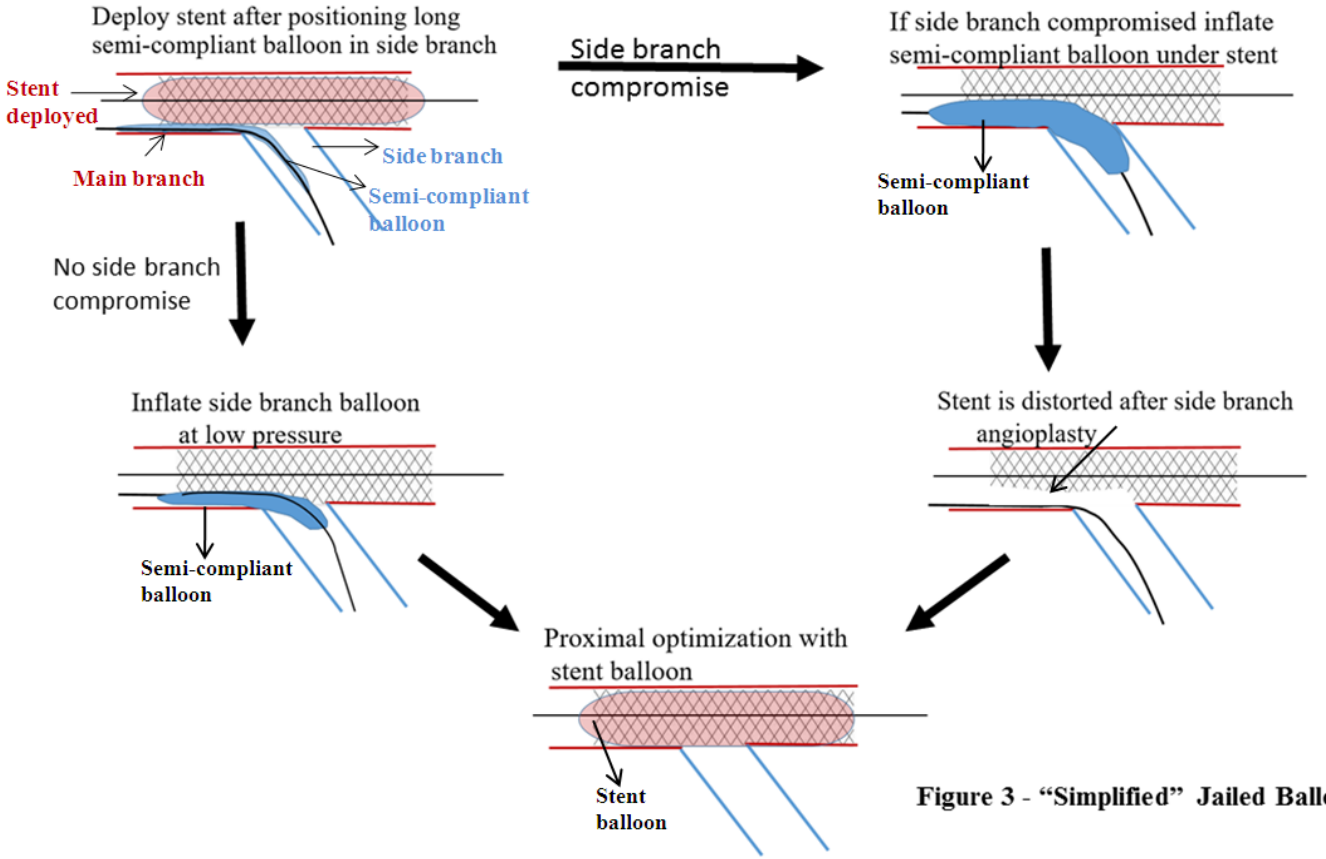

Figure 3 - "Simplified" Jailed BalloonTechnique

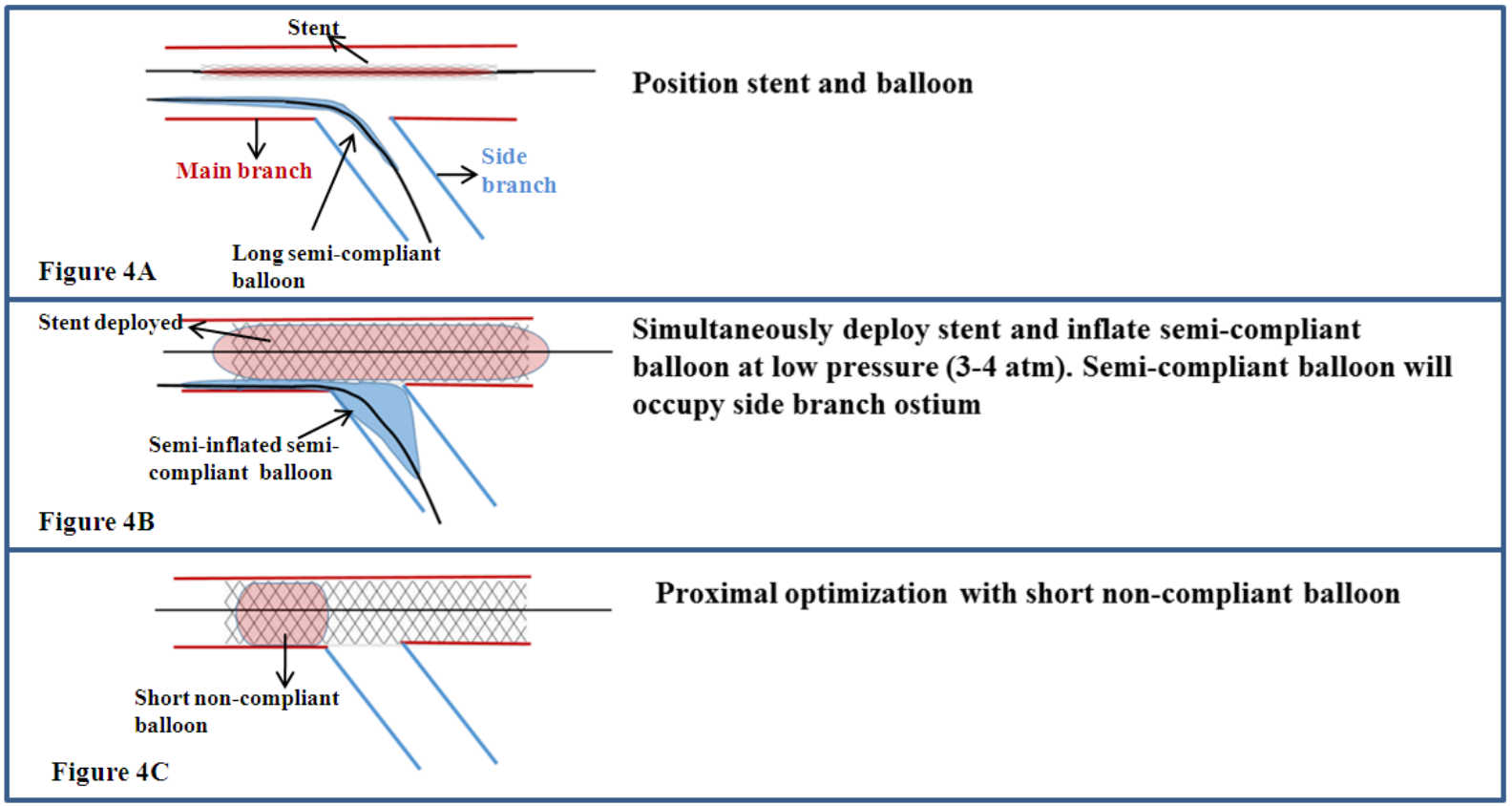

Figure 4A-C Jailed Semi-Inflated Balloon Technique

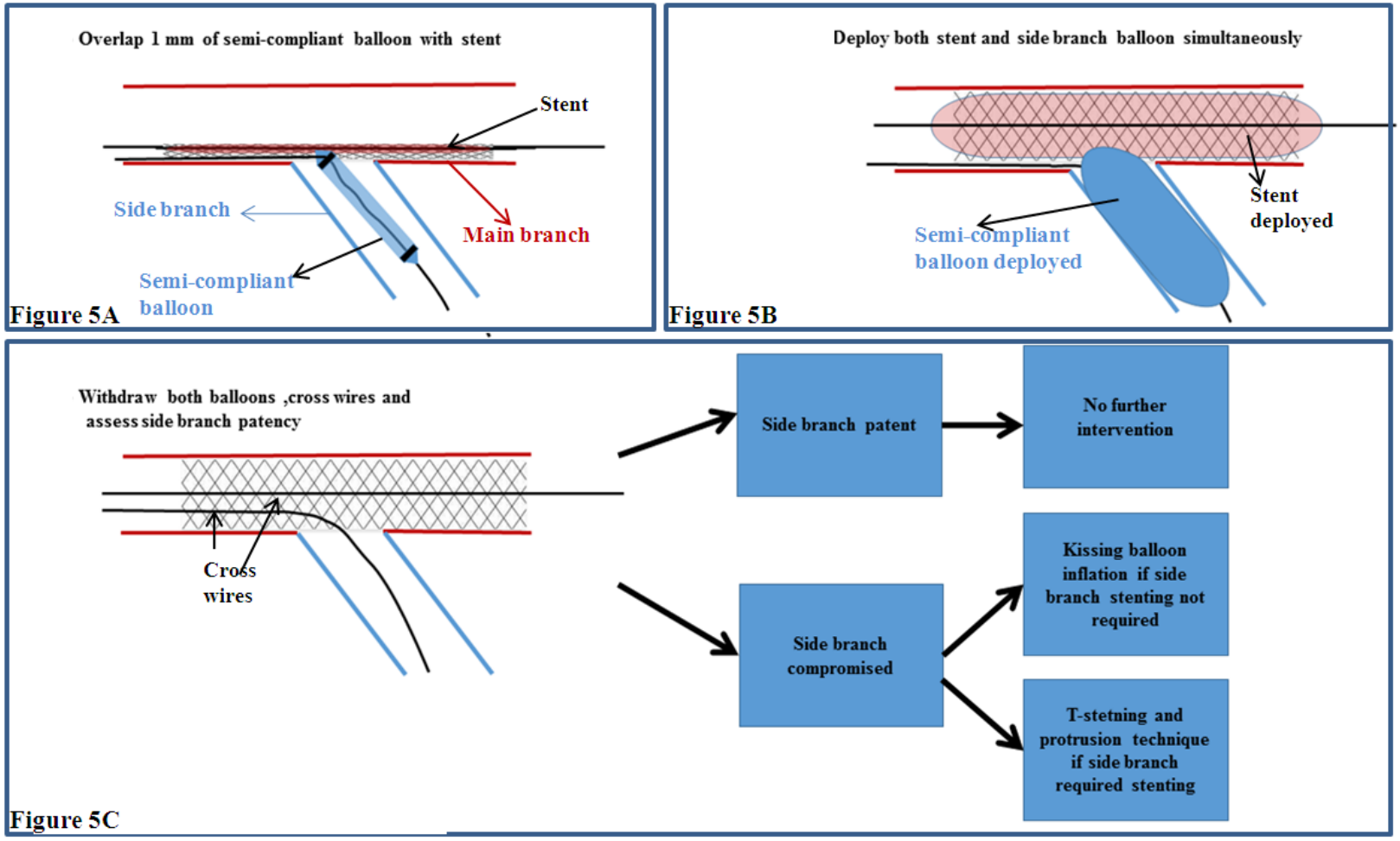

Figure 5A-C Modified Jailed Balloon Technique

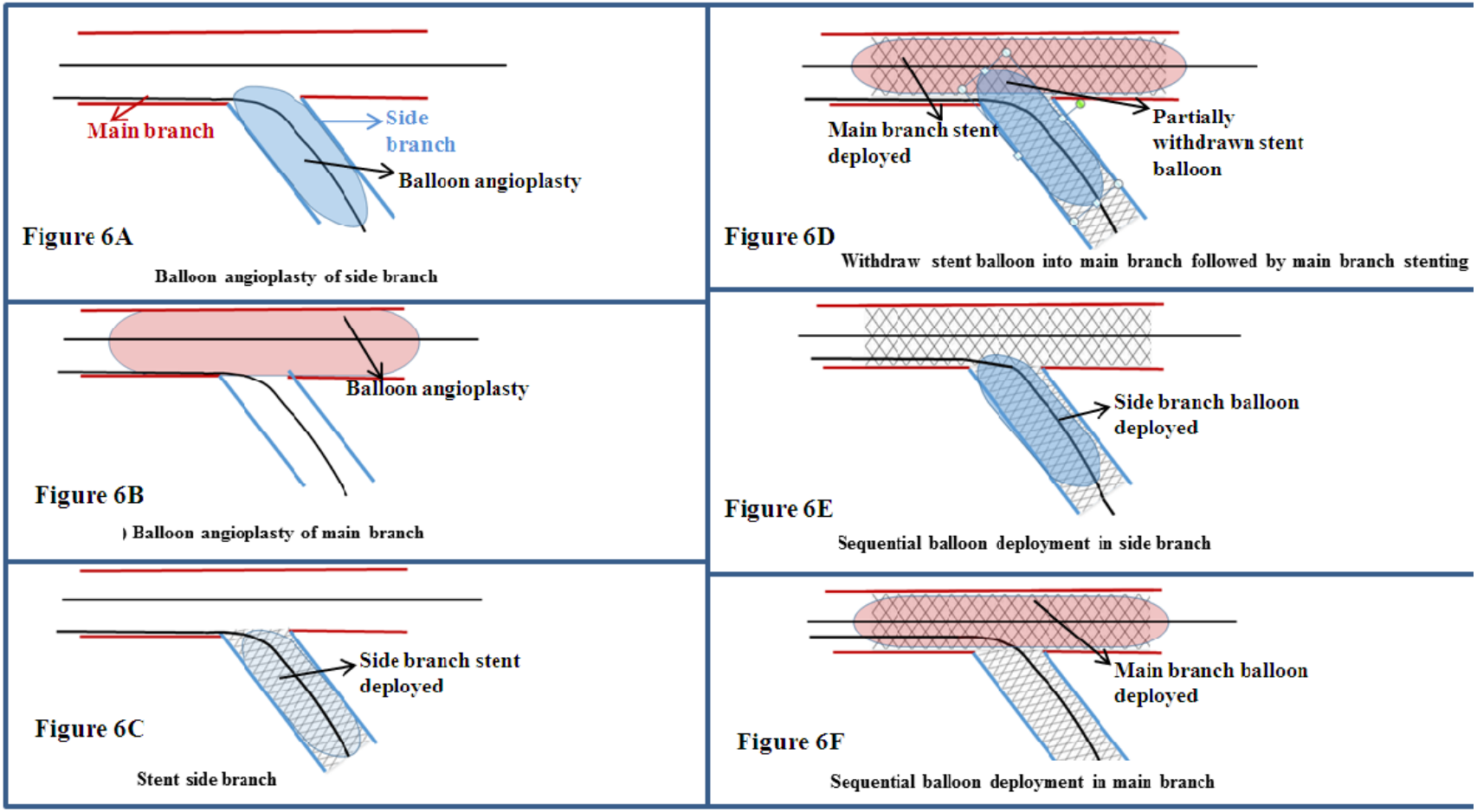

Figure 6A-F Jailed Stent Balloon Technique

AsiaIntervention

Official Journal of the Asian Pacific Society of Interventional Cardiology

(APSIC) and the Interventional Cardiology Foundation of India (ICFI)

www.asiaintervention.org

Title: **Ablation effect of additional low-speed rotational atherectomy following high-speed rotational atherectomy.**

Authors: Ruka Yoshida, M.D; Hideki Ishii, M.D, PhD; Itsuro Morishima, M.D, PhD; Akihito Tanaka, M.D, PhD; Takuma Tsuda, M.D, PhD; Kensuke Takagi, M.D; Yasuhiro Morita, M.D, PhD; Takashi Kataoka, M.D; Kiyoshi Niwa, M.D; Kenji Furusawa, M.D; Naoki Yoshioka, M.D; Hideyuki Tsuboi, M.D, PhD; Toyoaki Murohara, M.D, PhD

Manuscript number: AIJ-D-19-00022

Manuscript submission date: 06 May 2019

Revisions received: 26 July 2019

Accepted date: 04 March 2020

Ablation effect of additional low-speed rotational atherectomy following high-speed rotational atherectomy

Ruka Yoshida, MD[1,2]; Hideki Ishii MD, PhD[1]; Itsuro Morishima MD, PhD[2]; Akihito Tanaka MD, PhD[1]; Takuma Tsuda, MD, PhD[3];Kensuke Takagi, MD[2]; Yasuhiro Morita MD, PhD[2]; Takashi Kataoka, MD[1]; Kiyoshi Niwa[1], MD; Kenji Furusawa MD[1]; Naoki Yoshioka, MD[2]; Hideyuki Tsuboi MD, PhD[2]; and Toyoaki Murohara, MD, PhD[1]

[1]Department of Cardiology, Nagoya University Graduate School of Medicine, Nagoya, Japan

[2]Department of Cardiology, Ogaki Municipal Hospital, Ogaki, Japan

[3]Department of Cardiology, Nagoya Ekisaikai Hospital, Nagoya, Japan

Short title: low-speed RA following high-speed RA

Corresponding Author: Ruka Yoshida, MD

Department of Cardiology, Nagoya University Hospital,

65 Tsurumai-cho, Showa-ku, Nagoya 466-8560 Japan.

E-mail: lyoshida@hotmail.com

Abbreviations

CE clinical engineer

HS-RA high-speed rotational atherectomy

IVUS intravascular ultrasound

LS-RA low-speed rotational atherectomy

MLA minimal lumen area

PCI percutaneous coronary intervention

Classifications: Artherectomy; Calcified stenosis; Clinical research; Intravascular ultrasound; Rotablator; Stable angina

Introduction

Current expert opinion supports the use of low-speed rotational atherectomy (LS-RA) as an optimal technique[1] because slower burr speeds reduced platelet aggregation and heat injury associated with RA in previous *in vitro* experiments[2, 3]. However, a previous *in vivo* trial did not show benefits of LS-RA over high-speed RA (HS-RA) in terms of prevention of slow flow following RA[4]. In contrast, another effect of LS-RA may be that it ablates more plaques than does HS-RA because the burr axis vibrates to a greater extent while the burr rotates at slower speeds, such as the precessional movement of a spinning top. However, this additional ablation effect of LS-RA following HS-RA has not been completely elucidated. We hypothesized that LS-RA following HS-RA can achieve more acute gain by ablating more plaque than does HS-RA alone. To test this hypothesis, we conducted intravascular ultrasound (IVUS) analysis before and after LS-RA following HS-RA.

Methods

Of the 66 patients who underwent RA between January 2015 and July 2016, we examined 26 patients with 27 *de novo* severely calcified lesions who underwent LS-RA following HS-RA. Demographic, angiographic, and procedural data were collected from a prospectively entered dedicated database. This study was approved by the research review board of Ogaki Municipal Hospital and conducted according to the Declaration of Helsinki.

Rota Link PLUS™ (Boston Scientific, Marlborough, MA) was used in all patients. As wires, ROTAWIRE floppy™ or ROTAWIRE Extra Support™ (Boston Scientific) were used. The burr was advanced with a gradual push-forward/pull-back motion over short individual runs (<30 s) while attempting to avoid extreme deceleration. The rotational speed was set at 200,000 rpm at platform in the HS-RA protocol and at 115,000 rpm at platform in the

LS-RA protocol. RA in both protocols was continued until the rotational speed deceleration of <2000 rpm was achieved. Only one burr was used for each lesion. The study protocol was as follows: (1) HS-RA; (2) IVUS (before LS-RA); (3) LS-RA; and (4) IVUS (after LS-RA). Selection of wires and percutaneous coronary intervention (PCI) strategies, except for RA, was at the discretion of the treating physician.

The objective of this study was to compare the minimal lumen area (MLA) between IVUS findings before-and-after LS-RA. To obtain the corresponding MLA images before-and-after LS-RA, distances from at least two landmarks, such as side branches and calcifications, were used as references. Two experienced clinical engineers (CE) blinded to the study object independently measured IVUS. Any discrepancies between the two CEs were resolved by consensus.

MLA before-and-after LS-RA was compared using a paired t-test. All statistical analyses were performed using JMP software version 13.1 (SAS Institute Inc., Cary, NC, USA). $P < 0.05$ was considered statistically significant.

Results

Baseline characteristics are summarized in the Supplemental Table. Regarding PCI indication, most were cases of stable angina pectoris; however, there were 4 cases of non-ST-elevation acute coronary syndrome. The target lesions were the right coronary artery in 9, and the left anterior descending artery in 14 patients. Before RA, IVUS catheter could be passed through the lesion in 15 cases, and pre-dilatation was attempted in 9 lesions. All but 2 lesions were ablated using ROTAWIRE floppy™, and the burr size was 1.5 mm in 11, 1.75 mm in 11, and 2 mm in 5 lesions. While performing LS-RA, the rotational speed decreased to >3000 rpm even after HS-RA which ablated until rotational speed deceleration of <2000 rpm.

MLA after LS-RA was significantly larger than that before LS-RA (2.76 ± 1.03 mm^2 vs 3.29

± 0.95 mm^2; p<.0001; Figure 1A). The larger is the burr-to-minimum lumen diameter (before LS-RA) ratio, the greater is the change in the MLA before-and-after LS-RA (Figure 1B). A representative case is presented in Figure 1C. Slow flow occurred in 4 lesions after LS-RA, which recovered immediately after intracoronary nitroprusside injection. Final Thrombolysis in Myocardial Infarction flow grade 3 could not be attained in 3 lesions, in which slow flow developed before LS-RA. No major vessel perforation was observed.

Discussion

In this study, we demonstrated that significantly larger acute gain was achieved with additional LS-RA following HS-RA. Although we did not demonstrate the relationship between adding LS-RA and optimal stent expansion compared with standard RA, the mean additional ablation of 330 μm (calculated from MLA) may be helpful, considering previous study demonstrated the thresholds of calcium thickness of 450 μm as the predictor of calcium crack[5]. Because the burr-to-artery ratio is the significant determinant of slow flow[4], performing additional LS-RA following HS-RA, rather than the size-up of the burr, may be better to reduce complications and cost. The gyro effect may explain these results; the gyro effect is the principle that a burr rotating at a high-speed with a high moment of inertia proportional to the rotational speed produces less degree of change in the rotation axis direction[6].

LIMITATIONS

This is a pilot study with a retrospective nature. Eventually, this hypothesis needs to be tested in a prospective trial with proper randomization. Second, the wire bias may have influenced the ablation effect of LS-RA, suggesting that this technique may not be applied to all lesions, such as eccentric calcified lesions. Third, the burr speed used in HS-RA protocol was out-of-range from expert consensus[1], which might result in the compromise to increase in MLA or lead to more complication compared with that might

be achieved in the recommended high-speed protocol. Furthermore, optimal speed for LS-RA has not been elucidated yet. Fourth, although HS-RA was continued until the rotational speed deceleration of <2000 rpm was achieved, the increase in MLA might be gained by merely additional ablation rather than the effect of LS-RA. Furthermore, image analysis was not performed by the core laboratory.

CONCLUSIONS

Additional LS-RA following HS-RA ablated more plaque volume and gained significantly larger MLA than did HS-RA alone.

Impact on daily practice

Additional LS-RA following HS-RA could achieve more acute gain by ablating more plaque than does HS-RA alone, which might contribute to decreased incidence of slow flow and medical cost compared with burr size-up.

FUNDING

Supported by no-funding.

Conflict of Interest

H.I. received lecture fees from Astellas Pharma Inc., Bayer Pharmaceutical Co., Ltd., Daiichi-Sankyo Pharma Inc., and MSD K. K. T.M. received lecture fees from Bayer Yakuhin., Ltd., Daiichi-Sankyo Co., Ltd., MSD K. K., Mitsubishi Tanabe Pharma Co., Nippon Boehringer Ingelheim Co., Ltd. Department of Cardiology, Nagoya University Graduate School of Medicine received research grant from Astellas Pharma Inc., Daiichi-Sankyo Co., Ltd., Dainippon Sumitomo Pharma Co., Ltd., Kowa Co., Ltd., MSD K. K., Mitsubishi Tanabe Pharma Co., Nippon Boehringer Ingelheim Co., Ltd., Pfizer Japan Inc., and Teijin Pharma Ltd.

References

1. Barbato E, Carrie D, Dardas P, Fajadet J, Gaul G, Haude M, Khashaba A, Koch K, Meyer-Gessner M, Palazuelos J, Reczuch K, Ribichini FL, Sharma S, Sipotz J, Sjogren I, Suetsch G, Szabo G, Valdes-Chavarri M, Vaquerizo B, Wijns W, Windecker S, de Belder A, Valgimigli M, Byrne RA, Colombo A, Di Mario C, Latib A, Hamm C. European expert consensus on rotational atherectomy. *EuroIntervention*. 2015;11:30-6.

2. Reisman M, Shuman BJ, Dillard D, Fei R, Misser KH, Gordon LS, Harms V. Analysis of low-speed rotational atherectomy for the reduction of platelet aggregation. *Cathet Cardiovasc Diagn*. 1998;45:208-14.

3. Reisman M, Shuman BJ, Harms V. Analysis of heat generation during rotational atherectomy using different operational techniques. *Cathet Cardiovasc Diagn*. 1998;44:453-5.

4. Sakakura K, Funayama H, Taniguchi Y, Tsurumaki Y, Yamamoto K, Matsumoto M, Wada H, Momomura SI, Fujita H. The incidence of slow flow after rotational atherectomy of calcified coronary arteries: A randomized study of low speed versus high speed. *Catheter Cardiovasc Interv*. 2017;89:832-40.

5. Kubo T, Shimamura K, Ino Y, Yamaguchi T, Matsuo Y, Shiono Y, Taruya A, Nishiguchi T, Shimokado A, Teraguchi I, Orii M, Yamano T, Tanimoto T, Kitabata H, Hirata K, Tanaka A, Akasaka T. Superficial calcium fracture after PCI as assessed by OCT. *JACC Cardiovasc Imaging*. 2015;8:1228-9.

6. Provatidis CG. Revisiting the Spinning Top. *Int J Mater Mech Eng*. 2012;1:71-88.

Figure legends

Figure 1. (A) The change in MLA before and after low-speed rotational atherectomy (LS-RA) in each patient. (B) The relationship between minimal lumen area (MLA) change and burr-to-minimal lumen diameter (MLD) ratio. (C) Representative case. At each point, larger lumen areas were obtained following additional LS-RA.

(A)

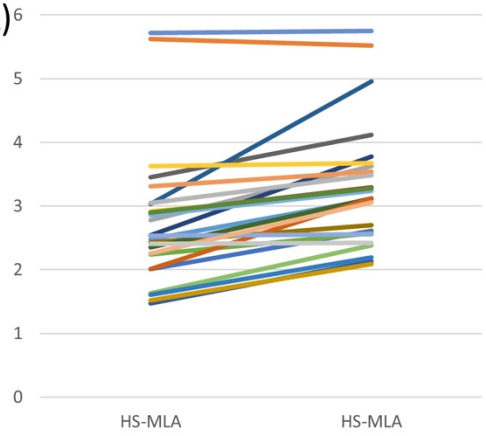

	Before LS-RA	After LS-RA	P value
MLA	2.76 ± 1.03	3.29 ± 0.95	<0.0001

(B)

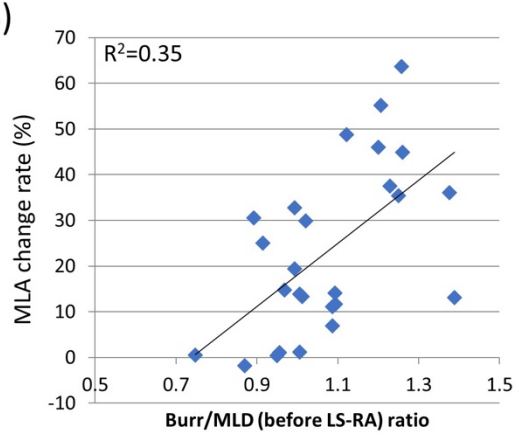

P=0.016

(C)

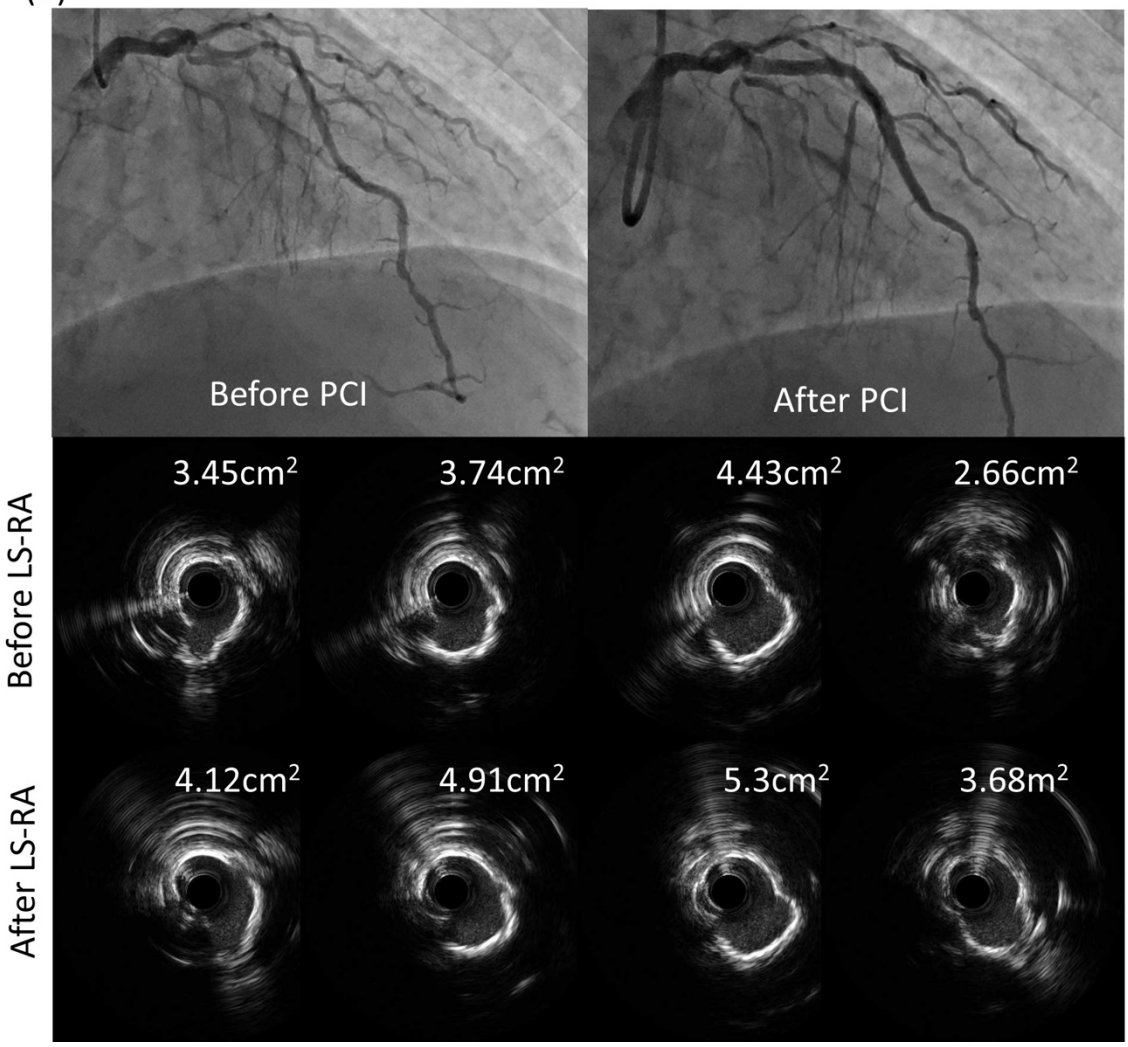

Supplemental Table: Patient's Clinical and Procedural Characteristics

Clinical baseline characteristics		N=26
	Age	74.6 (8.6)
	Male sex	18 (69.2%)
	Diabetes mellitus	16 (61.5%)
	Hypertension	17 (65.4%)
	Dyslipidemia	18 (69.2%)
	Hemodialysis	2 (7.7%)
	Smoking history	18 (69.2%)
	Prior PCI	20 (76.9%)
	Prior CABG	2 (7.7%)
Lesion and procedural characteristics		N=27
Indication for PCI	Stable angina pectoris	23 (85.2%)
	Non-ST-elevation acute coronary syndrome	4 (14.8%)
Target vessels	Right coronary artery	9 (33.3%)
	Left main	1 (3.7%)
	Left anterior descending	14 (51.9%)
	Left circumflex	3 (11.1%)
	Radial access	9 (33.3%)
	Chronic total occlusion	3 (11.1%)

	Procedure time (min)	100 [91, 126]
	Contrast volume (ml)	100 [60, 135]
	ROTAWIRE Floppy	25 (92.6%)
Burr size	1.5 mm	11 (40.7%)
	1.75 mm	11 (40.7%)
	2 mm	5 (18.5%)
	Burr-to-artery ratio	0.56 [0.53, 0.68]
High-speed RA	Session number	5.5 [4, 8]
	Total ablation time (sec)	70 [50, 113]
	Maximum speed deceleration (rpm)	5500 [4750, 7000]
Low-speed RA	Session number	5 [4, 7]
	Total ablation time (sec)	85 [51, 111]
	Maximum speed deceleration (rpm)	5500 [3000, 7000]
	Pre-intravascular ultrasound passed	15 (55.6%)
	Pre-dilatation	9 (33.3%)
	Small balloon un-passed before RA	2 (7.4%)
	Drug-eluting stent	21 (77.8%)
	Drug-coated balloon	6 (22.2%)
	Stent number	2 [1, 2.5]

Stent length (mm)	51 [29, 76]
Success and complication	
Final TIMI 3	24 (88.9%)
Peri-procedure myocardial infarction	3 (11.1%)
Slow flow	5 (18.5%)
Wire perforation	1 (3.7%)
Peak CK-MB (IU)	14 [11, 25]

Values are the mean ± standard deviation (SD), n (%), or median (interquartile range) as appropriate.

Peri-procedure myocardial infarction was defined as an increase in CK-MB above the normal upper limit.

CABG, coronary artery bypass graft; CK-MB, creatine kinase-myocardial band; PCI, pertcutaneous coronary intervention; RA, rotational atherectomy; TIMI, Thrombolysis in Myocardial Infarction.